REMOTE SENSING TO CHARACTERISE VEGETATION FUEL MOISTURE CONTENT IN THE UK UPLANDS

ABDULBASET HAMED A. BADI

Ecosystems and Environment Research Centre

School of Science, Engineering & Environment

University of Salford

Salford, M5 4WT, UK

Submitted in Partial Fulfilment of the Requirements of the Degree of Doctor of Philosophy, April 2019

Contents

List of tables

List of figures

DEDICATION

I would like to dedicate this thesis to my late father Hamed (God bless his soul), my mother Aisha and my brother Ahmed for trusting and supporting. I would like to dedicate it to my family specifically my wife Noura Elshebbah for her patience, encouragement, support and giving me her love more than I deserved. Also, my daughters Aisha, Asinat and all my friends who have been a source of inspiration and encouragement. Finally, I would like to dedicate it to my country Libya which supported me to complete my PhD in the UK.

Acknowledgments

First of all, thanks, and all praise is due to almighty Allah who gave me the strength and patience to complete my study.

I would like to acknowledge my country Libya, Omar AL-Mukhtar University/ /Derna branch, Faculty of Arts and Science, Environmental Science Department, for the study grant, which offered me this opportunity to complete a Ph.D. in the UK.

I would like to acknowledge Sheffield City Council, and Moors for the Future for access to the Peak District fire incidence data.

I wish to express my deep and sincere gratitude to my supervisors, Professor Mark Danson and Dr. Richard Armitage for their valuable advice, support and friendly help throughout this work. They were always there to listen and give advice. They did not only provide assistance and guidance, but also a good basis for the present thesis.

Salford University became a part of my life and I made many friends who helped me to enrich my knowledge and understanding of different cultures, experiences and backgrounds. I wish to extend my warmest thanks to all those who have helped me with my work in the School of Environment and Life Science, Geography Department at Salford University, UK.

I gratefully acknowledge the staff of the Libyan Cultural Bureau, London and particularly Dr. Abdelbasit Gadour and Dr. Atef Saeeh deserve my thanks.

I warmly thank my wife Noura Elshebbah and my daughters Aisha and Asinat for invaluable assistance during fieldwork and my special thanks and deepest gratitude go to all my friends in the UK, and I thank my cousin Prof. Mohamed Badi for proofreading.

Finally, I owe my loving thanks to my mother Aisha Abosif for her prayers, enduring sacrifice, extended support, understanding and patience, and my brother Ahmed Badi.

Declaration

I declare that the work presented in this thesis has not previously been submitted for a degree or similar award at Salford University or any other institution. To the best of my knowledge and belief, no material in this thesis has been previously published or written by another person, except where due reference is made. I further agree to give permission for fair use copying of this thesis for scholarly purposes

Signed: ……..

Date: …….

List of Acronyms

ASD	Analytical Spectral Devices
BOA	Bottom Of Atmosphere
BRDF	Bi-directional Reflectance Distribution Function
BRF	Bi-directional Reflectance Factor
EFFRFS	European Forest Fire Risk Forecasting System
EWT	Equivalent Water Thickness
FMC	Fuel Moisture Content
FRS	Fire and Rescue Services
IRS	Incident Recording System
JRC	Joint Research Centre
LAD	Leaf Angle Distribution
LAI	Leaf Area Index
LEDAPS	Landsat Ecosystem Disturbance Adaptive Processing System
LOO	Leave One Out
MSI	Moisture Stress Index
NDWI	Normalized Difference Water Index
NIR	Near Infrared
RS	Remote Sensing
RTM	Radiative Transfer Models
RWC	Relative Water Content
SAC	Special Areas of Conservation
Sen2Cor	Sentinel-2A Correction
SPA	Special Protected Areas
SSSI	Sites of Special Scientific Interest
SWIR	Short Wave Infrared
TIR	Thermal Infrared
TOA	Top-of-Atmosphere
VI	Vegetation Index

Abstract

Wildfires are an important hazard globally as they lead to significant land degradation, carbon losses and impact on human activities. Recent research has demonstrated how dynamic fire risk estimates can be informed by the use of remote sensing technology. The focus here is on improving methods for fire risk evaluation, so that prediction about where and when fires are likely to start can become more accurate. Fuel moisture content (FMC) is one of the most important factors influencing wildfire risk, as it controls the probability of ignition and the rate of spread of a fire. This work aims to assess the potential of calibrated time-series Sentinel-2A MultiSpectral Instrument (MSI) and Landsat-8 Operational Land Imager (OLI) data to estimate and map FMC in upland areas of the UK. The work employs laboratory and field-scale measurements, and radiative transfer modelling, to test the relationships between reflectance and FMC. *Calluna vulgaris* samples were collected from a test site in the UK Peak District, and their FMC determined. Near-coincident multi-temporal satellite imagery was acquired for the test site and maps of FMC generated using relationships tested through the laboratory work and modelling. The results showed a strong relationship between the normalized difference water index (NDWI) and moisture stress index (MSI) with FMC, which was independent of scale. The relationship was not strongly affected by variations in soil background properties or differences in solar zenith angle. Spatial mapping of FMC across the Peak District National Park revealed temporal and spatial variations in FMC in *Calluna*-dominated areas. The results have implications for wildfire risk management and for upland vegetation management and conservation.

CHAPTER 1: INTRODUCTION

1.1 Introduction

A wildfire is any unplanned, or uncontrolled, vegetation fire, which may require suppression, and where vegetation is the main 'fuel' component; wildfires can occur in a range of fuel types like grasslands, shrublands or forested areas (Hardy, 2005). Wildfire is a problem in many countries due to the interactions between people, fuel and climate (Hardy, 2005). There is therefore a need to minimise the negative effects of wildfires on ecosystems (Chuvieco et al., 2010).

The evaluation of the risk factors associated with wildfires helps the management of areas which are subjected to frequent fires. The established way to measure the dangers associated with wildfires is to use weather data to anticipate future climatic conditions (He, Shang, Crow, Gustafson, & Shifley, 2004). However, climatic conditions are just one factor influencing wildfires and other factors, like human causes of ignition, the availability of fuel, and vegetation moisture content, must also be considered (Shang, He, Crow, & Shifley, 2004).

The United Kingdom uplands normally occur above the limit of enclosed farmland, or above a certain altitude (e.g. 300m) (Clay, 2009), and they occupy about 27-30% of the land area (Thompson, MacDonald, Marsden, & Galbraith, 1995). The vegetation in the uplands of the UK is very important internationally, and some plant species found in these regions are rarely found elsewhere. The plant and animal species present in these area are also very important for the conservation of biodiversity (Albertson, Aylen, Cavan, & McMorrow, 2009; Clay, 2009).

Dry air and raised temperatures are causing frequent wildfires in the Peak District of Northern England (Albertson et al., 2009). Not only do these fires cause damage to the soil and vegetation but they also affect ecosystem processes and water quality in catchments of this upland area. In addition, significant releases of carbon dioxide are now seen as a major environmental problem (Albertson et al., 2009). Furthermore, wildfires contribute to increasing atmospheric levels of pollutants which are detrimental to human health and ecosystems, such as primary pollutants CO and NOx and the production of secondary pollutants (O_3 and secondary organic aerosols (SOA)) (Urbanski, Hao, & Baker, 2008). There have also been serious concerns about the impacts fires may have on land management and the tourism industry (Wotton, Martell, & Logan, 2003).

Advances in remote sensing (RS) technology over the last four decades have enabled better observations of burned areas, using sensors with a high-spatial and temporal resolution (Pleniou, Xystrakis, Dimopoulos, & Koutsias, 2012). RS is used to measure the quantitative and qualitative properties of the vegetation cover, and researchers have developed a range of vegetation indices to support this work. RS employs spectral measurements to help determine the characteristics of the vegetated areas, such as the different types of vegetation, soil properties, and topography (Bannari, Morin, Bonn, & Huete, 1995).

Remote sensing has proven itself as a valuable tool for monitoring wildfires because of its ability to detect variables like the frequency of fires or the fire return interval (Hardtke, Del Valle, & Sione, 2011). Other elements, such as the speed of fire ignition, and its impact on landscape dynamics can also be observed, allowing for better decision-making regarding the management of wildfires (Hardtke et al., 2011). Compared to other methods of observation, RS has also proven itself to be more efficient both in regard to the time required for analysis and associated costs (Pleniou et al., 2012).

This research will look to identify the factors that contribute to the relationship between vegetation fuel moisture content (FMC) and spectral measurements and combine this with spectral reflectance modelling for a specific species of shrubland vegetation.

In addition, to assess the spatial-temporal variation in FMC at landscape scale, satellite imagery can be used to map FMC over large areas with a focus on scaling-up FMC estimates to areas like the uplands of the Peak District. This research will therefore combine theoretical modelling of the relationship between spectral data and vegetation moisture content with both laboratory and field measurements. It will then employ time-series satellite imagery to map these relationships at landscape scale. It will use these findings to indicate the potential role of remote sensing in vegetation fire risk assessment in the UK uplands.

1.2 Research aims and objectives

One important hurdle to overcome in order to better evaluate fire risk is the lack of knowledge of vegetation fuel properties and their change in space and time (Keane, 2013). Fuels show wide variability in spatial extent, vegetation stand age, and species composition. Fuels also vary from year to year, and season to season, and are affected by both internal and external factors (Keane, 2015).

The main aim of this study is to investigate the spatial-temporal variation in vegetation fuel moisture content at the landscape scale in the UK uplands, and examine how this variation affects wildland fire risk by using remote sensing to estimate and map FMC for a specific shrubland species. The aim of the study can be split into the following three specific objectives (Figure 1.1):

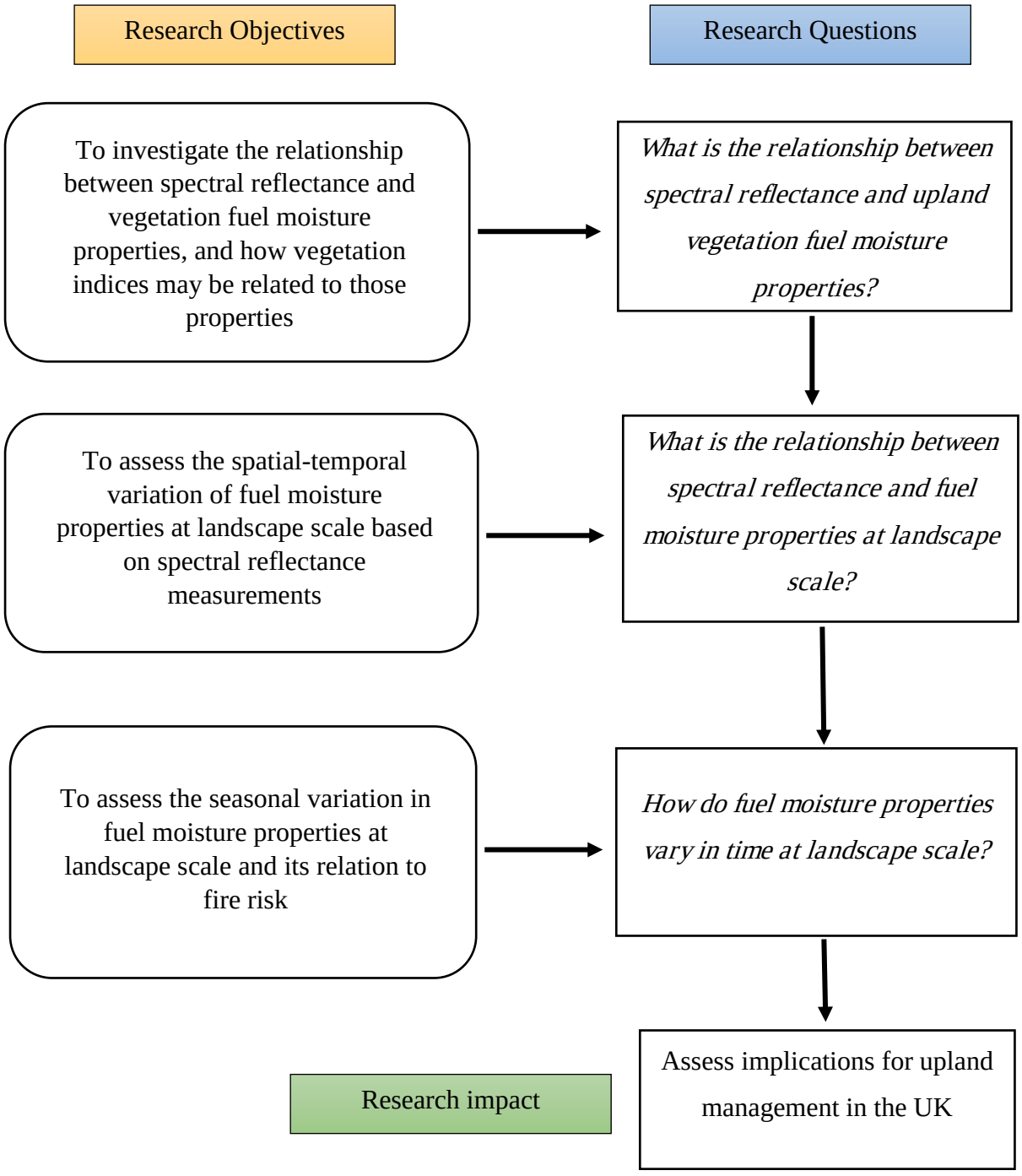

Figure 1.1: Research objectives and questions

(i) To investigate the relationship between spectral reflectance and vegetation fuel moisture properties, and how vegetation indices may be related to those properties.

Remote sensing technology is based on the ability to measure electromagnetic radiation, which interacts with material, at various wavelengths. Electromagnetic radiation is absorbed, reflected, or transmitted in a particular way that characterizes that material. By measuring radiation-material interactions at various wavelengths of the spectrum, the material's spectral signature can be plotted, which represents a characteristic shape (Sims & Gamon, 2002).

The interaction between vegetation and radiation differs from the interactions observed in other materials. Vegetation tends to absorb radiation in blue and red wavelengths due to the presence of chlorophyll, and also in water absorption wavebands which obscure biochemical features related to lignin and other carbon constituents (Fourty, Baret, Jacquemoud, Schmuck, & Verdebout, 1996). Healthy vegetation strongly reflects near-infrared radiation due to low absorption and high scattering at these wavelengths (Asner, 1998). Variations in spectral signatures are caused by differences in plant species, water levels, pigments, levels of nitrogen and carbon, as well as other characteristics (Asner, 1998). These differences make it possible to identify different Earth surface features or materials by analysing their spectral reflectance patterns or spectral signatures (Asner, 1998).

Vegetation indices have been widely used to monitor vegetation and to estimate vegetation biophysical parameters (Jackson & Huete, 1991). The Normalized Difference Water Index (NDWI) is a remote sensing-derived index related to liquid water which may be used to monitor changes in the water content of leaves, using near-infrared (NIR) and short-wave infrared (SWIR) wavelengths (Gao, 1996). The Moisture Stress Index (MSI) is a remote

sensing-derived index related to detection of plant water stress using near-Infrared (NIR) and mid-infrared (MIR) wavelengths (Hunt & Rock, 1989).

The combination of the NIR with the SWIR removes variations in the index induced by leaf internal structure and leaf dry matter content variation, improving the accuracy in retrieving the vegetation water content (Ceccato, Flasse, Tarantola, Jacquemoud, & Grégoire, 2001). Its usefulness for drought monitoring and early warning of wildfires has been demonstrated in many different studies (Ceccato, Gobron, Flasse, Pinty, & Tarantola, 2002; Zhang et al., 2010). To achieve this objective, three laboratory experiments were designed to investigate the effects of fuel moisture content, soil background and solar zenith angle on canopy reflectance using samples of *Calluna vulgaris,* and these results were then used to inform a radiative transfer modelling experiment using the ProSAIL model.

This objective leads to a specific research question:

What is the relationship between spectral reflectance and upland vegetation fuel moisture properties?

(ii) To assess the spatial-temporal variation of fuel moisture properties at landscape scale based on spectral reflectance measurements.

Landscape characterisation is a key area of study for many disciplines. Information regarding vegetation can be used in various research, from mapping of eco-regions and conservation studies, to fire mapping, global change research, or regional planning (Markon, Fleming, & Binnian, 1995). The scale of observation is often key to understanding the nature of a given phenomenon (Wu, Niu, Tang, & Huang, 2009). For instance, moisture content that is estimated from a small area cannot be used as a drought index for large-area drought

monitoring (Wu et al., 2009). In addition, local-scale information cannot be used as a substitute for regional scale information (Wu et al., 2009).

Consequently, the application of RS at landscape scale can help in assessing the role of such data in vegetation fire risk assessment in the UK. Through remote sensing technology, information can be obtained in an inexpensive manner; information that can be efficiently used for vegetation and fuel mapping. Images obtained through remote sensing, combined with environmental and vegetation inventory data can improve the accuracy of fuel and vegetation mapping (Poulos, Camp, Gatewood, & Loomis, 2007).

The relationship between FMC and VI is weaker in some vegetation types and stronger in others, namely in grasslands. This is potentially due to the fact that canopy structure varies spatially and temporally, for example variation in leaf area index (LAI) (Shen, Li, & Guo, 2014). FMC represents a relative index for quantifying water present in vegetation and cannot be scaled with the LAI. Two canopies that have the same FMC could potentially have significantly different LAI leading to different spectral responses (Wang, Xu, & Yang, 2009).

These relationships are further impacted by geometrical factors, such as sensor zenith view angle or temporal and spatial variability in solar illumination, and atmospheric properties. Before developing a way to more accurately estimate FMC, it is necessary to completely understand how spatial and temporal variability of geometrical and biophysical factors affect canopy and leaf reflectance (Bowyer & Danson, 2004). Fieldwork was the key tool to achieve this objective. Samples were collected to record the temporal variation in fuel moisture content (FMC) of upland vegetation sites coincident, or near-coincident, with

satellite images to allow investigation of the relationship between a vegetation index and FMC over a 12-month sampling frame.

This objective leads to a specific research question:

What is the relationship between spectral reflectance and fuel moisture properties at landscape scale?

(iii) To assess the seasonal variation in fuel properties at landscape scale and its relation to fire risk.

Fire patterns are constrained temporally and spatially by a series of both direct and indirect environmental gradients that work cumulatively (Rollins, Morgan, & Swetnam, 2002). Topography impacts at a regional scale on the occurrence and behaviour of fire (Rollins et al., 2002). Landscapes are not static by nature, and changes may occur over the course of days, weeks, months, years or decades. It is interesting to study these changes and assess how they influence ecological processes and how they affect fire risk. Fires that advance through a landscape will be met with varying fuels, weather, and topography, and these will influence the way in which fire behaves and how it will affect the landscape (Finney, 2004). In a more indirect way, the structure of the landscape is also linked with the configuration and composition of post-fire environments, which include plant mortality and regeneration. The landscape's structure is also influenced by fuel management. In order for fuel management to be efficient, it must take into account that vegetation canopy spatial patterns can interrupt fire flow across the landscape (Finney, 2004). This objective leads to a specific research question:

How do fuel properties vary in time at the landscape scale?

1.3 Original contribution of the research

The research aims to understand the use of remote sensing to estimate FMC for a specific species, and here the focus will be on uplands in the UK, and on *Calluna vulgaris* which is one of the most important species exposed to wildfires.

Many studies (Casas, Riaño, Ustin, Dennison, & Salas, 2014; Ceccato et al., 2001; Danson & Bowyer, 2004; Féret et al., 2011; Jacquemoud et al., 2009; Jacquemoud et al., 2006; Wang, Qu, Hao, & Hunt, 2011) have investigated the relationship between spectral reflectance and vegetation fuel characteristics using leaf and canopy reflectance models, generally focusing on using vegetation indices to assess the impact of physical and chemical properties of the canopy on the spectral reflectance. In addition, most of these studies did not look in detail at the spectral factors that contribute to the relationship between FMC and spectral measurements using different leaf or canopy structure, nor do they look at measurements specific to shrubland vegetation.

Some studies (Al-Moustafa, Armitage, & Danson, 2012; Almoustafa, 2011; Bisquert, Sánchez, & Caselles, 2014; Kodandapani, Cochrane, & Sukumar, 2008; Ustin, Riaño, Koltunov, Roberts, & Dennison, 2009; Yebra & Chuvieco, 2009) have assessed the spatial-temporal variation of fuel characteristics at landscape scale based on spectral reflectance measurements used to map FMC, in different environments, such as in Spain, California and moorlands in the UK, but the approach has never been applied for large areas. These studies have used remote sensing for mapping the spatial and temporal dynamics of vegetation FMC for small areas up to 10 km^2, and specifically for the study in the UK 0.15 km^2. This research will focus on scaling-up FMC measurements with satellite imagery to a much larger area of over 1400 km^2.

Some authors have employed time-series satellite imagery to map these relationships at landscape scale to assess the seasonal and inter-annual variation in fuel characteristics and its relation to fire risk (Allan, Johnson, Cridland, and Fitzgerald, 2003; Chuvieco, Cocero, Aguado, Palacios, and Prado, 2004; Cary et al. 2006). However, this has never been attempted for multi-temporal landscape scale mapping of FMC for uplands in the UK because the satellite data available has been inappropriate. In this research, FMC imagery is derived for a large area for one year of measurements, by extrapolating the relationships across space and time.

After achieving the research objectives, the results will be used to identify the role of remote sensing in vegetation fire risk assessment for uplands in the UK. FMC is one of the important variables for fire risk and spread models, along with vegetation type, topography and wind speed (Wang et al., 2017). This research will investigate the possibility of FMC mapping over large areas based on the relationship between VI (NDWI, MSI) and FMC using remote sensing technology, and test the effects of soil moisture, solar zenith angle on this relationship using a specific species of vegetation over a period of 12 months.

1.4 Structure of research

This thesis contains six chapters, followed by a list of references and appendices as follows:

Chapter 1 contains a general introduction relating to fire management and fire risk assessment and outlines the use of remote sensing. In addition, the research aim, objectives and questions to be addressed by this research, as well as the proposed scientific contribution, are presented.

Chapter 2 is a background literature review about the importance of the UK uplands, in terms of vegetation, wildfires, plant communities and fire risk modelling approaches. In addition, it highlights vegetation fuel characteristics which affect spectral reflectance. It also focuses on characterizing vegetation with remote sensing, relationships between remote sensing and vegetation biophysical properties and spectral measurements of leaf and canopy. Finally, this chapter presents the conclusions drawn from the literature review which form the rationale for this thesis.

Chapter 3 describes a laboratory experiment which addresses the first objective of the research. The setup of the laboratory and the methods used to test the hypotheses relating to fuel moisture content, soil, and solar zenith angle on canopy reflectance are described.

In addition, radiative transfer modelling is used to explore the sensitivity of these variables to spectral reflectance.

Chapter 4 describes the general background about the Peak District study area in terms of fire risk and vegetation, site and climate. In addition, it describes field data collection methods and laboratory analyses, including the sampling design and methodology. The techniques employed in generating and analysing the appropriate datasets are also outlined. This chapter also contains the satellite image processing procedures and explains the vegetation indices that were used to develop the relationship with FMC.

Chapter 5 explains the results of the fieldwork and investigates the potential of using remote sensing to estimate FMC and map the temporal variability of FMC across the test site. This chapter illustrates the importance of using remote sensing data to map spatial and temporal variations in vegetation FMC across large areas.

Chapter 6 comprises the final discussion and conclusions of the thesis. This involves discussion of a range of issues relating to the application of remote sensing in vegetation fire risk assessment in the uplands of the UK. In addition to the research challenges and problems, the chapter presents the overall conclusions of the work.

CHAPTER 2: LITERATURE REVIEW

Summary

This chapter reviews information about UK upland vegetation and wildfires, including the importance of uplands, details of plant communities, and a review of wildland fires and fire risk modelling approaches. In addition, the literature review focuses on vegetation fuel properties with a description of fuel moisture content and the most common methods used for its estimation. The literature review also touches on applications of remote sensing, including details about vegetation spectral reflectance and its relation to vegetation FMC and a review of vegetation indices which are used for investigating these relationships. The literature review finally focuses on radiative transfer models, explaining how they work to simulate the results of experimental measurements.

2.1 Introduction.

The aim of this literature review is to present an overview of the effects of wildfires on upland vegetation in the UK and highlight their importance in this environment. In addition, it will review how aspects of fire risk can be mapped with the use of remote sensing technologies and link this discussion to a brief review of the physical principles of remote sensing of vegetation.

2.2 UK upland vegetation and wildfires

Almost 15% of the world's blanket bog is found in upland Britain (Mehner, Cutler, Fairbairn, & Thompson, 2004). The vegetation in the uplands of the UK is very important internationally, and some plant species found in these parts are rarely found elsewhere (Clay, 2009). The species present in these areas have been in the region for a long time and are very important for the maintenance of biodiversity (Clay, 2009).

There are two zones into which the uplands of the United Kingdom can be divided: the montane zone and the sub-montane zone. The former is situated above the actual climax tree line, which is higher than 600-700 meters above sea level, whereas the latter is situated below this altitude. The area situated below the tree line constitutes 27-30% of the total area of the UK (Thompson et al., 1995).

2.2.1 Importance of uplands

Key aspects of the uplands of the UK include the cultural and economic contribution of these areas, the natural resources found, and the range of key landscapes (Tharme, Green, Baines, Bainbridge, & O'brien, 2001). Uplands cover about one third of the UK land surface and they consist of different habitats: granite tors, eroded peat plateaux and the arctic-like plateaus of Dartmoor, Derbyshire and Scotland (Davies, Legg, Smith, & MacDonald, 2006).

The uplands of the UK are also home to species and habitats that are globally rare. These species and habitats are often under pressure and are often protected in some way. In the UK, moorlands cover 38% of Scotland, 5.5% of England and Wales and 8% of Northern Ireland (Holden et al., 2007). These areas are dominated by small shrubs like heather (*Calluna vulgaris* (L) Hull) or bilberry (*Vaccinium myrtillus* (L)) and sedges such as cotton grass (*Eriophorum* spp.). There are variations in upland characteristics from north to south due to altitudinal variations. There are also variations east to west controlled by precipitation and local drainage conditions (Clay, 2009).

The Peak District National Park holds the title of being Britain's first National Park. Cultural and natural forces continuously change the landscapes of this park and it continues to evolve in reponse to climatic and environmental conditions. Millions of people visit this park each

year and the reasons include the fact that it has beautiful landscapes and a wide range of outdoor activities (Peak District National Park Authority (PDNPA), 2009).

The Peak District has been given much importance owing to the fact that it has attractions ranging from the purple heather moors and "featherbed" bogs of Kinder and Bleaklow, to verdant woodlands. Not to mention the rivers and dramatic limestone cliffs of Dovedale. All these individual attractions collectively make the Park stand out as a special place for tourists. The biggest attraction of the Peak District National Park is the fact that it is very diverse in terms of landscape and attractions (PDNPA, 2001). The total number of tourist visits to the Peak District National Park was around 12 million per annum from 2009 to 2013, based on a census of visitors who spent over 3 hours in the Peak District (PDNPA, 2014). A Peak District National Park Visitor Survey (PDNPVS, 2015) showed that most people visit the Peak District to enjoy outdoor activities in its spectacular landscapes (Table 2.1). The survey looked at data on tourism and visitor volume, and value for quantified behaviours and perceptions of visitors to the National Park.

Table 2.1: Reasons for visiting the Peak District; the percentages do not add up to 100 because some people chose more than one reason for visiting (Source: PDNPVS, 2015).

Reasons for Visiting	Percentages
Walk more than 10 miles	58%
Walk less than 2 miles	24%
Sightseeing	23%
Picnic	21%
Dog walking	16%
Tourist Attraction	10%
Other Count	8%
Bird watching	8%
Cycling	6%
Cultural Heritage	5%
Painting/ photography	5%
MTB (mountain biking)	4%
Climbing	4%
Running	2%

2.2.2 Plant communities in upland areas

The most notable plant communities in the British uplands, based on their vegetation characteristics, include 10 woodland, 15 heath, 30 mire (bog) and 27 grassland/sedge-dominated communities (total = 82); of these, 29%, are montane, 30% sub montane and 32% azonal (Birks & Ratcliffe, 1980). The rest are seven further graminoid-based upland communities that can often be found in close association with heather communities (Thompson et al., 1995). The dwarf shrub communities, which are abundant in the UK uplands, play a very important role in contributing to the biodiversity of the region (Humphrey, 2005).

Three factors affect vegetation distribution in the UK, the climate, the geology and the topography. Some of the geographical trends in the vegetation of the uplands of the UK, relating to these factors, are very striking. For example *Ulex gallii-agrostis curtisii* is geographically limited and is exclusive in the south-west region of Britain, while *Calluna vulgaris* and *Myrtillus-Sphagnum capillifolium* is most abundant in the north-west (Thompson et al., 1995). What is important is that these communities combine to form a complex mosaic of species. Based on the regional variation in climate, geology and topography the structure of these mosaics can be very different from one area to another (Usher & Thompson, 1993).

Calluna is the dominant species on UK moorland (Grime, Hodgson, & Hunt, 2014). It is a dwarf shrub which is relatively short-lived (usually under 30 years) and has a period of efflorescence starting in August (Fagúndez & Izco, 2004). *Calluna* produces its seeds inside capsules and then the wind helps to disperse them (Legg, Maltby, & Proctor, 1992). In addition, the seeds have the ability to survive for up to 100 years within the soil (Miller & Cummins, 1987). The seeds need between eight to fourteen days to germinate (Spindelböck

et al., 2013). The phenological cycle of *Calluna* starts with growth and maturing in spring then senescence during summer and autumn (Gilbert, 2008). *Calluna* has four phases during its life cycle which starts with the pioneer stage for 0-6 years, then the building stage for 7-15 years, the mature stage between 14-24 years and then the degenerate stage for 20-30 years (Figure 2.1) (Davies, 2005). Calluna moves through its life cycle the amount of woody material in the canopy increases as it ages.

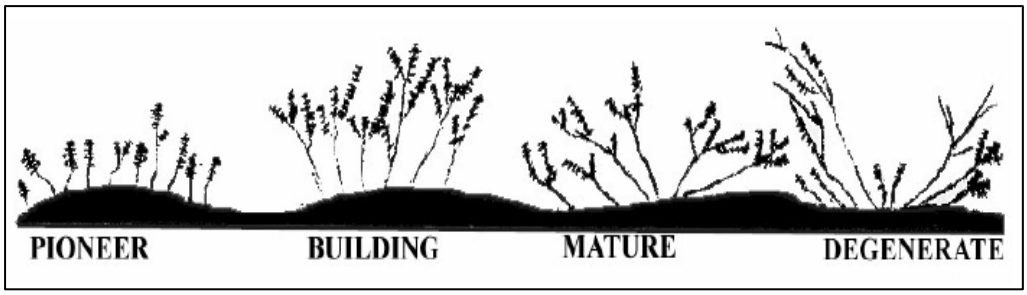

Figure 2.1: Life cycle of *Calluna* (Source: Davies, 2005).

2.2.3 Wildland fires in context

Wildland fires are considered an important environmental problem because of their effects on soil erosion, desertification, pollution, biodiversity and the landscape, in addition to potentially significant economic losses. Climate and vegetation are the main natural factors that affect the occurrence of fires, due to large regional differences in rainfall and temperature. Anthropogenic activities, terrain, fuel type, and causes of ignition, are also important factors affecting wildland fire occurrence (Hardy, 2005).

There is a wide range of terms used in the fire research literature to describe the potentially dangerous impacts of fire (Yakubu, Mireku-Gyimah, & Duker, 2015). Table 2.2 shows definitions for some of the important terms related to wildfires.

Table 2.2: Definition for wildfire terms

The term	Definition	Source
Fire danger	Sum of the constant and variable fire danger factors affecting the inception, spread and resistance to control and subsequent fire damage.	Potter (2012)
Fire hazard	A fuel complex, defined by volume, type, condition, arrangement, and location that determines the degree of ease of ignition and the resistance to control. It expresses the potential fire behaviour for a fuel type, regardless of the fuel type's weather influenced fuel moisture content.	Hardy (2005)
Fire risk	The chance that a fire might start, as affected by the nature and incidence of causative agents.	Hardy (2005)
Fire intensity	Represents the energy released during various phases of the fire and no single metric captures all the relevant aspects of fire energy. Different metrics, including reaction intensity, fire line intensity, temperature, residence time, radiant energy and others are useful for different purposes.	Keeley (2009)
Fire severity	Refers to the loss or decomposition of organic matter aboveground and belowground. Metrics for this parameter vary with the ecosystem. Including mortality is consistent with the definition of fire severity as a loss of organic matter.	Keeley (2009)

Uncontrolled fires are important in the ecology of upland areas, including those in the UK (Davies & Legg, 2008). Potential shifts in fire intensity and frequency may affect ecosystem function and biodiversity. Also, important is how people respond to fire management, the risks associated with wildfires and the suitability of conditions related to vegetation management with controlled fires (Davies, Gray, Hamilton, & Legg, 2008).

In the past, grazing and natural fires has negatively impacted the landscape, which has resulted in large areas of treeless moorland in the UK uplands (Palmer & Bacon, 2001). Fires that break out in these areas do not get extinguished easily and can last for several days and even weeks, due to the fact that the soil is very supportive of wildfires. Most of the time, these fires occur because of human negligence or occasionally as a result of lightning strikes.

Generally, the perception regarding wildfires is that they are caused accidently and are not intentional (Albertson et al., 2009).

Most of the controlled burning activity in the UK takes place in the months of February and March when the ground is rather wet and the shrubland vegetation is dry (McMorrow et al., 2009). These burning activities take place on a 10–20 year cycle. There is evidence that suggests that managed burning might have increased over time (Yallop et al., 2006).

Wildfires in the UK are considered a serious issue, and although they usually occur in remote areas, they can damage areas of more than 5000 ha, last for several days, and may need up to 100 firefighters to fight the fires. Additionally, affected areas may require extensive restoration (Davies et al., 2008).

There have been serious concerns raised by many organisations related with fire risk management about the possibility of fires breaking out because of climatic conditions in the uplands of the UK. These areas of the country are amongst the most frequently visited places and hence the tourism sector would be damaged if fire breakouts were not managed here (Wotton et al., 2003).

Some of the key years where wildfires became a common occurrence in the UK include 1976, 1995, 2003,2006 and 2018. Data also show that the UK is facing an increased threat of wildfires (Davies, Smith, MacDonald, Bakker, & Legg, 2010), with around 37,371 heathland and grassland fires recorded from 1986 to 1993, and around 60,332 per year recorded from 1994 and 2005. However, the reliability of these data is uncertain and there is little evidence quantifying the real damage caused by these wildfires (Davies et al., 2008).

McMorrow et al. (2009) studied fires in the Peak District between 1976 and 2003 and found that most fires had started accidentally, for example, one peat fire in the Peak District in

April 2003 burned 777 ha of moorland, including areas under statutory conservation protection. Another Peak District fire in July 2006 required 30 days of firefighting. This is likely to result in increased costs, divert focus to prevention, and increase demands for acquiring better risk assessment tools. Fire and Rescue Services (FRS) are required to identify risks to communities within their Integrated Risk Management Plans (McMorrow, 2011).

There is substantial variation in fire behaviour observed on heathlands, and these differences are closely related to the structure and age of the vegetation being burnt (Davies, Legg, Smith, & MacDonald, 2009). Additionally, it is acknowledged that assessing fire behaviour, including fire intensity, is not always accurate in evaluating the true effect of fires on environments and organisms (Keeley, 2009).

For example, in 1973 a *Calluna* wildfire occurred on the North York Moors, northern England, reported by Maltby, Legg, and Proctor (1990), was considered severe due to very dry peat conditions. The fire lasted for several weeks before it was controlled and put out. In the end it affected the *Calluna* root mats and natural seed banks over the areas which had been burned (McMorrow, 2011).

2.2.4 Fire risk modelling approaches

In a fire environment, there are several factors that define the concept of fire hazard such as the difficulty of control, the impact of the fire, the spread rate and the ease of ignition. This becomes fire risk if there is a chance of fire ignition by any causative agent (Bonazountas, Kallidromitou, Kassomenos, & Passas, 2005). One key activity involves measurements and monitoring to undertake damage assessment after a fire incident. These methods are implemented in order to provide information to various stakeholders and governmental agencies (Chuvieco et al., 2010).

Remote sensing is used to provide data on different phases of fire management. The phases include before a fire incident (prevention), during a fire (fire management), and damage assessment after the fire (Arroyo, Pascual, & Manzanera, 2008). In comparison to fire monitoring methods and conventional fire detection, observations from remote sensing have significant advantages. This is due to its spatial coverage and that it is repetitive and consistent over large areas of land (Arroyo et al., 2008). Fire monitoring can be undertaken from space, through the use of a number of satellites, in addition to airborne remote sensing systems. Appropriate satellites include Landsat-ETM, Landsat-8 OLI, ERS-ATSR, NOAA-AVHRR, SPOT, JERS, and DMSP (Yakubu et al., 2015).

Current systems for fire risk rating calculate fuel moisture content (FMC), and in particular 'dead FMC', by using meteorological indices. Dead FMC is suspended and dead biomass, which can ignite more easily than live fuel, and has a strong dependence on atmospheric conditions (Keane, 2015). Meteorological indices are harder to apply to live fuels because plants have the ability to draw water from the soil reservoir, even in cases of extreme temperatures (García, Chuvieco, Nieto, & Aguado, 2008).

Meteorological wildfire indices are determined on the basis that weather data are related to variable factors that may change rapidly in terms of time and space. Factors such as wind speed, temperature and moisture are often referred to in the literature as being 'fire danger indicators' (San-Miguel-Ayanz et al., 2003). For example, indices now use observational data, gathered from weather stations across Europe, interpolated to a 50km x 50km grid. First efforts in this area were initiated by the University of Torino, Italy which created prototype software called the European Danger Indices Calculator (EUDIC) (Perarnaud, Seguin, Malezieux, Deque, & Loustau, 2005).

Chuvieco (2003) shows that with this software, six indices were integrated within a GIS environment. Frequently used indices across European services for civil protection and forests were used in the EUDIC. Amongst them, The Canadian Fire Weather Index, or FWI, The Portuguese Index, The Spanish ICONA method, The Sol Numerical Risk and The Italian Fire Danger Index. This selection of indices was chosen because they were able to cover every meteorological index currently in use Chuvieco (2003).

FMC of both live and dead material, is one of the important variables in fire ignition and fire behaviour modelling, and it is used in most fire danger rating systems (Yebra et al., 2007). FMC is inversely related to the possibility of ignition, due to the energy necessary to start a fire being used in the process of evaporation before a fire starts (Dimitrakopoulos & Papaioannou, 2001). Furthermore, FMC affects fire spread because of the presence of moist vegetation ahead of the fire front (Yebra et al., 2007). For instance, the Canadian Fire Weather Index uses the Canadian Forest Fire Behaviour Prediction (FBP) as part of the Canadian Forest Fire Danger Rating System (CFFDRS) (figure 2.2), and needs inputs on fuel type, weather, topography, foliar fuel moisture content and duration of the prediction (figure 2.3).

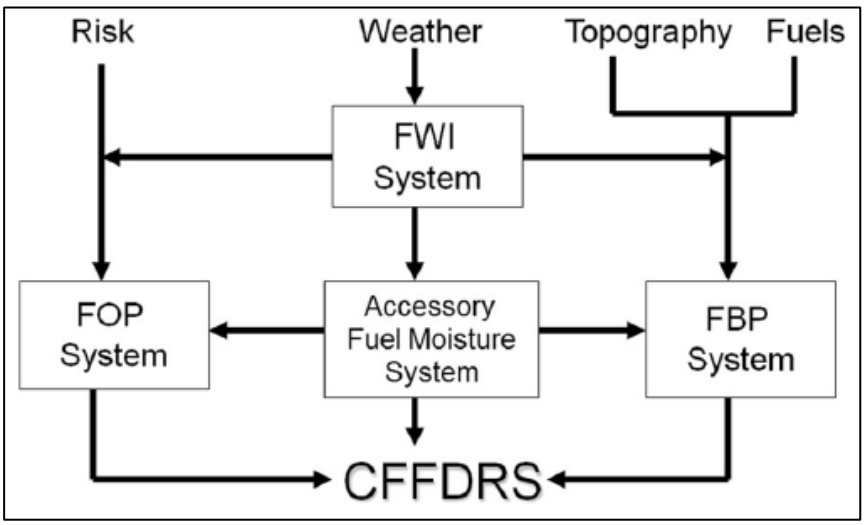

Figure 2.2: The Canadian Forest Fire Danger Rating System (Source: Wang et al., 2017).

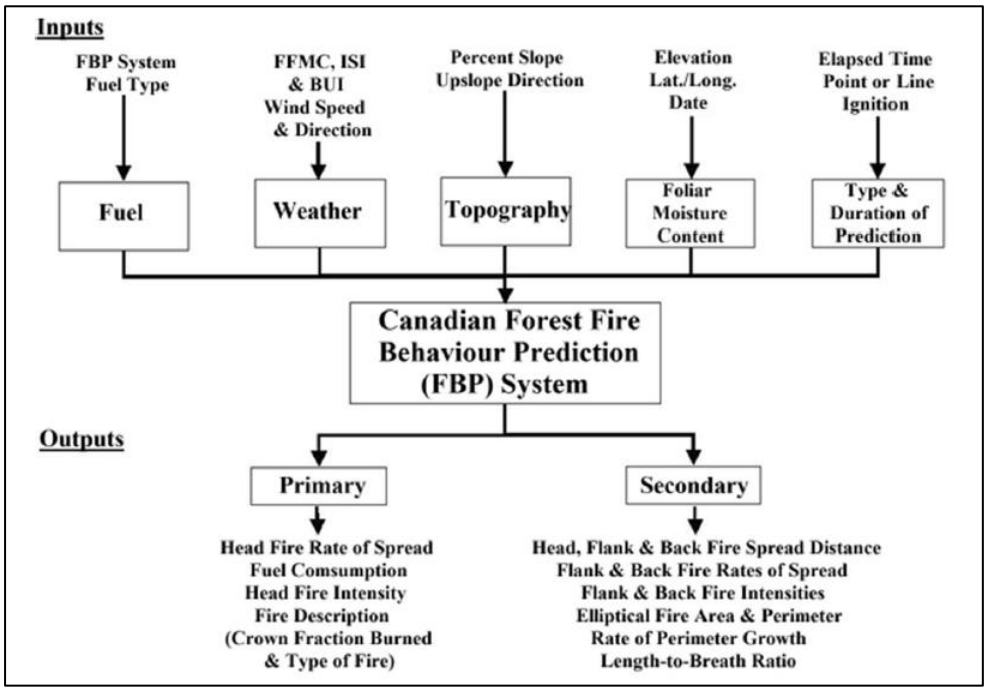

Figure 2.3: The Canadian Forest Fire Behaviour Prediction (FBP) System (Source: Wang et al., 2017).

However, FMC is not the only variable to consider in a wildfire risk system. There are also other variables affecting the probability of occurrence, such as socioeconomic factors. Consequently, modelling of all these variables will be required to provide spatial and temporal information on variations in fire danger rating levels (Lee et al., 2002).

Selected fire risk indices are utilized by forest fire administrations across Southern Europe and data from the European Commission is used to calibrate and validate the selected indices (Chuvieco, 2003). After forest fire services had become more accustomed to the risk maps, The Joint Research Centre (JRC) went on and developed forest fire forecasts. In order to achieve this data from the Action de Recherche Petite Echelle Grande Echelle (ARPEGE) model of Meteo France was utilized. By means of the EFFRFS (European Forest Fire Risk Forecasting System), the JRC offers fire risk forecasts for the next three days during the

season with high risk of fires, which is between the 1st of May and the 31st of October (Chuvieco, 2003).

Albertson et al. (2009) investigated the potential for fires under different conditions and times for Northern England using risk modelling. The modelling predicted fires during hot dry summers. Moreover, results revealed that climate change might shift the wildfire timings from a damper spring to drought-stressed summer. However, they also found that a small increase in temperature might not affect the risk of fire, given that the spring season starts earlier.

Albertson et al. (2010) examined the effect of climatic change on the number of wildfires occurring within the Peak District of Northern England. The simulations were generated by a Markov process model and then authenticated using baseline weather data. The results showed that wildfires will occur more frequently during summer, especially during reduced rainfall.

A two-tiered system reported UK wildfires until April 2009. This system was considered to be of a low standard because of its classification results (Kitchen, Marno, Legg, Bruce, & Davies, 2006). Now a new Web-enabled Incident Recording System (IRS) makes use of standard, consistent data records. There is in the UK a demand for consistency to improve the provision of fuller information, by Fire and Rescue Services (FRS) on wildfires, which include burned area and broad habitat type. Implementation of fire reporting and recording has traditionally been done locally. However, data quality and consistency has remained a concern. Geolocation of fires now has the possibility to produce more accurate spatial reporting and analysis (McMorrow, 2011).

2.3 Vegetation fuel properties

Fuel is considered an important aspect of the fire environment and some of its features can be changed by managing its composition or mass in the landscape (Fulé, Crouse, Cocke, Moore, & Covington, 2004). Properties of fuels contribute to the way fires break out, the production of air pollutants, and the energy generated. In addition, physical properties of fuel are significant factor for managing a fire. Such properties include moisture, size, loading, compactness, shape and fuel arrangement (Fulé et al., 2004).

2.3.1 Wildland vegetation fuel properties

Biological processes that are vital in controlling fuels are decomposition and deposition (referred to as litter fall/ fallen plant material). Fuel bed dynamics, fuel properties, and spatial distributions at scales from local to the landscape are governed by endogenous and exogenous disturbances with biomass deposition and decomposition and plant succession interactions (Ottmar, Sandberg, Riccardi, & Prichard, 2007). Fuels exist in various sizes, shapes and arrangements. These include are herb and shrub fuels, live and dead fuels, ladder fuels (small trees), twigs and branches, and canopy fuels (larger trees).

Any given fuel particle, type or component can be used to define wildland fuels as either dead or live. Dead fuel is composed of dead biomass that is mainly found beneath the canopy, while live fuel consist of living biomass (Keane, Gray, & Bacciu, 2012). Live biomass consists of vascular plants which are shrubs, trees and herbs, and can include lichens, mosses, and many other plant materials (Keane et al., 2012).

The main reason for this dichotomous stratification is to classify two different mechanisms that control both fuel dynamics and fuel moisture. Eco-physiological processes, including evaporation and transpiration and soil-water variations control live fuel moisture. Whereas

interaction of fuel physical properties such as density, size, and surface area dictate dead fuel moisture. In addition, shading of vegetation, climate, and topography make up the exogenous factors that affect dead fuel moisture. Dead fuels can be contained within some live fuel, for example, dead wood can be surrounded by live wood in trees (Jenkins, Page, Hebertson, & Alexander, 2012). The distribution of fuels across a fuel bed, or a landscape at coarser scales, governs fuel properties that are considered important to fire spread. The spatial scale of fire spread at the landscape level is important for fuel operations management and key in terms of designing fuel treatments (Agee & Skinner, 2005).

Heat, fuel, and oxygen are the three essential elements in the 'fire triangle' that can start a fire in any environment (Figure 2.4). They need to exist in the required proportions so as to allow a fire to develop. The combustion process requires oxygen due to its reactive property associated with the carbon content present in the fuel. Oxygen absence, will affect combustion in a suitable gaseous environment. Heat as a constituent has the role to excite combustion materials in the atoms of any available fuel (Moritz et al., 2005).

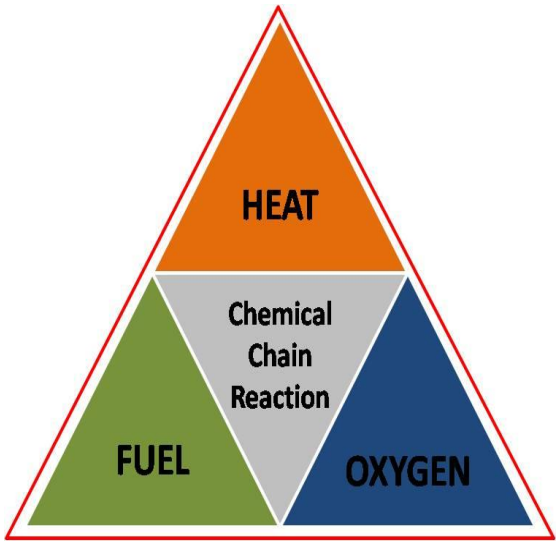

Figure 2.4: The fire triangle. (Source: Moritz, Morais, Summerell, Carlson, & Doyle, 2005)

2.3.2 Importance of fuel moisture content

Fuel moisture content, or FMC, is defined as the mass of water per mass of dry matter in the vegetation, and thus it is related to leaf water content and leaf dry matter content (Danson & Bowyer, 2004). It can be expressed using a percentage or fraction. Moreover, it can be measured for any tissue of the vegetation such as woody or herbaceous material (Maki, Ishiahra, & Tamura, 2004). FMC percentage values can exceed 100% where the dry mass is lower than the weight of water in the sample.

To understand how wildland fires are related to the structure, composition, and function of the landscape, it is essential to create fuel and fire pattern maps. This enables fire management and risk determination to be achieved from a perspective that takes into account the ecosystem characteristics. Such maps, created through modelling, could offer data that would identify the patterns and interactions between climatic and landscape parameters, which may lead to extensive fires (Rollins, Keane, & Parsons, 2004). FMC has great impact on whether a fire can ignite and how much it can spread. The level of moisture is an important element to take into account, as it can either facilitate or inhibit fire ignition (Yebra et al., 2013).

Santana and Marrs (2014) indicate that the flammability of fuel differs depends on the intrinsic characteristics of the species making up the fuel layer and these properties are also influenced strongly by their fuel moisture content. However, the probability of sustained ignitions varies across a wide range between 19 and 55% FMC (Santana & Marrs, 2014). When moisture levels are higher, fires will start more slowly, because the energy from high temperatures will initially lead to increased evaporation, thus leaving lower levels of energy to ignite the fire (Dimitrakopoulos & Papaioannou, 2001). FMC is also an essential variable to evaluate the subsequent behaviour of wildfires (Chuvieco, Riano, Van Wagtendok, &

Morsdof, 2003). Sandberg et al. (2001) indicates that dead fuels are composed of dead twigs and foliage, cured or dead grasses, litter, duff layers and branch wood. The moisture content of dead fuel depends on environmental conditions while in live fuel it depends on soil moisture and plant physiology (Figure 2.5).

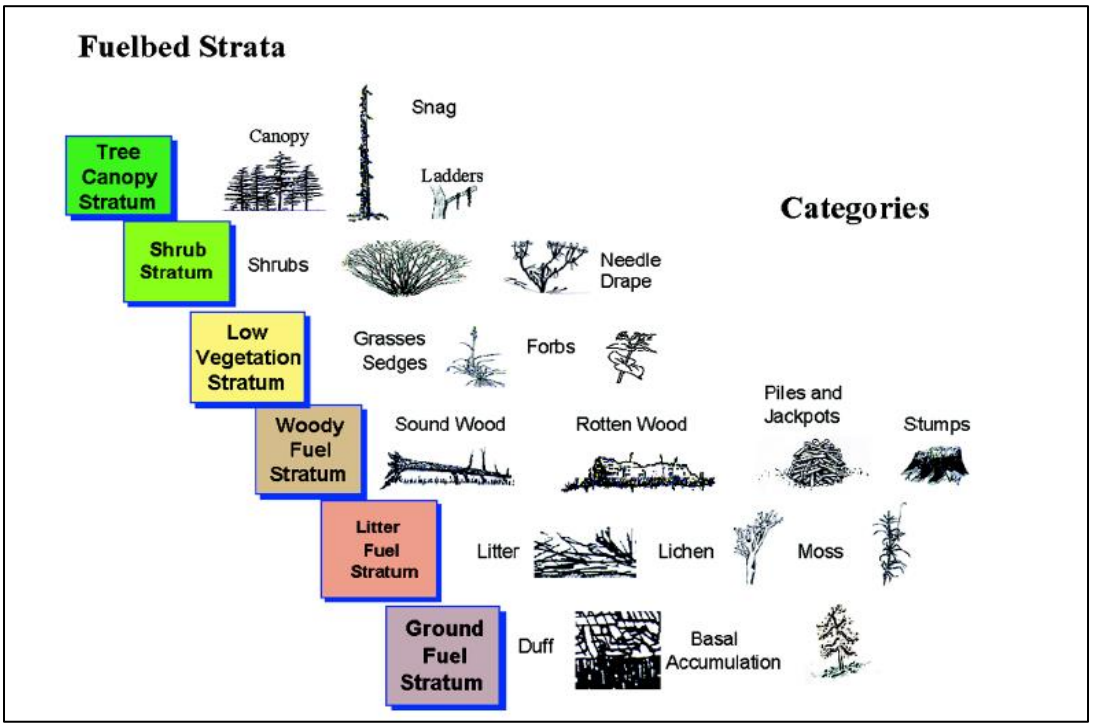

Figure 2.5: Fuel bed strata and categories (Source: Sandberg, Ottmar, & Cushon, 2001)

Dead fuels therefore depend more on atmospheric variables than live fuels. In field sampling, both dead and live FMC can be estimated from fresh and dry weights of vegetation samples (Danson & Bowyer, 2004).

Chuvieco, Riano, Aguado, and Cocero (2002) showed that FMC has an impact on combustion type due to the plant water content that acts as an inhibitor and may slow down the flaming process in vegetation. Even though fuel observations have represented an important element to determine fire risks, fire behaviour and spread patterns, the complexity

of how wildland fuels interact has not been fully explored (Sommers, Loehman, & Hardy, 2014).

2.3.3 Vegetation water content

Wildfires rely on the fuel present to support the fire. This fuel is made up of live or dead vegetation and be vulnerable to burning. Satellite technology may be used for the purpose of estimation of the characteristics of the fuel in the area being monitored (Ceccato et al., 2002). Research has shown that the mass of water in the vegetation is one of the important variables used in fire danger index and fire prediction models (Yebra et al., 2013). Recently, remote sensing technology has provided a means to monitor water content of vegetation over large areas with various spatial and temporal resolutions (Zhang et al., 2018).

In order to monitor vegetation water status, it is important to determine vegetation water content. This helps in the assessment of the risk of vegetation vulnerability to fire, and in vegetation fire mapping (Riaño et al., 2005). There are many terms that are used for the vegetation water content, including relative water content (RWC, %), equivalent water thickness (EWT, g/cm^2) and fuel moisture content (FMC, %) (Riaño, Vaughan, Chuvieco, Zarco-Tejada, & Ustin, 2005b). The relative water content is the ratio between the quantity of leaf water and the maximum quantity of leaf water at full capacity. The equivalent water thickness is defined as the ratio of the quantity of leaf water and the leaf area. Lastly the fuel moisture content is defined as the percentage of water weight over sample dry weight (Riaño et al., 2005b). Therefore, there is partial coupling of EWT and FMC, due to the fact that FMC is also affected by the dry matter in the leaves (Gao, Wang, Cao, & Gao, 2014).

2.3.4 Measured fuel moisture content

The moisture content of fuels is an essential variable in the assessment of fire danger. This is because it is strongly related to fire initiation and the potential of fire spread as discussed previously (Aguado, Chuvieco, Borén, & Nieto, 2007). There is an inverse relationship between the water content of fuels and the probability of ignition, because the energy that is necessary to initiate a fire is used up in the process of evaporation just before the flames start to take over. Conversely, the water content also has a serious effect on the fire propagation. This is because the source of the flames is decreased because of humid materials and this results in the reduction of flaming (Dimitrakopoulos & Papaioannou, 2001).

In the literature vegetation water content has been expressed as a percentage of the dry weight, this is usually referred to as 'fuel moisture content', (FMC) (Viney, 1991). FMC is determined through several methods. One of the methods is field sampling, and another is the standard fuel and meteorological indices. Field sampling is optimal as it provides very accurate FMC estimates (Aguado et al., 2007). A combination of two physical independent properties of vegetation determines FMC. One is the leaf equivalent water thickness (EWT) and the other is the leaf dry matter content (DM), both with units of g cm^{-2} (Eq. 2.1 and 2.2) (Danson, 2009).

FMC is expressed as:

$$\text{FMC } \% = \frac{\text{Wf -Wd}}{\text{Wd}} \times 100 \qquad (2.1)$$

Where (Wf) refers to the fresh weight of a vegetation sample and (Wd) refers to the dry weight of a vegetation sample. FMC is measured by looking of the ratio between dry matter and water content. This parameter is expressed as a percentage. In a situation where the leaf

water content is greater by weight than the leaf dry matter content, the FMC will be greater than 100% and *vice versa*. FMC may also be computed from:

$$\text{FMC } \% = \frac{\text{EWT}}{\text{DM}} \times 100 \tag{2.2}$$

Where (EWT) is leaf equivalent water thickness and (DM) is the leaf dry matter content.

According to Danson and Bowyer (2004), when the leaf dry matter is constant, either across the space or time, there is a direct correlation between leaf FMC and leaf EWT as shown by equation 2.2. Vegetation live FMC is highly variable when discussed either spatially and temporally because it is related to the interaction of plant physiology with the environment. The moisture in the soil and atmospheric conditions also come into play. It is hence very difficult to map FMC given that ground measurements cannot be acquired accurately at many places simultaneously (Chuvieco et al., 2002). Danson, Steven, Malthus, and Clark (1992) further studied this issue and used the already known physical relationships established between leaf EWT and spectral reflectance. These relationships were measured and tested in the near and middle-infrared, with the help of detailed laboratory-based experiments.

Several studies have been based on the fact that the relationship between FMC measured from field survey and vegetation indices have already been established (Danson et al., 1992). Remotely sensed images are used to drive this approach and have been used for the estimation of spatial and temporal variations in FMC (Yebra, Chuvieco, & Riaño, 2008).

2.4 Characterising vegetation with remote sensing

The assessment and monitoring of the Earth's surface is essential in the context of global change research. This means that researchers can be in a better position to forecast and estimate the future projections of environmental conditions (Jung, Henkel, Herold, &

Churkina, 2006). Similarly, it is imperative that the Earth's surface is carefully examined so that the forecasts can be made in an accurate manner. There are several influencing factors involved in global change research, including the technical assessment of managing natural resources, the influence of ever increasing CO_2 rates in the atmosphere, and the monitoring of vegetation cover change (Xiao et al., 2004). A remote sensing sensor can be a useful device for the acquisition of data about an object or scene in a remote manner, because all objects, including vegetation, have a spectral signature that serves as their identifier (Xie, Sha, & Yu, 2008).

2.4.1 Electromagnetic radiation

The physical quantity that can be successfully and conveniently measured with the use of remote sensing is electromagnetic radiation. Electromagnetic radiation is a form of energy which is capable of traveling through a vacuum (Hunt, 1980). However, like any other form of light, this energy becomes visible only after it has come in contact with physical matter. According to quantum theory, electromagnetic radiation can been viewed and defined as a stream of discrete particles, also called photons, which carry a fixed amounts of energy (Schowengerdt, 2006). Every time a molecule or atom falls from an excited energy state to a lower one such energy packets get released. In the same manner, electromagnetic radiation gets absorbed in proportion to the amount of energy that is required for promoting an atom or molecule from one energy state to a higher one (Schowengerdt, 2006). The same amount of energy is released when the atom falls from a higher energy state to a lower energy one. Optical and radar remote sensing frequencies and wavelengths can be used for the purpose of categorizing the types of radiation (Schowengerdt, 2006).

The optical domain stretches from around 0.4 to 14 μm and is the area in which passive remote sensing systems operate. This can be divided into two parts, a reflective and an

emissive part. The Earth's surface generally dominates the optical domain where wavelengths in excess of 5 μm represent most of the emitted radiation. TIR (thermal infrared) is the name that has been coined for this region (Giglio, Descloitres, Justice, & Kaufman, 2003).

A range of 2500 nm (at the maximum) is the signal that gets observed by the sensor when it is dominated by reflected solar radiance (Giglio et al., 2003). This reflective domain gets further categorized into the visible (0.4-0.7 μm), near infrared (0.7-1.3 μm) and shortwave infrared (1.3-2.5 μm). SWIR can be separated in two parts, based on the major atmospheric water absorption band at around 1.9 μm. (Justice et al., 2002).

2.4.2 Atmospheric interactions

Richter and Schläpfer (2002) show that different elements are responsible for the absorption or reflectance of incoming radiance by atmospheric gases, and that this is wavelength-dependent. The most important contributors to the process are:

(i) Ozone (O_3), absorbing part of the radiance in the blue and the ultraviolet.

(ii) Oxygen (O_2), responsible for increased absorption around 760 nm.

(iii) Carbon dioxide (CO_2) and water vapor (H_2O), that make the most important contributions to absorption at longer wavelengths.

The spectral bands used in remote sensing are positioned in atmospheric windows. Scattering and absorption have a combined effect that is related to the distance that exists between the Earth and the source of solar radiation (the Sun) and the position of the sensor (Liang, 2005). Martonchik, Bruegge, and Strahler (2000) show the combined effects of the atmospheric components in Figure 2.6. There are four major fluxes that can be distinguished from each other as follows:

(1) First is the path radiance which means that photons are scattered in the atmosphere between the ground and the sensor and reach the observation sensor without having first made contact of any sort with the ground.

(2) The second is the direct radiation coming from the Sun that falls on a target and then gets reflected and gets transmitted into the IFOV (instantaneous field of view) of the sensor.

(3) The third flux is the incident solar radiance that is incident upon a target and then gets reflected into the IFOV of that sensor. The global flux is the sum of direct and the diffuse flux that was incident on the surface.

(4) The fourth and the last flux is the adjacency radiance. This is the reflected radiation coming from the adjacent areas to the target that are scattered widely by the volume of air into the IFOV of the sensor.

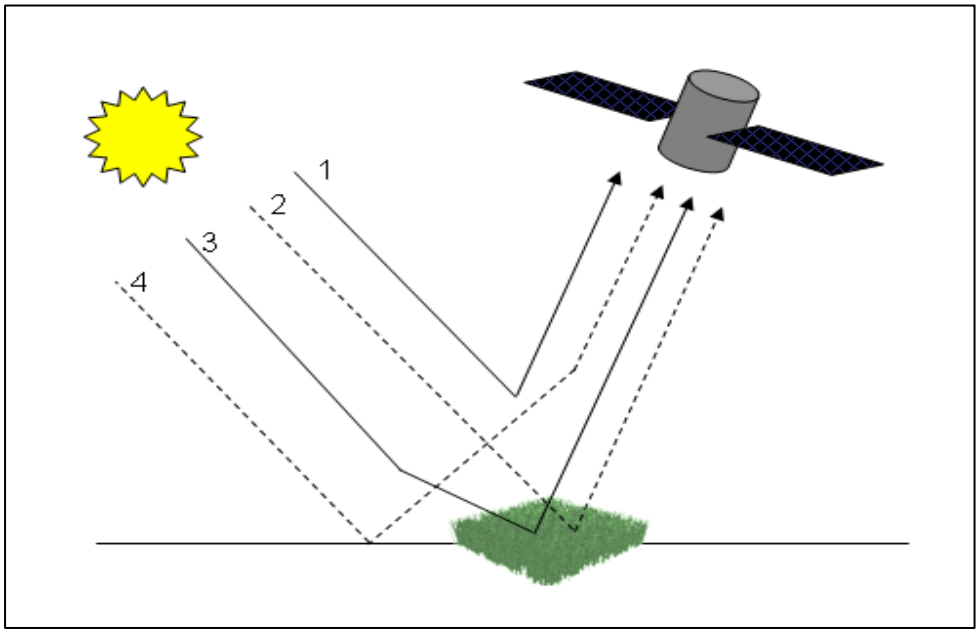

Figure 2.6: Schematic sketch of radiation components (Source: Richter, Bachmann, Dorigo, & Müller, 2006)

2.5 Remote sensing and vegetation biophysical properties

In order to drive a wide range of agricultural, ecological, and meteorological applications, there is need for accurate quantitative estimation of the properties of the vegetation (Houborg, Soegaard, & Boegh, 2007). The biochemical and biophysical characteristics of vegetation determine their remote sensing response (Turner, Cohen, Kennedy, Fassnacht, & Briggs, 1999).

2.5.1 Spectral properties of leaf and canopy

The tools for vegetation remote sensing have developed considerably in the past decades and optical remote sensing has expanded from the use of multi-spectral sensors to that of imaging spectrometers. Imaging spectrometry, or hyperspectral remote sensing, with sensors that typically have hundreds of narrow, contiguous spectral bands between 400 nm and 2500 nm, has the potential to measure specific vegetation variables that are difficult to measure using conventional multi-spectral sensors (Kennedy et al., 2009). In general, current remote sensing approaches to estimate vegetation biochemical and biophysical parameters include statistical and physically-based models. Both models (statistical/physical) have been used widely for estimating biochemical and biophysical parameters in agricultural and forestry environments with multi-spectral remote sensing data (Atzberger, 2004).

2.5.1.1 Leaf reflectance

Scattering and absorption are the two key processes that occur when solar radiation is incident upon a leaf. The scattering process is further categorized into transmission through the leaf and reflectance from the leaf (Figure 2.7) (Milton, 1987). Light absorption takes place when incoming solar radiation is absorbed within a leaf. The quantity of absorbed light is affected by the photons' energy or wavelength (Milton, 1987). Shorter wavelength photons take part in photochemical reactions, such as photosynthesis. On the other hand,

longer wavelength photons impact the energy balance of the leaf such as transpiration, heating and evaporation. Therefore, variation in the amount of light absorbed in a plant issue is induced by variations in concentration of tissue water content and leaf pigments (Carter & Knapp, 2001).

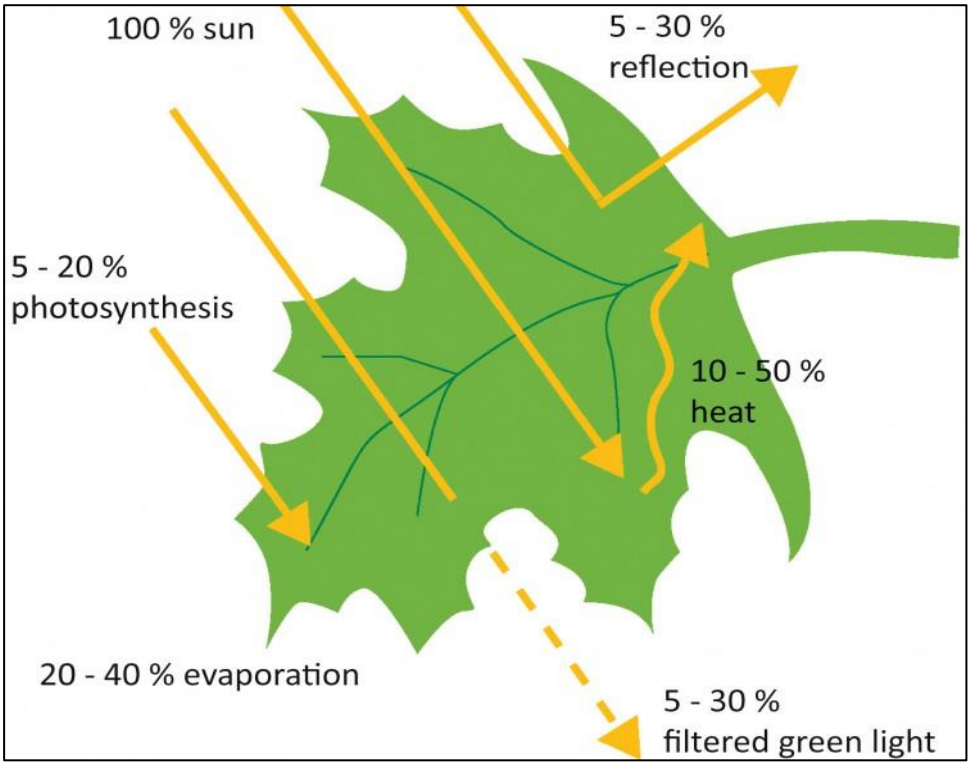

Figure 2.7: Scattering and absorption by leaf surface. (Source: Taiz and Zeiger, 2002)

In the visible region, pigments such as xanthophyll, carotene, and chlorophyll a and b dominate the absorption. In the NIR region, absence of absorbing media results in low absorption and high reflectance. In the MIR region, concentration of water in the tissue and leaf structure affects absorption. At 1450nm and 1950nm, strong water absorption takes place (Figure 2.8) (Hardisky, Klemas, and Smart (1983)

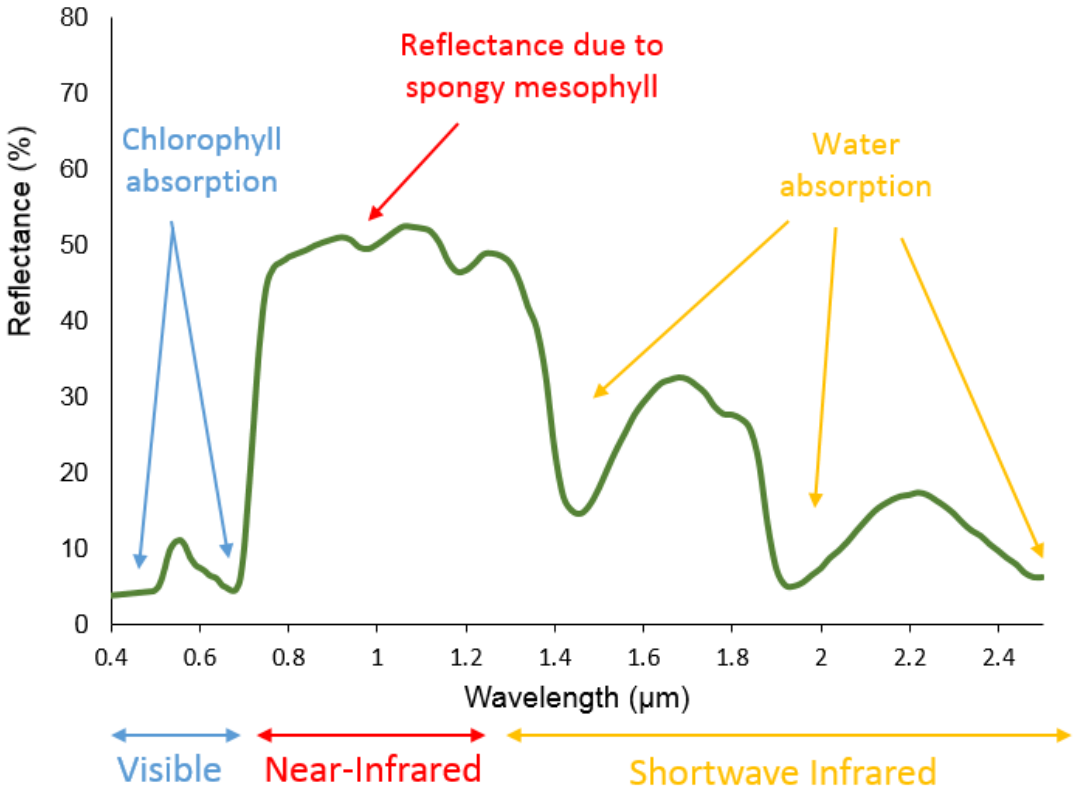

Figure 2.8: Leaf reflectance along the electromagnetic spectrum (Source: Humboldt State Geospatial Online, 2015).

The reflectance of leaves across the spectrum is affected by their internal structure. Consider the example of visible light which is reflected at the cell air-wall interface of the spongy layer and palisade of the mesophyll in the leaf (Figure 2.8). The whole spectrum is affected by the effects of the structure of the mesophyll and this is highly significant for the NIR where absorption by water and chlorophyll is negligible (Jacquemoud, Baret, Andrieu, Danson, & Jaggard, 1995).

Between 1000–2500 nm, the reflectance spectra of green plants is controlled mainly by liquid water and the bio-chemical components of a leaf, such as lignin, cellulose and protein (Gao & Goetz, 1994). Vegetation interacts with solar radiation and displays strong absorption features in wavelengths where different plant materials, water content, pigment,

carbon content, nitrogen content, and other properties cause variation. These variations provide information on plant health and water content using vegetation indices (VI) (Pfitzner, Bartolo, Carr, Esparon, & Bollhöfer, 2011).

2.5.1.2 Canopy reflectance

The vegetation canopy is a key example of a complex structure in which there is an assortment of various plant parts and leaves arranged in numerous planes, soil and other materials. As a result of this complex structure, when light is reflected from a canopy, it becomes a complex amalgamation of transmitted and reflected energy (Colwell, 1974).

According to (Asner, 1998) as the depth of a canopy increases the amount of reflected visible radiation is reduced to a great extent. Moreover, decreased radiation inside the canopy further lowers the canopy reflectance as compared to that of a single leaf. The optical signal at canopy level is based on the structure of the canopy, the optical features of the leaf, solar zenith angle, solar azimuth angles and the sensor position (Hatfield et al., 1985).

The structural properties and leaf level optical properties of a canopy, such as leaf area index, leaf size, and leaf orientation angles, all have an effect on canopy level reflectance (Williams, 1991). In vegetation spectra, the absorption characteristics are interlinked to biochemical compounds that are almost the same in all plant species. Therefore, information related to a plant canopy cannot be found from absence or presence of a particular absorption characteristic, rather, it is given by the comparative intensity of numerous absorption characteristics (Gao & Goetz, 1994). The key spectral absorption characteristics are caused by the presence of water and plant pigments, and the minor absorption characteristics are caused by sugars, cellulose, starches, proteins and lignin (Carter & Knapp, 2001).

One of the main variables controlling biophysical processes in a vegetation canopy is known as the Leaf Area Index (LAI). This index is linked to production of plant's biomass, rainfall interception, canopy micro-climate, radiation index and water and carbon exchange (van Wijk & Williams, 2005). LAI is the combined one-sided area of leaf tissue per unit ground surface area [LAI = leaf area / ground area, m^2/m^2] (Bréda, 2003). The common procedure for estimating LAI is to harvest vegetation in a particular area and calculate the one-side leaf area directly. It is used to estimate vegetation productivity, evapotranspiration and photosynthesis and depends on the composition of vegetation, season, site conditions and the stage of plant development (Fan, Gao, Brück, & Bernhofer, 2009).

Leaf Angle Distribution (LAD) is the parameter that affects the biophysical interaction of light with vegetation canopies (McNeil, Pisek, Lepisk, & Flamenco, 2016). Environmental factors such as light, water, nutrient supply and stress, in addition to genetic properties of vegetation, contribute to variations in canopy structure. LAD is important for measuring canopy properties using remote sensing (Müller-Linow, Pinto-Espinosa, Scharr, & Rascher, 2015). The capability to simulate the microclimate and surface energy balance within the plant canopy is dependent upon precise simulation of radiation exchange within the canopy. Accurate simulations of radiation require some assumptions about leaf angle distribution to calculate reflectance, transmissivity and scattering of radiation. The ellipsoidal LAD can approximate real plant canopies but requires complex integrations for several combinations of leaf area index, incident radiation angle, and density function (Flerchinger & Yu, 2007).

The surfaces of leaves have non-Lambertian transmittance and reflectance properties (Walter-Shea & Biehl, 1990). This means that radiant energy is not transmitted or reflected equally in all directions. Therefore, leaf properties vary with the angle of illumination and angle of view. The essential and intrinsic property that controls the behaviour of a scene

component and characterizes surface reflectance is known as the Bi-directional Reflectance Distribution Function (BRDF) (Walter-Shea & Biehl, 1990). This function is defined in terms of the source incidence direction (zenith and azimuth angles) and the direction of view angle. The BRDF cannot be measured directly because the infinitely small component of solid angle does not include a measurable quantity of radiant flux. Thus, real measurements that estimate the BRDF include the integration of the flux over finite solid angles that define the source and view directions (Figure 2.9). This integration produces the 'reflectance factor' that is actually determined in most field measurements (Walter-Shea & Biehl, 1990).

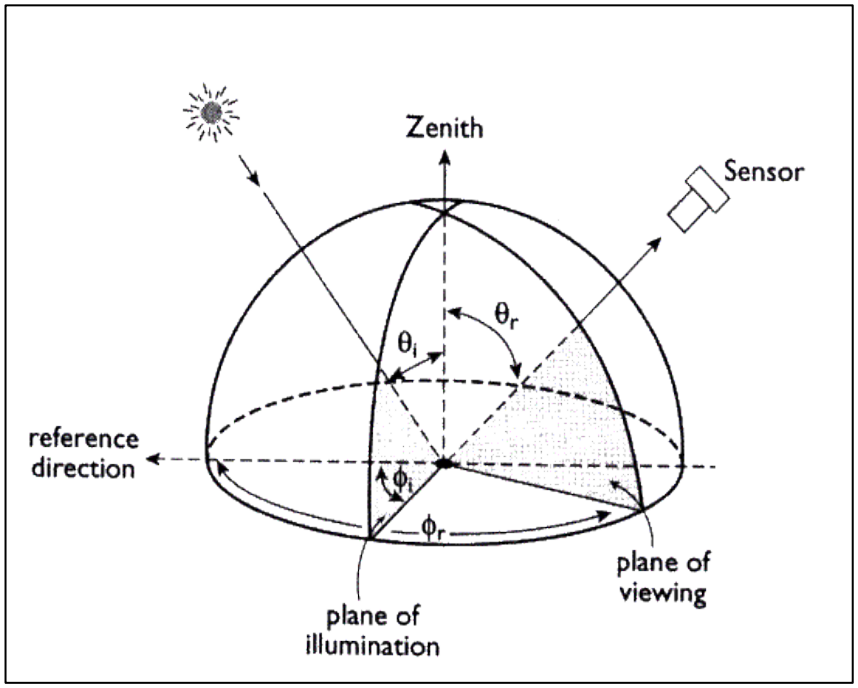

Figure 2.9: Model of the Bi-directional Reflectance Distribution Function (Source: NCAVEO, 2006).

The Bi-directional Reflectance Factor (BRF) is mostly used to describe the BRDF. It is defined as the ratio of radiant flux that is actually reflected by a sample surface on which it would be reflected in the same reflected beam by an ideal, perfectly diffused (Lambertian) standard irradiated in exactly the same way as the sample (Bruegge et al., 2004). It can be

measured using a calibrated reflectance panel (biconical mode) or a cosine-corrected receptor (cos-conical mode). Various techniques have been developed using hand-held radiometers to accurately measure the spectral directional reflectance of vegetation (Milton, 1987).

2.5.1.3 Soil reflectance

A range of factors including water content, mineral content, surface roughness and organic matter content affect the reflection of solar radiation from a soil surface. These factors vary across space and are complex. The solar radiation incident on soil is both absorbed and reflected by it. The radiation reflected from soil is further affected by viewing angle and wavelength. Generally, soil reflectance in the visible region is half that in the NIR region (Barrett, 2013). The findings of Whalley, Leeds-Harrison, and Bowman (1991) show that soil particle size is inversely proportional to reflectance. They also showed that an exponential decrease was observed in reflectance when, in a sandy loam soil, the water content was increased. However, the reflectance values were higher for sandy loam soil compared to clay soil and soil reflectance was determined by its primary minerals.

Organic matter present in the soil is comprised of decomposed materials to make a complex mixture known as humus, which is comprised of 65 – 75% of organic matter by weight in mineral soils. Organic matter can either exist in the form of a discrete soil substance or with mineral particles. It also binds particles throughout the soil. No matter how low the content is, organic matter greatly impacts properties of mineral soils including their reflectance, structure, water capacity and fertility (Schnitzer, 1982).

In the case where organic matter is more than 2%, then the reduction in organic matter conceals various absorption characteristics of the soil spectra. Additionally, decomposition

of organic material is interlinked to the reflectance spectra of organic soil (Figure 2.10) (Schnitzer, 1982). Lusch (1999) shows that the reflectance is affected by the extent of smoothness of the soil surface. For instance, the same amount of light is reflected by a dry rough soil surface as when a soil surface is wet and smooth. Moreover, the amount of shadow produced at the surface of the soil is impacted by the distribution and arrangement of particle sizes (Lusch, 1999).

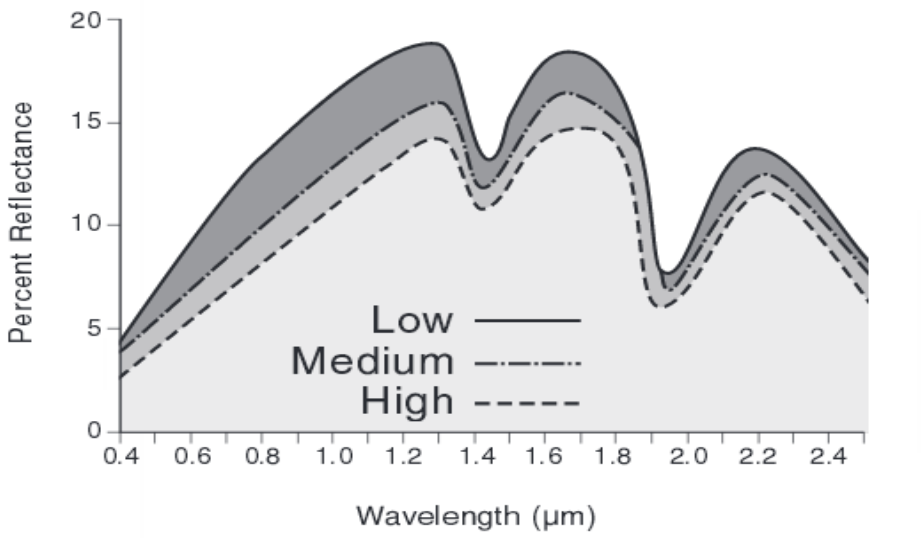

Figure 2.10: Spectral response to organic matter content. (Source: Lusch, 1999)

2.5.2 Vegetation Indices

For the assessment of biomass, water use, plant stress, plant health and crop production, remotely sensed spectral vegetation indices (VI) have been widely used (Jackson & Huete, 1991). An understanding of the way the architecture and the external environment of the vegetation canopy influences VI is also required for the effective use of these indices. There is no doubt that vegetation indices are well developed for the purpose of extracting the plant signal, from the soil background, the condition of moisture, the zenith angle of the sun, the view angle and lastly, and importantly, the atmosphere (Jackson & Huete, 1991).

The radiant flux that emanates from the surface of the Earth comprises spectral components that carry much useful information regarding the physical properties of soil, water, and vegetation features in the environments. More than one hundred vegetation indices have been established over the past four decades for the purpose of the enhancement of vegetation response and for the purpose of minimizing the effects of the features stated above (see appendix I for details) (Bannari et al., 1995; Hunt, Ustin, & Riaño, 2013; Xue & Su, 2017).

According to Jackson and Huete (1991) when an area that is covered with vegetation is considered the optical properties of this area evolve greatly and steadily with the passage of time. Factors affecting the reflectance of vegetation such as water content, leaf thickness, chlorophyll and leaf distribution in the canopy, affect the VI (Bannari et al., 1995).

From the long list of VI, shown in Appendix I, the NDWI and MSI are two widely used vegetation indices particularly for vegetation water content estimation. The NDWI has demonstrated potential to retrieve canopy water content of natural vegetation and irrigated fields, and it has been used by many researchers (Danson & Bowyer, 2004; Dawson, Curran, & Plummer, 1998; Serrano, Ustin, Roberts, Gamon, & Penuelas, 2000).

The NDWI is devised to be sensitive to vegetation water content and less sensitive to the effects of the atmosphere (Gao, 1996), and is therefore an appropriate water absorption index for monitoring live fuel moisture content (Dennison, Roberts, Peterson, & Rechel, 2005; Wang, Qu, Hao, & Zhu, 2008). MSI is a simple ratio of the reflectance in short-wave infrared, which is sensitive to water content and to the reflectance in the near-infrared, which is sensitive to changes in leaf internal structural (Hunt & Rock, 1989; Hunt, Rock, & Nobel, 1987). When the same NIR and SWIR wavebands are used, there is a functional relationship between NDWI and MSI.

2.5.2.1 Normalized Difference Water Index (NDWI)

The Normalized Difference Water Index (NDWI) is a satellite-derived VI using Near Infrared (NIR) and Short Wave Infrared (SWIR) channels. The SWIR reflectance reflects changes in both the vegetation water content and the spongy mesophyll structure in vegetation canopies, while the NIR reflectance is affected by leaf internal structure and leaf dry matter content, but not by water content. The combination of the NIR with the SWIR removes variations induced by leaf internal structure and leaf dry matter content, improving the accuracy in retrieving the vegetation water content (Ceccato et al., 2001). Satellite based indices have proven to be an effective way for drought monitoring and its usefulness for early warning has been demonstrated in different studies (Amalo, Ma'rufah, & Permatasari, 2018). Gao (1996) proposed two near-IR channels; one centred at 860 nm, and the other at 1240 nm (Eq. 2.3)

$$NDWI = \frac{NIR1 - NIR2}{NIR1 + NIR2} \tag{2.3}$$

2.5.2.2 Moisture Stress Index (MSI)

The Moisture Stress Index (MSI) is a vegetation index sensitive to moisture stress. It was originally developed by (Rock, Vogelmann, Williams, Vogelmann, & Hoshizaki, 1986) based on the Landsat Thematic Mapper Near Infrared (NIR) and short wave infrared (SWIR) bands, and is sensitive to moisture changes in vegetation. It was developed to compare one area of a scene to another for satellite sensor analyses. Hunt & Rock (1989) recommend the wavebands in the NIR around 800 nm and in the SWIR around 1600 nm (Eq. 2.4).

$$MSI = \frac{SWIR}{NIR} \tag{2.4}$$

2.5.3 Remote sensing of vegetation moisture content

Most vegetation targets are a mixture of components like leaves and other plant structures, as well as the background and shadow. Based on the incidence angle of the source of the radiation there are several angles from which these components can be illuminated. Because of this, there is a variation in radiance. Furthermore, the area that has been projected for each component when it is illuminated, and zenith viewed greatly depends on the zenith angle of the sun. Radiance also varies with the sensor view angle and the azimuth between the illumination and view angles (Gonzalo, Martinez, Arquero, & Ormeno, 1997).

The evaluation of vegetation, water, soil and materials are the most commonly derived using spectral information across the VIS-NIR-SWIR (Elvidge & Chen, 1995). There are a number of factors that influence the reflectance of leaves (e.g. water content, leaf thickness, chlorophyll, cellular structure and other biochemical) and this becomes even more important when plant and environmental interactions are included (Blackburn & Ferwerda, 2008).

The estimation of vegetation FMC is based on the physical relationship between leaf water content and spectral reflectance in the near- and middle-infrared (Danson et al., 1992). The basic foundation of vegetation fuel moisture content, when it is to be estimated using spectral reflectance, is that it is sensitive to the ratio the reflectance in the near infrared (NIR: 700-1300nm) and the short-wave infra-red (SWIR: 1300-2500nm) (Gao, 1996).

These wavelengths are influenced by changes in vegetation water content as described earlier. The incorporation of vegetation spectral reflectance in the regions of NIR and SWIR regions are required for making quantitative estimation of vegetation in a pigment-independent manner (Danson, 2009). According to Tucker (1980) the absorption features of liquid water in the leaves of plants are very visible and can be easily detected. The amount

of leaf water contained in these bodies can be measured through the use of spectroscopy. The basis of numerous remote sensing indices is the spectral reflectance at about 1240 and 1650 nm. Liquid water has absorption features in the near infrared and the shortwave infrared wavelengths, and these are readily identified in the spectral reflectance (Hunt et al., 2013). The basis for water content estimation is that the amount of water in the canopy affects the ratio of NIR to SWIR reflectance (Hunt et al., 2013).

The launch of the Landsat 8 OLI and Sentinel-2A MSI sensors provide an opportunity for vegetation monitoring with increased temporal frequency (Mandanici & Bitelli, 2016). The Landsat 8 OLI has a spatial resolution of 30 m for bands 1 to 7 and 9 (Barsi, Lee, Kvaran, Markham, & Pedelty, 2014), while Sentinel-2A MSI has finer spatial resolution (10, 20 and 60 m) and more spectral bands (13 bands from 443 to 2190 nm) (Van Der Werff & Van Der Meer, 2016). Landsat 8 OLI and sentinel 2A MSI have repeat coverage every 16 days and 10 days respectively (Zhang et al., 2018). The combination these sensors will allow high frequency of observation.

Gao (1996) indicate that the normalized difference water index (NDWI) can be derived using band 2 (841–876 nm) and band 5 (1230–1250 nm) of the Moderate Resolution Imaging Spectrometer (MODIS) data to retrieve vegetation water content. Both Landsat 8 OLI and Sentinel 2A MSI do not have a spectral wavelength near 1240 nm, however, the SWIR waveband around 1610 nm can be used as a replacement (Piragnolo, Lusiani, & Pirotti, 2018; Sakowska et al., 2015). Thus, both Landsat 8 OLI and Sentinel 2A MSI can be used to derive NDWI and MSI values across a landscape.

2.6 Radiative Transfer Models

Radiative transfer is the physical phenomenon of energy transfer in the form of electromagnetic radiation. The propagation of radiation through a medium is affected by absorption, emission, and scattering processes (Liu & Weng, 2006). Radiative Transfer Models (RTMs) calculate the flow of radiation through a plant canopy or planetary atmosphere (Liu & Weng, 2006). Radiative transfer models have greatly helped in the development of understanding about how light can be intercepted by plant canopies right from the beginning of optical remote sensing. They have also helped in the interpretation of reflectance in terms of vegetation biophysical characteristics, making use of the physical principles that they are based on, namely the absorption and scattering in different media (Jacquemoud et al., 2009).

There are many different radiative transfer models that have been developed and used to estimate vegetation structural and biochemical parameters (Table 2.3). There is a link required between the spectral variation and canopy reflectance, which is related to the leaf biochemical components, and the BRF variation. The variation is primarily related to the architecture of the canopy and the contrast between the soil and the vegetation (Jacquemoud et al., 2009).

With the use of radiative transfer theory, mathematical models are built to describe the reflectance behaviour of a canopy. Here the leaf model outputs are combined with the canopy such that there is a relationship between leaf and canopy variables and the fate of radiation. These are the properties that are modelled based on the radiative transfer model PROSPECT (Verhoef, 1984). Here, the leaf model outputs leaves are combined into are combined with the canopy radiative transfer model SAIL.

The combined model is called PROSAIL and it can effectively simulate the reflectance of a vegetation canopy in the range 400 nm to 2500 nm (Figure 2.11) (Verhoef, 1984).

Table 2.3: Types of model to simulate vegetation reflectance

Model	Using for	Author and Year
SUIT Model	For a homogeneous canopy	Goel and Strebel (1983)
SAIL Model	Canopy reflectance	Verhoef (1984)
PROSPECT Model	Determines leaf reflectance and transmittance signatures in the optical domain	Jacquemoud and Baret (1990)
FLIM model	To model forest canopies	Rosema, Verhoef, Noorbergen, and Borgesius (1992)
PROSAIL Model	Combined PROSPECT leaf optical properties model and SAIL canopy bidirectional reflectance model	Baret, Jacquemoud, Guyot, and Leprieur (1992).

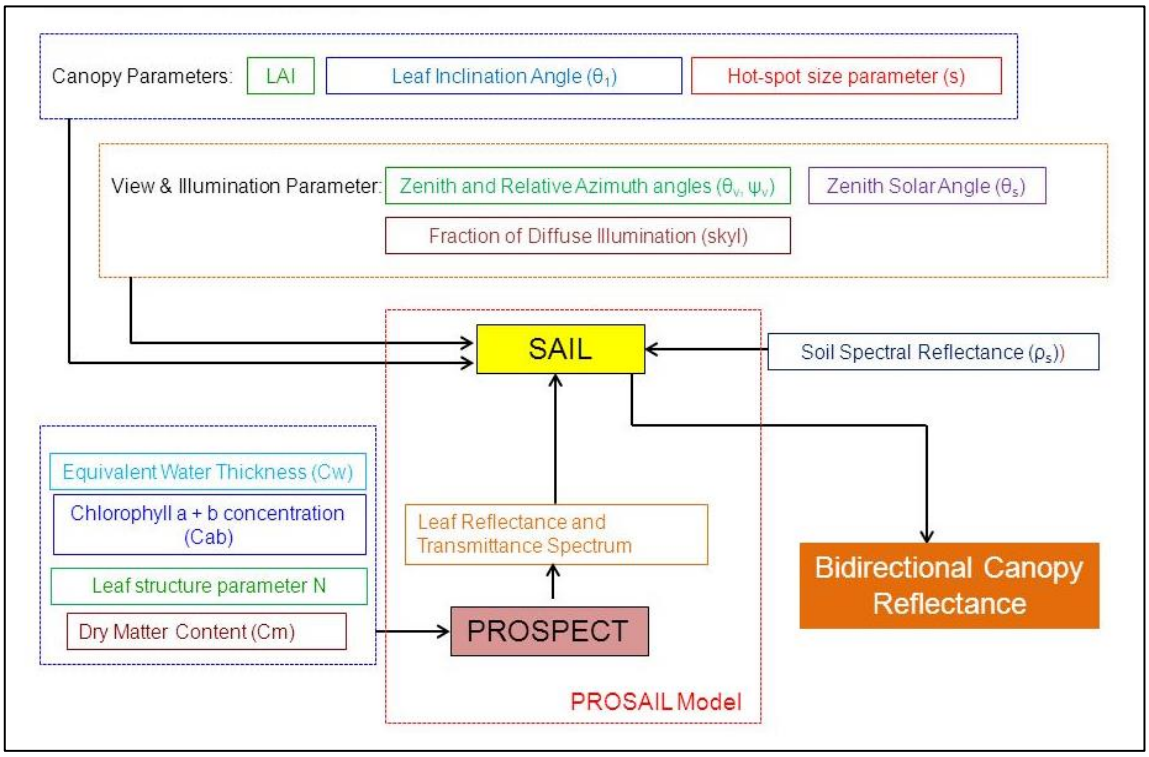

Figure 2.11: Input parameters for Radiative Transfer models PROSPECT and SAIL (Source: Nisha Upadhyay, 2016).

2.6.1 Scattering by arbitrary inclined leaves (SAIL) model

SAIL is one of the earliest canopy reflectance models and is an extension of the SUIT model. It uses the fraction of leaves at discrete leaf inclination at discrete angle distribution. SAIL considers the canopy as a horizontal, homogeneous, turbid, and infinitely extended vegetation layer composed of diffusely reflecting and transmitting elements. SAIL is a physically-based radiative transfer model used for simulating the BRF spectra of canopies under different viewing directions. The eight variables used as input to the SAIL canopy BRF are:

Structural canopy parameters [LAI, mean leaf inclination angle (θ1), hot-spot size parameter (s)], measurement configuration [zenith and relative azimuth viewing angles (θv, ψv), zenith solar angle (θs)], fraction of diffuse illumination (skyl), and soil spectral reflectance (ρs) (Verhoef, 1984).

2.6.2 Model of leaf optical properties spectra (PROSPECT)

The PROSPECT model describes the optical properties of plant leaves from the visible (400 nm) to the shortwave infrared (2500 nm). It is based on representation of the leaf as one or more absorbing plates with rough surfaces giving rise to isotropic scattering. The plate model of Allen, Gausman, Richardson, and Thomas (1969) states that the interactions that take place between electromagnetic radiation and a leaf depend on the physical characteristics of the leaves. Absorption is caused by the interaction between incoming light and substances within the leaf such as water, chlorophylls a and b, carotenoids, brown pigments and other accessory pigments. It can readily be coupled with SAIL to facilitate direct modelling of the impact of chlorophyll, water and leaf dry matter constituents on the reflectance of a complete plant canopy. The inputs to PROSPECT to derive leaf reflectance and transmittance signatures in the visible spectrum are:

Leaf structure parameter (N), chlorophyll a + b concentration (Cab) (µg/cm^2), equivalent water thickness (Cw) (cm), and dry matter content (Cm) (g/cm^2) (Jacquemoud & Baret, 1990).

2.6.3 PROSAIL model

The PROSAIL canopy reflectance model was developed by linking the PROSPECT leaf optical properties model and the SAIL canopy bidirectional reflectance model (Jacquemoud et al., 2009). It has been used to study plant canopy spectral and directional reflectance in the solar domain. Also, been used to develop new methods for retrieval of vegetation biophysical properties (Jacquemoud & Baret, 1990).

PROSAIL uses 14 input parameters to define leaf pigment content, leaf water content, canopy architecture, soil background reflectance, hot spot size, solar diffuse radiation fraction, and solar geometry. Based on these inputs, the model calculates canopy bidirectional reflectance from 400 to 2500 nm in 1 nm increments (Jacquemoud et al., 2009). PROSAIL is used in this research to simulate the relationships between FMC and VI (NDWI and MSI).

2.7 Conclusion

Most studies on the estimation of FMC have focused around spatial and temporal variations in FMC in various environments utilizing both field estimations and remote sensing methods. These studies have generally used VI to develop relationships with remotely sensed data. Few of these studies have looked in detail at the spectral factors that contribute to the relationship between FMC and spectral measurements and even fewer at measurements and modelling specific for shrubland vegetation.

Some studies have assessed the spatial-temporal variation of fuel characteristics at landscape scale based on spectral reflectance measurements, and have mapped FMC in different environments such as in Spain, California and moorlands in the UK, but never have looked at large areas of around 1000 km^2. These studies generally used remote sensing for mapping the spatial and temporal dynamics of vegetation FMC over small areas but in this research, the focus on will be scaling-up FMC to pixel size measurements over large areas.

The lack of such studies on the upland areas of the UK, is one motivation for the research described in this thesis. This research will combine theoretical modelling of the relationship between spectral data and moisture content with both laboratory and field measurements. It will employ time-series satellite imagery to map these relationships at landscape scale. It will use these finding to assess the role of remote sensing in vegetation fire risk assessment in the UK.

CHAPTER 3: LABORATORY EXPERIMENT AND RADIATIVE TRANSFER MODELLING

Summary

This chapter investigates the relationships between spectral reflectance and vegetation FMC and how vegetation indices may be related to vegetation characteristics. Small samples of *Calluna vulgaris* were brought from the study area for measurement using an ASD Fieldspec Pro Spectroradiometer in a dark room prepared in advance for this purpose. Three laboratory experiments assessed effects of the fuel moisture content, soil background and solar zenith angle on the canopy reflectance measurements. In the second part of the chapter a radiative transfer model is used to further explore these relationships and make comparisons with the results from the laboratory

3.1 Introduction

This chapter explores the relationships between vegetation canopy properties and spectral reflectance in a series of laboratory experiments, specifically investigating the effects of fuel moisture content (FMC), soil background, and solar zenith angle on spectral reflectance. Remote sensing of vegetation is based on the measurement of electromagnetic radiation fluxes reflected or emitted by the canopy. The observed signal is the combination of scattering, absorption, and emission processes that take place in the atmosphere and on the surface materials found within the field-of-view of the sensor. In order to interpret remote sensing observations, it is also possible to use computational tools like radiative transfer models (RTM). These can be used to predict the spectral transmission of the atmosphere, the light reflected or emitted from a plant canopy, and the amount of energy absorbed or emitted by different vegetation structures. In this chapter a RTM was used to extend the laboratory experiments to assess the sensitivity of the spectral reflectance to the range of measured variables.

Three hypotheses were proposed to examine the relationships between spectral reflectance and vegetation fuel moisture and how vegetation indices may be related to those characteristics. The hypotheses tested in the laboratory experiment were used to answer three questions which were:

(i) What is the relationship between canopy fuel moisture content and spectral reflectance?

(ii) How does soil moisture affect the relationship between canopy reflectance and fuel moisture content?

(iii) How does solar zenith angle affect the spectral reflectance?

3.2 Laboratory experiments

3.2.1 Preparation of vegetation samples

Calluna samples were collected from the Burbage Moor study area (describe in detail in the next chapter) by taking selected individual plants in July 2016 for use in the laboratory experiments. Samples were stored in airtight plastic bags to avoid loss of moisture and keep samples cool during transport to the laboratory. The samples were replanted in black 13 cm diameter pots in order to prepare them for the measurements. The samples were healthy, fresh and no irrigation was applied. One sample canopy was used in the experiment to measure fuel moisture content, a second sample was used to investigate the different soil background effects, and a further one for testing the effects of different solar zenith angles. For the FMC experiment, one canopy was used for the spectral measurements and a second 'near-identical' canopy used for destructively sampling FMC. The canopies were kept in the same conditions throughout the experiments.

3.2.2 ASD measurement protocol

The laboratory measurements were conducted at the University of Salford which has a purpose-built spectroscopy laboratory. Black curtains were used to cover six windows of the room which was used as a darkroom for spectral measurements to decrease the influence of light from other sources which may create some noise in the measurements. The support frame for the ASD was built on a table with the fibre optic pistol grip attached to a wooden stand at a height of 55 cm, with a 1 m-long fibre optic cable and lens with 8° field of view, so that there was enough space for the height of the container (approximately 30 cm) between canopy and lens. Illumination was provided by a tungsten-halogen 1000W lamp, which was set up on a tripod at the side of the table at a height of 65 cm, this was approximately 40 cm above the plant to provide sufficient light for accurate spectral measurements but without heating the canopy as shown in Figure 3.1.

A digital inclinometer was used for setting the illumination zenith angle at 45° during most of the measurements of the samples to ensure even distribution of radiation on the canopy (Figure 3.1). A calibrated reference panel (white panel) was horizontally positioned on a wooden holder at distance 30 cm from the canopy so that the diameter of the 'ground area' seen by the sensor was 4 cm with the 8° lens attached. The incident radiation on the panel was measured with every set of sample reflectance measurements. The small canopies of *Calluna* were placed under the wooden holder, and the centre point of the canopy was aligned using a thin thread hanging down from the lens.

Before starting the measurements, the ASD was warmed up for at least 30 min because the three spectrometer arrays warm up at different rates once they have been powered up which can result in spectral variations during the measurements. The ASD files were processed

using ViewSpec Pro, and the files converted into ASCII text files to be readable in Excel. The ASCII files were then saved in the output directory and inserted into Excel for analysis.

Following Zhang et al. (2018) the NDWI was calculated using Sentinel 2A MSI NIR b8a and SWIR b11 centred on wavelengths at 865 and 1610 nm respectively (see section 2.5.3). In order to calculate NDWI and MSI using simulated sentinel 2A datasets the ASD data were convolved with spectral response function for band8a and band11. The average of five spectral measurements, with the canopy rotated before each measurement, were used to calculate NDWI (equation 3.1) and MSI (equation 3.2).

$$\text{NDWI} = \frac{R_{865} - R_{1610}}{R_{865} + R_{1610}} \tag{3.1}$$

$$\text{MSI} = \frac{R_{1600}}{R_{865}} \tag{3.2}$$

where R_λ is the calibrated reflectance at wavelength λ

The first derivative of canopy reflectance was computed for each experiment because it is insensitive to variations caused by factors such as illumination intensity, and any changes observed in the spectra are more likely to be related to leaf biochemical composition, leaf structure, or water content (Blackburn and Ferwerda, 2008). The first derivative of spectral reflectance was calculated for the first and last measurement for experiments 1 and 2, while it was used for all measurements of solar zenith angle. The first derivative was computed as a simple difference function, based on a 7 nm gap either side of a given wavelength.

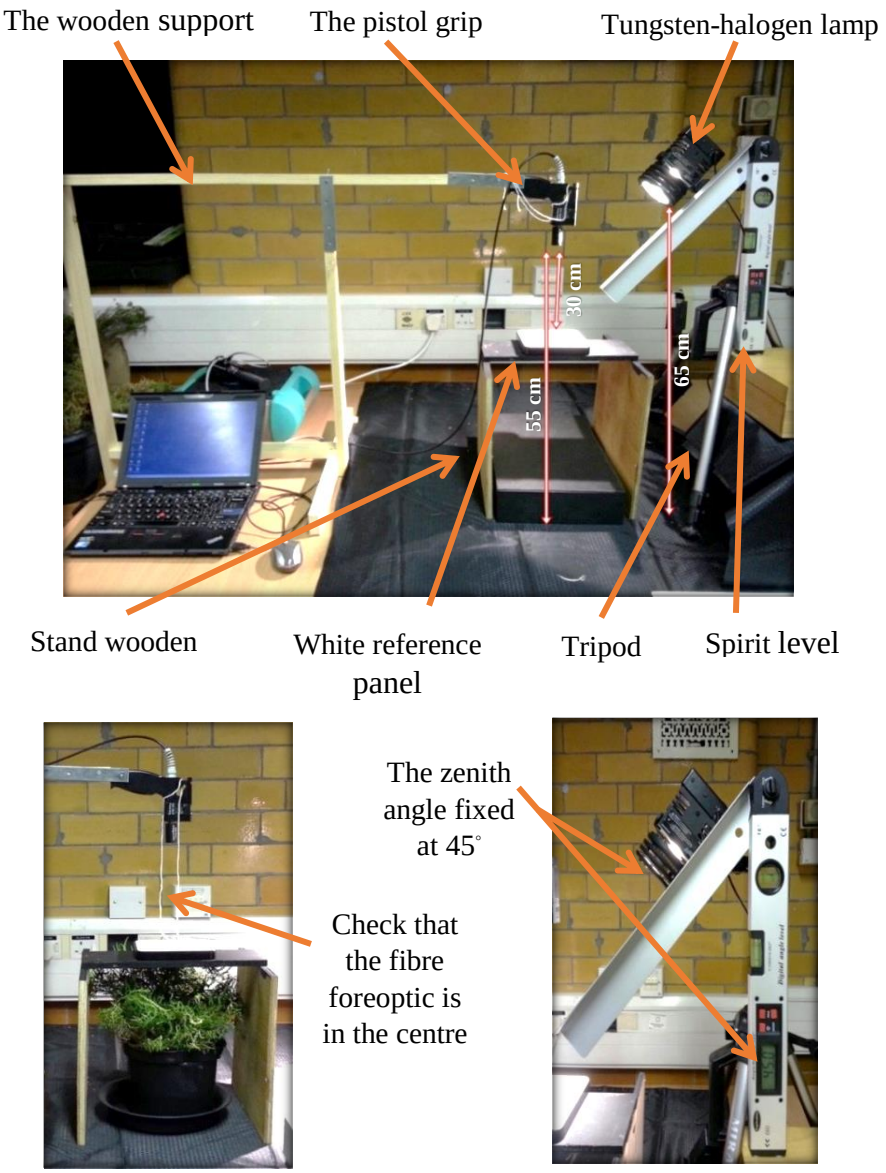

Figure 3.1: The ASD FieldSpec set-up for spectral reflectance measurements.

3.2.3 Experiment 1: Spectral reflectance with FMC variation

Calluna was chosen due to: (i) it being considered an important species in ecosystems of the uplands in the UK; (ii) most of the wildfires recorded in study area occur on this species; (iii) it dominates the study area which offered flexibility to find test plots that cover the pixel size of the two satellite sensors used to achieve the third objective of this study.

In this experiment, two samples of *Calluna* were used to measure the spectral reflectance of the canopy over 23 days in the laboratory; this period was long enough to dry the samples to low FMC. Spectral and leaf sample measurements were obtained on 12 separate days during the 23 day measurement period.

A sample of leaves was collected after every spectral measurement from the second canopy and used for estimating FMC. Whole terminal shots were sampled and placed in airtight plastic bags. Approximately 25 g of sample material was sampled. The leaf samples were dried in an oven for 48 hours at 60°C then fuel moisture content was calculated using equation (3.3).

$$FMC = \frac{Wf - Wd}{Wd} \times 100 \quad (3.3)$$

Where (Wf) refers to the fresh weight of a vegetation sample and (Wd) refers to the dry weight of a vegetation sample. The NDWI, MSI were computed as detailed earlier.

The samples brought from the study area were whole plants that were uprooted and then replanted in small containers. Only a small number of plants was used in the laboratory since uprooting of a large number of the plants is not permitted in the study area. This limitation may effect the accuracy of the FMC estimates because only a small sample of leaves was taken after each measurement.

3.2.3.1 Results

The results shown in Table 3.1 summarise the FMC values on the 12 measurements days and show clearly the gradual reduction in FMC. There was a noticeable change in the NDWI, with a high value of 0.38 at the first measurement and the lowest value of 0.22 when dry. The MSI changed from 0.46 to 0.70.

Table 3.1: The FMC, NDWI and MSI from small canopy of *Calluna* over 23 days

Measurements	FMC (%)	NDWI	MSI
1	53.01286	0.377122	0.463392
2	44.12425	0.313871	0.385696
3	35.44983	0.332657	0.520879
4	30.79151	0.32621	0.538882
5	23.03202	0.293376	0.572227
6	21.20154	0.236119	0.686189
7	15.47787	0.196237	0.724899
8	15.17416	0.245224	0.659072
9	14.22774	0.233534	0.679345
10	13.34251	0.219636	0.695666
11	12.62435	0.232585	0.676966
12	12.29369	0.217747	0.702667

Figure 3.2 shows the spectral reflectance of the sample canopy of *Calluna* at the start and end of the 23 day measurement period. There was a clear change in the shape of the water absorption features centred at 1450, 1900 nm; FMC was 53% and 12% at the start and end of the experiment respectively.

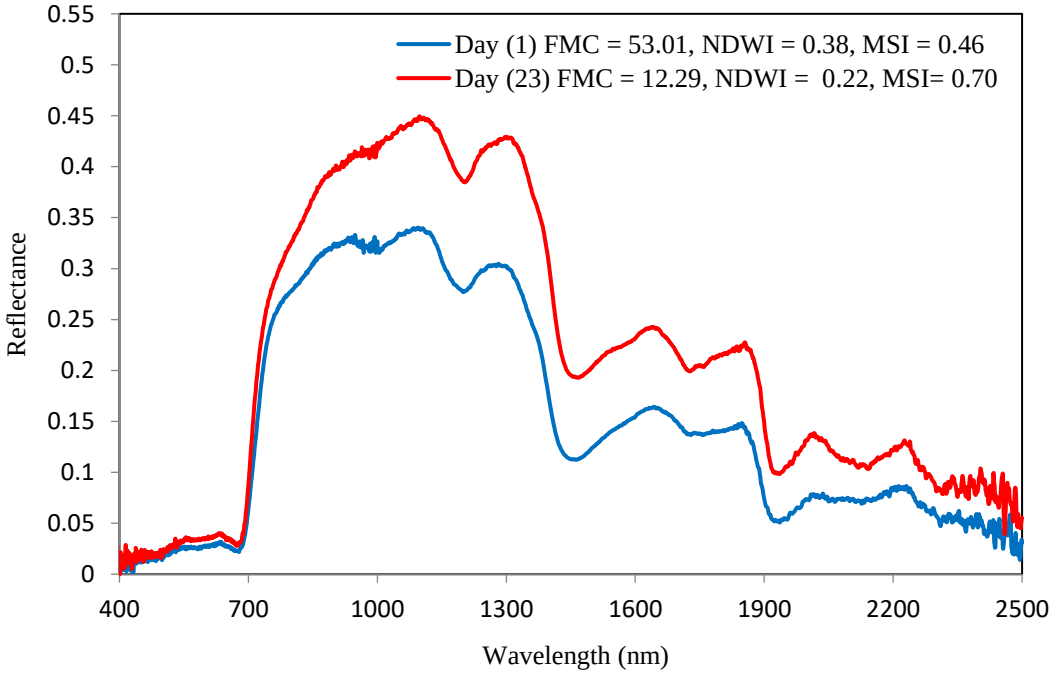

Figure 3.2: Spectral reflectance of *Calluna* canopy from fresh to dry

The first derivative of canopy reflectance was plotted for measurement day 1 and day 23 and compared in the wavelength regions of the NIR b8a (850-870 nm) and SWIR b11 (1560-1650 nm) of S2A MSI. Figure 3.3 shows the first derivative was not sensitive in these wavelength regions. This shows that the spectral reflectance is sensitive only to the magnitude of reflectance changes and suggests that the ratio indices used later will be related only to variation in FMC.

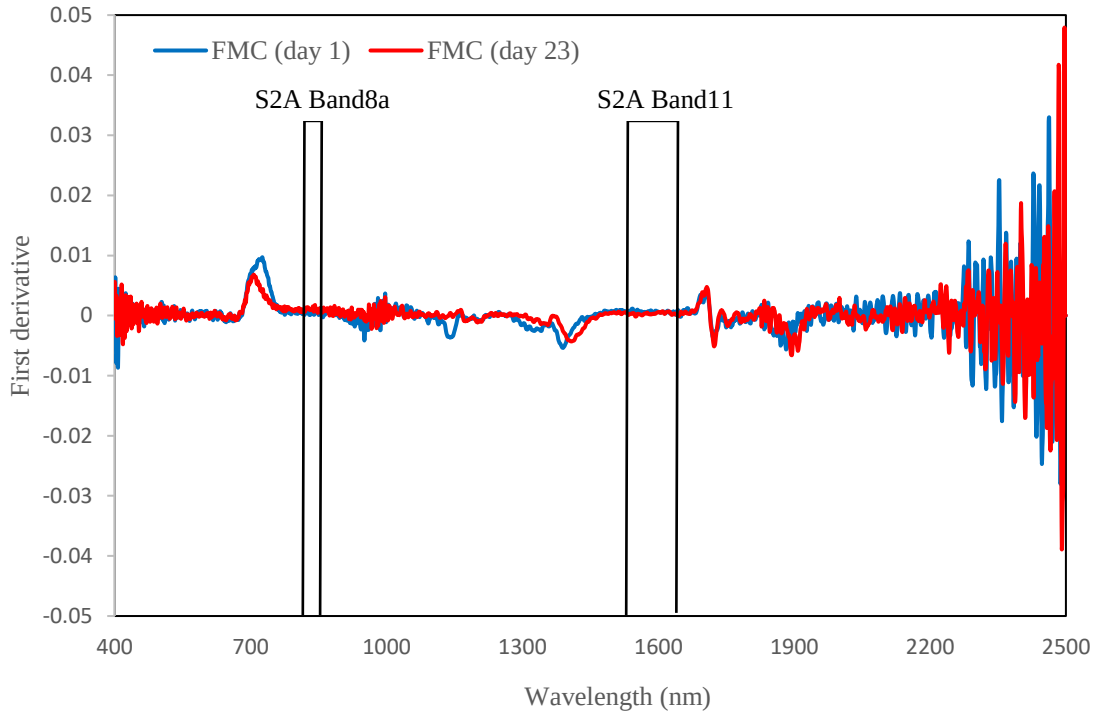

Figure 3.3: First derivative of canopy reflectance for day one and day 23 from FMC variations experiment.

The NDWI and MSI are two widely used vegetation indices, and the most frequently used for estimating plant water content (Almoustafa, 2011; Chen, Huang, & Jackson, 2005; Claudio et al., 2006; Danson & Bowyer, 2004; Stimson, Breshears, Ustin, & Kefauver, 2005; Yebra, Chuvieco, & Riaño, 2008; Yilmaz et al., 2008; Zhang et al., 2010). To investigate the relationships between vegetation FMC and the spectral indices, linear correlation was

used. The Pearson correlation r between vegetation FMC, NDWI and MSI, showed strong statistically significant correlations ($P < 0.05$). Figure 3.4 shows that there was a positive correlation between NDWI and FMC ($r = 0.9201$), and the correlation between MSI and FMC was strongly negative ($r = 0.9248$). These results confirm the relationship between FMC and the VI.

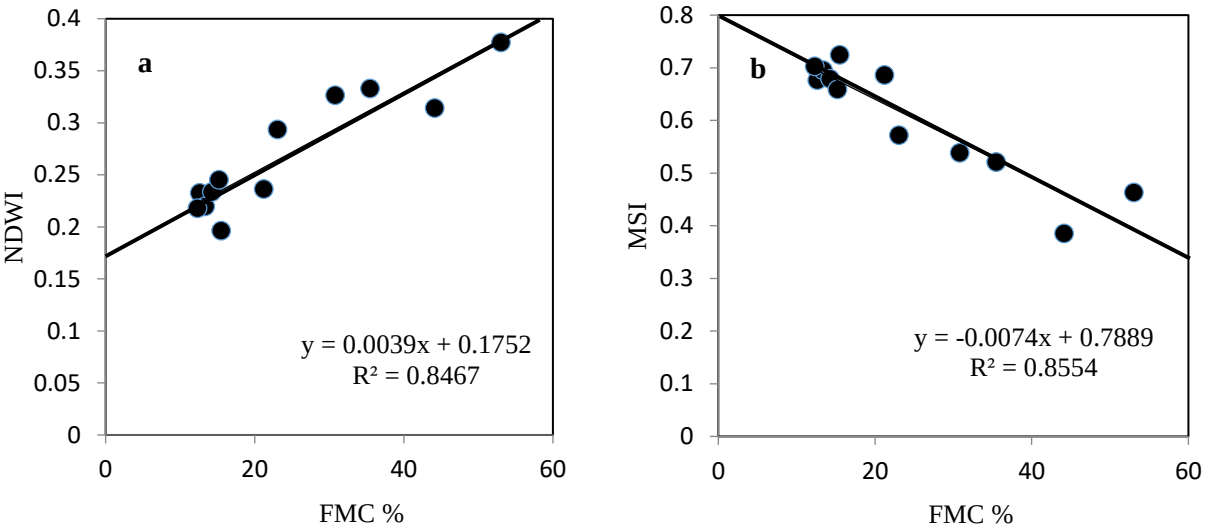

Figure 3.4: Relationship between vegetation indices and FMC

3.2.4 Experiment 2: Effects of soil background

Peat soil and loam soil were used in order to investigate the effects of the background on the spectral reflectance of the canopy. Both soils have different chemical and physical properties. Peat soil was brought from the study area and loam soil from adjacent place to the study area to test the extent of peat soil impact (dry and wet) on the canopy reflectance when compared with a different type of soil from the same area. In the laboratory, two containers were filled with the two types of dry soils. Two small canopies of *Calluna* were planted in each container using material from the study area (Figure 3.5). The spectral reflectance of the two canopies was measured separately. After measurement, the soils were watered to wet the soil to field capacity and after approximately 10 minutes the canopy

reflectance was measured again. Four measurements were therefore obtained from these experiments, canopy reflectance with dry and wet peat soil background, and canopy reflectance with dry and wet loam soil background. Five replicate spectral measurements were taken for each canopy, and the average was used to calculate the NDWI only. The MSI results were similar and are not discussed in detail.

Figure 3.5: Two different backgrounds with small canopy of *Calluna*

3.2.4.1 Results

The results showed that there were small differences in spectral reflectance of the canopies with the two different types of backgrounds, both in dry or wet conditions. Figure 3.6 shows that there was a small change in canopy reflectance between dry and wet peat soil backgrounds, where the NDWI values were 0.20 and 0.23 respectively. Spectral reflectance of the canopy with loam soil background showed less change compared with the peat soil background. NDWI was 0.22 when measured with the canopy with dry loam and 0.28 with wet loam (Figure 3.7).

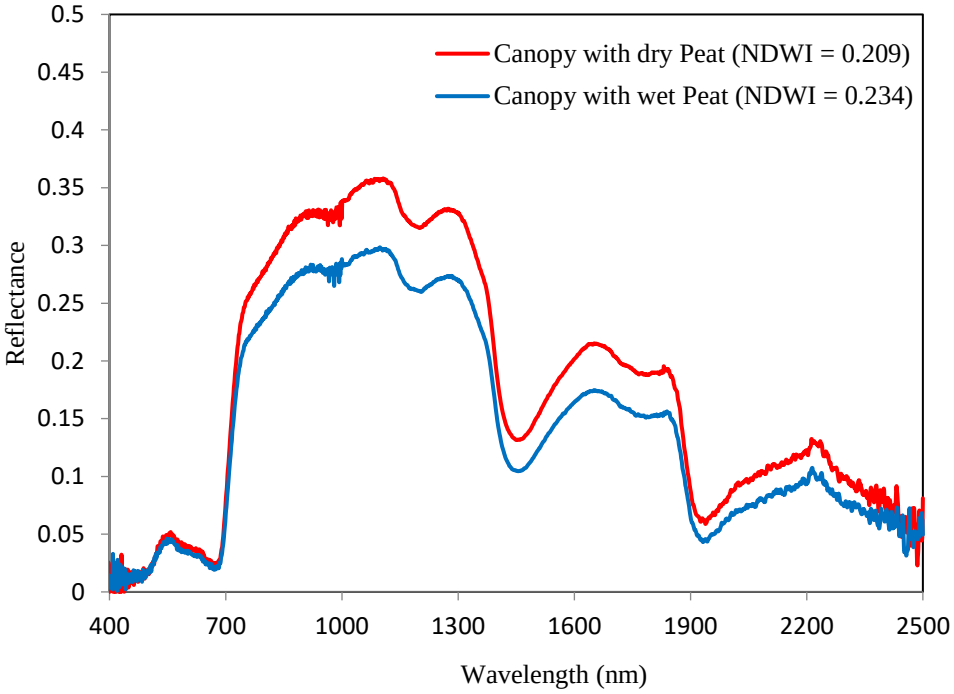

Figure 3.6: Spectral reflectance of sample canopy with dry and wet peat soil

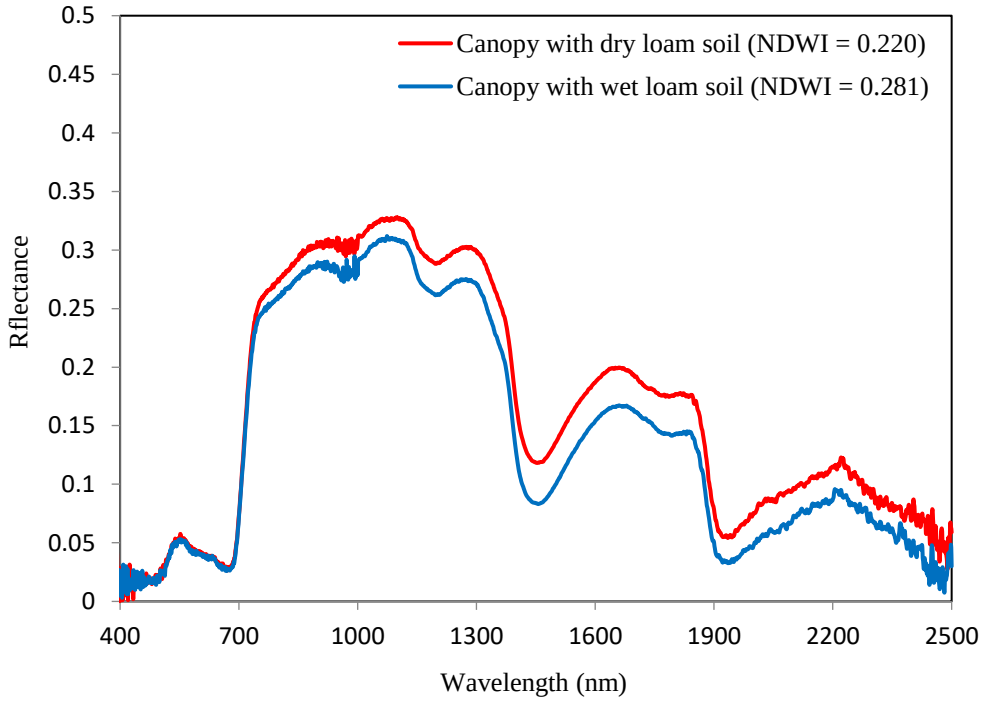

Figure 3.7: Spectral reflectance of sample canopy with dry and wet loam soil.

The first derivative of the canopy reflectance was used for the first measurement of wet and dry peat soil (figure 3.8), and wet and dry loam soil (Figure 3.9). The figures show the first derivatives were not sensitive in these wavelengths both for peat soil or loam soil with dry or wet conditions, so the ratio indices used later will be related only to change of moisture content in the vegetation which is influenced by magnitude of canopy reflectance.

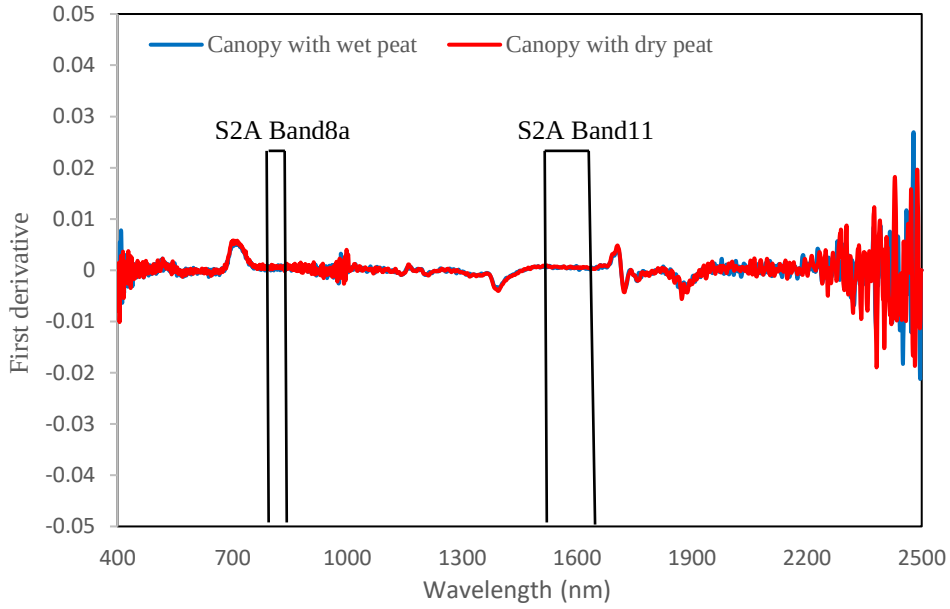

Figure 3.8: First derivative of canopy reflectance for wet and dry peat soil.

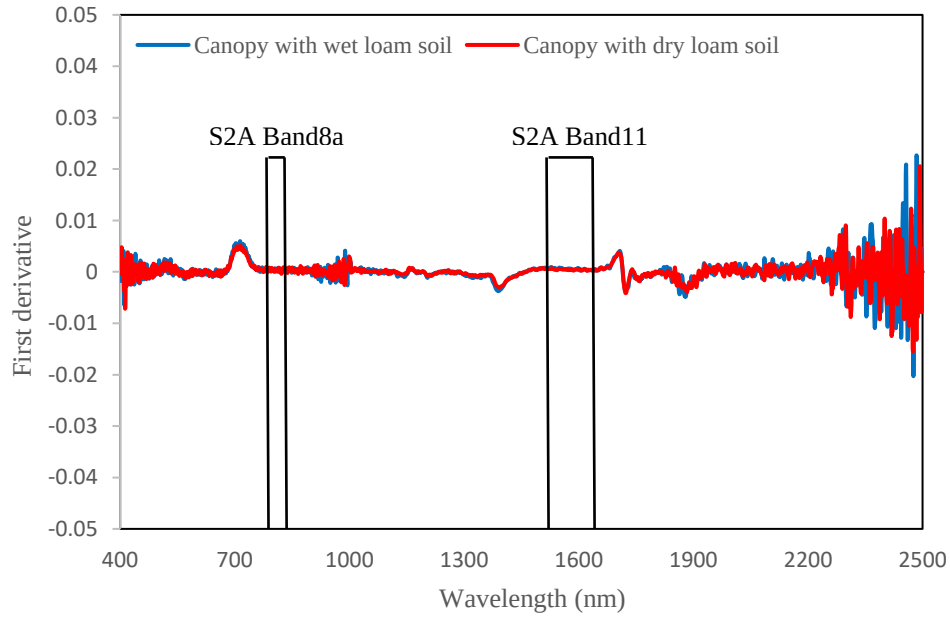

Figure 3.9: First derivative of canopy reflectance for wet and dry loam soil.

3.2.5 Experiment 3: Different 'solar' zenith angles

Small canopies of *Calluna* were used to test the effect of solar zenith angle on spectral reflectance in the laboratory. The sample was at a distance of 30 cm from the lens, where the diameter of the 'ground area' seen by the sensor was 4 cm with the 8° lens attached. Illumination was provided by the tungsten-halogen 1000W lamp, which was set up on a tripod at the side of the table at a height of 65 cm. A digital inclinometer was used to set the illumination zenith angle between 10° and 80° in 10° steps. The average of five spectral measurements were used to calculate NDWI for each illumination zenith angle measurement separately. Again the results for the MSI were similar and are not presented in detail.

3.2.5.1 Results

Figure 3.10 shows a gradual increase in reflectance with increasing solar zenith angle, where the highest reflectance was with the angle 80°, and the lowest with a solar zenith angle of 10°. However the NDWI showed a different pattern. The NDWI measurements were sensitive to change in solar zenith angle, and was highest (0.390) at 40°, while the value gradually dropped to 0.267 at 80° and to 0.334 at 10°. There were very small change between 40° and 60° degree (Figure 3.11), and over this range of solar zenith angles, typical of the range for the satellite data used in chapter 5, there is likely to be very little effect on FMC estimation.

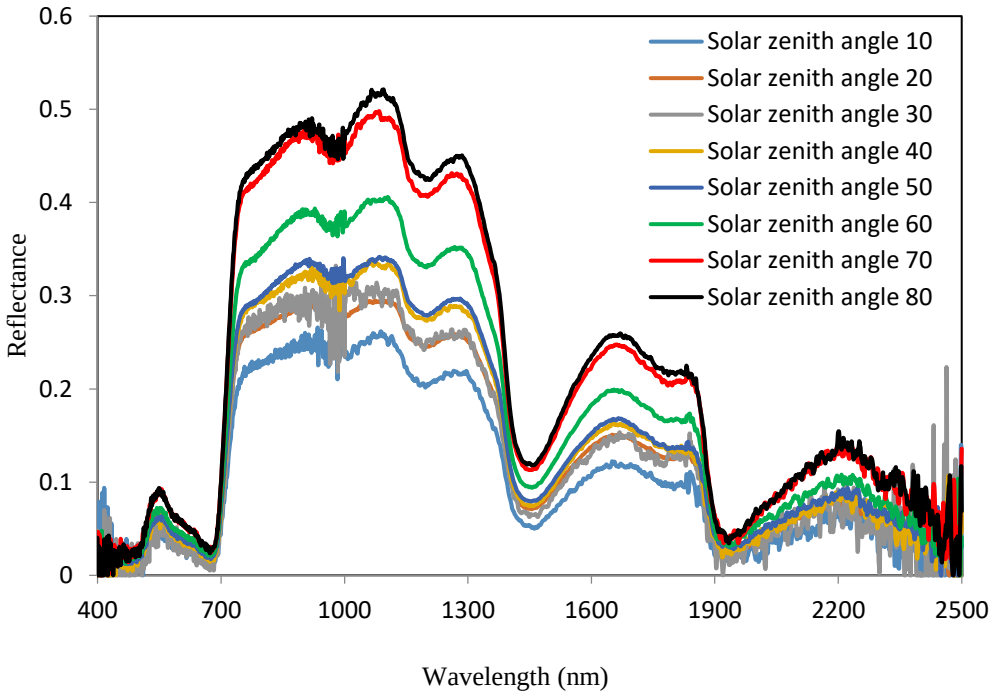

Figure 3.10: Reflectance measurements with different solar zenith angles (degrees) using ASD in the laboratory.

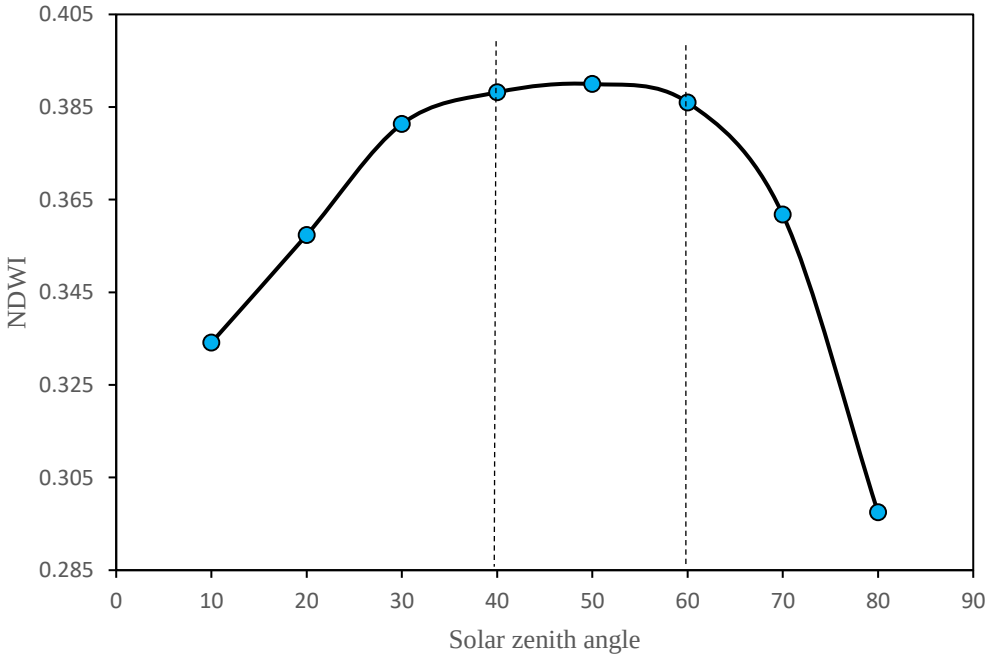

Figure 3.11: Measured NDWI with change of solar zenith angle.

The first derivative of canopy reflectance was plotted for the first measurement of each solar zenith angle. Figure 3.12 shows the first derivatives were not sensitive in these wavelengths with eight different solar zenith angles, and the only sensitivity was with the magnitude of canopy reflectance.

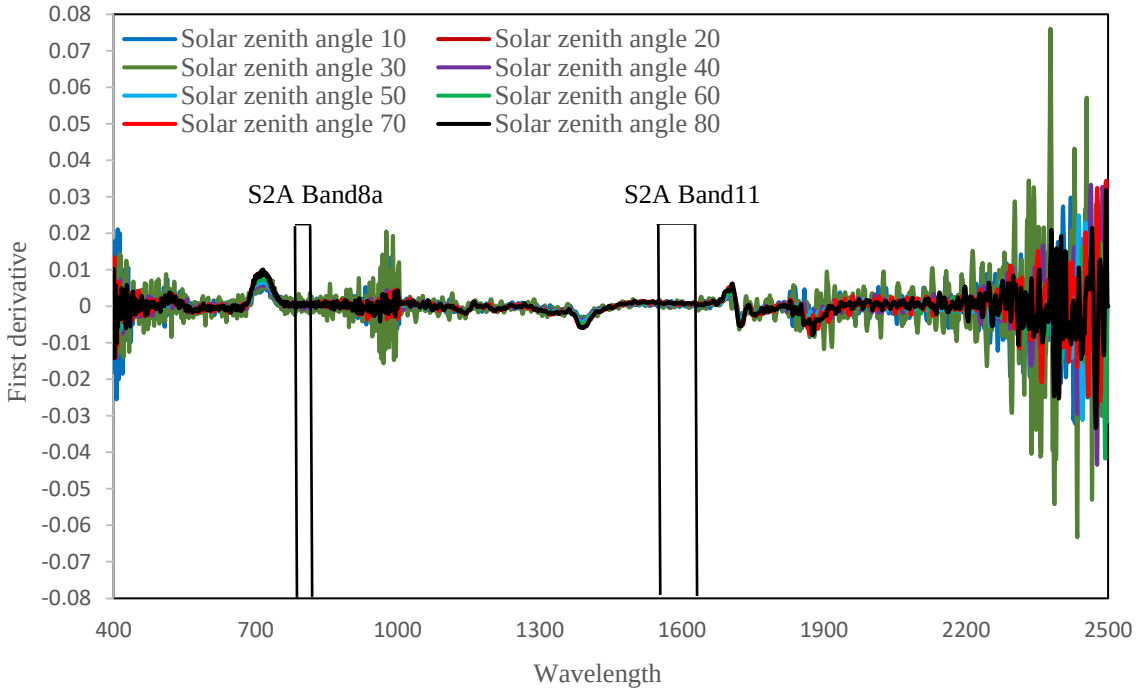

Figure 3.12: First derivative of canopy reflectance for different solar zenith angles.

3.3 Radiative Transfer Modelling

The Scattering by Arbitrarily Inclined Leaves (SAIL) model describes canopy bidirectional reflectance considering the leaf optical properties, the canopy structure (leaf area index (LAI) and mean leaf inclination angle), illumination and viewing geometry (zenith and relative azimuth viewing angles and, zenith solar angle), and the wavelength-dependent reflectance of the underlying soil (Jacquemoud et al., 2009).

Atmospheric conditions are considered by the fraction of diffuse illumination (skyl). As SAIL requires leaf reflectance and transmittance spectra as input variables, it was coupled with the PROSPECT leaf model (Jacquemoud et al., 2009).

In PROSPECT, leaf reflectance and transmittance is described as a function of the leaf mesophyll structure parameter (N), the chlorophyll a + b concentration, the leaf equivalent water thickness, and the leaf dry matter content (Figure 3.13).

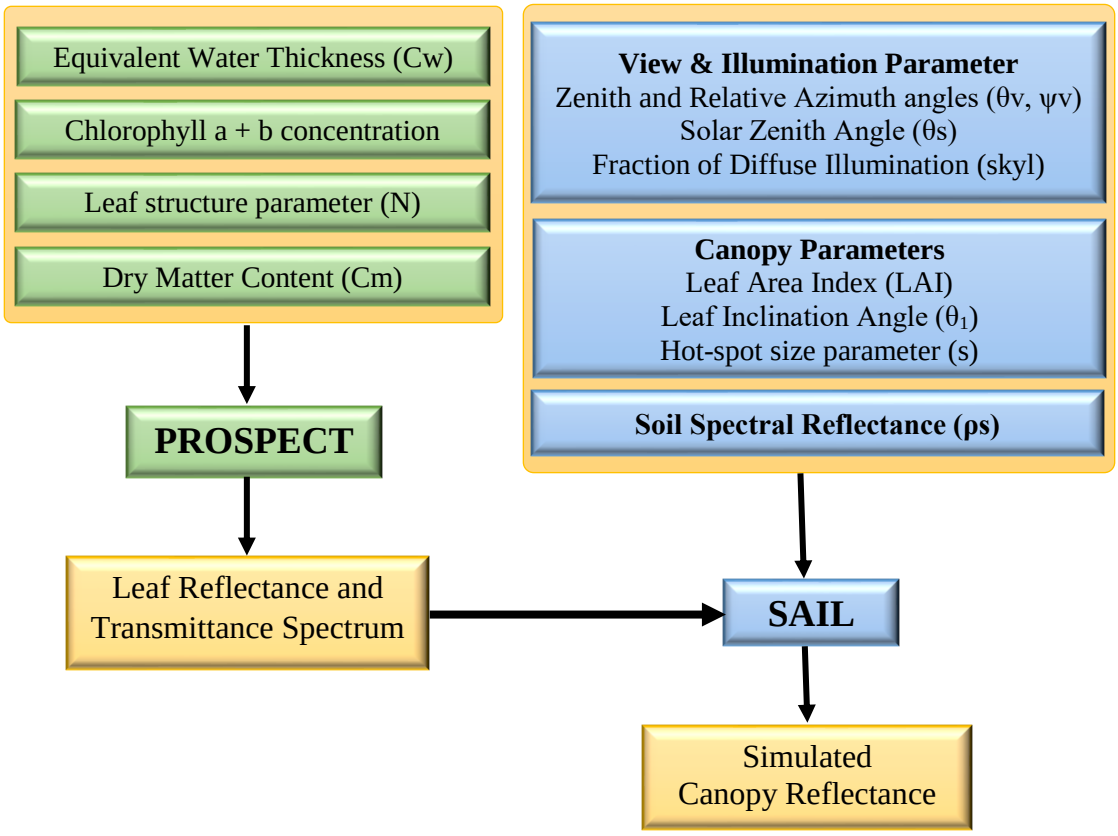

Figure 3.13: Parameters to simulate canopy reflectance using the PROSAIL model.

Radiative transfer models (RTM) allow us to describe the interactions of electromagnetic radiation with plant canopies and here the SAIL model and PROSPECT model were combined as the Pro-SAIL model (Jacquemoud & Baret, 1990) which simulates canopy

reflectance over the range 400-2500 nm using a set input of variables. The model uses 12 input parameters, and based on these inputs, the model calculates canopy BRF (Table 3.2).

Table 3.2 Parameters used to establish the reflectance simulation using PROSAIL.

	Input variable	Units
Leaf parameters: **PROSPECT-4**	Leaf structure index (N)	unitess
	Leaf chlorophyll content (LCC)	µg/cm^2
	Leaf dry matter content (Cm)	g/cm^2
	Leaf water content (Cw)	g/cm^2
Canopy variables: **SAIL**	Leaf area index (LAI)	m^2/m^2
	Soil scaling factor (asoil)	unitess
	Hot spot parameter (HotS)	-
	Diffuse incoming solar radiation (sky)	fraction
	Average leaf angle (ALA)	degrees
	Solar zenith angle (Θs)	degrees
	View zenith angle (Θv)	degrees
	Sun-sensor azimuth angle (Ø)	degrees

The model was used here to explore the relationships between plant canopy water content and specifically FMC and spectral reflectance. Forward simulations were used to assess the sensitivity of vegetation indices to variations in FMC and to understand how other variables, like soil background reflectance, and change solar zenith angle, may affect these relationships. The approach was developed to estimate FMC using Sentinel-2A wavebands in order to link to the laboratory experiments and field-based work that follow in the next chapter. In the simulations, the FMC was derived from the leaf water content and leaf dry matter parameter values.

3.3.1 Simulating the relationship between FMC and VI

Two sets of simulations were conducted. First a "global" simulation where the model variables were allowed to vary over their full range (Danson & Bowyer, 2004). Second a "laboratory" simulation where the model variables were set at values representing the

variation in the laboratory plant canopies (Table 3.3). The soil background spectra used were derived directly from the laboratory measurements and were the loam and peat soils in "wet" and "dry" conditions.

To derive the NDWI and MSI the output spectra were convolved with the spectral response functions for Sentinel 2A MSI bands 11 and 8a and the NDWI and MSI computed. The model was run 500 times drawing randomly from each parameter range at each run.

Table 3.3: Range and fixed input values used to establish the reflectance simulations.

Input variable	Global	Experiment
Leaf structure index (N)	1	1
Leaf chlorophyll content (LCC)	40	40
Leaf dry matter content (C_m)	0.0014-0.05	0.009-0.01
Leaf water content (C_w)	0.001-0.085	0.001-0.004
Leaf area index (LAI)	0.5-5	0.5-5
Soil spectral reflectance (a_{soil})	measured	measured
Hot spot parameter (HotS)	0.1	0.1
Diffuse incoming solar radiation (sky)	0.2	0.2
Average leaf angle (ALA)	40	40
Solar zenith angle (Θ_s)	45	45
View zenith angle (Θ_v)	0	0
Sun-sensor azimuth angle (Ø)	0	0

3.3.1.1 Results

Figure 3.14 shows the modelled relationship between FMC and vegetation indices (NDWI and MSI) for the global simulation and FMC range of 10-200 %. The combination of variables gives rise to a wide scatter of points although there is a clear positive relationship here. It is clear that there will be a weak relationship between FMC & NDWI when there is large variation in LAI. Figure 3.15 shows the simulation for the laboratory experiment variables range. Here the FMC range is very narrow, and LAI is allowed to vary from 0.5 to 5. The red points show the outputs for a fixed LAI of 3.0. Also shown is the experimentally-derived regression equation from the laboratory work.

The model results are close to the relationship from the laboratory further confirming the use of NDWI or MSI for FMC estimation.

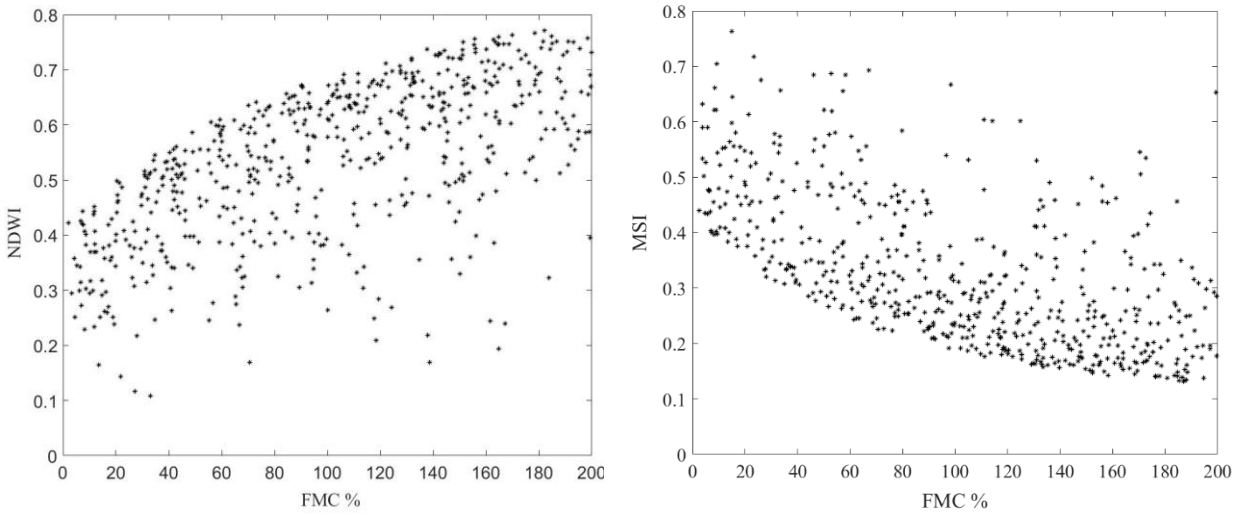

Figure 3.14: Global simulation of the relationship between vegetation indices and FMC with LAI 0.5-5.

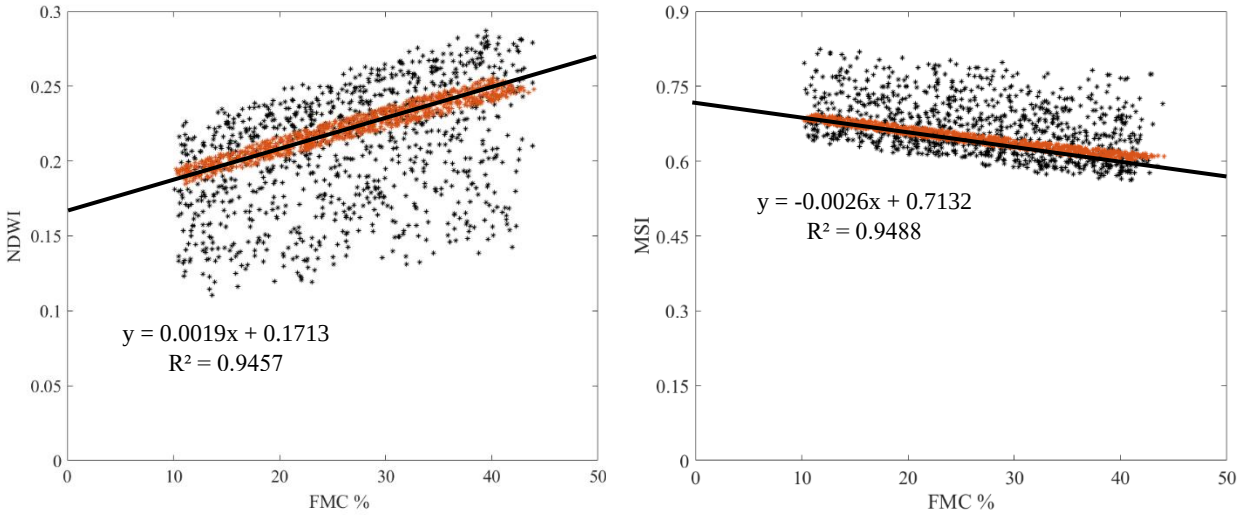

Figure 3.15: Simulation of the relationship between vegetation indices and FMC from laboratory experiment with LAI 3.0 (red points) and LAI 0.5-5 (black points).

3.3.2 Simulating the effects of different soil backgrounds

The sensitivity of canopy reflectance to variation in soil background and soil moisture was simulated using the PROSAIL model. All parameters were fixed at the values for the laboratory experiment (Table 3.4). Four different soil background reflectance spectra were used in the simulation to test the sensitive of canopy reflectance to them: wet and dry loam soil, wet and dry peat soil.

Table 3.4: Input values used to simulate the sensitivity of soil background

Input variable	Fixed value
Leaf structure index (N)	1
Leaf chlorophyll content (LCC)	40
Leaf dry matter content (C_m)	0.01
Leaf water content (C_w)	0.01
Leaf area index (LAI)	2
Soil spectral reflectance (a_{soil})	measured
Hot spot parameter (HotS)	0.1
Diffuse incoming solar radiation (skye)	0.2
Average leaf angle (ALA)	40
Solar zenith angle (Θ_s)	45
View zenith angle (Θ_v)	0
Sun-sensor azimuth angle (Ø)	0

3.3.2.1 Results

Figure 3.16 shows the effects of wet and dry loam soil background on canopy reflectance. The spectra were very similar in shape although the reflectance is very slightly (less than 1%) lower with the wet soil background. There was a very small difference between the computed NDWI of 0.304 for the wet loam soil background, compared to 0.318 for the dry loam soil background. There were also no large differences in canopy reflectance between the wet and dry peat background, with NDWI for wet and dry peat of 0.273 and 0.316 respectively (Figure 3.17). Based on the laboratory-derived relationship the difference in estimated FMC for the four soils was between 25 and 36%. Therefore, it is likely that

variation in soil background and soil wetness may give rise to 11% variation in estimated FMC, for a given canopy LAI. The differences in NDWI between the wet and dry soils are similar in magnitude to those in the laboratory experiment confirming further the likely effects of variation in soil background.

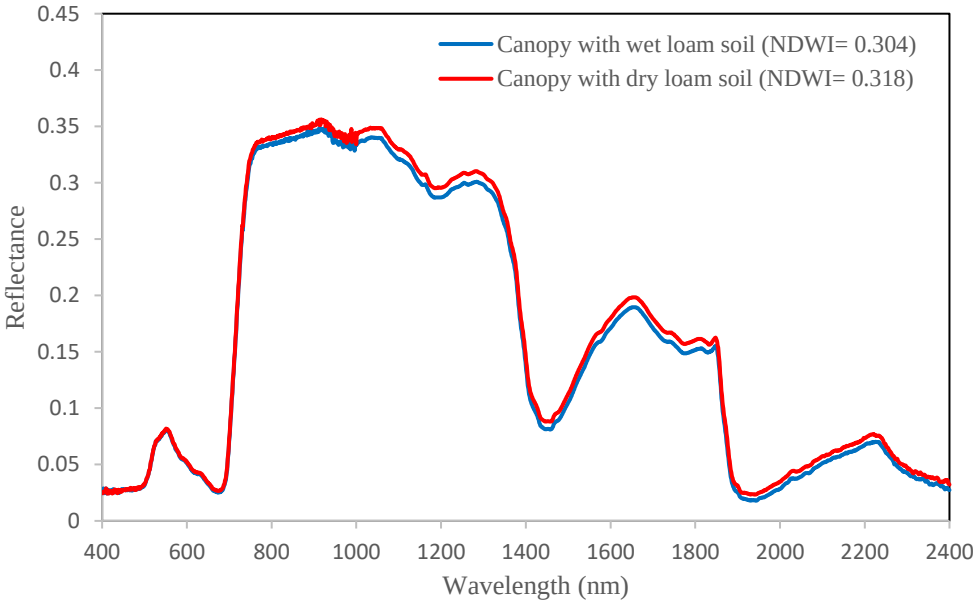

Figure 3.16: Simulating canopy reflectance with wet and dry loam soil backgrounds.

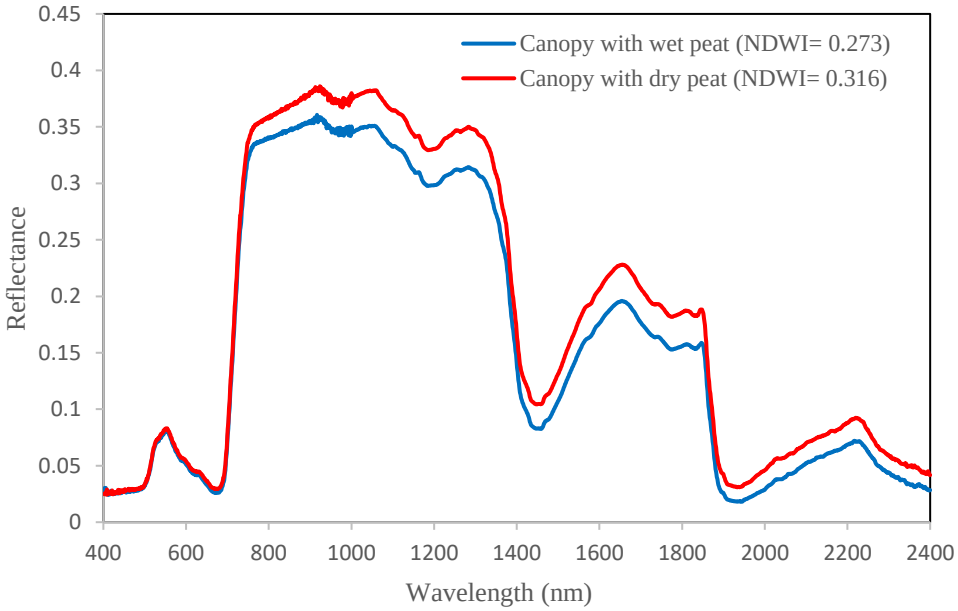

Figure 3.17: Simulating canopy reflectance with wet and dry peat soil backgrounds.

3.3.3 Simulating the effects of different solar zenith angles

The PROSAIL model was used to simulate the effects of change in solar zenith angle on canopy spectral reflectance and NDWI. The parameters were again set to typical values, with the solar zenith angle varied between 10° and 80° in steps of 10° (Table 3.5). The spectral reflectance and NDWI were again computed for each run of the model.

Table 3.5: Input values used to simulate the sensitivity of different solar zenith angles

Input variable	Value
Leaf structure index (N)	1
Leaf chlorophyll content (LCC)	40
Leaf dry matter content (C_m)	0.01
Leaf water content (C_w)	0.01
Leaf area index (LAI)	2
Soil spectral reflectance (a_{soil})	fixed
Hot spot parameter (HotS)	0.1
Diffuse incoming solar radiation (skyI)	0.2
Average leaf angle (ALA)	40
Solar zenith angle (Θ_s)	10°-80°
View zenith angle (Θ_v)	0
Sun-sensor azimuth angle (Ø)	0

3.3.3.1 Results

The reflectance distribution in figure 3.18 shows that there is a connection between the change in the zenith view angle and the canopy reflectance. With every change in the solar zenith angle, there is change in the canopy reflectance. The figure shows that the highest values of reflectance are recorded at 80° zenith angle and the lowest value at 10°. Moreover, it was noticed that there was only a slight change in the reflectance for the angles 40°, 50°, and 60° respectively. In addition, there were small changes in the NDWI values with different view zenith angles (Figure 3.19). The highest value of NDWI was 0.312 at 50°, while the lowest NDWI was 0.286 at 80°. There were again small changes between 40° and 60°. The solar zenith angle range for the satellite data used in the next chapter was between

41.46 to 58.90 degrees for seven images obtained across a 12 month period. The NDWI range for these solar zenith angles was between 0.311 and 0.312. This is equivalent to an FMC range of 34.82% to 35.07%, and suggests that variations solar zenith angle is unlikely to have a large effect on FMC estimation. Again, the change in NDWI with solar zenith angle was similar to those in the laboratory experiment, although the magnitude of the NDWI was different.

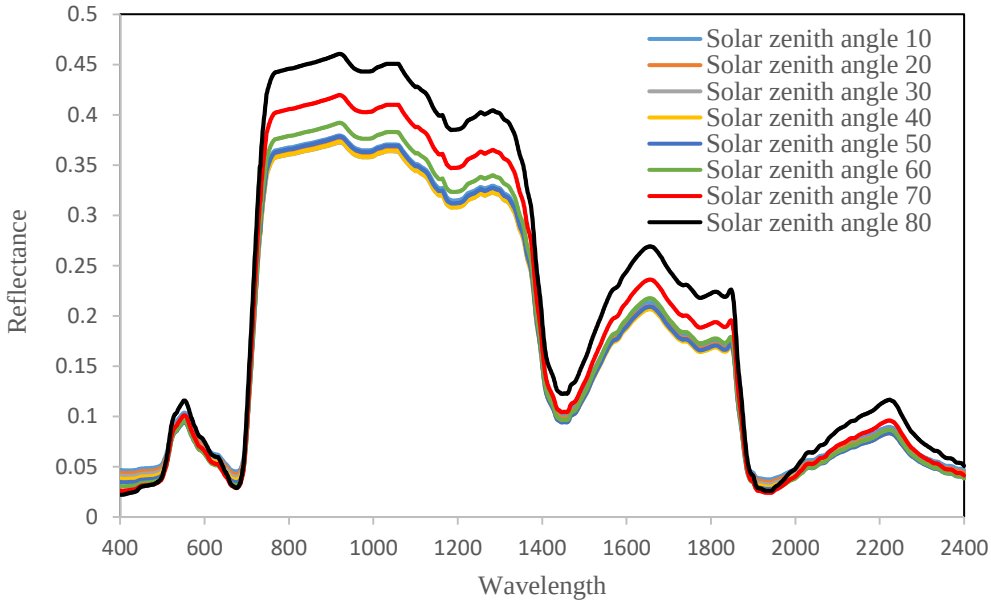

Figure 3.18: Simulating canopy reflectance with different solar zenith angles

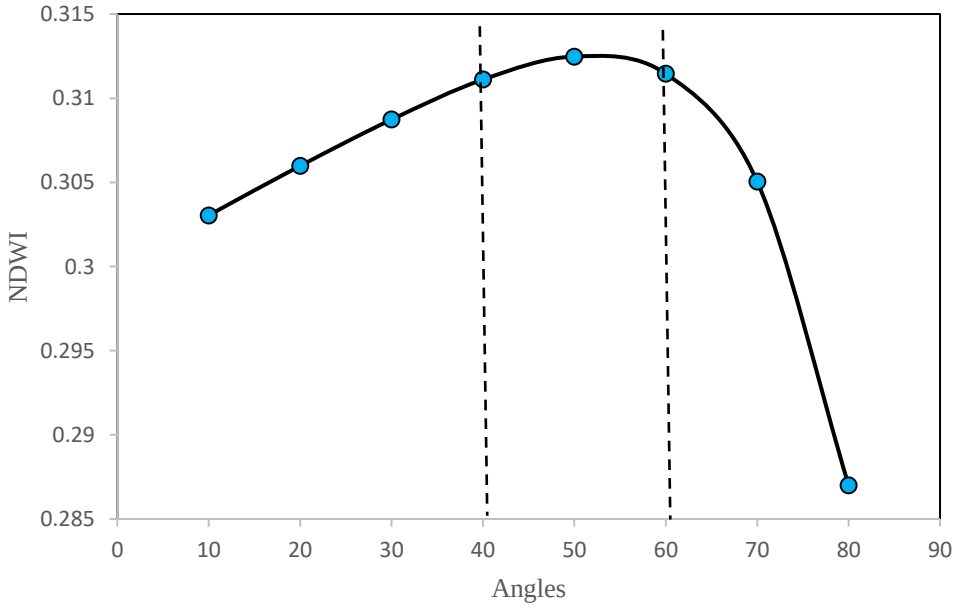

Figure 3.19: Sensitivity of NDWI to change in solar zenith angle.

3.4 Conclusion

This chapter has provided initial datasets which were required to investigate the three hypotheses which relate to the first objective. It demonstrated that experimental work is essential to get a better understanding of the canopy characteristics that effect reflectance measurements. It also demonstrated the application of a RTM to both confirm and explore these relationships. The main conclusions that may be drawn from these experiments are:

(i) There is a strong correlation between NDWI and MSI, and FMC in *Calluna* and therefore both indices can be reliably used to estimate FMC.

(ii) Wet and dry soil backgrounds have a significant effect on canopy reflectance and the NDWI (and MSI by implication), and may therefore lead to some variability in FMC estimations.

(iii) Solar zenith angle had a limited effect on NDWI (and MSI) over the range of 40° - 60° and is therefore unlikely to affect FMC estimations from satellite data.

The next chapter describes the setting of a field-based experiment to explore the application of satellite-derived NDWI and MSI for FMC estimation for a moorland test site in the Peak District, UK.

CHAPTER 4: STUDY AREA, FIELD WORK AND IMAGE DATA ANALYSIS

Summary

This chapter aims to provide a general description of the chosen study area in the Peak District National Park, UK. The chosen sampling site was a small part of Burbage Moor, near Hathersage, a *Calluna*-dominated managed moorland. Sampling was undertaken at five plots of 20 x 20 m. The sampling period extended from April 2016 to March 2017 so that the temporal variation in fuel moisture content (FMC) of the vegetation could be recorded. Weighing of all samples was done in the laboratory, prior to and after drying the samples in an oven. Seven satellite images were retrieved from Landsat-8 OLI and Sentinel-2A MSI. Only three of these images coincided exactly with the field sampling, due to logistical and weather constraints. Pre-processing and calibration of images was done in order to calculate a time-series VI (NDWI and MSI), to allow investigation of the relationship between VI (NDWI and MSI) and FMC over the 12-month sampling frame.

4.1 Introduction

The main aim of this chapter is to provide a description of the study site, and explain the fieldwork undertaken to sample variation in FMC. The chosen field site was Burbage Moor, which is situated in the Peak District National Park, UK. FMC was measured over a sampling period from April 2016 to March 2017. Sentinel-2A MSI (Multi Spectral Imager) and Landsat 8 OLI (Operational Land Imager) data were used to provide digital imagery for the study.

4.2 Study area

The Peak District forms the southern end of the Pennines and much of the area is uplands above 300m, with a high point on Kinder Scout at 636m. It covers 1,440 km^2 of Derbyshire, Staffordshire, Cheshire, Greater Manchester and South and West Yorkshire, and includes

most of the area commonly referred to as the Peak (Figure 4.1). It is the fifth largest National Park in England and Wales (PDNPA, 2015).

The Park includes many Sites of Special Scientific Interest (SSSI) and has several ecological landscape qualities that are unique. By the end of March 2013, there were a total of 60 SSSI sites covering 49,919 hectares (35% of the National Park). The Park has been protected by various cultural and area protection organizations such as the European Natura 2000 Sites, Special Areas of Conservation (SAC) and Special Protected Areas (SPA) (PDNPA, 2015).

The Peak District National Park is a rural upland area valued for its diverse landscapes and scenery. It is surrounded by major conurbations and is at the hub of trans-Pennine road routes. The landscape ranges from the broad open moorlands and gritstone formations of the Dark Peak, to the varied river corridor habitats of the Derwent Valley, and the limestone plateaux and deeply cut dales and gorges of the White Peak. These landscapes are interspersed by enclosed farmlands, wooded valleys and villages (Albertson et al., 2009). The park provides timber resources, grazing land and water supplies, and is popular for activities like trekking, climbing, bicycling, paragliding and walking (Holden et al., 2007).

This rural area of the UK is amongst the busiest areas of the country because of its landscapes (Wotton et al., 2003). This creates a conflict between recreation and conservation that requires careful land management. One key issue emerging as a result of this conflict, and also due to climatic changes, is the incidence of moorland fires. These have increased soil erosion and affected water quality (Davies et al., 2016).

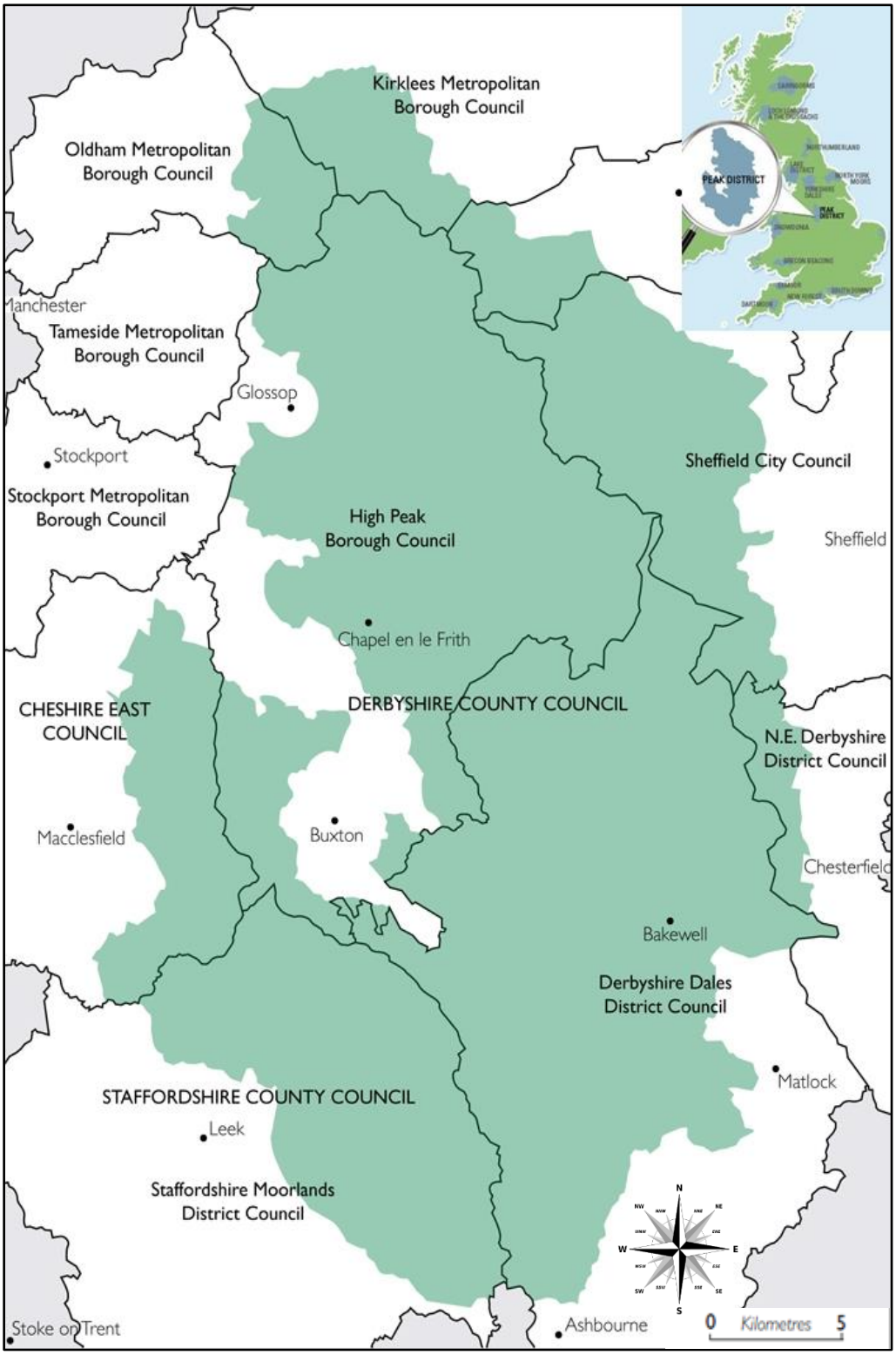

Figure 4.1: Peak District National Park, UK (Source: Peak District National Park, 2018)

4.3 Climate

There is significant spatial variation in climate across the Peak District National Park, with cooler, wetter uplands in the north and west, and warmer drier southern and eastern areas (McMorrow et al., 2009). The following data are based on weather station data from 1981 to 2010 from nearby Sheffield, located at 53.38ºN, 1.48ºW at 131.0 m above mean sea level (Met Office, 2017). Figure 4.2 shows the mean monthly temperatures for Sheffield, UK. The maximum mean monthly temperature was 21.1ºC in July, while the mean minimum temperature was 1ºC in January.

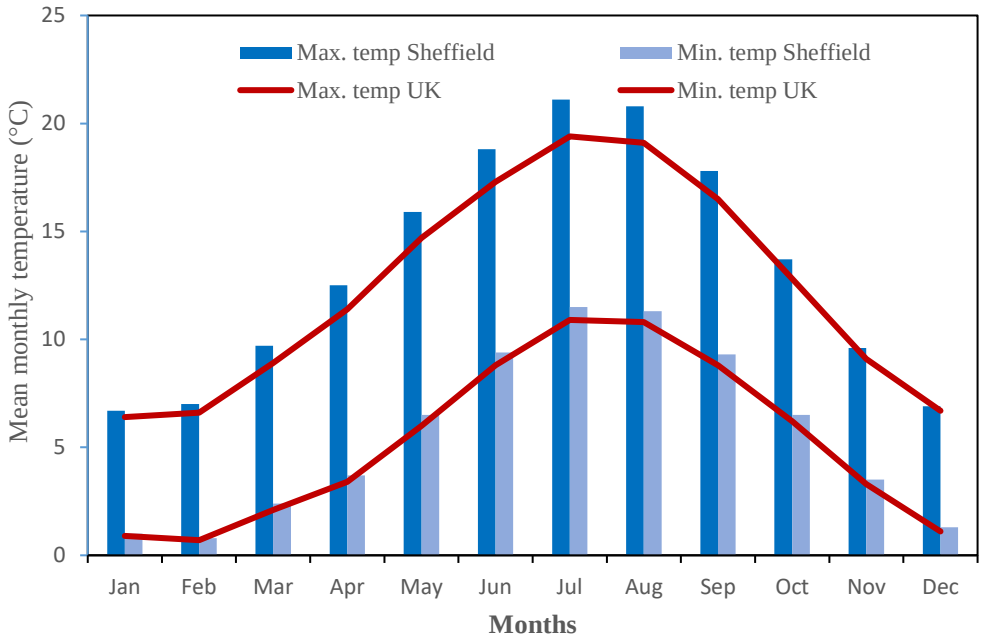

Figure 4.2: Mean monthly temperature 1981-2010 (Source: Met Office, 2017).

Figure 4.3 shows the mean monthly rainfall for the weather station. The maximum mean rainfall recorded was in October and the minimum recorded was in February, however, there are no great variations in rainfall through the year.

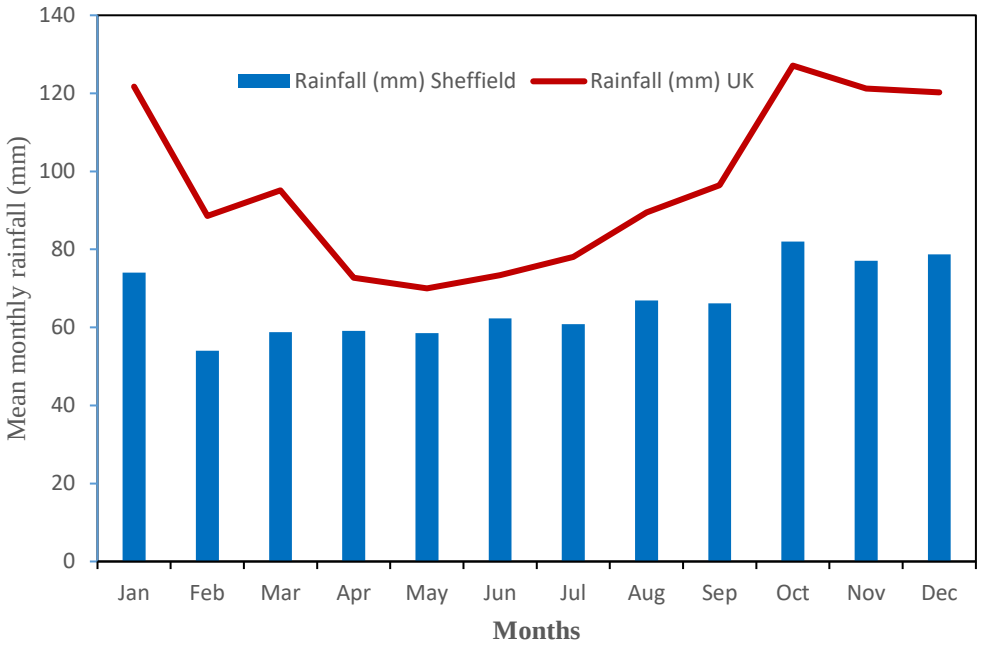

Figure 4.3: Mean monthly rainfall 1981-2010 (Source: Met Office, 2017).

Figure 4.4 shows that for mean monthly sunshine hours, the maximum was in July and the minimum was in December.

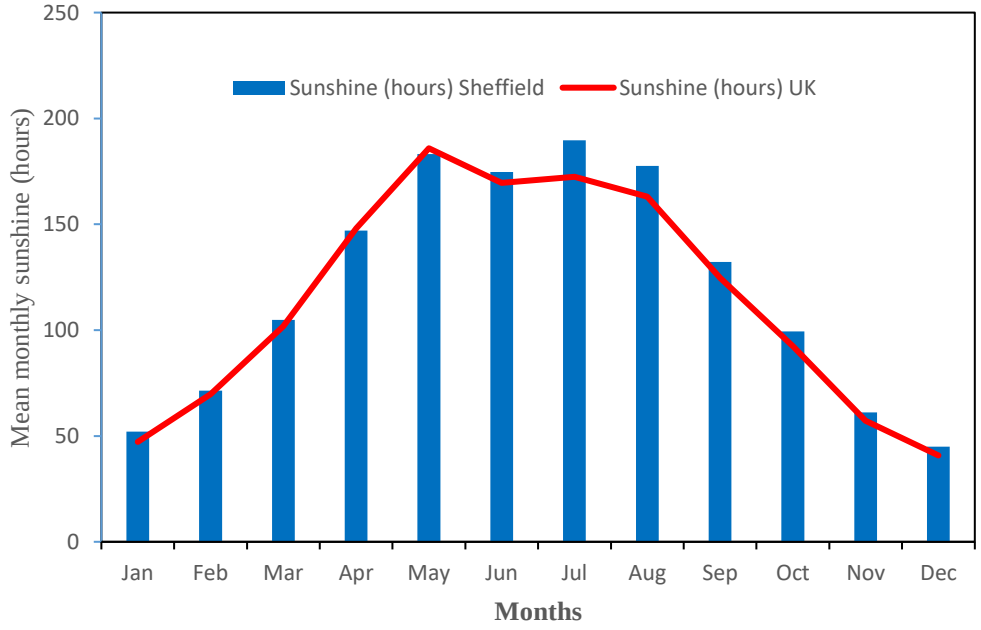

Figure 4.4: Mean monthly sunshine 1981-2010 (Source: Met Office, 2017).

The figure shows comparisons with UK weather, where the mean maximum monthly temperatures was 19.4^{o}C in July, while the minimum was 0.7^{o}C in February. For rainfall Sheffield is a little drier and has a more even spread of rainfall across the year than the UK on average. In terms of sunshine hours, Sheffield is fairly similar to the yearly variation across the UK.

The Burbage Moor field site is located approximately 7 km south-west of the Sheffield weather station at an altitude of around 420 m. It can therefore be expected to be cooler and wetter than the Sheffield station.

4.4 Vegetation

The carboniferous limestone area of the White Peak, the Gritstone and shale areas of the Dark Peak and the South West Peak are the three parts comprising the Peak District (Figure 4.5) (Ashbourn, 2011). These three areas have distinctive vegetation communities related to the geology, climate and land use.

A gently rolling limestone plateau incised by deep river valleys makes up the White Peak. These areas are composed of productive meadows where sheep and cattle permanently graze on scattered farms (PDNPA, 2009). Areas of rough grazing land are situated on the higher unenclosed limestone hills that can be found around Castleton and Bradwell in the north, and in the south-east above Dovedale. Other notable limestone areas nearby are the Manifold Valley and Earl Sterndale. These areas are considered important meadow habitat and have exceptional landscapes which are rich in wild flowers providing habitats for species like skylark and brown hare (Albertson et al., 2010).

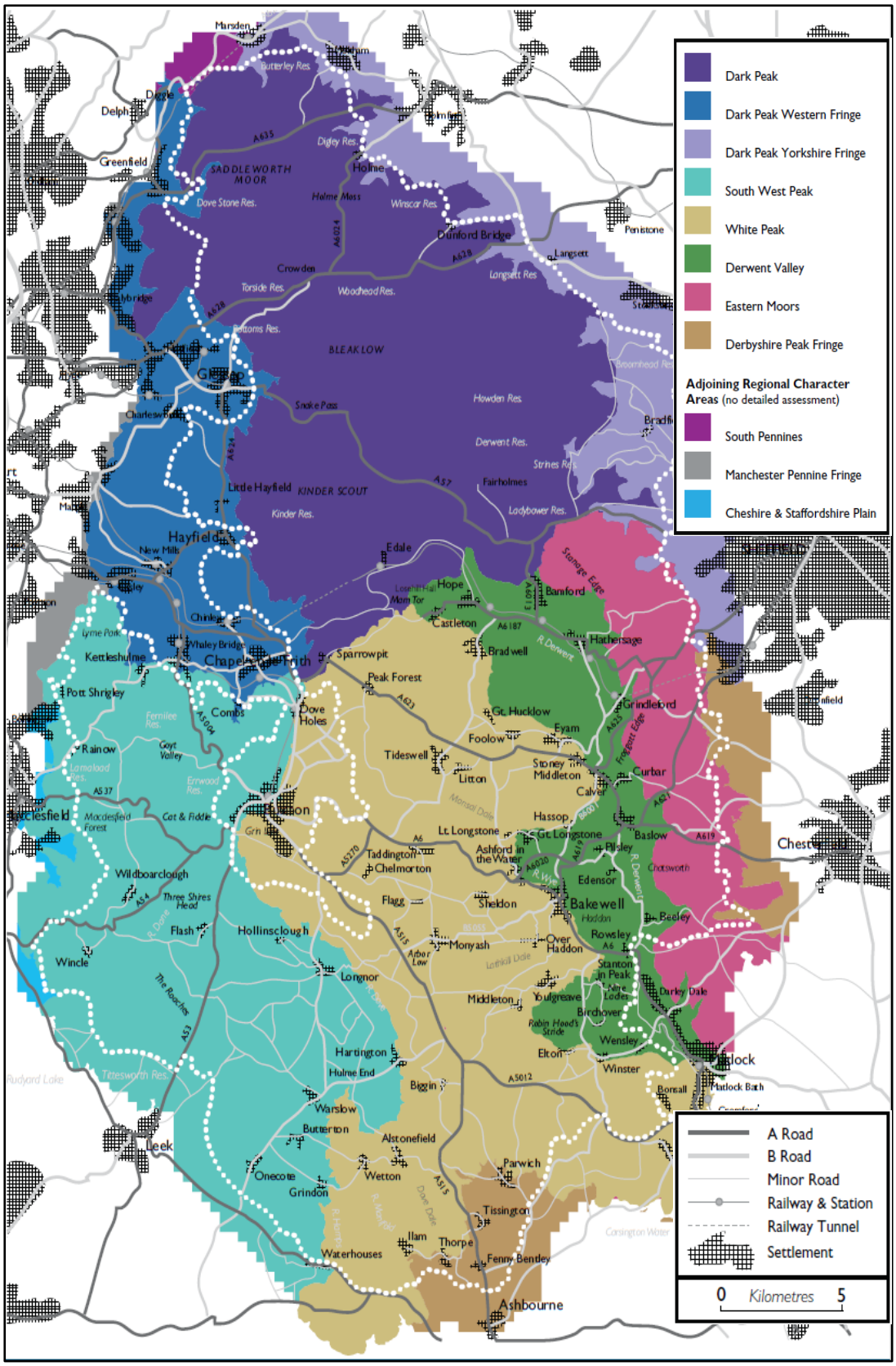

Figure 4.5: Landscape character areas of the Peak District National Park (Source: Ashbourn, 2011).

The Dark Peak is characterised by extensive areas of moorland with steep-sided valleys or cloughs cut by fast-flowing streams; oak woodland is mostly found in the cloughs and on the valley sides. Reservoirs have been constructed in some of the valleys and the surrounding land has been planted with conifer forests (PDNPA, 2001).

There is a wide range of habitats (vegetation communities) and vegetation types within the Dark Peak such as: grassland, heaths, woods, bogs, screes, cliffs, scrub, and high rocky summits (Albertson et al., 2009). The area is considered a distinctive landscape with species including dwarf shrub heath with bilberry (*Vaccinium myrtillis*), heather (*Calluna vulgaris*), cotton grass (*Eriophorum vaginatum*), purple moor grass (*Molinia caerulea*) and tracts of bracken (*Pteridium aquilinum*) and eroding bare peat (Holden et al., 2007; Yallop et al., 2006).

The South-West Peak supports a similar range of habitats to the Dark Peak, but generally in a much more intimate mosaic. The main ridges such as the Roaches, Morridge, Lum Edge and the Ipstones Ridge, are classical examples of such landscapes (PDNPA, 2001).

Continuous grazing over a period of several decades has caused the ecosystem of this area to vary greatly, specifically on the slopes west of the Kinder Estate which lies within the moorland zone of the Peak District National Park. The largest change and the most visible effect of this extensive grazing comes in the form of replacement of the hilltop moorland by rough acid grassland. Moving towards the eastern and western edges of the area, the land is extensively farmed (Anderson & Radford, 1994). The Peak District has high habitat and species diversity. However, the continued pressure of climate change, land use change and recreational activities threatens its fragile ecosystems (Albertson et al., 2010).

4.5 Wildfires in the Peak District

McMorrow et al. (2009) studied wildfires in the Peak District using data between 1976 and 2003, and found that most fires had started accidentally. One peat fire in the Peak District in April 2003 burned 777 ha of moorland, including areas under statutory conservation protection. Another Peak District fire in July 2006 required 30 days of firefighting.

Albertson et al. (2010) refers to 34 years of daily data on wildfire incidents from 1 June 1976 to 31 December 2008. There were a total of 399 wildfires in this period, recorded on 279 days. Furthermore, there were a total 112 wildfires from 1 January 2009 to 31 December 2017 recorded on 94 days (the data obtained from Moors for the Future).

Figure 4.6 shows a total of 511 wildfires in the Peak District over 41 years, with the highest number of 81 wildfires in 1976, while there were no recorded fires in 1979. Also, there were some fluctuations in the total of wildfires in other years, specifically in 2003 when there were 39 fires, most likely due to warm weather increasing number of visitors as well as periods of drought and high temperatures which increased fire risk.

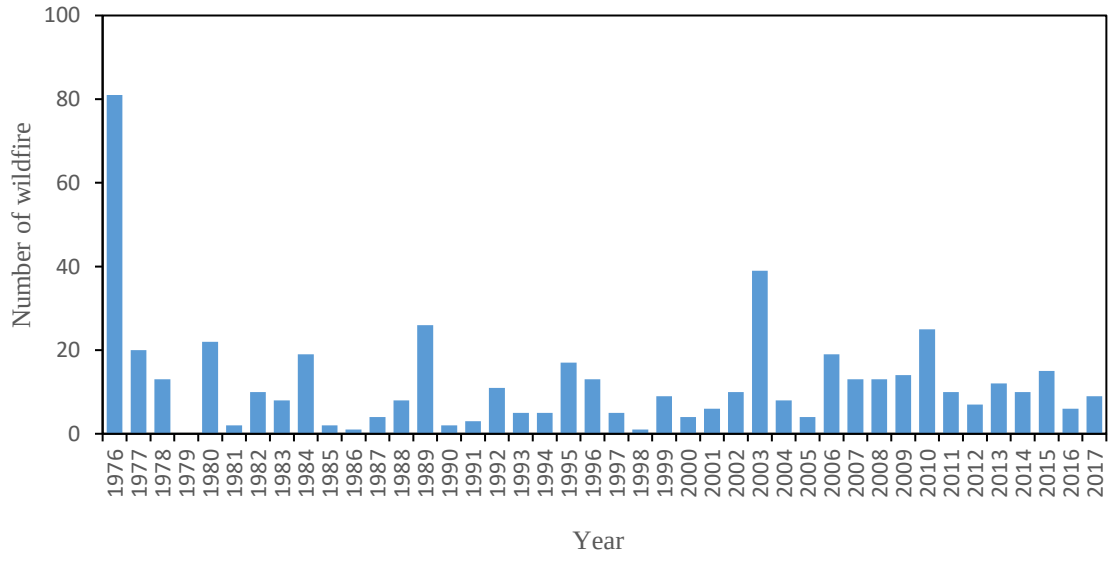

Figure 4.6: Total number of wildfires in the Peak District National Park from June 1976 to December 2017 (Source: Moorland Centre-Edale, 2018)

Most of wildfires during this period occurred in the north west and the south west of Peak District which are covered by wide areas of *Calluna* (Figure 4.7).

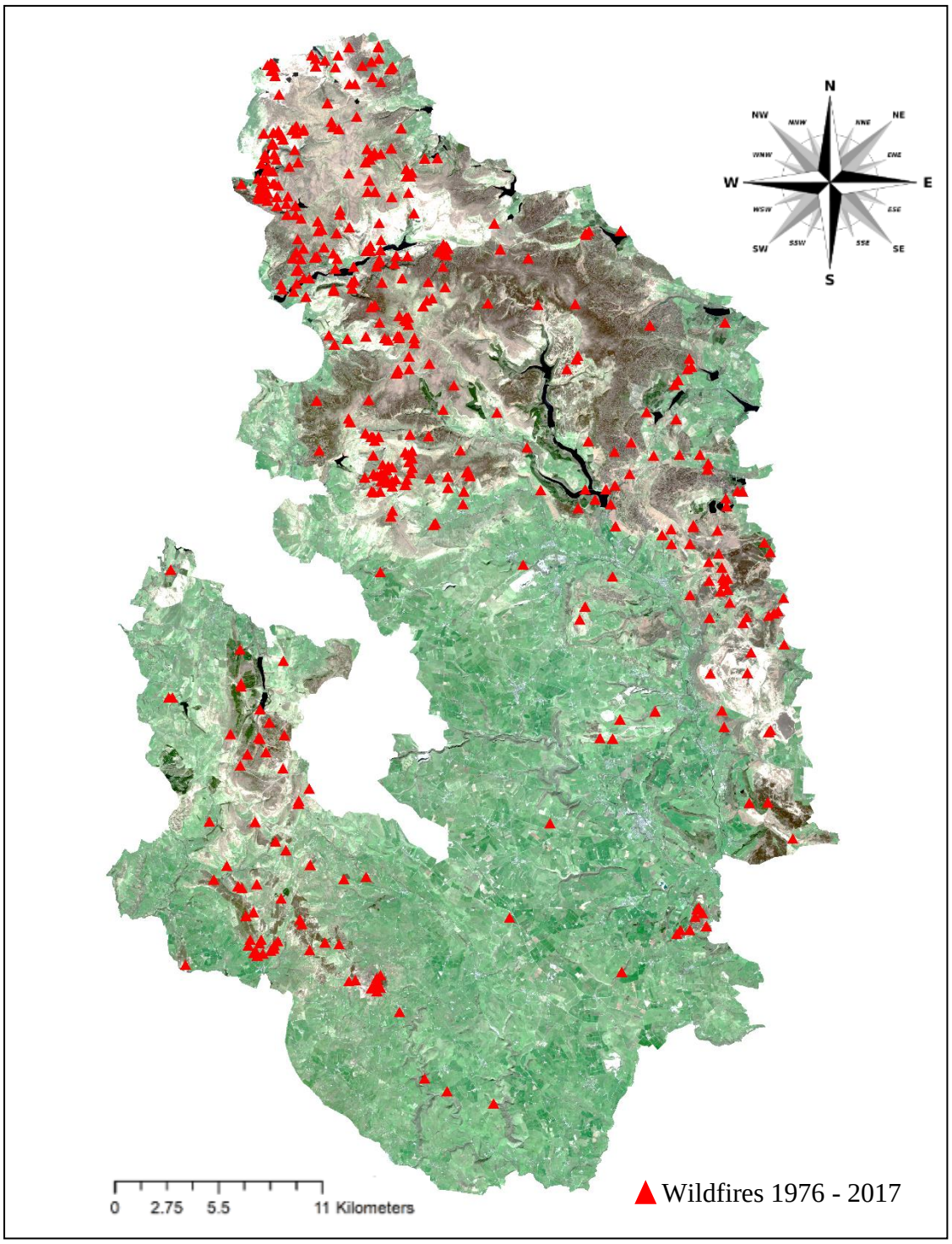

Figure 4.7: Distribution of wildfires in the Peak District National Park recorded from June 1976 to December 2017 using S2A base-image recorded 20th April 2016.

Figure 4.8 illustrates the monthly distribution of wildfires over the course of 41 years, where May was the peak month in terms of recurrence of fires and there were no fires recorded in January and December. More wildfires were reported at weekends (Figure 4.9) and on bank holidays.

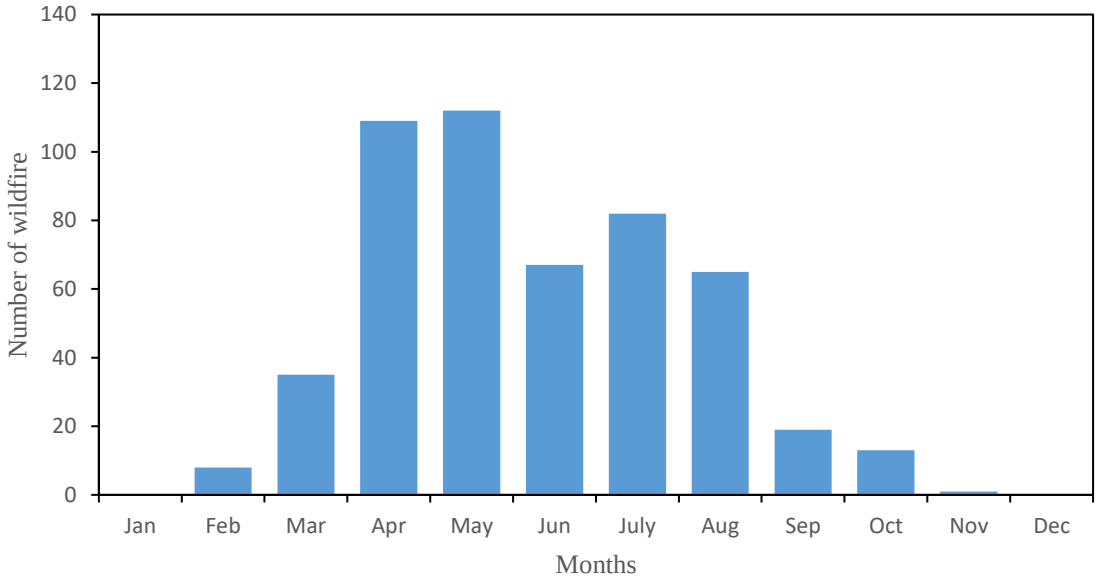

Figure 4.8: Total number of wildfires in the Peak District National Park recorded by month from June 1976 to December 2017 (Source: Albertson et al., 2010).

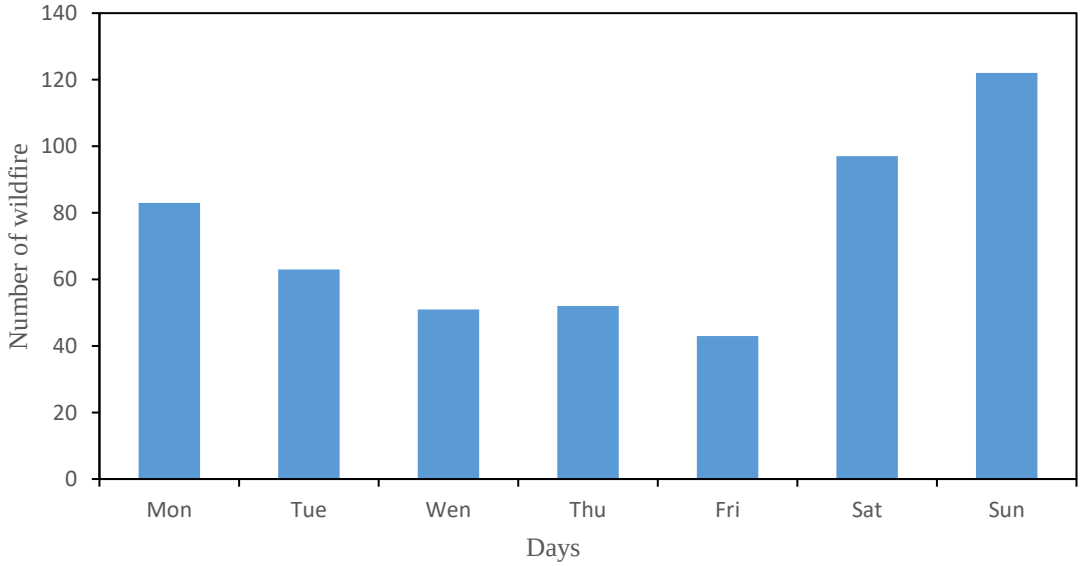

Figure 4.9: Total number of wildfires in the Peak District National Park recorded by day of week from June 1976 to December 2017 (Source: Albertson, Aylen, Cavan, & McMorrow, 2010).

However, in general, the percentage of incidence of wildfires during week days were as follows; 43% occurred on the weekend (Saturday and Sunday), while 4% were on Bank holidays and 53% occurred on weekdays (Monday to Friday) (Figure 4.10).

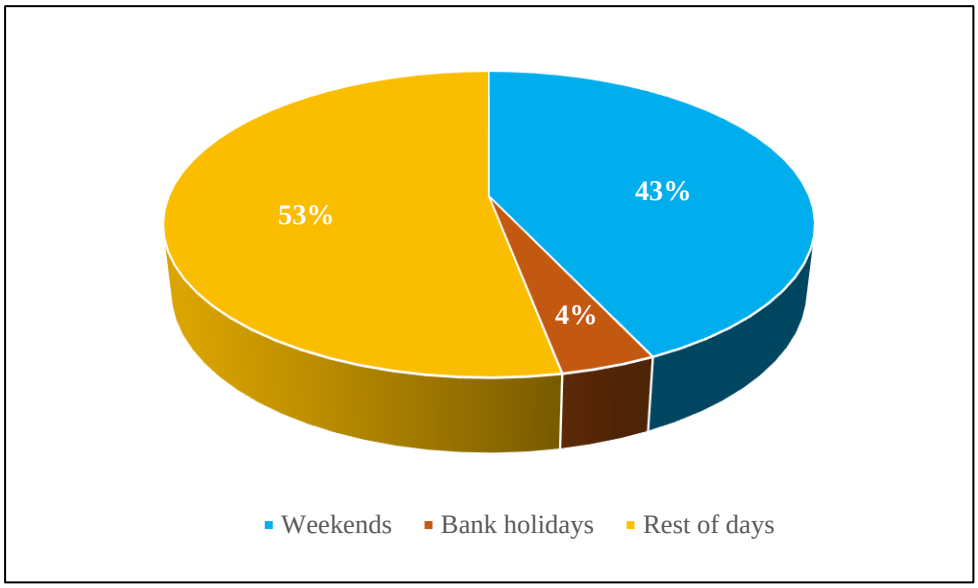

Figure 4.10: Percentage of wildfires during days of week in the Peak District National Park across 41 years.

There is a legal burning period which helps in land management of the UK uplands and moorland by optimizing productivity and ecosystem services; this period is from October until mid-April (Table 4.1) (Harper, Doerr, Santin, Froyd, & Sinnadurai, 2018). This period is suitable for periodic fire management due to soil moisture and/or frozen soil (Santana & Marrs, 2014). Wildfires are considered a threat during spring because they occur in the aboveground vegetation due to the soils retention of moisture, by contrast in summer wildfires can be more dangerous due to soil dryness (Rein, Cleaver, Ashton, Pironi, & Torero, 2008). Severe wildfires burn into the peat and destroy seed banks, preventing natural regeneration and encouraging erosion, therefore, they are recognised as a significant threat to biodiversity in the park (PDNPA, 2001).

Table 4.1: Legal prescribed burn seasons with relevant legislation (Source: Harper et al., 2018)

Uplands	legal burning period	Legislation	Code
England	1st October–15th April	The Heather and Grass Burning Code Regulations (England) 2007	The Heather and Grass Burning Code (Defra, 2007)
Wales	1st October–31st March	The Heather and Grass Burning Code Regulations (Wales) 2008	The Heather and Grass Burning Code for Wales (Welsh Assembly Government, 2008
Scotland	1st October–30th April	Hill Farming Act 1946	Muirburn Code (SEERAD, 2001)
Northern Ireland	1st September–14th April	Game Preservation Act 1928.	The Heather and Grass Burning Code (Defra, 2007)

4.6 Fieldwork study area

The study area used for the fieldwork was Burbage Moor, located 7 km south-west of Sheffield, UK, and 4 km east of Hathersage. Burbage Moor is a *Calluna*-dominated upland plateau with thin peaty soils and outcrops of Millstone Grit bedrock forming small tors and bedrock exposures (Almoustafa, 2011). The Moor is mostly above 400m and reaches a height of 438 m at Ox Stones tor in the east (Figure 4.11) (Hutchinson & Armitage, 2009). The site is part of the Eastern Moors Site of Special Scientific Interest (SSSI) and is currently managed to allow *Calluna* regrowth following severe fires in 1959 and 1976. Burbage is not managed by burning like many privately owned moorlands in the Peak District but strips of mature heather are mown every 10-15 years for conservation and fire management purposes (Anderson & Radford, 1994).

These strips of even-aged *Calluna* are often only 30-40 m wide and 70 – 100 m long and are therefore close to the spatial resolution cell size of the imagery produced by many remote sensing satellites.

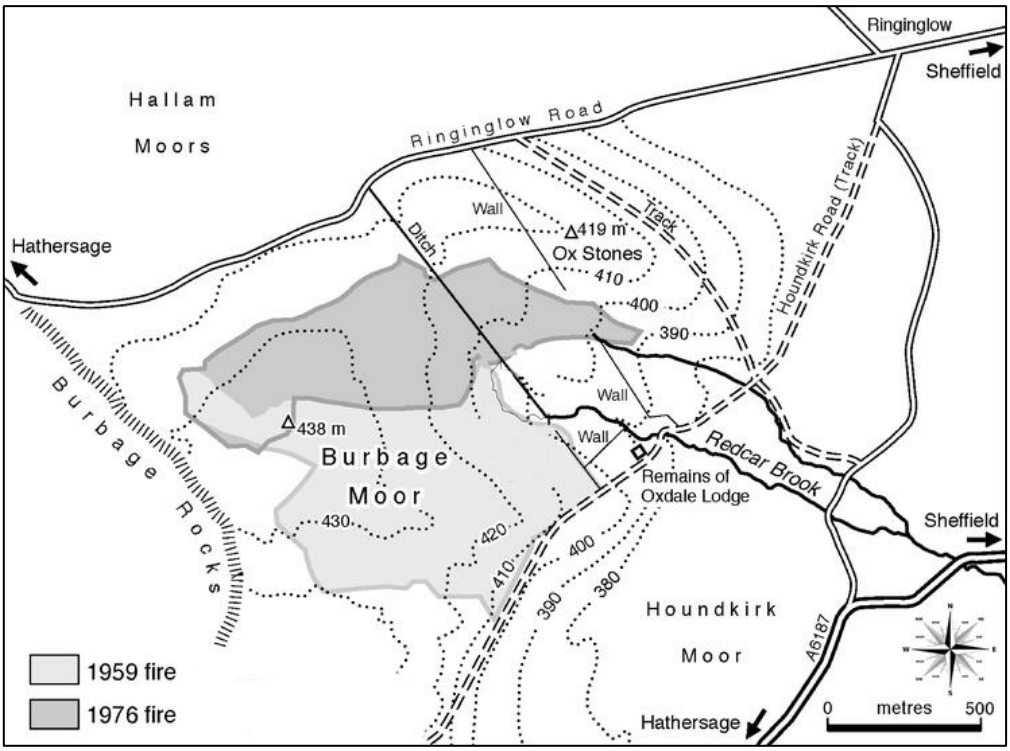

Figure 4.11: Study area Burbage Moor (Adapted from (Hutchinson & Armitage, 2009)

4.6.1 Sampling design

The fieldwork at Burbage Moor was carried out over a one year period from April 2016 to March 2017 (Figure 4.12). Measurements were acquired at five plots selected to meet a range of criteria. The plots were located within a sampling area of approximately 600 m x 200 m and each plot centre was located in a flat area with continuous *Calluna* cover (Figure 4.13). The plots were selected so as to be visually homogeneous over an area of at least 20 m in all directions from the centre point. The centre points were marked with wooden pegs as were the four corners of a north-south oriented 20 m × 20 m plot, which is representative of the pixel resolution for the satellite sensors used (Figure 4.14).

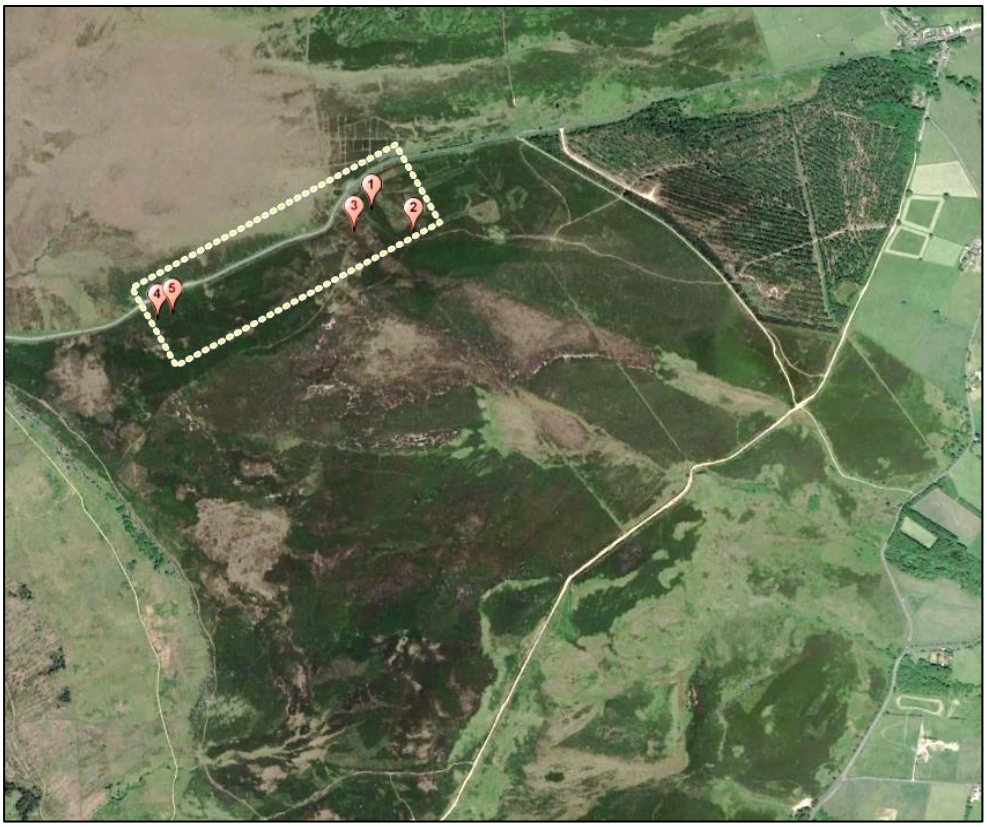

Figure 4.12: Study area Burbage Moor, showing the five sampling plots within square boundary (yellow line) (Source: Google Earth, 2018).

Figure 4.13: Establishing the field plots in the continuous cover *Calluna*.

The plot centre points were surveyed with a GPS with sub-metre accuracy. At each date five sampling locations within each plot were used to collect samples (Table 4.2), to provide a better estimate of the average moisture for each plot. In addition, this avoided the logistic difficulties of sampling randomly and ensured that all part of the plot was represented in the sampling design.

The sampling locations were the centre point and four additional points located 7 m from the centre point in a NE, NW, SE and SW direction (mid points) selected to optimise the sampling of the 20 x 20 m plot area that corresponded to the Sentinel-2A MSI spatial resolution. The five plots had small differences in terms of location, plant density and height, and soil moisture conditions (Table 4.3).

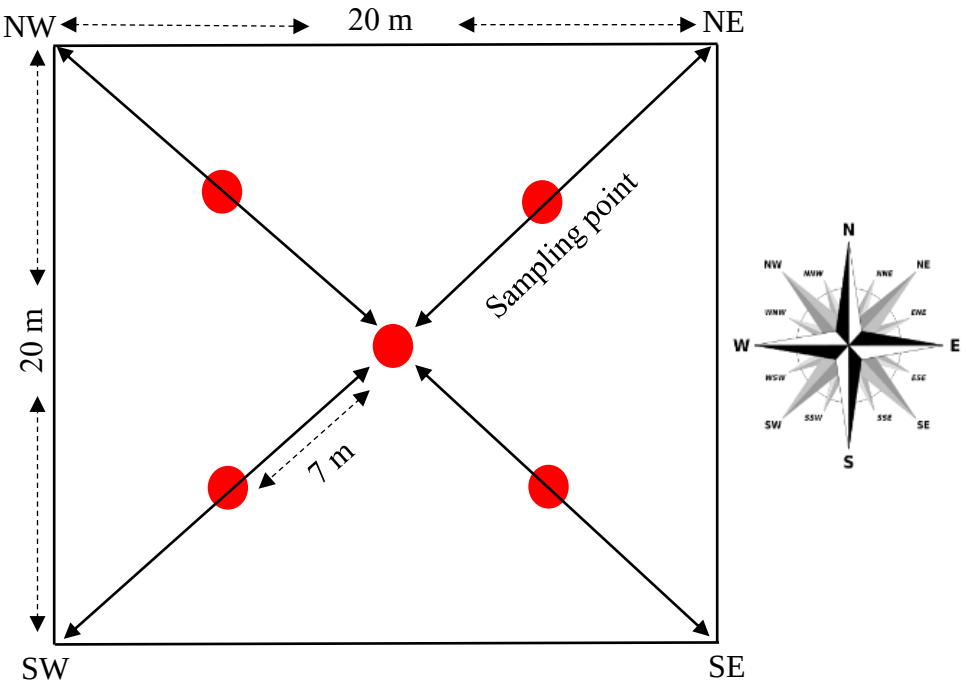

Figure 4.14: Sampling within each sample plot. The points sampled within each plot are shown by the red circles: At each point vegetation was sub-sampled in a circle to estimate FMC.

Table 4.2: Sampling locations in Peak District (Burbage Moor)

No of plot	GPS of the plot centre (OSGB)	Coordinate converter (UTM)
1	E/N:427429, 383257	30U E/N:593901,5911633
2	E/N:427545, 383186	30U E/N:594018,5911563
3	E/N:427377, 383197	30U E/N:593850,5911572
4	E/N:426815, 382962	30U E/N:593291,5911329
5	E/N:426857, 382976	30U E/N:593333,5911344

Table 4.3: Description of sampling locations in study area (Burbage Moor)

Plot	Description
Plot 1	Located around 80 m East of the main road. The plot is covered by homogeneous *Calluna*, with an average height around 49 cm in the summer and 46 cm in the winter.
Plot 2	Located around 135 m North East of plot 1. Here, pure *Calluna* denser than plot 1, and with an average height around 59 cm in the summer and 57 cm in the winter.
Plot 3	Located around 78 m North West of plot 1. Calluna was relatively sparse compared to plot 1 and 2. Plant maximum height did not exceed 43 cm in the summer, while in the winter the height was 40 cm. Plot 3 was located at a lower altitude compared to the others plots. Due to this, water remained in this plot for long time, which kept the peat soil wetter than the other plots.
Plot 4	Located around 610 m North West of plot 3 and around 60 m East of the main road. The height of the *Calluna* was 52 cm and 49 cm in the summer and winter respectively. There was a moss layer under the canopy which covered the peat soil.
Plot 5	Located around 42 m North of plot 4. The height of the *Calluna* was 50 cm in the summer and 44 cm in the winter.

Following previous research (Stonex et al. 2004; Pollet and Brown, 2007) field data were collected every three to four weeks over the 12 month sampling period reflecting the expected slow changes in moisture content of the vegetation but encompassing the full annual change of plant moisture content. Where possible field data were collected on the day of the overpass of either Sentinel-2A MSI or Landsat 8 OLI with potential clear skies, but otherwise the data were collected at least once per month.

The field data were acquired between approximately 10 am and 2pm, as recommended by Countryman and Dean (1979) since this period is associated with minimum diurnal variation in foliar moisture content (Chuvieco, Aguado, Cocero, & Riaño, 2003). Days with rain or heavy dew formation were avoided so that the surface of the canopy was always dry.

4.6.2 Vegetation and soil sampling

Vegetation samples were collected from the five plots and five sampling locations within each plot. Approximately 20g of terminal shoot material was clipped using scissors from randomly selected *Calluna* plants at each sampling point. All sampled plant material was immediately transferred to labelled airtight plastic bags in order to prevent moisture loss before weighing (Figure 4.15). In addition to the FMC sampling, small surface samples of soils of approximately 50 g were collected at the centre point of each plot. The samples were again placed in sealed plastic bags in preparation for weighing in the laboratory.

Figure 4.15: Sampling approximately 20g of terminal shoot material by using scissors.

4.7 Laboratory work

4.7.1 FMC and soil moisture measurements

Carefully labelled plastic bags were used to store soil and vegetation samples from the plots. The bags were sealed to avoid loss of moisture while being transported and the gravimetric moisture analysis was conducted in the laboratory. The analysis was done on the same day as the collection of the samples. In the case of the *Calluna* samples, an electronic balance (Metter pc 440) was used in order to record the fresh overall weight of the vegetation samples. This was followed by drying all samples for 48 hours at a temperature of 60°C in an oven. This led to the determination of their dry weight. Desbois, Deshayes, and Beudoin (1997) showed that carbonisation cannot be observed at 60°C, since at this temperature only highly volatile elements and water in vegetation are eliminated. The same electronic balance was used to record the sample's dry weight. Equation (4.1) was used to calculate the FMC of the bulk plant shoot sample. In order to estimate the soil moisture, the determination of the wet weight was followed by drying all samples for 48 hours in an oven at 45°C and thus, dry weight was identified. Equation (4.2) was used to calculate the Soil Moisture (SM).

$$FMC = \frac{Wf - Wd}{Wd} \times 100 \quad (4.1)$$

where Wf refers to the fresh weight of vegetation samples and Wd refers to the dry weight.

$$SM = \frac{Sf - Sd}{Sd} \times 100 \quad (4.1)$$

where Sf is the soil wet weight and Sd is the soil dry weight.

4.8 Remote sensing data sets

The research relied on Sentinel-2A (S2A) MSI and Landsat-8 (L8) OLI images between April 2016 and March 2017. Seven cloud-free images were identified. Other images were

rejected due to the presence of clouds. Three images coincided with field sample data collection (Table 4.4). The Earth Explorer website was used to download images from L8 OLI with acquisition dates of 04 May, 05 June, and 28 November 2016; these images were all surface reflectance. Likewise, the Scihub Copernicus website was used to download images from S2A MSI with acquisition dates of 20 April, 06 June, 19 July 2016, and 26 March 2017 and these were also processed to surface reflectance images.

Table 4.4: Dates of satellite images downloaded for the study area

Image date	Sensor	Day of year	Test Site location in image	Time	Field data collection
20-04-2016	S2A MSI	111	West side	11:22:42	√
04-05-2016	L8 OLI	125	West side	11:03:42	
05-06-2016	L8 OLI	157	West side	11:03:46	
06-06-2016	S2A MSI	158	East side	11:06:24	
19-07-2016	S2A MSI	201	West side	11:21:17	√
28-11-2016	L8 OLI	333	West side	11:04:25	
26-03-2017	S2A MSI	85/2017	West side	11:21:08	√

4.8.1 Atmospheric correction

Atmospheric correction is essential for multi–temporal or multi-site quantitative analysis of remotely sensed data (Gao, Montes, Davis, & Goetz, 2009). When computing ratio transformations, surface reflectance is a pre-requisite and this depends on the atmospheric correction method, surface attributes, and sensor design (Martins et al., 2017). There are many atmospheric correction methods for remotely sensed data. The data used here were all pre-corrected using well-established algorithm, Sen2Cor for Sentinel-2A MSI and the Landsat Ecosystem Disturbance Adaptive Processing System (LEDAPS) for Landsat 8 OLI.

4.8.1.1 Sen2Cor

Sen2Cor is used to correct Sentinel-2 Level-1C products for the effects of the atmosphere in order to deliver a Level- 2A surface reflectance product (Louis et al., 2016). The product affords Bottom-of-Atmosphere (BOA) reflectance images that are extracted from the associated Level-1C products. The Level-2A product involves a scene classification and an atmospheric correction applied to the Top-of-Atmosphere (TOA) Level-1C orthoimage products (Main-Knorn, Pflug, Debaecker, & Louis, 2015). The Level-2A main output is an orthoimage BOA corrected reflectance product. The algorithm is a combination of state-of-the-art atmospheric corrections and cirrus clouds correction, which have been tailored to the S2A sensor (Gašparović & Jogun, 2018). The Sentinel Application Platform (SNAP) software was used to correct band 8a and band 11 of the Sentinel-2A MSI data. SNAP was downloaded from the ESA Scihub website.

4.8.1.2 LEDAPS

The National Aeronautics and Space Administration (NASA) Goddard Space Flight Centre and the University of Maryland developed LEDAPS to apply atmospheric corrections to create surface-reflectance products. In addition, LEDAPS creates cloud masks to minimize the effect of clouds on the images, which can partially affect their clarity (Martins et al., 2017). LEDAPS depends on deriving the aerosol optical thickness from each Landsat image obtained, and rectifying every pixel assuming a fixed continental aerosol type (Ju, Roy, Vermote, Masek, & Kovalskyy, 2012).

4.8.2 Spectral measurements

The Normalized Difference Water Index (NDWI) is calculated by using short-wave infrared and near-infrared bands, which for L8 OLI are bands 6 and 5, and for S2A MSI the equivalent bands are 11 and 8a. In order to use both sensors, it was necessary to test for

similarity in relative spectral response curves for the spectral bands used to calculate the NDWI and MSI (Table 4.5). The metadata of the relative spectral response (RSR) profiles for the spectral bands are available from the web page of the Spectral Characteristics Viewer (USGS, 2017) provided by the US Geological Survey. Figure 4.16 shows that the spectral response function of the Landsat-8 OLI band 5 was slightly wider compared with Sentinel-2A band 8a. Landsat-8 OLI band 6 and Sentinel-2A MSI band 11 were very similar in shape (Figure 4.17). A key difference between sensors was that the spatial resolution of these bands is 20 m for S2A MSI and 30 m for Landsat 8 OLI.

Table 4.5: Comparison of Sentinel-2A MSI and Landsat-8 OLI spectral bands (Source: (Zhu & Liu, 2015)

<table>
<tr><td colspan="3">Sentinel -2A MSI</td><td colspan="3">L8 OLI</td></tr>
<tr><td>Bands</td><td>Wavelength (µm)</td><td>Resolution (m)</td><td>Bands</td><td>Wavelength (µm)</td><td>Resolution (m)</td></tr>
<tr><td>Band 1</td><td>0.43 - 0.45</td><td>60</td><td>Band 1</td><td>0.43 - 0.45</td><td>30</td></tr>
<tr><td>Band 2</td><td>0.45 - 0.52</td><td>10</td><td>Band 2</td><td>0.45 - 0.51</td><td>30</td></tr>
<tr><td>Band 3</td><td>0.54 - 0.57</td><td>10</td><td>Band 3</td><td>0.53 - 0.59</td><td>30</td></tr>
<tr><td>Band 4</td><td>0.65 – 0.68</td><td>10</td><td>Band 4</td><td>0.64 - 0.67</td><td>30</td></tr>
<tr><td>Band 5</td><td>0.69 - 0.71</td><td>20</td><td>Band 5</td><td>0.85 - 0.88</td><td>30</td></tr>
<tr><td>Band 6</td><td>0.73 – 0.74</td><td>20</td><td>Band 6</td><td>1.57 - 1.65</td><td>30</td></tr>
<tr><td>Band 7</td><td>0.77 - 0.79</td><td>20</td><td>Band 7</td><td>2.11 - 2.29</td><td>30</td></tr>
<tr><td>Band 8</td><td>0.78 – 0.89</td><td>10</td><td>Band 8</td><td>0.50 - 0.68</td><td>15</td></tr>
<tr><td>Band 8a</td><td>0.85 – 0.87</td><td>20</td><td>Band 9</td><td>1.36 - 1.38</td><td>30</td></tr>
<tr><td>Band 9</td><td>0.93 – 0.95</td><td>60</td><td>Band 10</td><td>10.60 - 11.19</td><td>100*(30)</td></tr>
<tr><td>Band 10</td><td>1.36 – 1.39</td><td>60</td><td>Band 11</td><td>11.50 - 12.51</td><td>100*(30)</td></tr>
<tr><td>Band 11</td><td>1.56 – 1.65</td><td>20</td><td colspan="3" rowspan="3">Approximate scene size
170 km north-south by 183 km east-west</td></tr>
<tr><td>Band 12</td><td>2.10 - 2.28</td><td>20</td></tr>
<tr><td colspan="3">Approximate scene size
290 km swath width</td></tr>
</table>

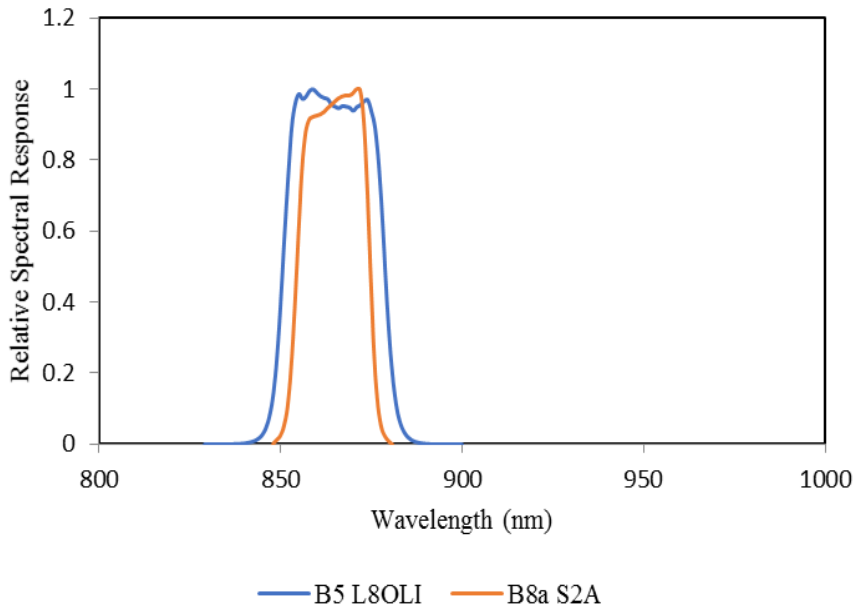

Figure 4.16: Spectral response functions for band 5 of L8 OLI and band 8a of Sentinel-2A MSI.

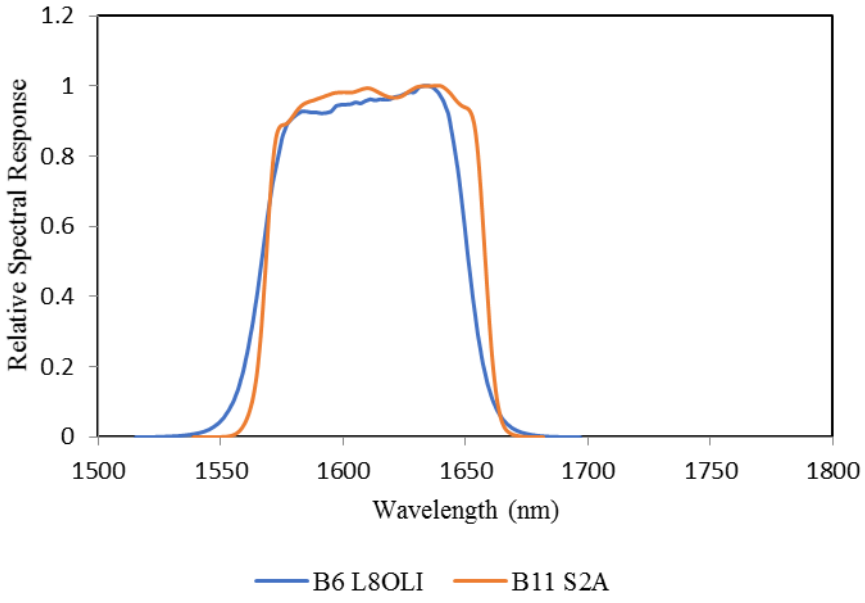

Figure 4.17: Spectral response functions for band 6 of L8 OLI and band 11of Sentinel-2A MSI.

4.8.3 Surface reflectance validation

Surface reflectance products are required for all images used. In order to check the relative accuracy of the surface reflectance products, 12 targets were selected from two images with close acquisition dates, those being 05-06-2016 and 06-06-2016 for L8 OLI and S2A MSI respectively. The reflectance values were collected from both images for a range of surfaces including quarries, airports and lakes, with a range of reflectance values. The results confirmed that the atmospheric correction procedures were accurate. There were very strong correlations between the reflectance for both the NIR and SWIR band for the two sensors (Figure 4.18). This result provided confidence that the SR products could be used in the time series NDWI and MSI analysis.

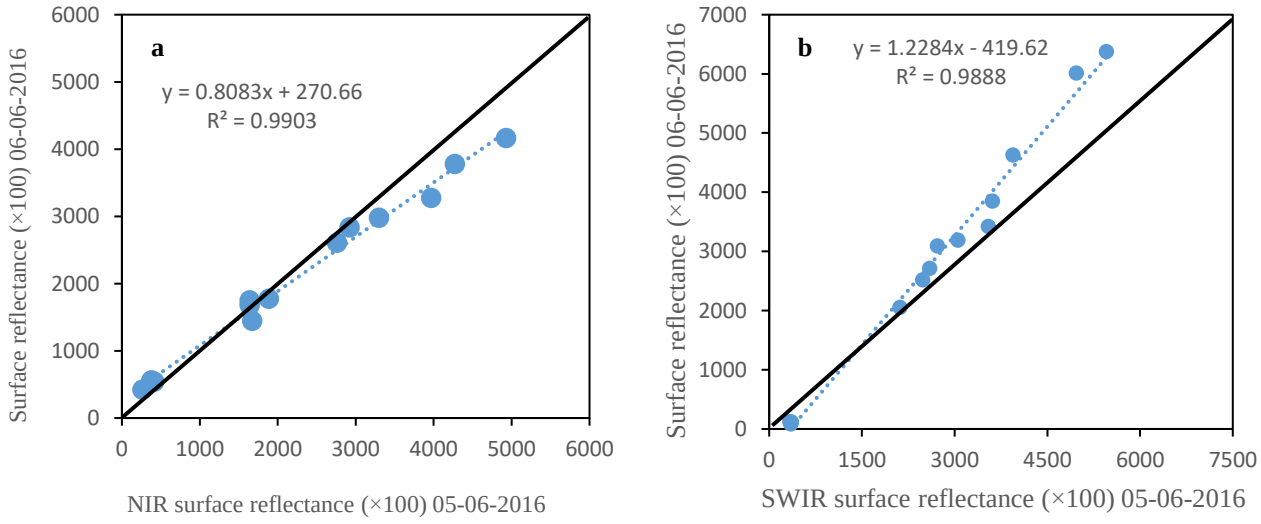

Figure 4.18: Linear regression comparison between surface reflectance for (a) the Near Infrared (NIR) band 8a of S2A MSI and the L8 OLI equivalent band 5. (b) Comparison between Shortwave Infrared (SWIR) band 11 from S2A MSI with the L8 OLI equivalent band 6.

4.9 Spectral sampling of remote sensing data

To extract the spectral reflectance from each image it was necessary to extract the data for specific pixels corresponding to the field sampling plots, recalling there is a difference in pixel resolution between S2A SMI and L8 OLI. Although, the plots were designed primarily for the 20 m pixels of S2A MSI, it was also necessary to extract data for the L8OLI. The plots were located on homogeneous areas of *Calluna* approximately 40 m across and were oriented N-S. As a result, the plot centre points were used to identify a single pixel to represent the spectral reflectance of each study plot (Figure 4.19).

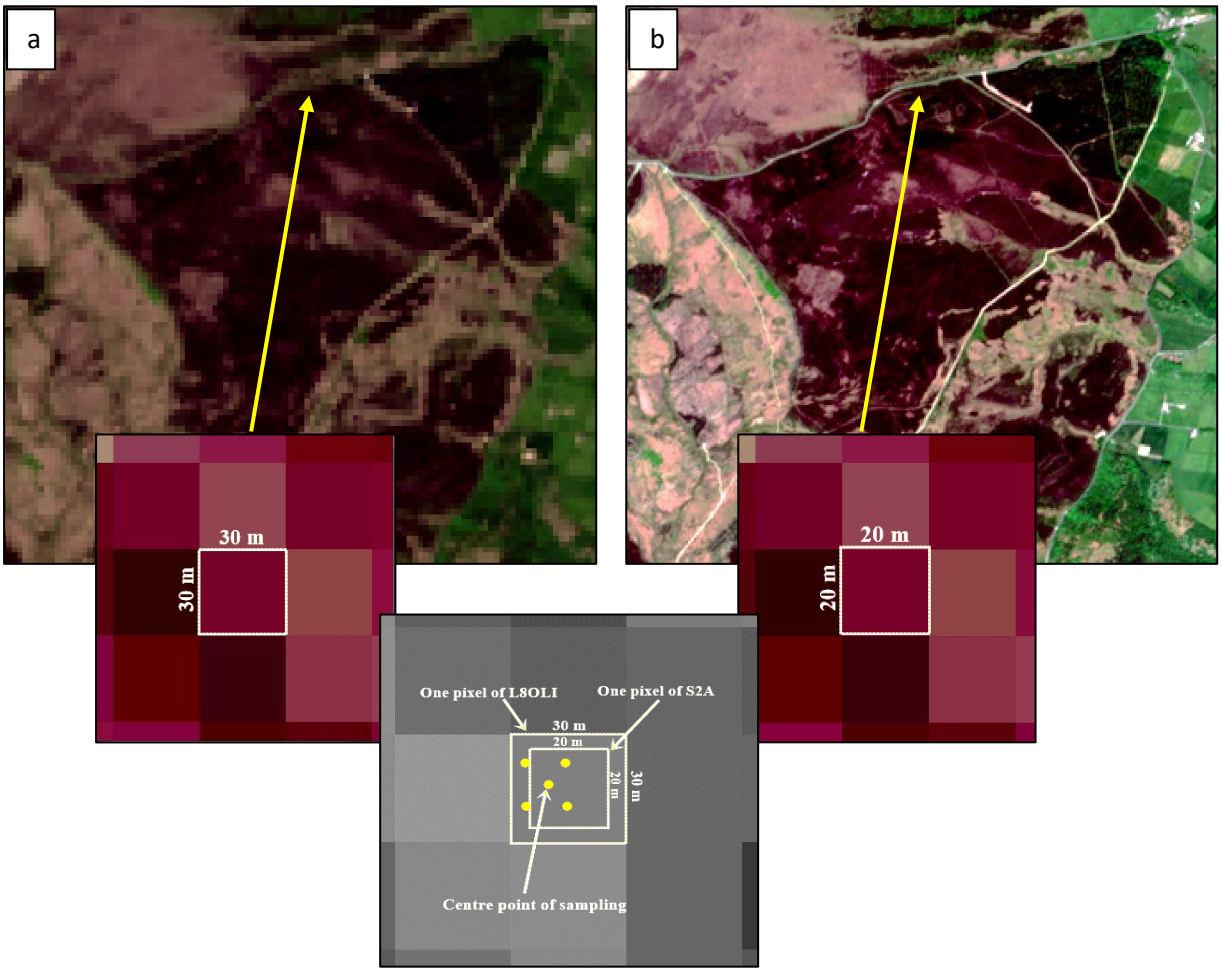

Figure 4.19: Comparison of (a) One pixel of L8 OLI image 05-06-2016 with centre point of plot and (b) One pixel of S2A MSI image 06-06-2016 with centre point of plot.

4.10 Conclusion

This chapter has described the general background on the study area, the sampling design, measuring fuel moisture content and soil moisture content and the approaches for pre-processing the satellite imagery. Weather constraints meant that only a limited number of cloud-free satellite images were available over the 12 month sampling period. Field data were collected simultaneously on three dates and close to a satellite over-pass on other dates. Therefore, only three images were obtained during 12 months which matched field and satellite, although the aim was to collect data monthly with coincident images on the same day. The next chapter will use the field data on FMC to examine the variation of FMC during the year. In addition, the image data will be used to investigate the relationship between FMC and both the Normalized Difference Water Index and Moisture Stress Index across time, which will then be used to map these relationships at landscape scale.

CHAPTER 5: FUEL MOISTURE CONTENT AT PLOT AND LANDSCAPE SCALE

Summary

This chapter reports the results of the field experiment to investigate the estimation of FMC across space and time at Burbage Moor. FMC values of five plots measured over 12 months were plotted against the measurement date in order to assess temporal FMC trends. Standard errors of FMC values were calculated to quantify the errors in the measured FMC values. Soil moisture was assessed to characterise the temporal variability across the test site and the likely effects on FMC estimation. Seven images from Sentinel-2A MSI and Landsat-8 OLI were used to calculate NDWI and MSI at Burbage Moor, three near-coincident with sampling. These data were used in order to obtain a relationship between FMC and VI (NDWI and MSI) and, from this FMC maps of the Peak District. The results show that FMC can be estimated with an accuracy of around 15.74% using the MSI. The landscape scale mapping shows the spatial and temporal variation in FMC in areas of *Calluna* at a range of scales.

5.1 Introduction

This chapter presents the results of the fieldwork-based analysis of the relationships between remotely sensed data and *Calluna* FMC estimated using direct fieldwork measurements. FMC was measured across five plots at Burbage Moor over 12 months. Results of the soil moisture sampling are also presented. Remotely sensed data were used to investigate the relationship between FMC and VI (NDWI and MSI) by analysis of images from two different sensors (S2A MSI and L8 OLI) during the study period. This relationship was assessed in order to determine the likely accuracy of FMC estimates derived from such data sources. The plot-based results are then extended to allow FMC mapping at landscape scale to assess the possible application of this approach to modelling fire risk in UK uplands using remote sensing data.

5.2 Fuel moisture content variations of *Calluna*

The variability in *Calluna* FMC measured at Burbage Moor is shown in Figure 5.1, both temporally and spatially. For all plots, the FMC tended to increase up to a value of around 172% in July (Julian data 201). However, the maximum value of around 212% was reached in December (Julian date 351) in plots 4 and 5 (refer table 4.3). The variation was large for FMC values between the different samples at a given date (see section 2.2.2 for phenological cycle). Overall plots 3, 4 and 5 showed the lowest FMC values while plot 4 and 5 showed the highest FMC values (Figure 5.1).

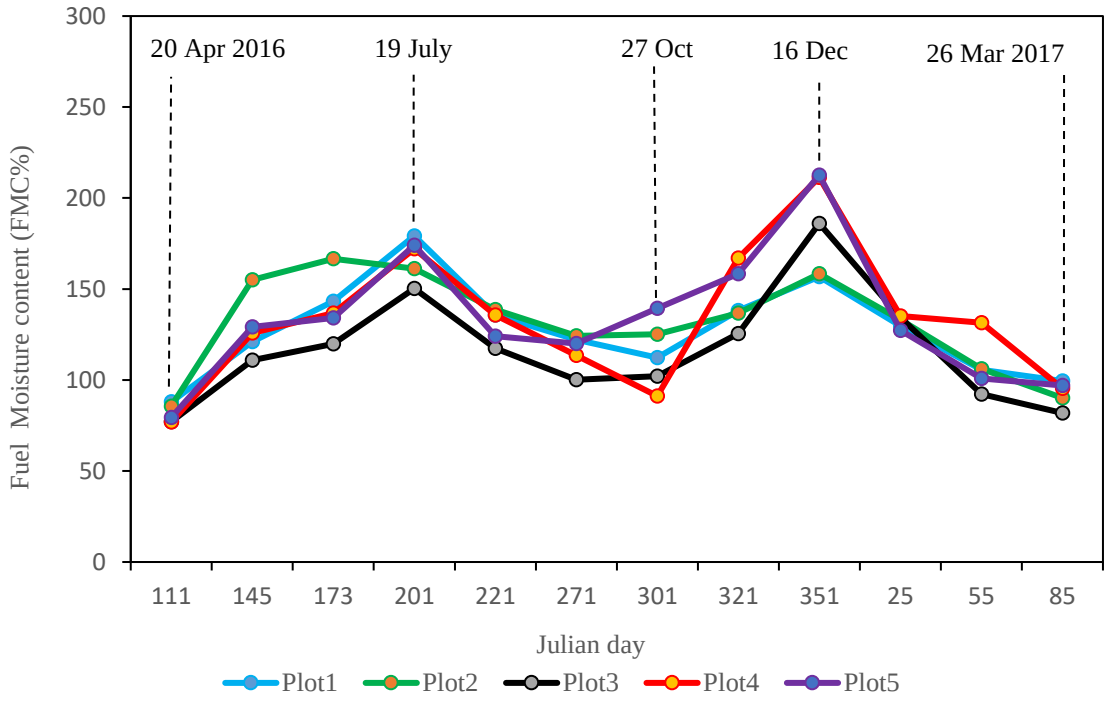

Figure 5.1: FMC values versus day of year for sample plots

Table 5.1 shows the meteorological conditions on the sampling date and suggests that there was no obvious explanation of the high and variable FMC in December 2016. High soil moisture may have been a factor but there are insufficient data on this to be certain.

Table 5.1: Meteorological data for days of sampling (Source: Met Office)

Date of sampling	Day of year	Average Temperature (°C)	Rain (mm)			Average Wind speed (km/hr)
		Day of Sampling	Week Before	Day Before	Day of Sampling	Day of Sampling
20-04-2016	111	9.1	13.6	0	0	6.1
25-05-2016	145	8.2	18.4	0.2	5.0	14.5
21-06-2016	173	15.9	31.2	1.4	0	7.2
19-07-2016	201	24.2	0.6	0	0	3.1
08-08-2016	221	14.1	1.8	0.8	0.6	12.3
27-09-2016	271	14.0	16.8	4.4	0	13.3
27-10-2016	301	11.8	0.8	0	0	15.9
16-11-2016	321	8.2	9.4	0	0.4	16.9
16-12-2016	351	7.8	7.0	0.2	0	9.8
25-01-2017	25	3.6	0.8	0	0.2	15.6
24-02-2017	55	4.8	21.2	19.2	0.2	16.1
26-03-2017	85	7.1	13.0	0	0	8.6

Across the course of data collection, the same general pattern was followed by the temporal variation in mean FMC of the plots (Figure 5.2). Summer months (June and July) are associated with the largest amount of live green material in the canopies and FMC values are normally at their highest. From April 2016 to March 2017 the FMC values at all plots show the same pattern of variation (Figures 5.2), although there is evidence of some variation in the level of FMC values between the plots. Plot 3 showed the lowest temporal variation while plot 4 and 5 showed the largest temporal variation (Table 5.2). The lowest mean value of FMC for the *Calluna* was 76% in plot 4 at 20th Apr (Julian date 111) while highest value recorded was 212% in plot 5 at 16 Dec (Julian date 351). A paired two sample t-test was used to compare between mean FMC at each successive sampling date. All differences were

significant at the 95% confidence level, apart from the September - October 2016 dates (Figures 5.2).

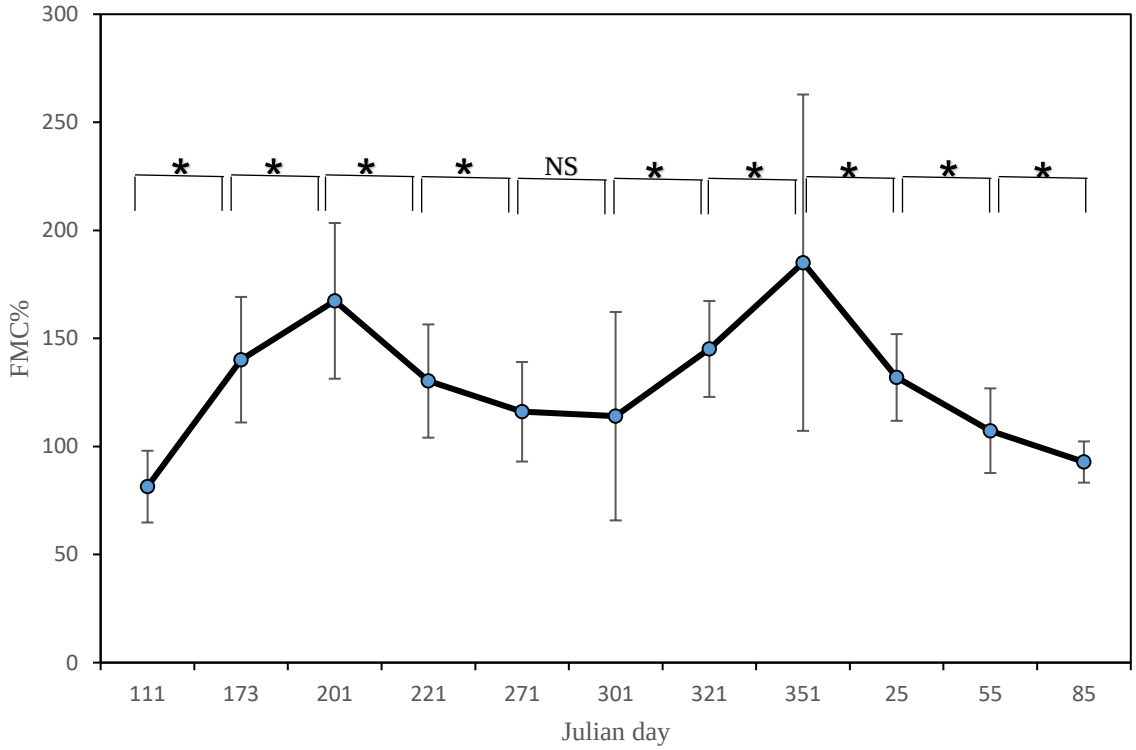

Figure 5.2: Mean FMC value versus day of year for the five plots. Vertical bars show -/+ one standard deviation (n = 25). * indicates two sample t-test, P significant at 95% confidence level, (NS) = not significant.

Table 5.2: FMC of the plots at each measurement date

Date of sampling	Julian day	Average FMC of each plot				
		P1	P2	P3	P4	P5
20/04/2016	111	87.94	85.64	77.11	76.91	79.49
25/05/2016	145	121.18	155.08	110.96	125.81	129.27
21/06/2016	173	143.35	166.61	119.78	136.83	134.16
19/07/2016	201	179.22	161.19	150.31	172.12	174.05
08/08/2016	221	135.71	138.61	117.38	135.67	124.02
27/09/2016	271	122.22	124.34	100.13	113.59	119.96
27/10/2016	301	112.38	125.07	102.05	91.12	139.41
16/11/2016	321	138.13	136.81	125.43	166.95	158.31
16/12/2016	351	156.87	158.33	186.03	211.32	212.63
25/01/2017	25	129.79	132.98	134.33	135.25	127.28
24/02/2017	55	105.59	106.13	92.32	131.54	100.92
26/03/2017	85	99.54	90.17	81.83	95.44	97.08

Figure 5.3 shows FMC variation for each plot during the 12 months. The highest FMC in the five plots was in December (Julian day 351), while the lowest FMC values were recorded in April (Julian day 111). In addition, there was an increase in FMC in summer, and particularly in July (Julian day 201) in all of the plots.

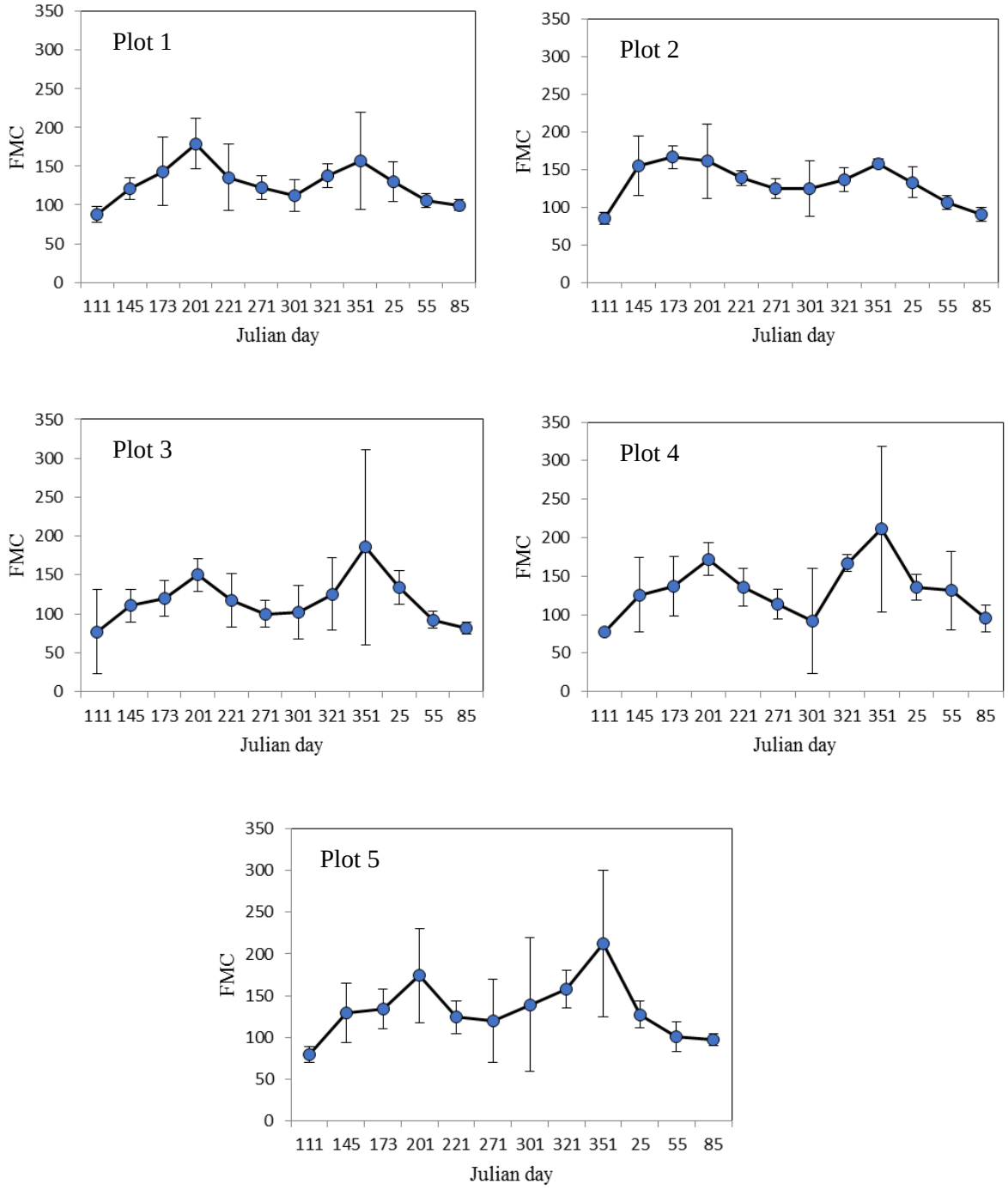

Figure 5.3: FMC versus day of year for each plot

5.3 Soil moisture variations

Samples from all the plots were used to measure the soil moisture (SM) during the period of data collection. Soil moisture did not show a large variation across the plots although insufficient samples were collected to test this statistically (Figure 5.4). The maximum SM was recorded in April (Julian day 111), while the minimum value of SM% was in August (Julian day 221). There was quasi stability in SM% from December 2016 to March 2017, in addition to decreased SM% in the plots particularly in summer. Table 5.3 illustrates that the highest value of SM% was 90% in plot 3 on 20th April, while the lowest SM was 48% in plot 2 on 8th August.

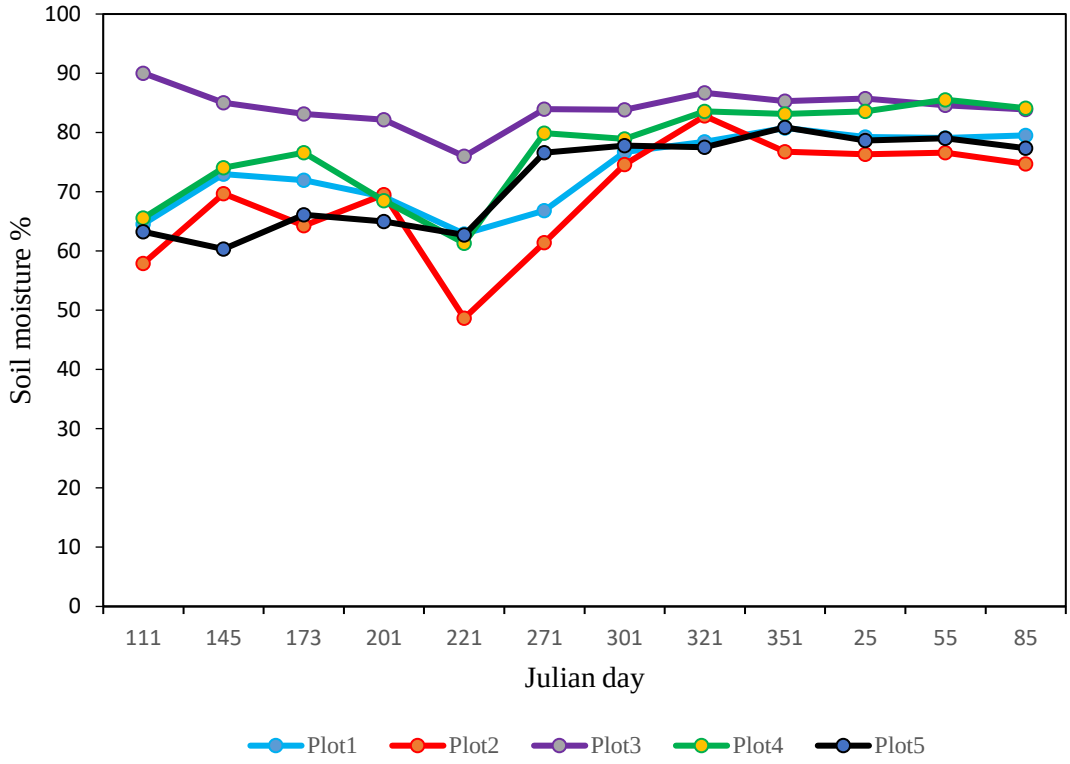

Figure 5.4: Soil moisture variations at each plot during period of data collection

Table 5.3: Soil moisture (SM) variations at each plot

Date of sampling	Julian day	SM% of each plot				
		P1	P2	P3	P4	P5
20/04/2016	111	64.52	57.91	90.02	65.58	63.26
25/05/2016	145	73.00	69.68	85.02	74.07	60.32
21/06/2016	173	71.94	64.27	83.13	76.59	66.10
19/07/2016	201	69.10	69.50	82.14	68.51	64.99
08/08/2016	221	62.89	48.65	75.98	61.31	62.71
27/09/2016	271	66.81	61.43	83.95	79.87	76.58
27/10/2016	301	76.72	74.60	83.83	78.93	77.78
16/11/2016	321	78.40	82.79	86.72	83.54	77.49
16/12/2016	351	80.76	76.78	85.28	83.12	80.86
25/01/2017	25	79.27	76.30	85.75	83.55	78.67
24/02/2017	55	79.05	76.57	84.61	85.53	79.04
26/03/2017	85	79.52	74.68	83.90	84.11	77.34

5.4 Relationship between FMC and VI

The centre coordinates of all plots were recorded by GPS, and the coordinates were changed to UTM as explained in the previous chapter (Table 4.2). These locations were identified on the satellite images and then used for calculating the NDWI and MSI for the plots. One 20×20 m pixel for S2A MSI image and one 30×30 m pixel for L8 OLI image was located using the plot centre coordinates. The FMC of each plot on the day of satellite overpass was determined by linear interpolation of the FMC of the closest dates of sampling before and after the overpass. The largest 'gap' from ground sampling to satellite overpass was 21 days (between 04 May 2016 and 21 May 2016) (Table 5.4), but most gaps were less than 2-3 days. Surface reflectance was extracted for the two bands (NIR and SWIR) and used to compute the NDWI and MSI for each plot at each date using the NDWI equation 5.1 and MSI equation 5.2.

$$NDWI = \frac{NIR\text{-}SWIR}{NIR+SWIR} \tag{5.1}$$

$$MSI = \frac{SWIR}{NIR} \tag{5.2}$$

Where NIR and SWIR are the surface reflectance in the near-infrared and shortwave infrared bands of MSI and OLI as described earlier.

Table 5.4: The gaps between ground sampling and satellite overpass dates

Data	20 Apr 2016	04 May	25 May	05 Jun	06 Jun	21 Jun	19 July	08 Aug	27 Sep	27 Oct	16 Nov	28 Nov	16 Dec	25 Jan	24 Feb	26 Mar 2017
Sampling																
Overpass																

Table 5.5 shows the values of NDWI and MSI extracted from one pixel centred on the centre coordinates of the plots. Simple linear regression and coefficient of determination were used to measure the form and strength of the relationship between the VI (NDWI and MSI) and FMC.

Table 5.5: NDWI and MSI values calculated by using one pixel from each plot

Data of image	**Satellite overpass**	**Value of NDWI and MSI from one pixel at each plot**									
		P1		**P2**		**P3**		**P4**		**P5**	
		NDWI	**MSI**	**NDWI**	**MSI**	**NDWI**	**MSI**	**NDWI**	**MSI**	**NDWI**	**MSI**
20/04/2016	S2A MSI	0.083	0.846	0.076	0.858	0.060	0.841	0.092	0.830	0.077	0.856
04/05/2016	L8 OLI	0.098	0.795	0.102	0.826	0.088	0.824	0.141	0.765	0.159	0.728
05/06/2016	L8 OLI	0.147	0.721	0.162	0.703	0.098	0.812	0.173	0.705	0.157	0.729
06/06/2016	S2A MSI	0.141	0.745	0.154	0.728	0.102	0.811	0.124	0.779	0.132	0.767
19/07/2016	S2A MSI	0.311	0.526	0.245	0.606	0.173	0.705	0.297	0.542	0.263	0.583
28/11/2016	L8 OLI	0.246	0.593	0.242	0.603	0.223	0.631	0.301	0.531	0.281	0.564
26/03/2017	S2A MSI	0.151	0.737	0.131	0.768	0.084	0.845	0.141	0.753	0.128	0.772

Figure 5.5 shows the data for the five sample plots with each date as a different colour. The general trend shows a statistically significant linear relationship ($P < 0.05$) with an R^2 of 0.82. For any single date, there is generally a weak linear relationship between NDWI and FMC because the FMC range is small. For the closely paired S2A MSI and L8 OLI dates the NDWI was very similar (yellow and black colours), though again there was some scatter about the regression line. Although, the data for both S2A MSI and Landsat 8 OLI are plotted together, there was a similar underlying relationship for both sensors.

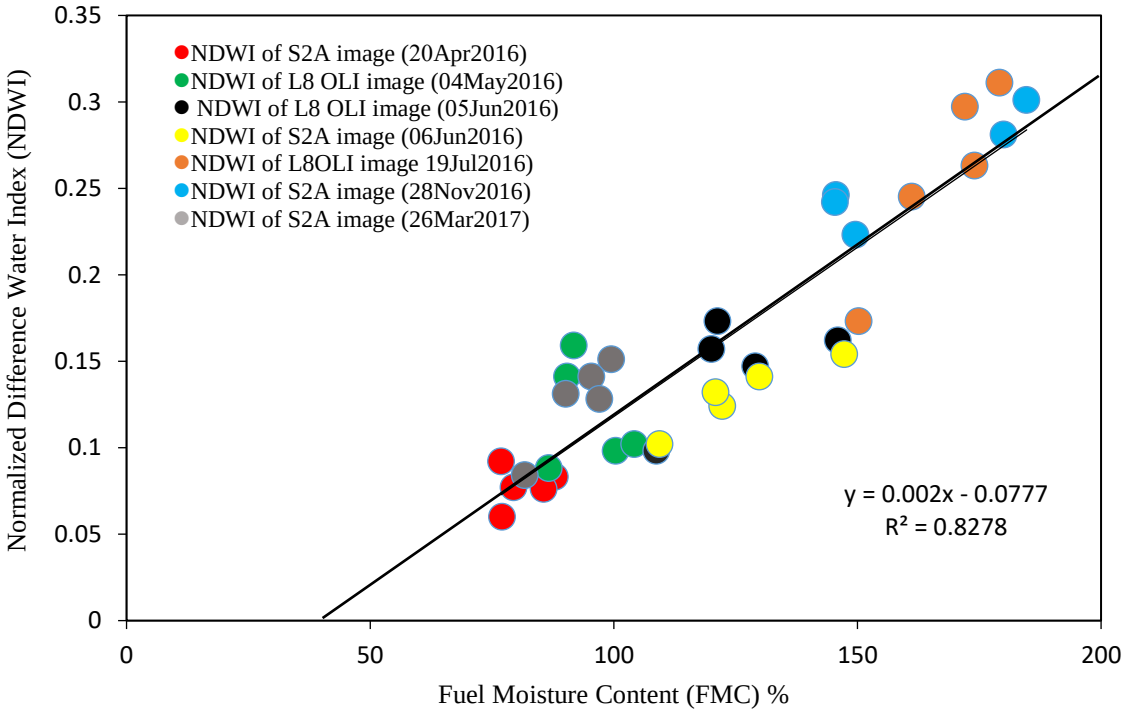

Figure 5.5: Relationship between Normalized Difference Water Index and FMC using seven satellite images.

Figure 5.6 shows a strong relationship between FMC and MSI with a statistically significant negative linear relationship ($P < 0.05$) with an R^2 of 0.84, and relatively little scatter about the regression line. Since the MSI gave the strongest correlation with FMC, this regression equation forms the basis of a validation test in the next step (section 5.5) and for the spatial prediction of FMC at landscape scale in the last part of this chapter (section 5.6).

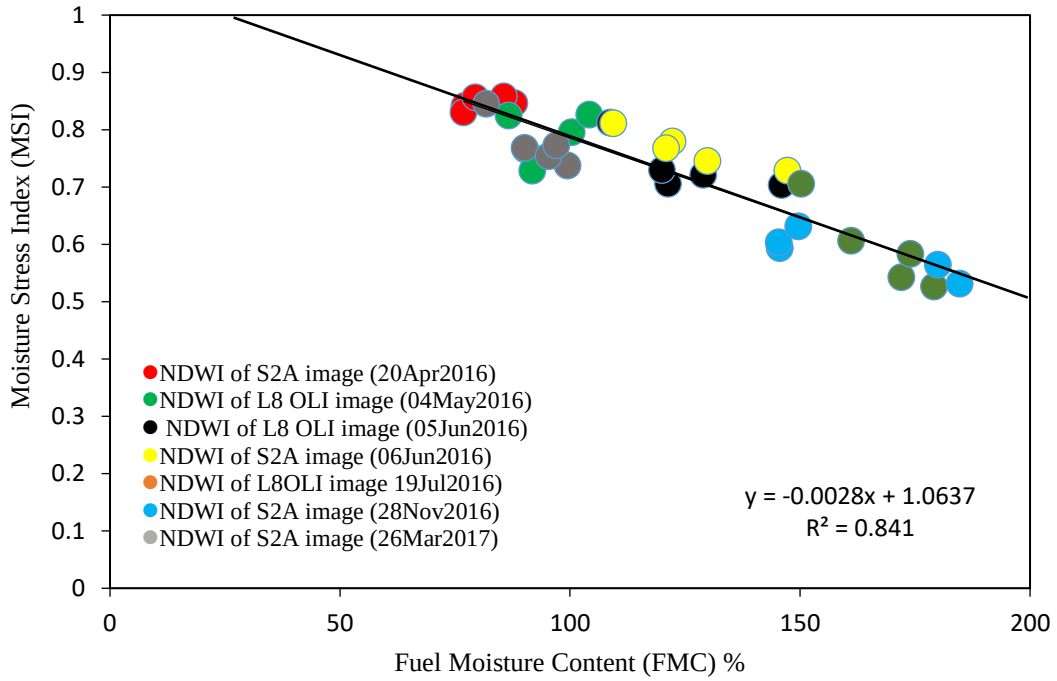

Figure 5.6: Relationship between Moisture Stress Index and FMC using seven satellite images.

5.5 Testing the accuracy of FMC estimation

The Leave One Out (LOO) cross-validation approach was used to test the accuracy of the FMC estimation across the test site. It is mainly used to estimate how accurately a predictive model will perform in practice and is useful as it makes maximum use of small samples. RMSE is a frequently used measure of the differences between values predicted by a model or an estimator and the values observed and is used here as an accuracy metric (Olden and Jackson, 2000). The measured and estimated FMC and root-mean-square error (RMSE) are calculated to test the ability of each regression model to estimate FMC. The use of r, in this case, assesses the model accuracy whereas the use of RMSE assesses model precision. Lower values of RMSE show that it is more precise while higher values indicate that the model is less precise. The LOO approach was applied to the MSI-FMC regression relationships.

In LOO, one sample is first omitted before computing the regression equation, and FMC estimated for the omitted sample. This process is continued with each sample leaving one out in turn. Figure 5.7 shows FMC estimated using the MSI. The correlation was 0.84 and the RMSE 15.74% (sample size = 25). This result is the first demonstration of FMC estimation for moorland vegetation in the UK derived from satellite imagery. This finding is comparable with Yebra, Chuvieco, and Riaño (2008) who obtained an R^2 of 0.72 and RMSE 16.01% for FMC estimation in Mediterranean shrublands with a sample size of 40, Al-Moustafa et al. (2012) for upland vegetation in UK with an R^2 of 0.71 and RMSE of 16.8% (n=20), and Quan et al. (2017) for forests in Sichuan province, China, with an R^2 of 0.86 and RMSE 32.35% (n=41).

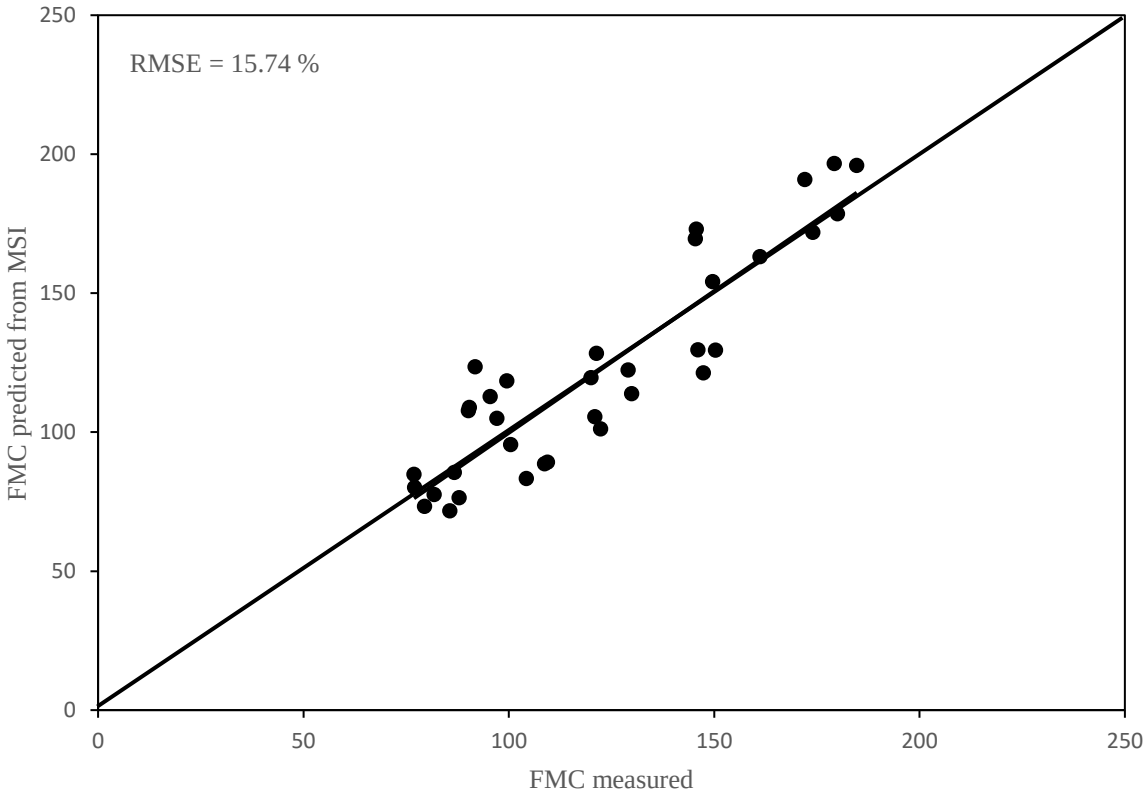

Figure 5.7: Measured versus estimated FMC values for all plots

5.6 Mapping FMC variations at landscape scale

5.6.1 Methods

The relationship between FMC and MSI (Figure 5.6) was used to produce seven FMC images, obtained from the two different sensors (L8 OLI and S2A MSI). The imagery was a sub-set of the original data sets covering the upland of the Peak District National Park and encompassing a wide range of land cover types. The 2015 UK Land cover map (Version 1.2) was used to select *Calluna* areas across the Peak District at landscape scale (the 'Heather' class in the UKLCM 2015). The map is a parcel-based land cover map for the UK, created by classifying satellite data into 21 land cover classes. The classes are based on the UK Biodiversity Action Plan Broad Habitat definitions (Figure 5.8). *Calluna* areas (purple color) were extracted from the land cover map using ArcMap software to create a shapefile, and this was then used as a mask on the FMC images (Figure 5.9). These maps were not validated independently as visiting a larger number of test sites across a large area on each of the sampling dates was impractical. However, it is assumed for the purpose of interpretation that the mapped FMC has the same error characteristics as that of validation data for the Burbage test site.

5.6.2 FMC variations

The estimated FMC values in these images varied from 0% to 349% for some areas of *Calluna*. The FMC values exhibit large variation across the Peak District area at all seven dates. Figure 5.10a-g shows that there was a general trend of higher FMC across the areas as summer progresses, shown by a change from yellow/orange color to blue/green in the images. There was also a trend of lower FMC in the eastern areas of *Calluna*, compared to the west, although this pattern was not always clear. At a more local scale there was also spatial variability in the FMC estimates, particularly in areas that correspond to extensive

areas of moorland managed by burning strips of heather to promote game bird populations. These areas appear like a chequer-board in the imagery and have the same appearance in the FMC images suggesting that the different aged strips of *Calluna* have different FMC.

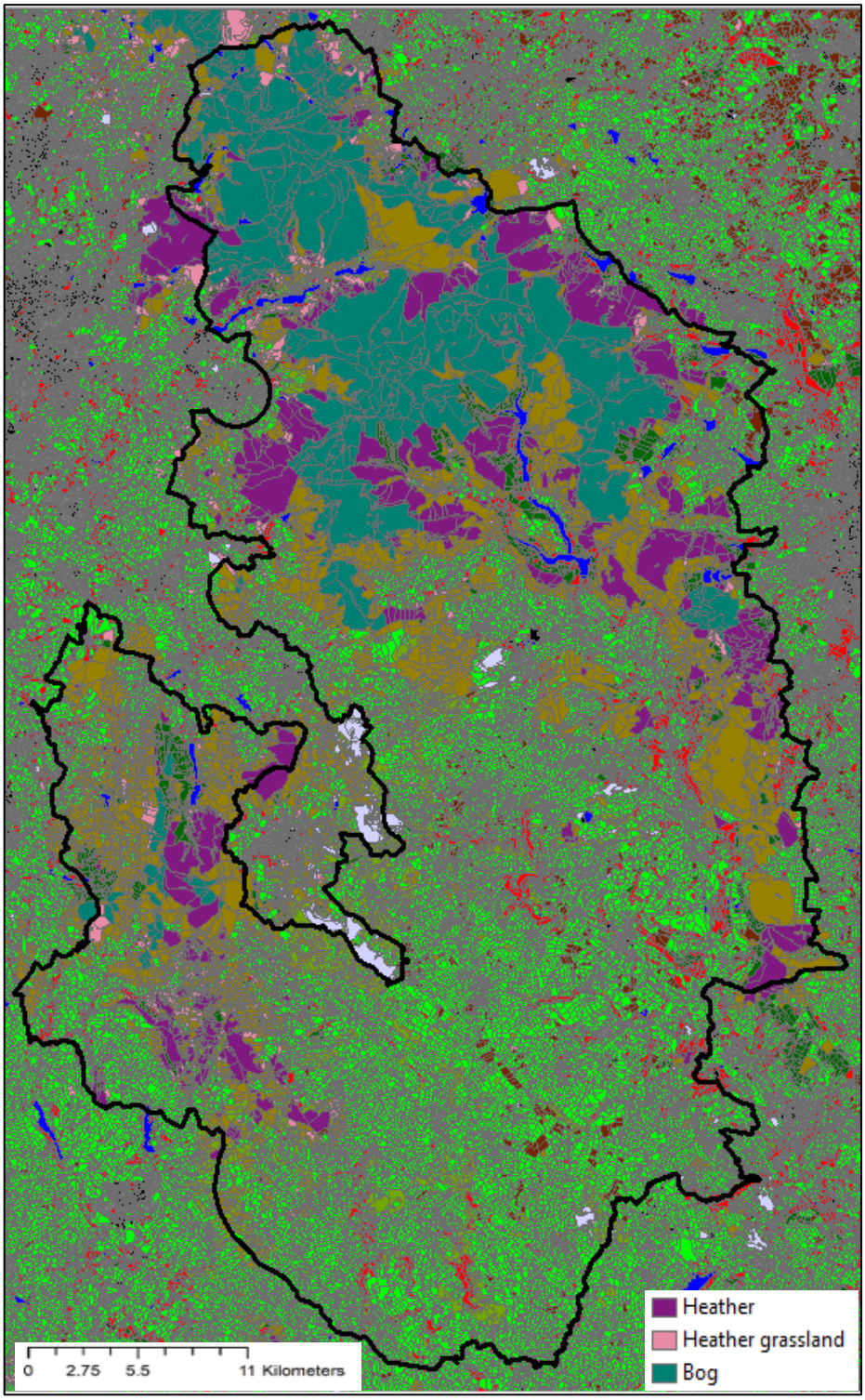

Figure 5.8: UK Land Cover Map 2015 with the Peak District National Park boundary (black line) (Source: Rowland et al, 2017).

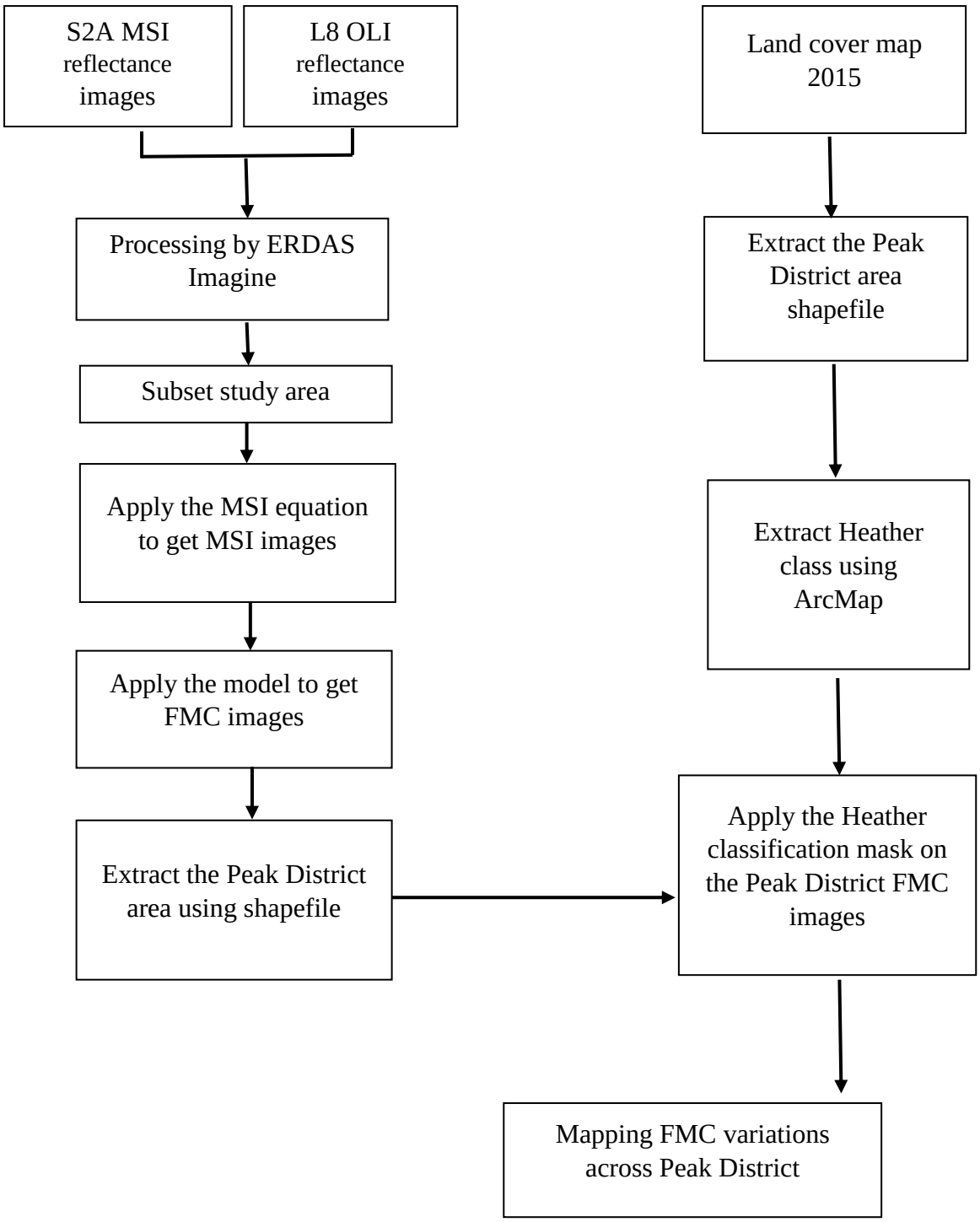

Figure 5.9: Method for mapping FMC variations at landscape scale

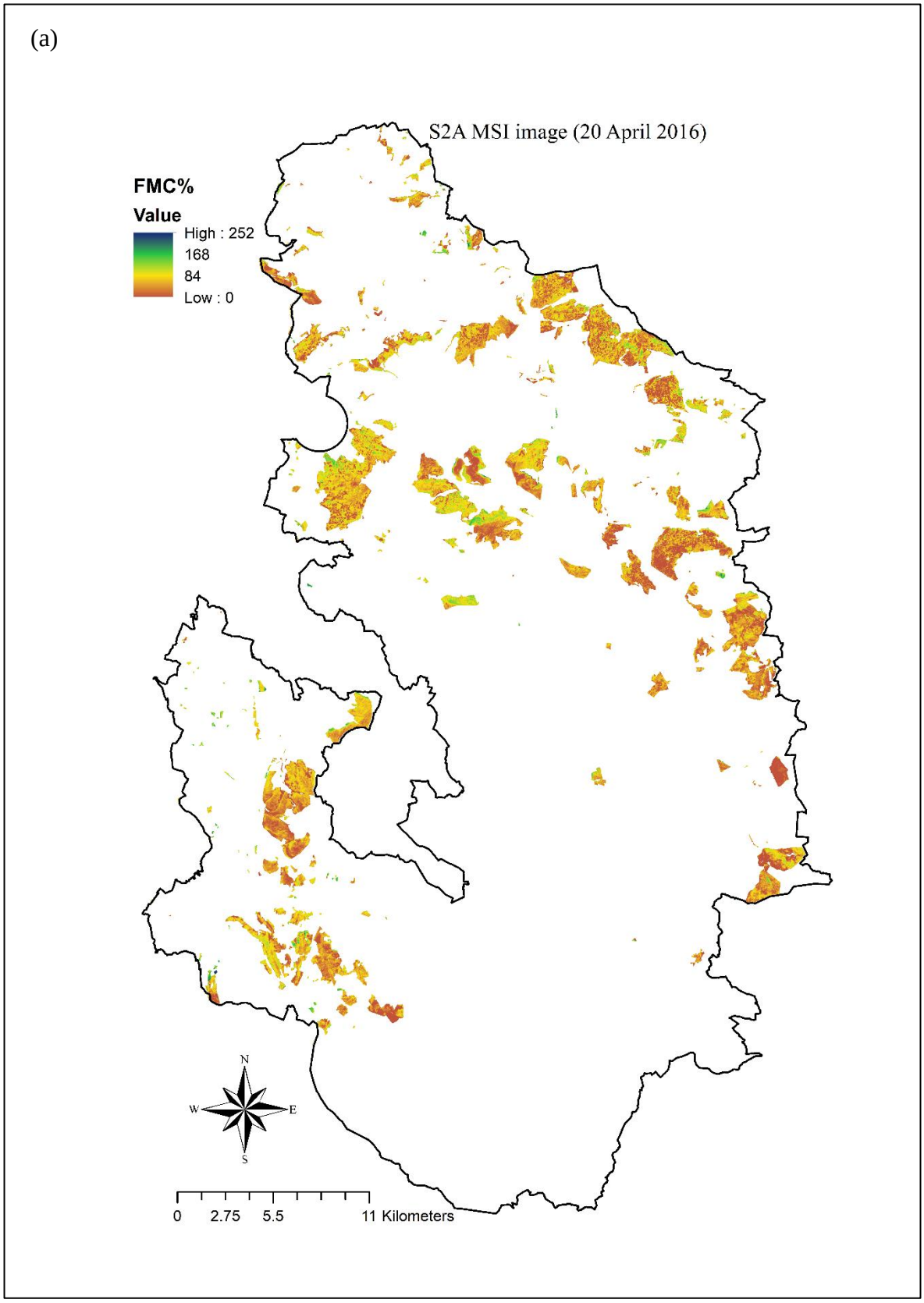

Figure 5.10 a-g: Mapping estimated FMC at landscape scale for *Calluna* areas based on the relationship between MSI and FMC for *Calluna* plots at Burbage Moor. Square shows the area with different patches of FMC used later in the chapter.

(b)

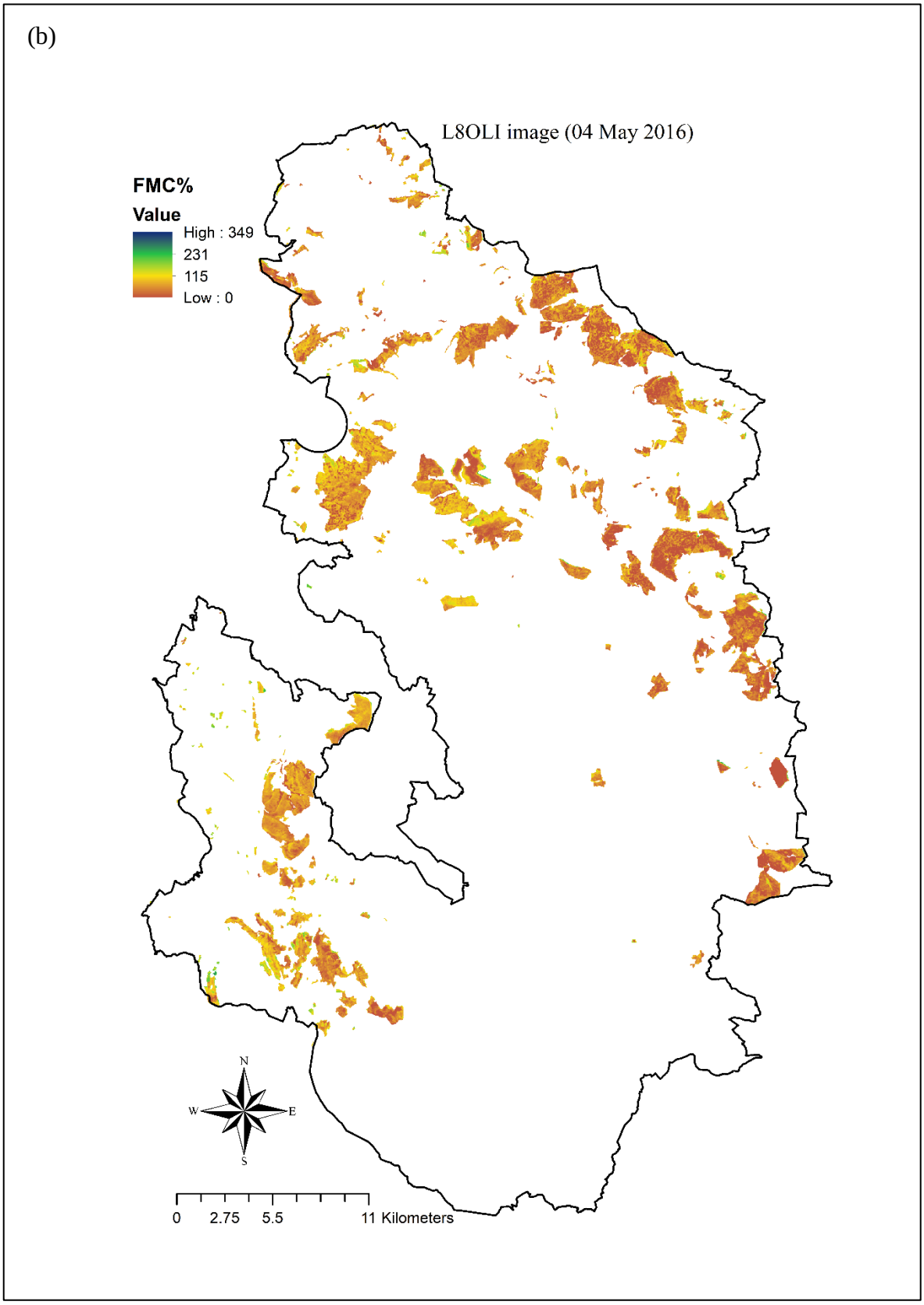
L8OLI image (04 May 2016)
FMC%
Value
High : 349
231
115
Low : 0
N
W
E
S
0
2.75
5.5
11 Kilometers

(c)

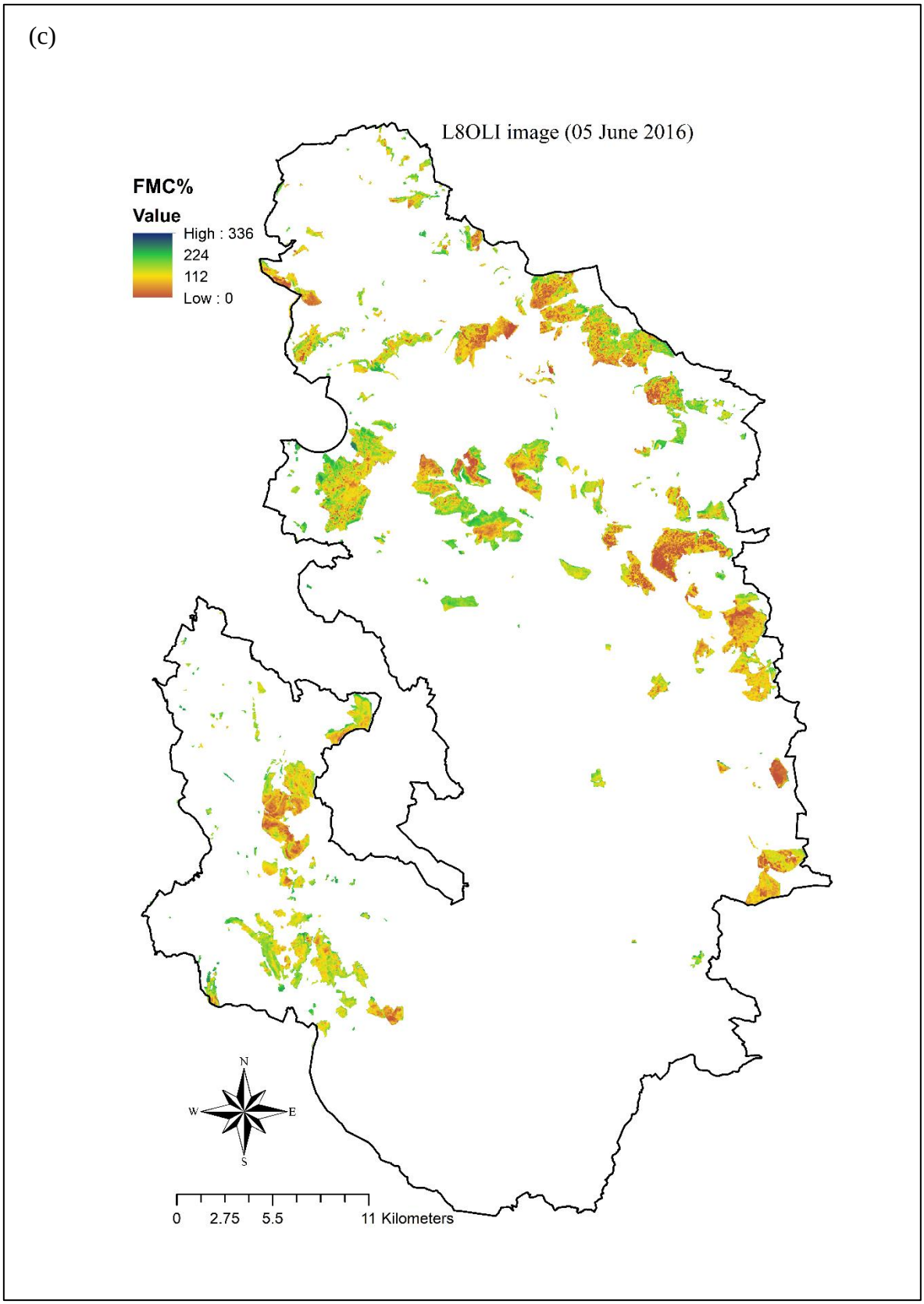
L8OLI image (05 June 2016)
FMC%
Value
High : 336
224
112
Low : 0
N
W
E
S
0
2.75
5.5
11 Kilometers

(d)

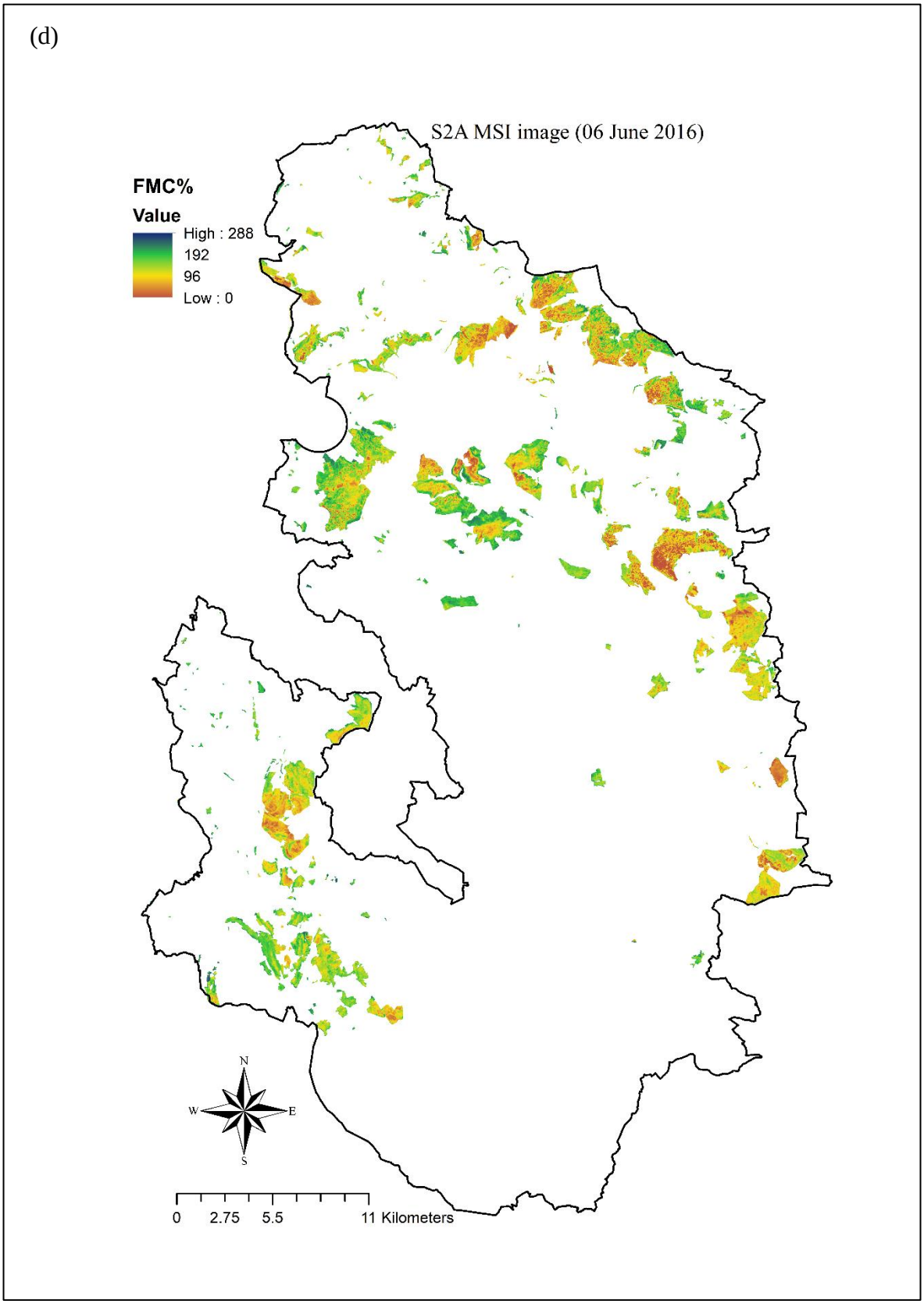
S2A MSI image (06 June 2016)
FMC%
Value
High : 288
192
96
Low : 0
N
W
E
S
0
2.75
5.5
11 Kilometers

(e)

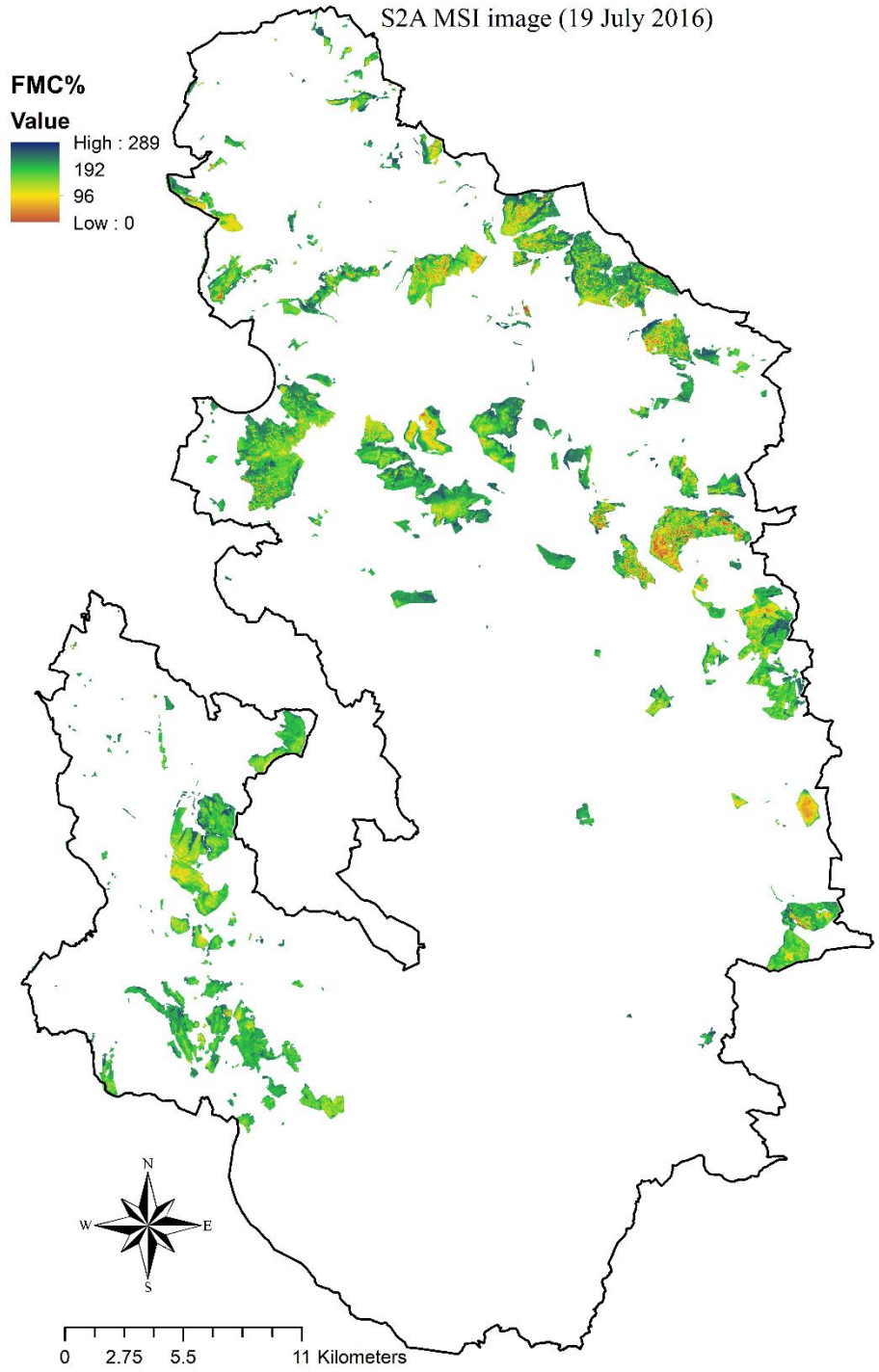
S2A MSI image (19 July 2016)
FMC%
Value
High : 289
192
96
Low : 0
N
W
E
S
0
2.75
5.5
11 Kilometers

(f)

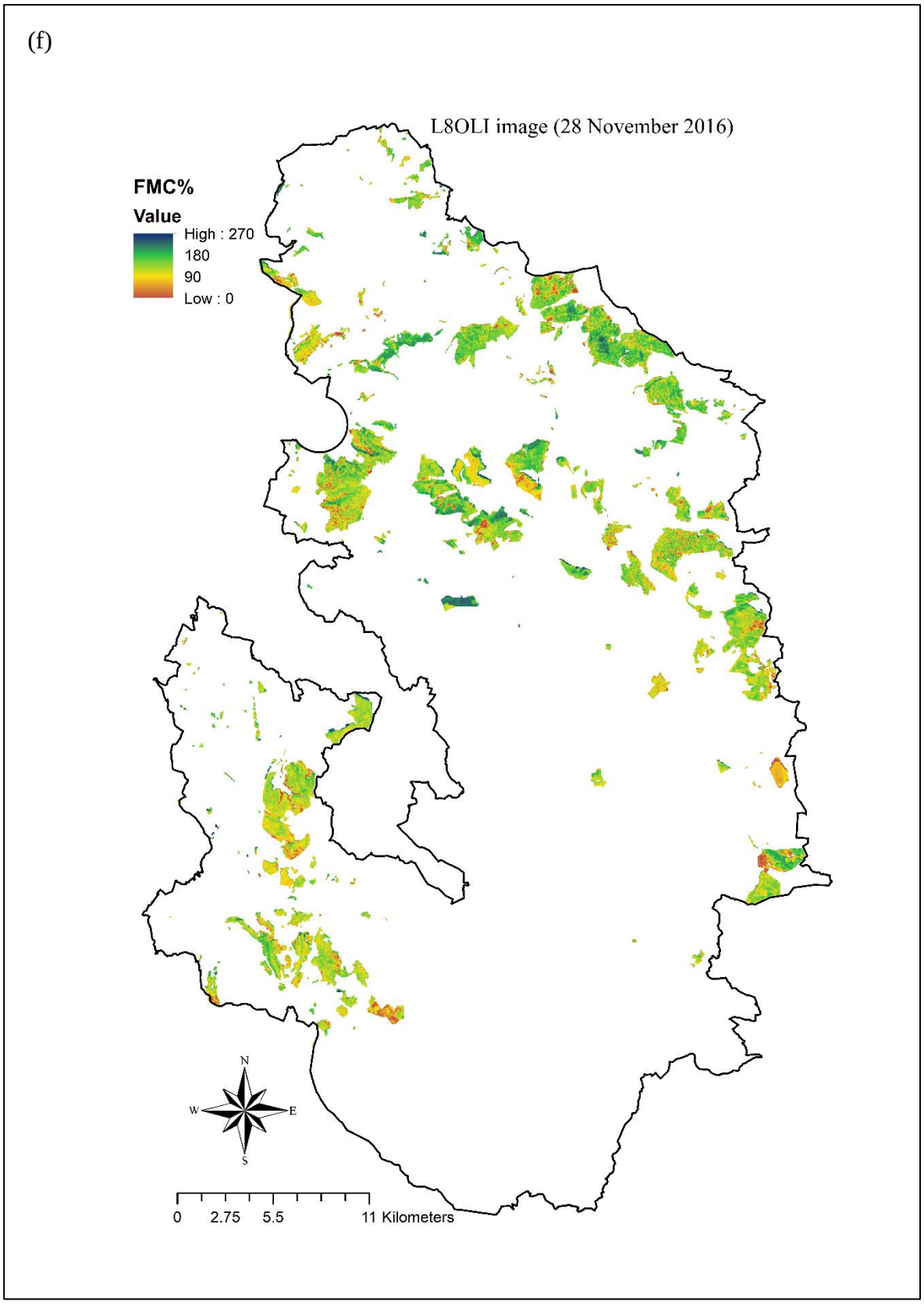
L8OLI image (28 November 2016)
FMC%
Value
High : 270
180
90
Low : 0
N
W
E
S
0
2.75
5.5
11 Kilometers

(g)

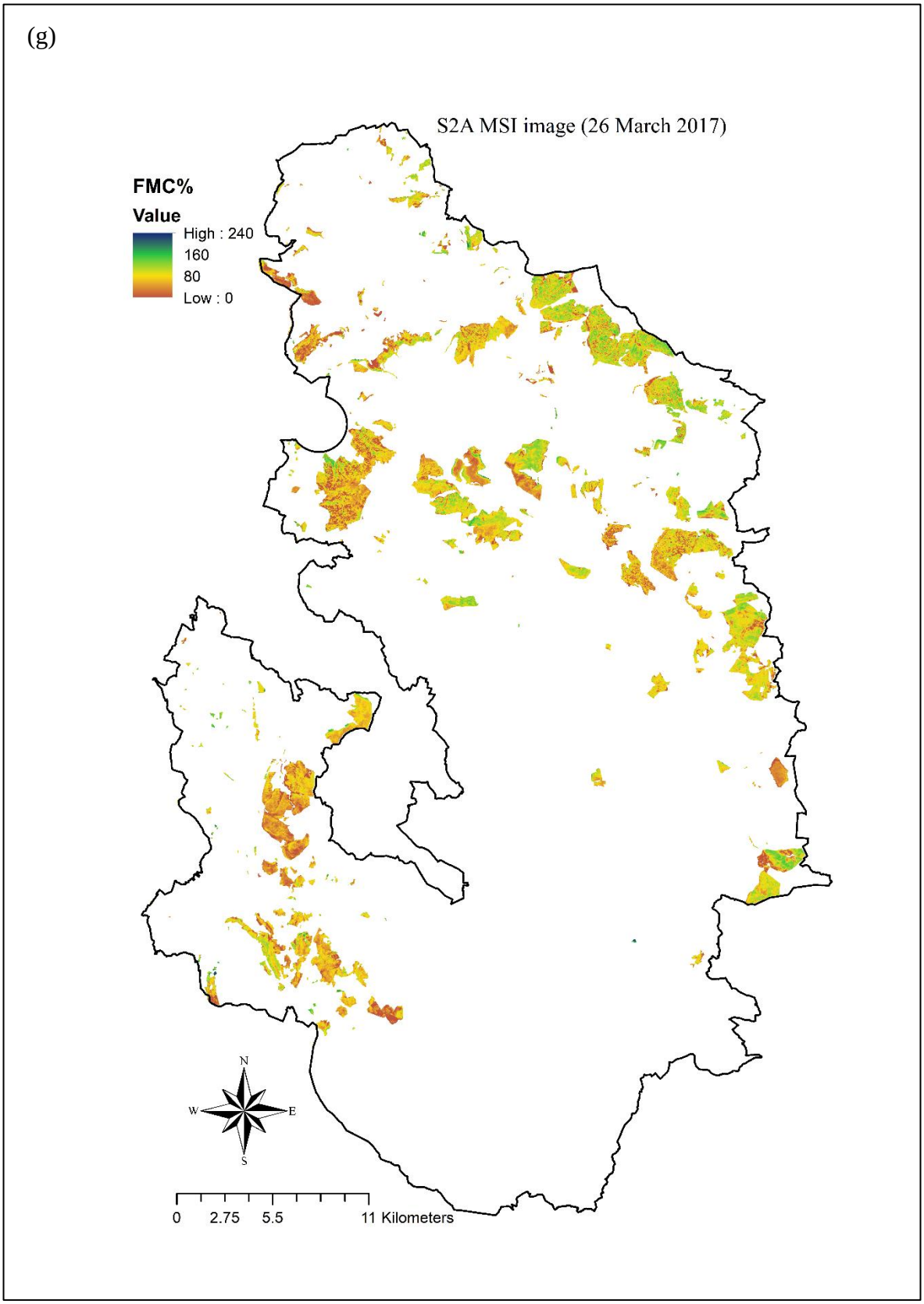
S2A MSI image (26 March 2017)
FMC%
Value
High : 240
160
80
Low : 0
N
W
E
S
0
2.75
5.5
11 Kilometers

To examine the variation across the dates, histograms of the FMC distributions were computed for each date (Figure 5.11). The histograms were arranged according to the date of data acquisition. A general look at the results shows that the FMC values fluctuated according to the time of data collection. It is noted that there are different frequency totals between the two sensors because of the different spatial resolutions. The histograms highlight the wide variation in FMC across the area at given date. They also show the general shift to higher FMC values in summer (5.11e), compared to spring (5.11a) and autumn (5.11f). The general trend in FMC at landscape scale is shown in Figure 5.12, which shows the modal FMC value extracted for each date.

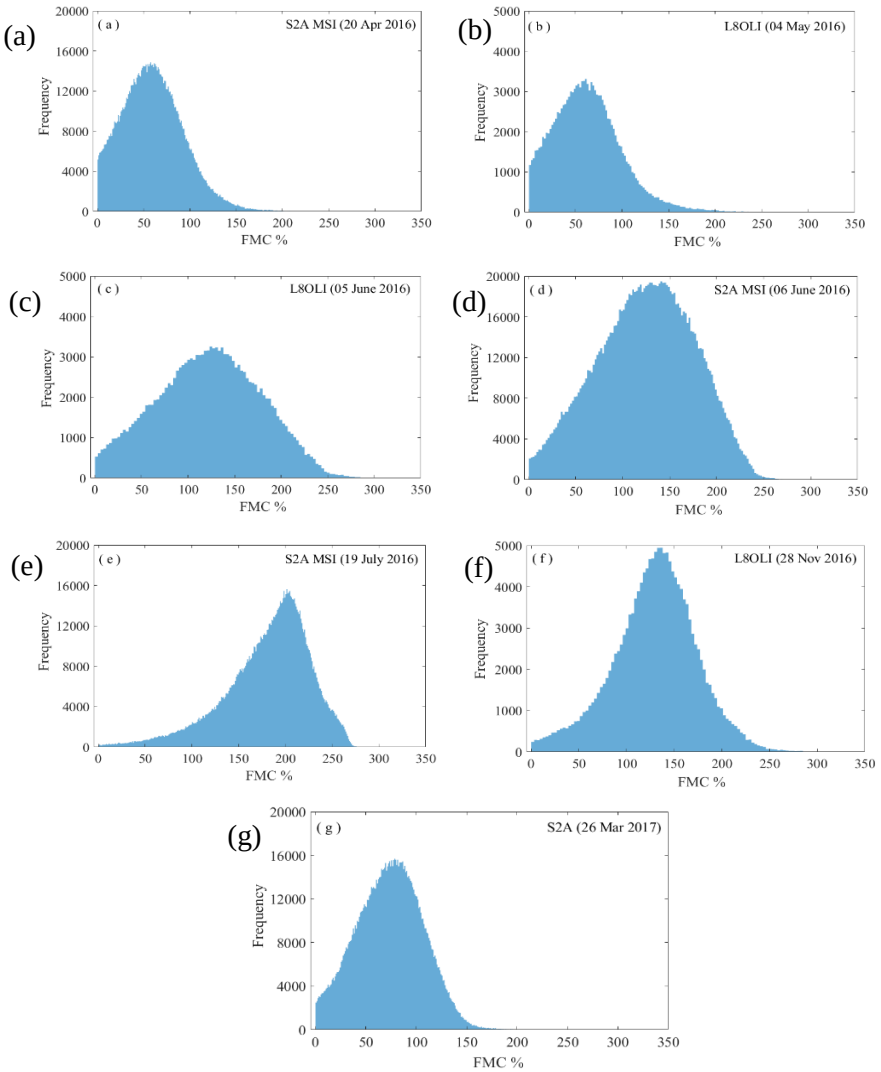

Figure 5.11: Frequency distribution of FMC obtained from S2A MSI and L8 OLI images from April 2016 to March 2017

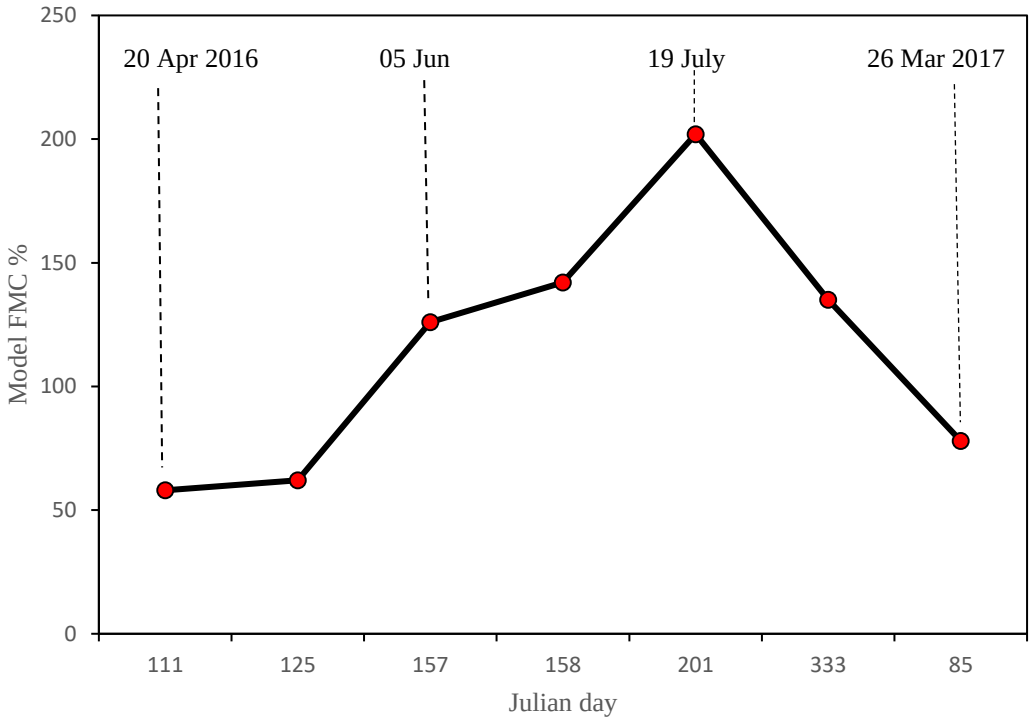

Figure 5.12: Modal FMC at landscape scale of the modelled FMC values.

The results shown above indicate significant spatial variability within individual patches of *Calluna* at the seven dates. To examine this in further detail a sub-area was extracted that included Burbage Moor and other areas nearby that were subject to intensive management by burning strips of *Calluna* on a rotation of 12-15 years (Figure 5.13). In Figure 5.14 the spatial variation in FMC across the managed area in the north-west corner of the sub-image is very clear. The spatial variation across the less intensively managed area of Burbage Moor, located in the south-east of the sub-image, appears to be lower, reflecting the more extensive full cover of *Calluna* in this area. This series of high resolution image shows the local patch-scale variability in estimated FMC. From this figure a range of observation are made:

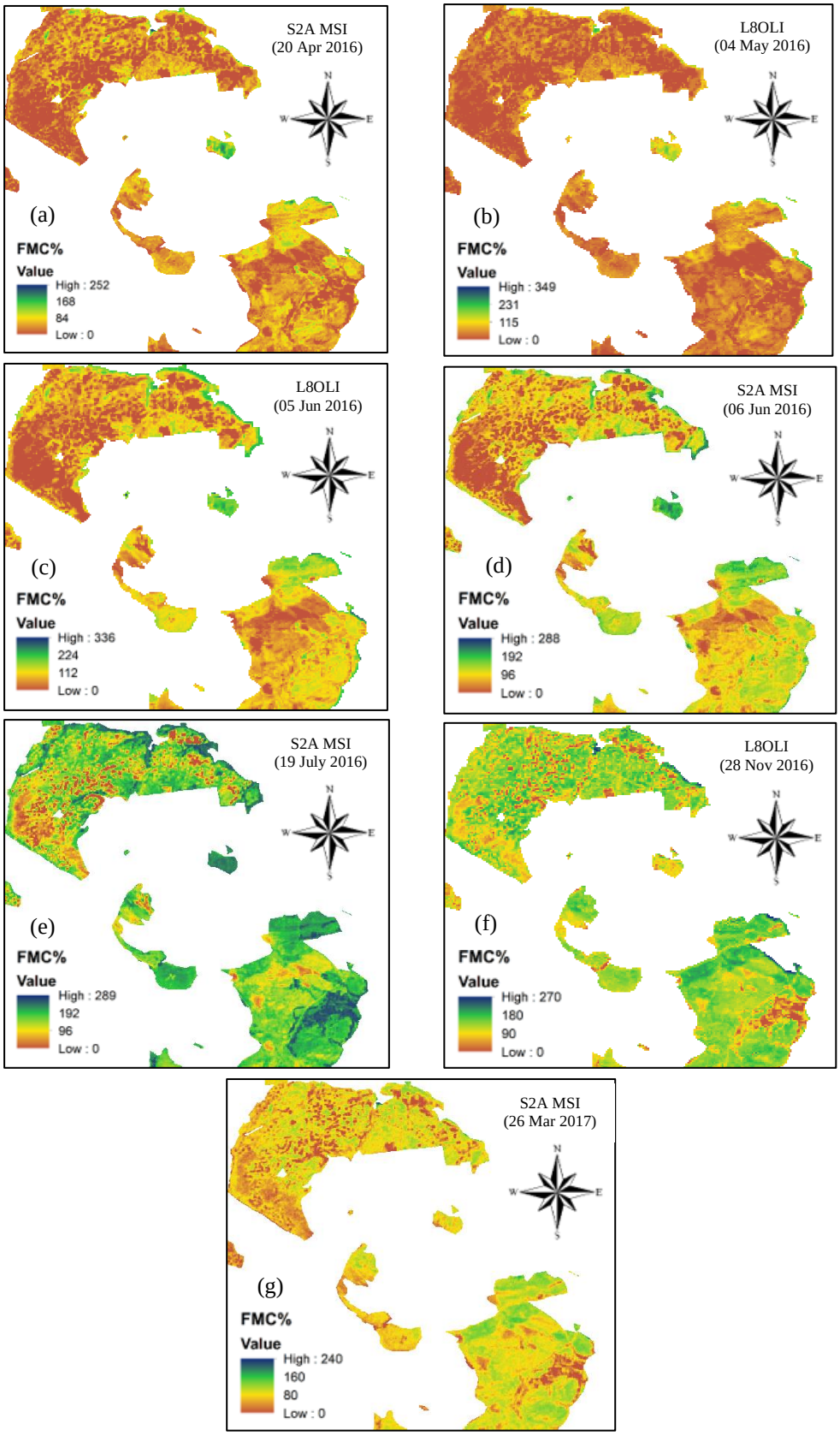

Figure 5.13: Part of the Peak District showing the changes in FMC values between April 20th 2016 and March 26th 2017, including Burbage Moor.

(i) There are clear differences in FMC within the chequer-board areas of managed moor. This pattern reflects the management of these areas by managed burning. There appears to be different FMC in different patches of regrowth (see the north-west corner of the sub-image).

(ii) The more homogeneous vegetation on less intensively managed Burbage Moor shows more even FMC values across the sites (see the south-east of the sub-image).

(iii) There were some small areas with extremely high values of FMC (dark green) that may be due to the overlap of some other plant species, especially on the edges of the *Calluna* patches (see the dark green areas in the sub-image).

These observations can also be applied to the time-series of seven images of the whole of the Peak District since areas of continuous *Calluna* cover, and areas managed by burning, are present across the area.

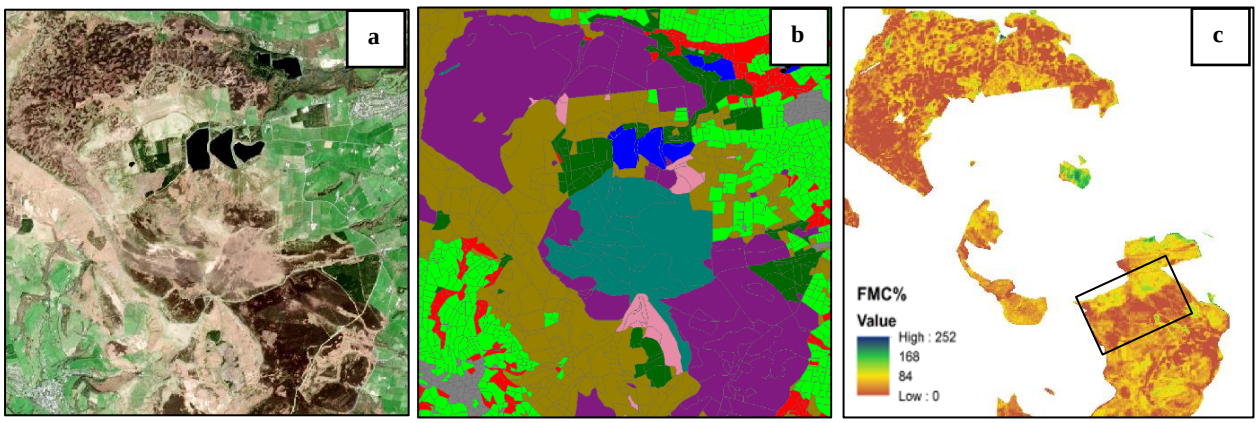

Figure 5.14: Three parts of same area from Peak District. (a) Part of the Peak District from S2A MSI image on 20 April 2016 including Burbage Moor. (b) Part of shape file from land cover map 2015 showing *Calluna* classification with purple colour. (c) Part of FMC mapping using MSI with black box showing area from which ground data were collected.

Figure 5.15 shows three different lines representing average FMC values from three different patches in this sub-image: Burbage Moor, an area of managed moor, and a burned area. The average FMC values were calculated from 25 pixels (100x100m) for S2A MSI and 9 pixels (90x90m) for L8 OLI.

The general trend of the three patches was of higher FMC in summer (19th July) compared to spring and autumn. The Burbage Moor site and the managed moor showed similar trends and FMC, whereas the burned area showed lower FMC at all dates. These results show for the first time the clear potential of using satellite data to map sub-patch scale variations in *Calluna* FMC using satellite data.

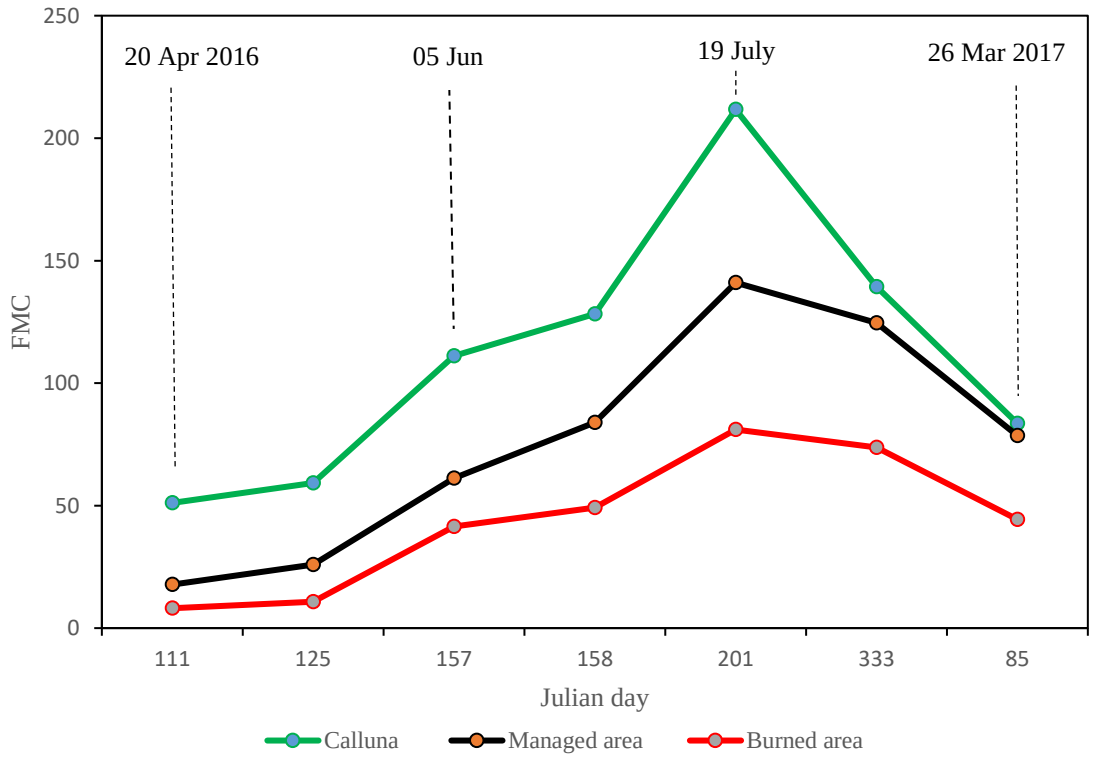

Figure 5.15: Average FMC value of three different patches in part of the Peak District.

5.7 Conclusion

It is evident that the flush of young green summer growth explains the large difference between consistently low moisture content during spring and autumn and consistently high live FMC during summer as referred to in Gilbert (2008). There were clear patterns of variation in the soil moisture over the period, but there was no significant correlation between vegetation FMC and soil moisture. A strong relationship was found between FMC and MSI, and the RMSE was relatively low at 15.74% compared to the results of Al-Moustafa et al. (2012), Yebra, Chuvieco, and Riano (2008) and Quan et al. (2017) where the RMSE was 16.01%, 16.8% and 32.35% respectively. The variation in measured FMC followed a similar pattern to a previous study in a similar environment, with higher FMC in the summer during greening of the canopy (Al-Moustafa et al., 2012). The high measured FMC in November/December was unusual and at the time of writing is unexplained.

The results of the relation between FMC and MSI at landscape level were applied on seven images to test whether FMC can be mapped using a satellite-derived vegetation index (MSI) over large areas of upland vegetation. The results showed there were FMC variations at different times during the year. Some areas showed very high or very low FMC and further detailed investigation of these areas at 'patch scale' is warranted.

CHAPTER 6: DISCUSSION AND CONCLUSIONS

6.1 Introduction

Wildfires are a global problem affecting a wide range of ecosystems and causing degradation of vegetation, soil, plant and animal biodiversity, and affecting the hydrological cycle. At global scale there is growing evidence of an increase in wildfire frequency that may be related to climate change (Jolly et al., 2015). At the national scale there were nearly 260,000 wildfire incidents recorded in England between 2009 and 2017, and further evidence that increasing fire frequency is related to periods of hot dry weather (Forestry Commission England, 2019). Wildfires also present a danger to humans and to property and are notoriously difficult to fight (Chen, 2006). This is particularly the case when wildfires occur in remote and inaccessible areas (Davies & Legg, 2016).

The research in this thesis contributes to work aimed at measurement of fire hazard, and in particular to the management of wildland fire fuels. It is hoped that the work highlights the potential application of satellite remote sensing for fuel management in UK uplands, but that it also illustrates future challenges for operational implementation of such data for fire management at the landscape scale.

This research aimed to investigate the spatial-temporal variation in vegetation fuel moisture at landscape scale in one fire-prone ecosystem in the UK uplands. In order to achieve this aim, the research used a series of laboratory experiments to investigate the relationship between spectral reflectance and vegetation fuel moisture, and then looked at how this is related to vegetation indices. In addition, the work assessed the spatial-temporal variation of fuel moisture at landscape scale based on satellite-derived spectral reflectance measurements. The results of this work could be used to assess the seasonal and inter-annual

variation in *Calluna* moorland fuel moisture characteristics at landscape scale and how this relates to fire hazard and fire risk. The aim of this chapter is to synthesise the main findings of the research, highlight the key outcomes, identify the methodological and operational challenges encountered, and consider the next steps required to extend the research towards operational applications.

6.2 Laboratory experiments on FMC and vegetation indices

Laboratory experiments were used to investigate three hypotheses related to vegetation canopy and to observation properties that effect canopy spectral reflectance, those being FMC, soil background and solar zenith angle. The results of the experiments showed that there were statistically significant relationships between FMC and vegetation indices (NDWI and MSI with $R^2 = 0.84$ and 0.85 respectively, sample size 12). These relationships were consistent with those found for other species and provided strong justification for the use of these relationships later in the research. For example Dennison, Roberts, Peterson, and Rechel (2005) showed that there was a positive correlation between NDWI and live fuel moisture for chamise (*Adenostoma fasciculatum*) in the Angeles National Forest, Los Angeles County, California, USA; the relationship established had an R^2 of 0.80 using 56 samples. The FMC of Mediterranean shrubland (*Cistus ladanifer*) in Cabaneros National Park, Central Spain, was shown to have a strong relationship ($R^2 = 0.85$, sample size 40) with NDWI (Yebra, Chuvieco, & Riaño, 2008). Sow, Mbow, Hély, Fensholt, and Sambou (2013) found relationships between MSI and FMC for different vegetation types in Senegalese grassland ecosystems, these included grasslands, savanna vegetation, shrub savannas and woodlands, where the relations were R^2 of 0.92, 0.82 and 0.80 respectively (sample size 36).

Other authors have looked at the relationship between fuel moisture content of vegetation and spectral reflectance using a modelling approach for a range of different species including

grassland, shrubland and forest. For example Riaño, Vaughan, Chuvieco, Zarco-Tejada, and Ustin (2005) estimated FMC by inversion of the PROSPECT leaf model, on measured reflectance data and used a sensitivity analysis to examine responses to changes in EWT and dry matter. Spectroradiometric measurements for leaves of three Mediterranean species *Quercus pyrenaica*, *Rosmarinus oficinalis* and *Cistus ladanifer* were used. The results indicated difficulties in estimating dry matter and FMC at a canopy level because of confounding factors like canopy LAI and structure.

Wang, Hunt, Qu, Hao, and Daughtry (2013) used the leaves of *Quercus alba*, *Acer rubrum* and *Zea mays* to test simulations of spectral reflectance data in the laboratory for potential use in estimating FMC from satellites. The results showed that the ratio of the water index with the dry-matter index was strongly related to FMC using the PROSPECT and the SAIL models. However, to the author's knowledge the experiments described in this thesis are the first investigations of the relationship between *Calluna* canopy FMC and spectral reflectance carried out in the laboratory. The only previous related research on *Calluna* was by MacArthur (2011) who used radiative transfer modelling and field spectroscopy to gain an understanding of the complex interactions between light and individual shoots of *Calluna*. The key strength of working in a laboratory setting is that the researcher can control variables such as soil background, canopy properties and solar zenith angle, and that there are no complicating atmospheric effects. Such experiments allow the target variables (in this case FMC and spectral reflectance) to be studied whilst minimizing the effects of other variables.

A key issue encountered was that the FMC measurements had a small range of values due to the experimental set-up. Moving plants from the field to the laboratory resulted in low FMC values for the canopies at the start of the experiment. In addition, it was difficult to recreate 'realistic' canopies in the laboratory because of the need to replant the whole plant

and keep the soil background properties the same as those in the field. Furthermore, only one sample was used for the spectral reflectance measurements and another one was used for destructively sampling of FMC, and it is recognized that the response to drying of the two canopies may have been different.

Future laboratory experiments may be more effective if whole canopies with their soil are extracted and fully watered before transfer to the laboratory to keep the FMC closer to field conditions at the start of measurements. Using replicates for the two canopies would increase the statistical power of tests applied. Extraction of complete canopies was not possible at Burbage Moor because of its SSSI status, but samples from other less sensitive sites could be used.

This study focused on NDWI and MSI because they are the most widely used VI for estimating water content using broadband data. However, some studies have used high-spectral resolution data and employed VI designed to be used with such data. Almoustafa (2011) found that broadband indices, such as the NDWI, produced similar results to hyperspectral indices when estimating water content in *Calluna* shrublands. For this reason, and because the later chapters worked with broadband image data, the application of hyperspectral approaches was not pursued. However, in the laboratory experiment hyperspectral measurements were acquired with the ASD and converted to broadband measurements to simulate the satellite image data spectral properties, and so, these data may in future be used to explore the application of a range hyperspectral indices as used by Danson, Steven, Malthus, and Clark (1992) for example.

6.3 Radiative transfer modelling (RTM)

In the laboratory and field, the variables of interest have a narrow range in reality. For example, in the laboratory experiment the FMC ranged from 12 to 53%, and in the field experiments between 76 and 212%. With the application of the radiative transfer model FMC could be varied over a much larger range, for example 0 to 1000%, and it also allowed exploration of the effects of a wide range of variables interacting together at the same time. Simulations from models can give results close to reality and it is possible to do thousands of simulations very quickly. However, the effectiveness of simulation outputs depends on setting the model parameters to best simulate reality, which is not always possible.

For example, in this study the range of LAI for *Calluna* canopies measured in the field was not known. Zarco-Tejada, Rueda, and Ustin (2003) showed good correlation between a time series of MODIS-estimated EWT and measured FMC using the PROSPECT leaf model and the SAIL canopy reflectance model where viewing geometry and LAI were used as additional inputs. A knowledge of *Calluna* LAI variations in time and space would therefore be useful in further understanding the spectral response of such canopies. However, as MacArthur (2011) showed, leaf clumping and canopy gaps cause LAI estimation errors, therefore the heterogeneity of *Calluna* canopies will complicate attempts to model their reflectance.

Radiative transfer modelling depends on sensitivity analyses to study the effect of variables on the spectral response of vegetation. In this study the variables were LAI, solar zenith angle, leaf dry matter content, leaf water content, and soil spectral reflectance. The results of the modelling work presented in this research further supported the strong relationships between FMC and VI and illustrated the likely impacts of variations in soil spectral reflectance and solar zenith angle. Future application of RTM should consider collecting

field measurements of all model variables in the field in order to better constrain the model before carrying out more sophisticated sensitivity analyses like those in Bowyer and Danson (2004), who used a global sensitivity analysis to examine the contribution and interactions of each model variable separately.

6.4 The challenges of FMC field measurement

In this study, the field measurements were made in a typical *Calluna*-dominated UK upland environment. Regular FMC measurements were obtained at Burbage Moor across a year from five plots to capture the seasonal variation. Sampling was undertaken within one hour of the satellite overpass time to avoid diurnal changes in FMC (Danson 2018, pers comm.). It is probable that there is a decline in fuel moisture content during the day due to the high mid-morning transpiration rates, which leads to stomatal closure to avoid wilting. Stomata may then reopen around midday and fuel moisture content may fall in the afternoon (Agee, Wright, Williamson, & Huff, 2002; Chuvieco, Aguado, Cocero, & Riaño, 2003; Davies, 2006). The data sets in this research represent one of the few studies collecting data on seasonal FMC variations in this type of environment; with additional resources spatial and diurnal patterns of FMC variation could easily be established following the same approaches.

However, the limited number of plots within the study area may be insufficient to properly represent the different communities of *Calluna*, which are distributed across areas of the Peak District. There are many differences between *Calluna* canopy structures within the sampling area alone, with variations in age, species and homogeneity as indicated by Almoustafa (2011). Across the Peak District *Calluna* areas are managed by burning and by mowing, and the resulting structural differences may cause some variations in FMC measurement between one area and another. Davies (2005) showed that the structure of *Calluna* canopies influences their moisture content, even though this is primarily dependent

on plant phenological changes. In these experiments Davies (2005) suggested that this variability in *Calluna* moisture content, in the canopy specifically, is due to the leaves on older shoots in the middle and basal canopy layers having lower moisture content than new shoots at the top of the canopy. Thus, this result supports the hypothesis generated in this study that there are variations in FMC measurement with different canopy structures as a result of the management both by fire or cutting.

In addition to these structural differences, there were also some logistical issues with sampling in the research described here. For example some field visits were made soon after heavy rainfall which may have led to short-term increase in fuel moisture content as suggested by Lopes, Viegas, de Lemos, and Viegas (2014). Lopes et al. (2014) measured fuel moisture content from *Calluna vulgaris* and *Chamaespartium tridentatum* in the forests of Central Portugal using field sampling over a four-year period. The total daily rainfall was measured at the Lousã Weather Station during the same period. The result suggested a moderate positive correlation with between the FMC on one day and the FMC on the day before. In addition, in this research, on one occasion there was a large gap between the field sampling and the nearest cloud-free satellite overpass, and the linear interpolation of FMC across these dates may have introduced an error in the FMC estimate for the overpass day.

To estimate FMC in the study area it was necessary to strike a balance between the timing of the sampling and the number of plots. Sampling a larger number of plots distributed across different areas may represent the FMC variations more accurately. However, collecting such data over large areas simultaneously with a satellite overpass would require more resources. Sampling a larger number of points within each plot may also help increase the accuracy of field estimates of FMC. It is also suggested that on-site weather station data measured before

sampling and on the day of sampling may help explain some of the fluctuations in the FMC measurements that were present in the monthly measurements.

6.5 Remotely sensed data sets

Sentinel-2A MSI and Landsat 8 OLI were the sources of imagery used in this research. These sensors are a new generation of orbital optical sensors that deliver images with high spatial and temporal resolution. In addition, they may be obtained as surface reflectance images which provide the primary input for all higher-level surface geophysical parameters, including vegetation indices. Furthermore, these images are freely accessible from their respective websites. In this research seven cloud-free images of the study area were obtained, including three images that coincided with a field sampling day.

To obtain accurate FMC estimates across a year will require high spatial resolution sensor data on at least a weekly basis. The UK weather is the main impediment to image acquisition because of cloud cover. For example, for the study area 49 images from L8 OLI were cloudy and only three images were cloud free, while there were 89 images from S2A MSI recorded during the study period that were cloudy and only four images that were cloud free. The seven images from L8 OLI and S2A MSI used in Chapter 5 were not evenly spaced temporally across the study period, with two of the images being acquired only one day apart.

The difference in spatial resolution between the two sensors may also have played an important role in affecting the accuracy of the relationships between FMC and VI. The pixel sizes and plot sizes were only approximately coincident, and the measured FMC may not have accurately represented the FMC of the sensor's pixels.

In addition, the application of surface reflectance products is dependent on the accuracy of the atmospheric corrections and this is always subject to some uncertainties. The accuracy of any product derived from optical-domain satellite borne sensors is related to the accuracy of surface reflectance or, more precisely, to the accuracy of the atmospheric correction that is applied to level 1 products of Top-of-Atmosphere (TOA) reflectance for generating land surface reflectance. Claverie et al. (2018) investigated the uncertainties in the atmospheric correction products from L8 OLI and Sentinel 2A MSI and the results showed uncertainties in reflectance estimates of up to 11% and 7% for L8 OLI and Sentinel 2A respectively. Such errors are likely to be present, and unquantified, in the data sets used in the present research with implications for VI data extracted from them.

Villaescusa-Nadal et al. (2019) showed that there may also be variance in the reflectance data from different sensors as a result of differences in their relative spectral response functions. When comparing Landsat 8 OLI and Sentinel 2A MSI, this difference was found to be small in the NIR (0.03%) because of the similar spectral response. In the red waveband the difference was found to be 3% and required correction. However, the authors did not quantify the differences in the SWIR bands used in this study and clearly this work needs to be done.

Franch et al. (2019) showed that differences in sensor view geometry lead to the emergence of variations in time series data when using measurements from Landsat 8 OLI and Sentinel-2 MSI together. They also found that the surface reflectance values in these data were affected by the seasonal variations in the solar zenith angle. Both of these factors are in turn related to the surface bidirectional reflectance distribution function (BRDF). Franch et al. (2019) addressed these issues through a correction procedure to normalize the data and reduce the coefficient of variation in time-series data sets.

Using larger plots to represent the pixels from the different sensor resolutions might increase the accuracy of the FMC measurements. However, one of the limitations is that there are different contiguous patches of *Calluna*, which may have variable FMC. High-spatial resolution satellite images are prone to geometric distortions, and algorithms have been designed to correct and removal these distortions in satellite imagery (Zheng, Huang, Wang, Wang, & Zhang, 2018). Some distortions, such as the effects of the Earth's rotation and sensor angles, are predictable and referred to as systematic distortions. In addition, random distortions can also occur due to changing terrain and variations in the sensor altitude. Therefore, the use of Ground Control Points (GCP) to correct the geometry of the satellite imagery on an image-by-image basis may give more confidence when co-locating areas in multi-temporal, multi-sensor imagery.

This research used satellite data from Landsat-8, launched in 2013 and Sentinel-2A launched in 2015 offering 30 and 20m spatial resolution data and multi-spectral global coverage. During the research Sentinel-2B was launched in March 2017, and together the S2A and S2B satellites can obtain image data globally every five days and over Europe every two to three days (Revel et al., 2019). This expansion of the Sentinel family adds to the potential number of images that could be used in future research, improving the multi-temporal data sets required to track FMC at landscape scale. If the challenges of calibrating between different sensors can be overcome, it may be possible to develop a virtual constellation of satellites to maximise the probability of acquiring could-free data for this type of application (Wulder et al., 2015).

A further notable addition to such constellations could be the WorldView-3 satellite sensor, launched in 2014, which provides the only satellite data with both NIR and SWIR bands at a resolution less than 5m. The area coverage of such sensors is very limited however (16 x

16 km for Worldview-3), and routine monitoring with commercial satellites is still likely to be prohibitively expensive (Longbotham, Pacifici, Baugh, & Camps-Valls, 2014; McKenna, Phinn, & Erskine, 2018).

6.6 Comparing the FMC VI relationships

A strong linear relationship between FMC and MSI was found in the laboratory experiment, RTM modelling and fieldwork measurements as discussed in sections (3.2.3), (3.3.1) and (5.4). However, although 'surface reflectance' was used in all experiments, the form of the relationship differed between the three experiments (Figure 6.1).

The form for the laboratory data and RTM simulations was similar but for the field experiment it was quite different. The cause of this variation requires further investigation, but it is suggested that soil characteristics in the field were not adequately reproduced either in the laboratory experiments or RTM modelling. On the other hand, it is also possible that, as discussed above, the absolute surface reflectance of the image data sets was biased in some way, leading to a bias in the MSI and FMC estimates.

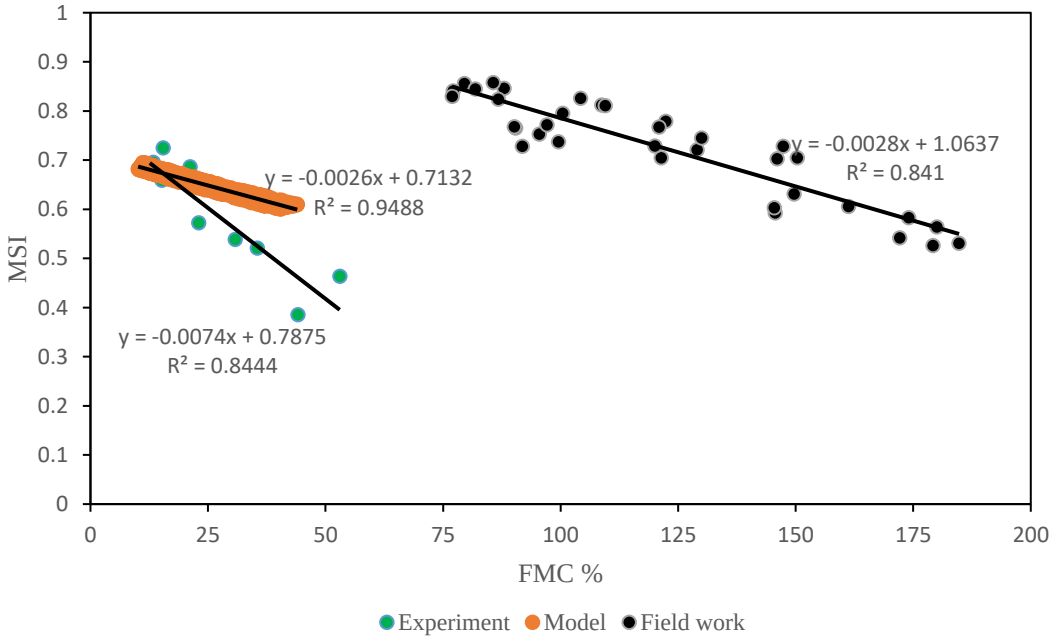

Figure 6.1: Comparison of FMC and MSI relationships for the three experiments.

The overall accuracy of the field-based FMC estimation was tested using the RMSE. It was used here to assess model precision, and the correlation to assess model accuracy (Olden & Jackson, 2000). The RMSE of the relationship between FMC and MSI was 15.74% which may be accurate enough for some operational applications. This finding can be compared directly with several previous studies where the RMSE was higher (Al-Moustafa, Armitage, and Danson (2012); Yebra, Chuvieco, and Riano (2008) and Quan et al. (2017)) although there were differences in sample size and/or vegetation type in these studies (see section 5.5). The results from this study might be more accurate after investigating the range of potential error sources. These may be summarised as:

(i) Differences in spatial resolution and alignment of pixels with sample plots.

(ii) Errors in atmospheric correction of S2A MSI and/or Landsat 8 OLI.

(iii) Time gap between field sampling and satellite overpass.

(iv) Errors in FMC measurement at plot scale (including diurnal variations).

6.7 Relating wildfire occurrence to the FMC maps

Data on wildfire occurrence in the Peak District obtained from Moors for the Future for 1976 to 2017 could potentially indicate relationships between FMC and fire occurrence. However, this data is very difficult to work with in a systematic way. There were 354 fires without information on vegetation type and reasons for ignition, out of a total of 511 (Table 6.1). There was also ambiguity in the classes used with Moorland, Heather and Peat included as separate classes. In addition, there were frequent errors in the coordinates which gave rise to spurious fire locations (e.g. in water bodies). However, two of the FMC images produced in this research were selected to assess the spatial relationship between FMC and occurrence of fires as one of the key factor influencing the probability of ignition. These FMC images were for the *Calluna* areas only in the Peak District. Fire occurrence data for last ten years

from 2007 to 2017 were used and each point plotted on the FMC maps produced. Wildfire occurrences for April and May only were selected. The S2A MSI image on 20th April 2016 represented the lowest FMC values of *Calluna* across the year (see section 5.2), while the L8OLI image on 5th May 2016 was selected because the highest number of wildfires occurred in May (see section 4.5).

Table 6.1: Occurrence of wildfires on different types of vegetation in the Peak District from 1976 to 2017 (Source: Moors for the Future)

Type of vegetation	Number of fires
Moorland	54
Heather	45
Peat	19
Grass	13
Grassland, woodland and crops	11
Woodland	9
Tree scrub	3
Roadside fire	3
No information	354
Total	511

Figure 6.2 shows that most of the wildfires occurred in the north west and south west of the Peak District over the last 10 years in April and May specifically. Wildfires in this period appear to be distributed on the areas with generally lower FMC values (dark red colour) compared to the rest (orange, yellow and green colour). These maps provide a first indication that there may be a relationship between the value of *Calluna* FMC and the probability of fire ignition and that the maps may be able to highlight fire hazard in the future. More detailed and more reliable fire occurrence data are now being collected by fire services in the UK and wildfires statistics were included in the National Risk Register for the first time in 2013 (Gazzard, McMorrow, & Aylen, 2016). As result, wildfire research is now considered an important area for many agencies and beneficiaries interested in this field.

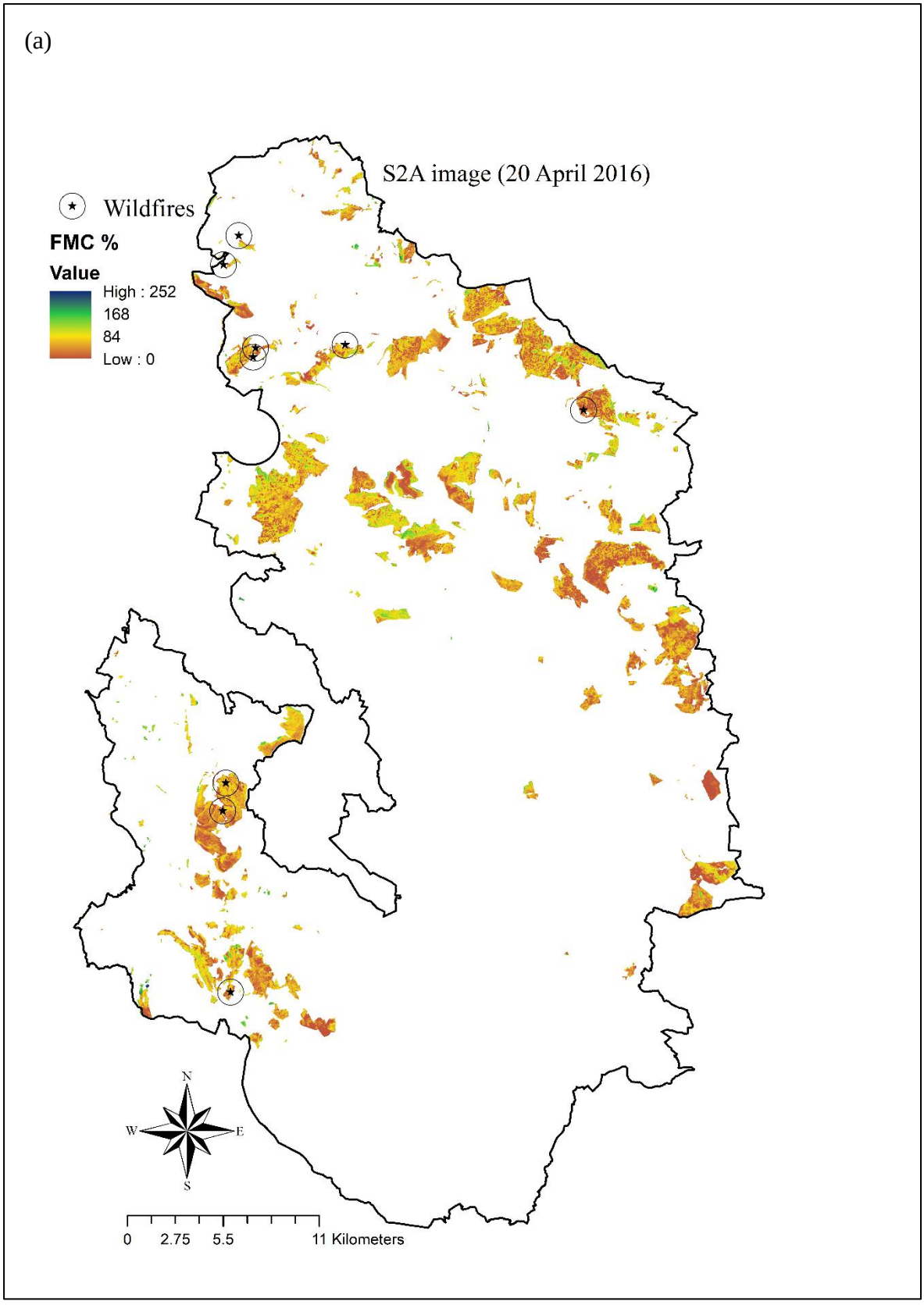

Figure 6.2 a-b: Distribution of wildfires on the FMC map using data from April and May from 2007 to 2017 using data from Moors for the Future.

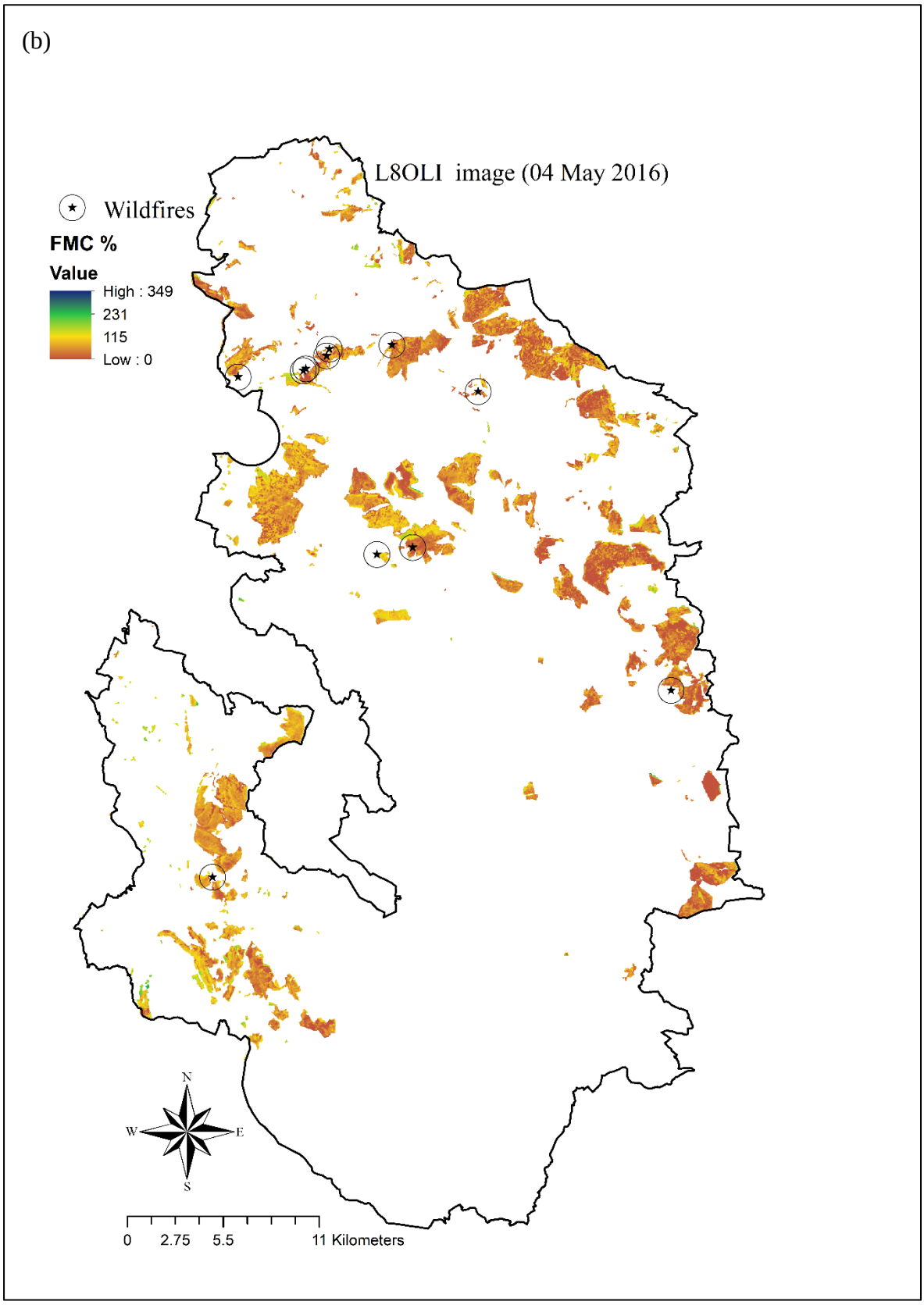
(b)
L8OLI image (04 May 2016)
Wildfires
FMC %
Value
High : 349
231
115
Low : 0
N
W
E
S
0
2.75
5.5
11 Kilometers

6.8 FMC and fire ignition

Fuel moisture content is one of the key variables in fire ignition and fire behaviour because vegetation FMC is inversely related to the probability of ignition, and in addition it effects fire propagation (Jurdao, Chuvieco, & Arevalillo, 2012). Live fuels have different physiological characteristics which can give rise to differences in water content as result of adaptation to local conditions, for example soil moisture and phenological stage (Pivovaroff et al., 2019). In this research, the minimum value for FMC of *Calluna* across the year in the Peak District was 76% in April, while most fires observed to have occurred in this species took place during May and June when the lowest values of FMC were 110% and 119% respectively. These results suggest that a threshold of FMC of around 100% for *Calluna* may be an indicator of fire ignition hazard.

Dennison, Moritz, and Taylor (2008) and Dennison and Moritz (2010) indicated that large fires occur with low values of FMC of around 79% in Mediterranean ecosystems in North America, using field-derived FMC data. Another study by Chuvieco, González, Verdú, Aguado, and Yebra (2009) showed that large fires occurred in the Mediterranean Basin when the FMC was < 35% in grasslands and between 84% to 110% in different shrub species. Jurdao et al. (2012) found a relation with the outbreak of fires in Spain when the FMC was 40% in grasslands and around 100% shrublands. Argañaraz, Landi, Scavuzzo, and Bellis (2018) showed differences in FMC with land cover in the Sierras Chicas in the Chaco Serrano sub region (Argentina) where the fire hazard thresholds for grasslands were 55% and 67%, 72%, for forests 105% and for shrublands 106% and 121%.

Fuel moisture content differs between ecosystems and affects the relationships between FMC and fire activity. In addition, there is a wide range of other relevant variables affecting ignition such as the structural and chemical properties of vegetation, live and dead fuel loads

as well as weather condition and topography (Yebra et al, 2007). Data from this thesis has recently been used to contribute to a global database of fuel moisture content measurements that included 11 countries: Argentina, Australia, China, France, Italy, Senegal, Spain, South Africa, Tunisia, United Kingdom and the United States of America (Yebra et al., 2019). This database, Globe-LFMC, aims to calibrate and validate remote sensing algorithms used to predict FMC. It also aims to help with the validation of dynamic global vegetation models and to better understand the eco-physiology of models of plant water stress. The database will also help investigations on how fuel moisture content effects wildfire occurrence and behaviour (Yebra et al., 2019). The global database has many interesting features, one being that the main leaf FMC is often around 100% for the wide range ecosystem and species represented.

6.9 Future work and new technology

Mapping fuel moisture content of vegetation through remotely sensed data involves a wide range of processes and techniques. To improve this work research on other shrubland areas, with different physiological properties should be pursued. In addition, transferring this work to different environments, such as the Mediterranean, would provide further validation of the approach. Weather usually plays an important role in obtaining cloud free images and obtaining a larger number of images in a time-series from another area with lower cloud frequencies will help establish patterns of spatial and temporal FMC variation at landscape scale. Moreover, using sensors with higher spatial resolutions and ground data sampling from different places across a larger area that might result in more accurate FMC estimates.

Franch et al. (2019) recently developed a new method to account for BRDF changes in Landsat 8 OLI and Sentinel 2a data called the Harmonized Landsat/Sentinel-2 (HLS) project. This method reduces the effect of solar angle changes and view angle changes that may lead

to more accurate time-series remote sensing data to develop this research in future. A recent has investigated the application of satellite-derived synthetic aperture radar for burn scar mapping in the UK uplands (Johnston et al., 2018). These data have not yet been used to measure soil moisture or vegetation water content in fire-prone areas, but show some potential for this application.

6.10 Potential Beneficiaries

The UK routinely experiences wildfires in spring and summer specifically (Davies & Legg, 2016), but recent large-scale wildfire events in the UK have led to heightened concern from organizations responsible for fire prevention and moorland management. In the UK, statutory responsibility for wildfires rests with the FRS under the Fire and Rescue Services Act 2004. The FRS have indicated that the costs of vehicle response alone for vegetation fires in the UK is around £55 million/year (Gazzard et al, 2016). There are many sectors and agencies that contribute to wildfire management in England (see appendix IX). However, the key stakeholders that may be able to take advantage of this research include the England and Wales Wildfire Forum, Scottish Wildfire Forum and the Chief Fire Officers Association Wildfire Group, all of which are research and knowledge exchange initiatives. In addition, the Forestry Commission has experience of land management for improved fire resilience in UK forests specifically (Forestry Commission England, 2019). This research may also contribute to studies that aim to develop a UK fire danger rating system. The current Met Office Fire Severity Index (MOFSI) has been shown to be not fit for purpose (Met Office, 2019). One improvement will be inclusion of fuel type and FMC in future. In general, all these institutions seek to expand the approaches available to reduce wildfire risk, and to support effective responses when fires threaten a community or ecosystem.

6.11 Conclusions of research

The main aim of this research was to investigate the potential of using satellite data for landscape scale assessment of vegetation fuel moisture content in UK uplands and to examine how this could aid wildland fire risk assessment for a specific shrubland species. To achieve this aim, the work used laboratory experiments and radiative transfer modelling, fieldwork and image data analysis.

The first objective was to investigate the relationship between spectral reflectance and vegetation fuel moisture characteristics and how vegetation indices may be related to those characteristics. This objective was achieved using a laboratory experiment and radiative transfer modelling to test three hypotheses on the relationships between FMC, soil background and solar zenith angle, and canopy spectral reflectance. The results confirmed the strong relationship between FMC and VI although there was some variability in FMC estimation as a result of variations in soil background (dry/wet), and in addition a limited effect from changing solar zenith angle on canopy reflectance.

The second objective was to assess the spatial-temporal variation of fuel moisture characteristics at landscape scale based on spectral reflectance measurements. Fieldwork and satellite data were used to achieve this objective. Field sampling was planned to be coincident with the overpass of the satellite sensors, however, the weather played a role in the logistics and in obtaining a limited number of images.

The last objective was to assess seasonal variation in fuel characteristics at landscape scale and its relation to fire risk. The relationship between FMC and MSI from fieldwork was used to achieve this objective. The results emphasized the potential for FMC mapping at landscape scale using the whole of the Peak District as the test area. In spite of these results

there is a clear need to improve the accuracy with which FMC can be estimated at the landscape scale.

Mapping FMC at the landscape scale depends on the relationship between FMC and MSI derived from the remotely sensed data. The different morphologies of areas of *Calluna* cover were clear at the landscape scale, representing burned areas, managed areas and areas of continuous cover *Calluna*. Finer-scale analysis is necessary to better understand FMC variation at this local scale. For effective use of this information in fire risk models it must also be coupled with data relating to topography, vegetation composition and meteorological conditions.

Wildfires in the Peak District continue to present a challenge for land management and conservation and, at the time of writing the Conclusions to this thesis, there was a large wildfire on Goyt Moor, near Buxton in the Peak District. The Buxton Advertiser reported on Thursday 10th May 2018 that an uncontrolled fire covering around 35 ha of the moor broke out on Sunday 6th May 2018 and required a large number of agencies to control it. In addition, the Guardian reported on Sunday 1st July 2018 that, a large fire broke out on Tuesday 26th June 2018 near Saddleworth Moor during Britain's summer heatwave. The fire damaged at least 2,000 ha of moorland. Firefighters from across the north of England and Midlands travelled to Greater Manchester to help control the fires (Figure 6.3).

These incidents show the need for improved methods to predict and manage wildfires in sensitive ecosystems like the UK uplands. The work described in this thesis provides clear evidence that satellite remote sensing has a role to play in developing such methods, and also highlights the technical, methodological and logistical barriers that have yet to be overcome.

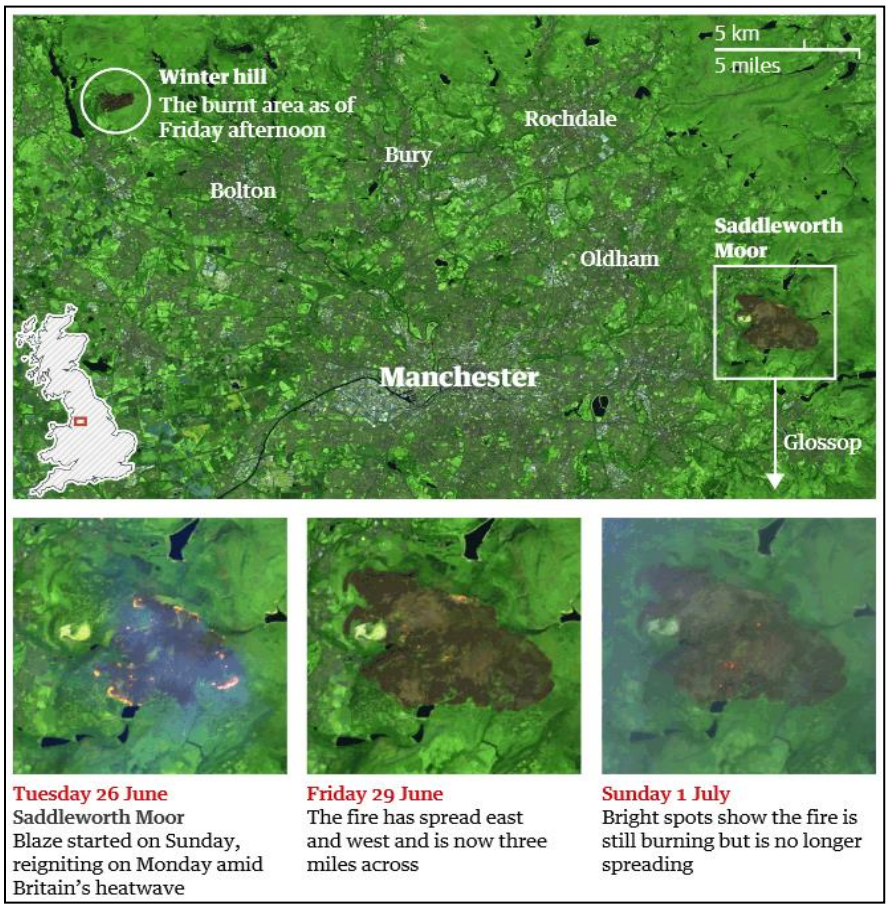

Figure 6.3 Saddleworth Moor wildfires (Source: The Guardian, 2018).

This research has shown that vegetation fuel moisture content can be estimated with satellite data, and this may help to assess the hazard related to wildfires in the UK uplands. However, for evaluating fire risk assessment, it is necessary to include other factors such as probability of ignition and pre-existing meteorological condition.

This research has made a significant contribution to wildfire risk assessment and the methods developed may be used in the management of the UK uplands in the future.

References

Agee, J. K., & Skinner, C. N. (2005). Basic principles of forest fuel reduction treatments. *Forest Ecology and Management, 211*(1), 83-96.

Agee, J. K., Wright, C. S., Williamson, N., & Huff, M. H. (2002). Foliar moisture content of Pacific Northwest vegetation and its relation to wildland fire behavior. *Forest Ecology and Management, 167*(1), 57-66.

Aguado, I., Chuvieco, E., Borén, R., & Nieto, H. (2007). Estimation of dead fuel moisture content from meteorological data in Mediterranean areas. Applications in fire danger assessment. *International Journal of Wildland Fire, 16*(4), 390-397.

Al-Moustafa, T., Armitage, R. P., & Danson, F. M. (2012). Mapping fuel moisture content in upland vegetation using airborne hyperspectral imagery. *Remote Sensing of Environment, 127*, 74-83.

Albertson, K., Aylen, J., Cavan, G., & McMorrow, J. (2009). Forecasting the outbreak of moorland wildfires in the English Peak District. *Journal of Environmental Management, 90*(8), 2642-2651.

Albertson, K., Aylen, J., Cavan, G., & McMorrow, J. (2010). Climate change and the future occurrence of moorland wildfires in the Peak District of the UK. *Climate Research (Open Access for articles 4 years old and older), 45*(1), 105.

Allan, G., Johnson, A., Cridland, S., & Fitzgerald, N. (2003). Application of NDVI for predicting fuel curing at landscape scales in northern Australia: can remotely sensed data help schedule fire management operations? *International Journal of Wildland Fire, 12*(4), 299-308.

Allen, W. A., Gausman, H. W., Richardson, A. J., & Thomas, J. R. (1969). Interaction of isotropic light with a compact plant leaf. *JOSA, 59*(10), 1376-1379.

Almoustafa, T. (2011). *Optical remote sensing for estimating fuel moisture content in upland vegetation.* PhD Thesis. University of Salford. UK.

Amalo, L. F., Ma'rufah, U., & Permatasari, P. A. (2018). *Monitoring 2015 drought in West Java using Normalized Difference Water Index (NDWI).* Paper presented at the IOP Conference Series: Earth and Environmental Science. Bogor, Indonesia.

Anderson, P., & Radford, E. (1994). Changes in vegetation following reduction in grazing pressure on the National Trust's Kinder Estate, Peak District, Derbyshire, England. *Biological Conservation, 69*(1), 55-63.

Argañaraz, J. P., Landi, M. A., Scavuzzo, C. M., & Bellis, L. M. (2018). Determining fuel moisture thresholds to assess wildfire hazard: a contribution to an operational early warning system. *PloS one, 13*(10), e0204889.

Arroyo, L. A., Pascual, C., & Manzanera, J. A. (2008). Fire models and methods to map fuel types: the role of remote sensing. *Forest Ecology and Management, 256*(6), 1239-1252.

Ashbourn, J. (2011). An Overview of the Geology of Britain. *Geological Landscapes of Britain* (pp. 17-33): Springer. Netherlands.

Asner, G. P. (1998). Biophysical and biochemical sources of variability in canopy reflectance. *Remote Sensing of Environment, 64*(3), 234-253.

Atzberger, C. (2004). Object-based retrieval of biophysical canopy variables using artificial neural nets and radiative transfer models. *Remote Sensing of Environment, 93*(1), 53-67.

Badhwar, G. (1981). *The use of parameters to separate and identify spring small grains.* Paper presented at the Quarterly Technical Interchange Meeting NASA Johnson Space Flight Center, Houston, Tex.

Bannari, A., Asalhi, H., & Teillet, P. (2002). *Transformed difference vegetation index (TDVI) for vegetation cover mapping.* Paper presented at the Geoscience and Remote Sensing Symposium, IEEE International. Ontario, Canada.

Bannari, A., Morin, D., Bonn, F., & Huete, A. (1995). A review of vegetation indices. *Remote Sensing Reviews, 13*(1-2), 95-120.

Bannari, A., Morin, D., & He, D. (1994). *High spatial and spectral resolution remote sensing for the management of the urban environment.* Paper presented at the The First International Airborne Remote Sensing Conference and Exhibition, Strasbourg, France.

Baret, F., & Guyot, G. (1991). Potentials and limits of vegetation indices for LAI and APAR assessment. *Remote Sensing of Environment, 35*(2-3), 161-173.

Baret, F., Jacquemoud, S., Guyot, G., & Leprieur, C. (1992). Modeled analysis of the biophysical nature of spectral shifts and comparison with information content of broad bands. *Remote Sensing of Environment, 41*(2-3), 133-142.

Barrett, E. C. (2013). *Introduction to environmental remote sensing*: Routledge.London.

Barsi, J. A., Lee, K., Kvaran, G., Markham, B. L., & Pedelty, J. A. (2014). The spectral response of the Landsat-8 operational land imager. *Remote Sensing, 6*(10), 10232-10251.

Birks, H., & Ratcliffe, D. (1980). Upland vegetation types. A list of National Vegetation Classification plant communities. *Nature Conservancy Council, Peterborough*.

Bisquert, M., Sánchez, J. M., & Caselles, V. (2014). Modeling fire danger in Galicia and Asturias (Spain) from MODIS Images. *Remote Sensing, 6*(1), 540-554.

Blackburn, G. A. (1998). Quantifying chlorophylls and caroteniods at leaf and canopy scales: An evaluation of some hyperspectral approaches. *Remote Sensing of Environment, 66*(3), 273-285.

Blackburn, G. A., & Ferwerda, J. G. (2008). Retrieval of chlorophyll concentration from leaf reflectance spectra using wavelet analysis. *Remote Sensing of Environment, 112*(4), 1614-1632.

Bonazountas, M., Kallidromitou, D., Kassomenos, P., & Passas, N. (2005). Forest fire risk analysis. *Human and Ecological Risk Assessment, 11*(3), 617-626.

Bowyer, P., & Danson, F. (2004). Sensitivity of spectral reflectance to variation in live fuel moisture content at leaf and canopy level. *Remote Sensing of Environment, 92*(3), 297-308.

Bréda, N. J. (2003). Ground-based measurements of leaf area index: a review of methods, instruments and current controversies. *Journal of Experimental Botany, 54*(392), 2403-2417.

Broge, N. H., & Leblanc, E. (2001). Comparing prediction power and stability of broadband and hyperspectral vegetation indices for estimation of green leaf area index and canopy chlorophyll density. *Remote Sensing of Environment, 76*(2), 156-172.

Bruegge, C., Schaepman, M., Strub, G., Beisl, U., Itten, K., Demircan, A., . . . Abdou, W. (2004). Field measurements of bi-directional reflectance. In *Reflection Properties of Vegetation and Soil with a BRDF Database* (pp. 195-224). Wissenschaft und Technik Verlag.

Carter, G. A., & Knapp, A. K. (2001). Leaf optical properties in higher plants: linking spectral characteristics to stress and chlorophyll concentration. *American Journal of Botany, 88*(4), 677-684.

Cary, G. J., Keane, R. E., Gardner, R. H., Lavorel, S., Flannigan, M. D., Davies, I. D., . . . Mouillot, F. (2006). Comparison of the sensitivity of landscape-fire-succession models to variation in terrain, fuel pattern, climate and weather. *Landscape Ecology, 21*(1), 121-137.

Casas, A., Riaño, D., Ustin, S., Dennison, P., & Salas, J. (2014). Estimation of water-related biochemical and biophysical vegetation properties using multitemporal airborne hyperspectral data and its comparison to MODIS spectral response. *Remote Sensing of Environment, 148*, 28-41.

Ceccato, P., Flasse, S., Tarantola, S., Jacquemoud, S., & Grégoire, J.-M. (2001). Detecting vegetation leaf water content using reflectance in the optical domain. *Remote Sensing of Environment, 77*(1), 22-33.

Ceccato, P., Gobron, N., Flasse, S., Pinty, B., & Tarantola, S. (2002). Designing a spectral index to estimate vegetation water content from remote sensing data: Part 1: Theoretical approach. *Remote Sensing of Environment, 82*(2), 188-197.

Chamard, P., Courel, M., Docousso, M., Guénégou, M., Le Rhun, J., Levasseur, J., . Togola, M. (1991). Utilisation des bandes spectrales du vert et du rouge pour une meilleure évaluation des formations végétales actives. *Télédétection et Cartographie*, 203-209.

Chappelle, E. W., Kim, M. S., & McMurtrey III, J. E. (1992). Ratio analysis of reflectance spectra (RARS): an algorithm for the remote estimation of the concentrations of chlorophyll a, chlorophyll b, and carotenoids in soybean leaves. *Remote Sensing of Environment, 39*(3), 239-247.

Chen, D., Huang, J., & Jackson, T. J. (2005). Vegetation water content estimation for corn and soybeans using spectral indices derived from MODIS near-and short-wave infrared bands. *Remote Sensing of Environment, 98*(2), 225-236.

Chen, J. M. (1996). Evaluation of vegetation indices and a modified simple ratio for boreal applications. *Canadian Journal of Remote Sensing, 22*(3), 229-242.

Chen, Z. (2006). Effects of fire on major forest ecosystem processes: an overview. *Ying yong sheng tai xue bao. TheJournal of Applied Ecology, 17*(9), 1726-1732.

Chuvieco, E., Riano, D., Van Wagtendok, J., & Morsdof, F. (2003). Fuel loads and fuel type mapping. In: E.Chuvieco (Ed.), *Wildland fire danger estimation and mapping.*

The role of remote sensing data, (pp 119-142). World Scientific Publishing. London.

Chuvieco, E., Aguado, I., Cocero, D., & Riaño, D. (2003). Design of an empirical index to estimate fuel moisture content from NOAA-AVHRR images in forest fire danger studies. *International Journal of Remote Sensing*, *24*(8), 1621-1637.

Chuvieco, E., Aguado, I., Yebra, M., Nieto, H., Salas, J., Martín, M. P., . . . Ibarra, P. (2010). Development of a framework for fire risk assessment using remote sensing and geographic information system technologies. *Ecological Modelling*, *221*(1), 46-58.

Chuvieco, E., Cocero, D., Aguado, I., Palacios, A., & Prado, E. (2004). Improving burning efficiency estimates through satellite assessment of fuel moisture content. *Journal of Geophysical Research: Atmospheres, 109*(D14).

Chuvieco, E., González, I., Verdú, F., Aguado, I., & Yebra, M. (2009). Prediction of fire occurrence from live fuel moisture content measurements in a Mediterranean ecosystem. *International Journal of Wildland Fire*, *18*(4), 430-441.

Chuvieco, E., Riano, D., Aguado, I., & Cocero, D. (2002). Estimation of fuel moisture content from multitemporal analysis of Landsat Thematic Mapper reflectance data: applications in fire danger assessment. *International Journal of Remote Sensing, 23*(11), 2145-2162.

Claudio, H. C., Cheng, Y., Fuentes, D. A., Gamon, J. A., Luo, H., Oechel, W., . . . Sims, D. A. (2006). Monitoring drought effects on vegetation water content and fluxes in chaparral with the 970 nm water band index. *Remote Sensing of Environment, 103*(3), 304-311.

Claverie, M., Ju, J., Masek, J. G., Dungan, J. L., Vermote, E. F., Roger, J.-C., . . . Justice, C. (2018). The Harmonized Landsat and Sentinel-2 surface reflectance data set. *Remote Sensing of Environment, 219*, 145-161.

Clay, G. D. (2009). *The impacts of heather and grassland burning in the Uplands: creating sustainable strategies.* PhD Thesis. Durham University.

Clevers, J. (1986). Application of a weighted infrared-red vegetation index for estimating leaf area index by correcting for soil moisture. *Remote Sensing of Environment, 29*(1), 25-37.

Colwell, J. E. (1974). Vegetation canopy reflectance. *Remote Sensing of Environment, 3*(3), 175-183.

Countryman, C. M., & Dean, W. A. (1979). Measuring moisture content in living chaparral: a field user's manual. *General Technical Report PSW-036. Berkeley, CA: US Department of Agriculture, Forest Service, Pacific Southwest Research Station. 28 p, 36*. Berkeley, California.

Danson, F., & Bowyer, P. (2004). Estimating live fuel moisture content from remotely sensed reflectance. *Remote Sensing of Environment, 92*(3), 309-321.

Danson, F., Steven, M., Malthus, T., & Clark, J. (1992). High-spectral resolution data for determining leaf water content. *International Journal of Remote Sensing, 13*(3), 461-470.

Danson, F. M. (2009). Remote sensing of fuel moisture content: advances in measurement and modelling. In: Chuvieco, E., and Lasaponara, R., (Eds.), *Advance in remote sensing and GIS applications in forest fire management twords an operational use of remote sensing in forest fire managemnet*. Proceeding of the VII International EARSeL. Workshop Matera, Italy.

Daughtry, C., Walthall, C., Kim, M., De Colstoun, E. B., & McMurtrey Iii, J. (2000). Estimating corn leaf chlorophyll concentration from leaf and canopy reflectance. *Remote Sensing of Environment, 74*(2), 229-239.

Daughtry, C. S. (2001). Discriminating crop residues from soil by shortwave infrared reflectance. *Agronomy Journal, 93*(1), 125-131.

Davies, G. M. (2005). *Fire behaviour and impact on heather moorland*. PhD Thesis. University of Edinburgh.

Davies, G. M., Kettridge, N., Stoof, C. R., Gray, A., Ascoli, D., Fernandes, P. M., . . . Clay, G. D. (2016). The role of fire in UK peatland and moorland management: the need for informed, unbiased debate. *Phil. Trans. R. Soc. B, 371*(1696), 20150342.

Davies, G. M., Legg, C., Smith, A., & MacDonald, A. (2006). Developing shrub fire behaviour models in an oceanic climate: burning in the British Uplands.V International Conference on Forest Fire Research. Figuera da Foz, Portugal.

Davies, G. M., & Legg, C. J. (2016). Regional variation in fire weather controls the reported occurrence of Scottish wildfires. *PeerJ, 4*, e2649.

Davies, G. M., Legg, C. J., Smith, A. A., & MacDonald, A. J. (2009). Rate of spread of fires in Calluna vulgaris-dominated moorlands. *Journal of Applied Ecology, 46*(5), 1054-1063.

Davies, G., Adam Smith, A., MacDonald, A. J., Bakker, J. D., & Legg, C. J. (2010). Fire intensity, fire severity and ecosystem response in heathlands: factors affecting the regeneration of Calluna vulgaris. *Journal of Applied Ecology, 47*(2), 356-365.

Davies, M. G., Gray, A., Hamilton, A., & Legg, C. J. (2008). The future of fire management in the British uplands. *The International Journal of Biodiversity Science and Management, 4*(3), 127-147.

Dawson, T. P., Curran, P. J., & Plummer, S. E. (1998). Liberty-Modeling the effects of leaf biochemical concentration on reflectance spectra. *Remote Sensing of Environment, 65*(1), 50-60.

Dennison, P. E., & Moritz, M. A. (2009). Critical live fuel moisture in chaparral ecosystems: a threshold for fire activity and its relationship to antecedent precipitation. *International Journal of Wildland Fire, 18*(8), 1021-1027.

Dennison, P. E., Moritz, M. A., & Taylor, R. S. (2008). Evaluating predictive models of critical live fuel moisture in the Santa Monica Mountains, California. *International Journal of Wildland Fire, 17*(1), 18-27.

Dennison, P., Roberts, D., Peterson, S., & Rechel, J. (2005). Use of normalized difference water index for monitoring live fuel moisture. *International Journal of Remote Sensing, 26*(5), 1035-1042.

Desbois, N., Deshayes, M., & Beudoin, A. (1997). Protocol for fuel moisture content measurements. *A review of remote sensing methods for the study of large wildland fires*, 61-72. Department of geography, University of Alcalá. Spain.

Dimitrakopoulos, A., & Papaioannou, K. K. (2001). Flammability assessment of Mediterranean forest fuels. *Fire Technology, 37*(2), 143-152.

Eitel, J. U., Gessler, P. E., Smith, A. M., & Robberecht, R. (2006). Suitability of existing and novel spectral indices to remotely detect water stress in Populus spp. *Forest Ecology and Management, 229*(1), 170-182.

Elvidge, C. D., & Chen, Z. (1995). Comparison of broad-band and narrow-band red and near-infrared vegetation indices. *Remote Sensing of Environment, 54*(1), 38-48.

Escadafal, R., & Huete, A. (1991). Etude des propriétés spectrales des sols arides appliquée à l'amélioration des indices de végétation obtenus par télédétection. *Comptes Rendus de l'Académie des Sciences. Série 2: Mécanique... 312*, 1385-1391.

Fagúndez, J., & Izco, J. (2004). Seed morphology of Calluna salisb.(Ericaceae). *Acta Botánica Malacitana, 29*, 215-220.

Falkowski, M. J., Gessler, P. E., Morgan, P., Hudak, A. T., & Smith, A. M. (2005). Characterizing and mapping forest fire fuels using ASTER imagery and gradient modeling. *Forest Ecology and Management, 217*(2-3), 129-146.

Fan, L.-y., Gao, Y.-z., Brück, H., & Bernhofer, C. (2009). Investigating the relationship between NDVI and LAI in semi-arid grassland in Inner Mongolia using in-situ measurements. *Theoretical and Applied Climatology, 95*(1-2), 151-156.

Fensholt, R., & Sandholt, I. (2003). Derivation of a shortwave infrared water stress index from MODIS near-and shortwave infrared data in a semiarid environment. *Remote Sensing of Environment, 87*(1), 111-121.

Féret, J.-B., François, C., Gitelson, A., Asner, G. P., Barry, K. M., Panigada, C., . . . Jacquemoud, S. (2011). Optimizing spectral indices and chemometric analysis of leaf chemical properties using radiative transfer modeling. *Remote Sensing of Environment, 115*(10), 2742-2750.

Finney, M. A. (2004). Landscape fire simulation and fuel treatment optimization. *Methods for Integrated Modeling of Landscape Change*, 117-131.

Flerchinger, G., & Yu, Q. (2007). Simplified expressions for radiation scattering in canopies with ellipsoidal leaf angle distributions. *Agricultural and Forest Meteorology, 144*(3), 230-235.

Fourty, T., Baret, F., Jacquemoud, S., Schmuck, G., & Verdebout, J. (1996). Leaf optical properties with explicit description of its biochemical composition: direct and inverse problems. *Remote Sensing of Environment, 56*(2), 104-117.

Forestry Commission England (2019) Wildfire Statistics for England 2009-10 to 2016-17. Available at https://www.gov.uk/government/publications/forestry-commission-england-wildfire-statistics-for-england-2009-10-to-2016-17 (accessed 29th September 2019).

Franch, B., Vermote, E., Skakun, S., Roger, J.-C., Masek, J., Ju, J., . . . Santamaria-Artigas, A. (2019). A method for Landsat and Sentinel 2 (HLS) BRDF normalization. *Remote Sensing, 11*(6), 632.

Fulé, P. Z., Crouse, J. E., Cocke, A. E., Moore, M. M., & Covington, W. W. (2004). Changes in canopy fuels and potential fire behavior 1880–2040: Grand Canyon, Arizona. *Ecological Modelling, 175*(3), 231-248.

Gamon, J., Penuelas, J., & Field, C. (1992). A narrow-waveband spectral index that tracks diurnal changes in photosynthetic efficiency. *Remote Sensing of Environment, 41*(1), 35-44.

Gao, B.-C. (1996). NDWI-a normalized difference water index for remote sensing of vegetation liquid water from space. *Remote Sensing of Environment, 58*(3), 257-266.

Gao, B.-C., & Goetz, A. F. (1994). Extraction of dry leaf spectral features from reflectance spectra of green vegetation. *Remote Sensing of Environment, 47*(3), 369-374.

Gao, B.-C., Montes, M. J., Davis, C. O., & Goetz, A. F. (2009). Atmospheric correction algorithms for hyperspectral remote sensing data of land and ocean. *Remote Sensing of Environment, 113*, S17-S24.

Gao, Z., Wang, Q., Cao, X., & Gao, W. (2014). The responses of vegetation water content (EWT) and assessment of drought monitoring along a coastal region using remote sensing. *GIScience & Remote Sensing, 51*(1), 1-16.

García, M., Chuvieco, E., Nieto, H., & Aguado, I. (2008). Combining AVHRR and meteorological data for estimating live fuel moisture content. *Remote Sensing of Environment, 112*(9), 3618-3627.

Gašparović, M., & Jogun, T. (2018). The effect of fusing Sentinel-2 bands on land-cover classification. *International Journal of Remote Sensing, 39*(3), 822-841.

Gazzard, R., McMorrow, J., & Aylen, J. (2016). Wildfire policy and management in England: an evolving response from Fire and Rescue Services, forestry and cross-sector groups. *Philosophical Transactions of the Royal Society B: Biological Sciences, 371*(1696), 20150341.

Geller, C. (2018). *Automated burned area identification in real-time during wildfire events using WorldView imagery for the insurance industry.* Paper presented at the Earth

Resources and Environmental Remote Sensing/GIS Applications IX. Berlin, Germany

Ghulam, A., Li, Z.-L., Qin, Q., Yimit, H., & Wang, J. (2008). Estimating crop water stress with ETM+ NIR and SWIR data. *Agricultural and Forest Meteorology, 148*(11), 1679-1695.

Giglio, L., Descloitres, J., Justice, C. O., & Kaufman, Y. J. (2003). An enhanced contextual fire detection algorithm for MODIS. *Remote Sensing of Environment, 87*(2), 273-282.

Gilbert, J. A. (2008). *Calluna vulgaris regeneration on upland moorland post-wildfire.* PhD Thesis. University of Central Lancashire. UK.

Gitelson, A. A. (2004). Wide dynamic range vegetation index for remote quantification of biophysical characteristics of vegetation. *Journal of Plant Physiology, 161*(2), 165-173.

Gitelson, A. A., Kaufman, Y. J., & Merzlyak, M. N. (1996). Use of a green channel in remote sensing of global vegetation from EOS-MODIS. *Remote Sensing of Environment, 58*(3), 289-298.

Gitelson, A. A., Kaufman, Y. J., Stark, R., & Rundquist, D. (2002). Novel algorithms for remote estimation of vegetation fraction. *Remote Sensing of Environment, 80*(1), 76-87.

Gitelson, A. A., Merzlyak, M. N., & Chivkunova, O. B. (2001). Optical properties and nondestructive estimation of anthocyanin content in plant leaves¶. *Photochemistry and Photobiology, 74*(1), 38-45.

Goel, N. S., & Strebel, D. E. (1983). Inversion of vegetation canopy reflectance models for estimating agronomic variables. I. Problem definition and initial results using the Suits model. *Remote Sensing of Environment, 13*(6), 487-507.

Gonzalo, C., Estibaliz Martinez, M., Arquero, A., & Ormeno, S. (1997). Use of satellite images and laboratory data to determine the influence of the photosynthetic pigments content on vegetation canopies spectral answer. *WIT Transactions on Ecology and the Environment, 19.*

Grime, J. P., Hodgson, J. G., & Hunt, R. (2014). *Comparative plant ecology: a functional approach to common British species*: Springer. Chapman & Hall, London.

Haboudane, D., Miller, J. R., Tremblay, N., Zarco-Tejada, P. J., & Dextraze, L. (2002). Integrated narrow-band vegetation indices for prediction of crop chlorophyll content for application to precision agriculture. *Remote Sensing of Environment, 81*(2-3), 416-426.

Hardisky, M., Klemas, V., & Smart, R. M. (1983). The influence of soil salinity, growth form, and leaf moisture on the spectral radiance of Spartina alterniflora canopies. *Photogrammetric Engineering and Remote Sensing, 49*, 77-83.

Hardtke, L. A., Del Valle, H. F., & Sione, W. (2011). Spatial distribution of wildfire risk in the Monte biome (Patagonia, Argentina). *Journal of Maps, 7*(1), 588-599.

Hardy, C. C. (2005). Wildland fire hazard and risk: Problems, definitions, and context. *Forest Ecology and Management, 211*(1), 73-82.

Harper, A. R., Doerr, S. H., Santin, C., Froyd, C. A., & Sinnadurai, P. (2018). Prescribed fire and its impacts on ecosystem services in the UK. *Science of The Total Environment, 624*, 691-703.

Hatfield, J., Kanemasu, E., Asrar, G., Jackson, R., Pinter Jr, P., Reginato, R., & Idso, S. (1985). Leaf-area estimates from spectral measurements over various planting dates of wheat. *International Journal of Remote Sensing, 6*(1), 167-175.

Hay, C., Kuretz, C., Odenweller, J., Scheffner, E., & Wood, B. (1979). Development of AI procedures for dealing with the effects of episodal events on crop temporal spectral response. *AGRISTARS SR-B9-00434*.

He, H. S., Shang, B. Z., Crow, T. R., Gustafson, E. J., & Shifley, S. R. (2004). Simulating forest fuel and fire risk dynamics across landscapes—LANDIS fuel module design. *Ecological Modelling, 180*(1), 135-151.

Holden, J., Shotbolt, L., Bonn, A., Burt, T., Chapman, P., Dougill, A., . . . Kirkby, M. (2007). Environmental change in moorland landscapes. *Earth-Science Reviews, 82*(1), 75-100.

Houborg, R., Soegaard, H., & Boegh, E. (2007). Combining vegetation index and model inversion methods for the extraction of key vegetation biophysical parameters using Terra and Aqua MODIS reflectance data. *Remote Sensing of Environment, 106*(1), 39-58.

Huete, A., Didan, K., Miura, T., Rodriguez, E. P., Gao, X., & Ferreira, L. G. (2002). Overview of the radiometric and biophysical performance of the MODIS vegetation indices. *Remote Sensing of Environment, 83*(1), 195-213.

Humboldt State Geospatial Online (2015). Vegetation Spectral Reflectance Curves. Retrieved 12 March 2018, from http://gsp.humboldt.edu/olm_2015/Courses/GSP_216_Online/lesson2-1/vegetation.html.

Hunt, E. R., & Rock, B. N. (1989). Detection of changes in leaf water content using near- and middle-infrared reflectances. *Remote Sensing of Environment, 30*(1), 43-54.

Hunt, E. R., Rock, B. N., & Nobel, P. S. (1987). Measurement of leaf relative water content by infrared reflectance. *Remote Sensing of Environment, 22*(3), 429-435.

Hunt, G. R. (1980). Electromagnetic radiation: the communication link in remote sensing. *Remote Sensing in Geology, 2*, 5-45.

Hunt Jr, E. R., Ustin, S. L., & Riaño, D. (2013). Remote sensing of leaf, canopy, and vegetation water contents for satellite environmental data records *Satellite-based applications on climate change* (pp. 335-357): Springer. USA.

Hutchinson, S. M., & Armitage, R. P. (2009). A peat profile record of recent environmental events in the South Pennines (UK). *Water, Air, and Soil Pollution, 199*(1-4), 247-259.

Idso, S., Jackson, R., Pinter Jr, P., Reginato, R., & Hatfield, J. (1981). Normalizing the stress-degree-day parameter for environmental variability. *Agricultural Meteorology, 24*, 45-55.

Jackson, R., Printer, P., Paul, J., Reginato, R., Robert, J., & Idso, S. (1980). Hand-held radiometry. Agricultural Reviews and Manuals ARM-W-19. Okland, CA. *US Department of Agriculture, Science and Education Administration, ARM-W-19, Phoenix, Arizona, USA.*

Jackson, R., Slater, P., & Pinter, P. (1983). Discrimination of growth and water stress in wheat by various vegetation indices through clear and turbid atmospheres. *Remote Sensing of Environment, 13*(3), 187-208.

Jackson, R. D., & Huete, A. R. (1991). Interpreting vegetation indices. *Preventive Veterinary Medicine, 11*(3), 185-200.

Jacquemoud, S., & Baret, F. (1990). PROSPECT: A model of leaf optical properties spectra. *Remote Sensing of Environment, 34*(2), 75-91.

Jacquemoud, S., Baret, F., Andrieu, B., Danson, F., & Jaggard, K. (1995). Extraction of vegetation biophysical parameters by inversion of the PROSPECT+ SAIL models on sugar beet canopy reflectance data. Application to TM and AVIRIS sensors. *Remote Sensing of Environment, 52*(3), 163-172.

Jacquemoud, S., Verhoef, W., Baret, F., Bacour, C., Zarco-Tejada, P. J., Asner, G. P., . . . Ustin, S. L. (2009). PROSPECT+ SAIL models: A review of use for vegetation characterization. *Remote Sensing of Environment, 113*, S56-S66.

Jacquemoud, S., Verhoef, W., Baret, F., Zarco-Tejada, P., Asner, G., Francois, C., & Ustin, S. (2006). *PROSPECT+ SAIL: 15 years of use for land surface characterization.* Paper presented at the 2006 IEEE International Symposium on Geoscience and Remote Sensing. (pp. 1992-1995). IEEE. USA.

Jenkins, M. J., Page, W. G., Hebertson, E. G., & Alexander, M. E. (2012). Fuels and fire behavior dynamics in bark beetle-attacked forests in Western North America and implications for fire management. *Forest Ecology and Management, 275*, 23-34.

Johnston, A., Millin-Chalabi, G., & Quincey, D. (2018). *Identifying and Characterising UK Upland Wildfires Using Sentinel-1 Radar*. 127. Poster session presented at UK National Earth Observation Conference 2018, Birmingham, United Kingdom.

Jolly, W. M., Cochrane, M. A., Freeborn, P. H., Holden, Z. A., Brown, T. J., Williamson, G. J., & Bowman, D. M. (2015). Climate-induced variations in global wildfire danger from 1979 to 2013. *Nature Communications, 6*, 7537.

Ju, J., Roy, D. P., Vermote, E., Masek, J., & Kovalskyy, V. (2012). Continental-scale validation of MODIS-based and LEDAPS Landsat ETM+ atmospheric correction methods. *Remote Sensing of Environment, 122*, 175-184.

Jung, M., Henkel, K., Herold, M., & Churkina, G. (2006). Exploiting synergies of global land cover products for carbon cycle modeling. *Remote Sensing of Environment, 101*(4), 534-553.

Jurdao, S., Chuvieco, E., & Arevalillo, J. M. (2012). Modelling fire ignition probability from satellite estimates of live fuel moisture content. *Fire Ecology, 8*(1), 77-97.

Justice, C., Giglio, L., Korontzi, S., Owens, J., Morisette, J., Roy, D., . . . Kaufman, Y. (2002). The MODIS fire products. *Remote Sensing of Environment, 83*(1), 244-262.

Kaufman, Y. J., & Tanre, D. (1992). Atmospherically resistant vegetation index (ARVI) for EOS-MODIS. *IEEE Transactions on Geoscience and Remote Sensing, 30*(2), 261-270.

Kauth, R. J., & Thomas, G. (1976). *The tasselled cap--a graphic description of the spectral-temporal development of agricultural crops as seen by Landsat.* Paper presented at the LARS Symposia. (p. 159). Purdue University. USA.

Keane, R. E. (2013). Describing wildland surface fuel loading for fire management: a review of approaches, methods and systems. *International Journal of Wildland Fire, 22*(1), 51-62.

Keane, R. E. (2015). *Wildland fuel fundamentals and applications*: Springer International Publishing Switzerland.

Keane, R. E., Gray, K. L., & Bacciu, V. (2012). *Spatial variability of wildland fuel characteristics in northern Rocky Mountain ecosystems*: US Department of Agriculture, Forest Service, Rocky Mountain Research Station.

Keeley, J. E. (2009). Fire intensity, fire severity and burn severity: a brief review and suggested usage. *International Journal of Wildland Fire, 18*(1), 116-126.

Kennedy, R. E., Townsend, P. A., Gross, J. E., Cohen, W. B., Bolstad, P., Wang, Y., & Adams, P. (2009). Remote sensing change detection tools for natural resource managers: Understanding concepts and tradeoffs in the design of landscape monitoring projects. *Remote Sensing of Environment, 113*(7), 1382-1396.

Khanna, S., Palacios-Orueta, A., Whiting, M. L., Ustin, S. L., Riaño, D., & Litago, J. (2007). Development of angle indexes for soil moisture estimation, dry matter detection and land-cover discrimination. *Remote Sensing of Environment, 109*(2), 154-165.

Kim, M. S., Daughtry, C., Chappelle, E., McMurtrey, J., & Walthall, C. (1994). The use of high spectral resolution bands for estimating absorbed photosynthetically active radiation (APAR). CNES, Proceedings of 6th International Symposium on Physical Measurements and Signatures in Remote Sensing; pp. (299-306). France.

Kitchen, K., Marno, P., Legg, C., Bruce, M., & Davies, G. (2006). Developing a fire danger rating system for the UK. *Forest Ecology and Management, 234*, S21.

Kodandapani, N., Cochrane, M. A., & Sukumar, R. (2008). A comparative analysis of spatial, temporal, and ecological characteristics of forest fires in seasonally dry

tropical ecosystems in the Western Ghats, India. *Forest Ecology and Management, 256*(4), 607-617.

Kogan, F. N. (1995). Application of vegetation index and brightness temperature for drought detection. *Advances in Space Research, 15*(11), 91-100.

Lee, B., Alexander, M., Hawkes, B., Lynham, T., Stocks, B., & Englefield, P. (2002). Information systems in support of wildland fire management decision making in Canada. *Computers and Electronics in Agriculture, 37*(1-3), 185-198.

Legg, C., Maltby, E., & Proctor, M. (1992). The ecology of severe moorland fire on the North York Moors: seed distribution and seedling establishment of Calluna vulgaris. *Journal of Ecology*, 80, 737-752.

Li, F., Miao, Y., Feng, G., Yuan, F., Yue, S., Gao, X., . . . Chen, X. (2014). Improving estimation of summer maize nitrogen status with red edge-based spectral vegetation indices. *Field Crops Research, 157*, 111-123.

Liang, S. (2005). *Quantitative remote sensing of land surfaces* (Vol. 30): John Wiley & Sons.Canada.

Liu, Q., & Weng, F. (2006). Advanced doubling–adding method for radiative transfer in planetary atmospheres. *Journal of the Atmospheric Sciences, 63*(12), 3459-3465.

Longbotham, N., Pacifici, F., Baugh, B., & Camps-Valls, G. (2014). *Prelaunch assessment of worldview-3 information content.* Paper presented at the 2014 6th Workshop on Hyperspectral Image and Signal Processing: Evolution in Remote Sensing (WHISPERS). Lausanne, Switzerland.

Lopes, S., Viegas, D. X., de Lemos, L., & Viegas, M. T. (2014). Rainfall effects on fine forest fuels moisture content. *Advances in Forest Fire Research; Imprensa da Universidade de Coimbra: Coimbra, Portugal*, pp. 427.

Louis, J., Debaecker, V., Pflug, B., Main-Knorn, M., Bieniarz, J., Mueller-Wilm, U., . . . Gascon, F. (2016). *Sentinel-2 Sen2Cor: L2A Processor for Users.* Paper presented at the Proceedings Living Planet Symposium 2016. Prague, Czech Republic.

Lusch, D. (1999). Introduction to Environmental Remote Sensing. *Center for Remote Sensing and GIS, Michigan State University*.

MacArthur, Alasdair A. (2011) *Field spectroscopy and spectral reflectance modelling of Calluna vulgaris*, PhD Thesis, University of Edinburgh, Edinburgh.

Mahlein, A.-K., Rumpf, T., Welke, P., Dehne, H.-W., Plümer, L., Steiner, U., & Oerke, E.-C. (2013). Development of spectral indices for detecting and identifying plant diseases. *Remote Sensing of Environment, 128*, 21-30.

Main-Knorn, M., Pflug, B., Debaecker, V., & Louis, J. (2015). Calibration and validation plan for the L2a processor and products of the Sentinel-2 mission. *The International Archives of Photogrammetry, Remote Sensing and Spatial Information Sciences, 40*(7), 1249.

Maki, M., Ishiahra, M., & Tamura, M. (2004). Estimation of leaf water status to monitor the risk of forest fires by using remotely sensed data. *Remote Sensing of Environment, 90*(4), 441-450.

Maltby, E., Legg, C., & Proctor, M. (1990). The ecology of severe moorland fire on the North York Moors: effects of the 1976 fires, and subsequent surface and vegetation development. *Journal of Ecology*, 490-518.

Mandanici, E., & Bitelli, G. (2016). Preliminary comparison of Sentinel-2 and Landsat 8 Imagery for a combined use. *Remote Sensing, 8*(12), 1014.

Markon, C. J., Fleming, M. D., & Binnian, E. F. (1995). Characteristics of vegetation phenology over the Alaskan landscape using AVHRR time-series data. *Polar Record, 31*(177), 179-190.

Martins, V. S., Barbosa, C. C. F., de Carvalho, L. A. S., Jorge, D. S. F., Lobo, F. d. L., & Novo, E. M. L. d. M. (2017). Assessment of atmospheric correction methods for Sentinel-2 MSI images applied to Amazon floodplain lakes. *Remote Sensing, 9*(4), 322.

Martonchik, J. V., Bruegge, C. J., & Strahler, A. H. (2000). A review of reflectance nomenclature used in remote sensing. *Remote Sensing Reviews, 19*(1-4), 9-20.

Matt, D. G., & Legg, C. J. (2008). The effect of traditional management burning on lichen diversity. *Applied Vegetation Science, 11*(4), 529-538.

McKenna, P., Phinn, S., & Erskine, P. (2018). Fire severity and vegetation recovery on mine site rehabilitation using WorldView-3 imagery. *Fire, 1*(2), 22.

McMorrow, J. (2011). *Wildfire in the United Kingdom: status and key issues.* Paper presented at the Proceedings of the Second Conference on the Human Dimensions of Wildland Fire GTR-NRS-P.

McMorrow, J., Lindley, S., Aylen, J., Cavan, G., Albertson, K., & Boys, D. (2009). Moorland wildfire risk, visitors and climate change: patterns, prevention and policy. *Drivers of Change in Upland Environments*, 432-459. Routledge. UK.

McNairn, H., & Protz, R. (1993). Mapping corn residue cover on agricultural fields in Oxford County, Ontario, using Thematic Mapper. *Canadian Journal of Remote Sensing, 19*(2), 152-159.

McNeil, B. E., Pisek, J., Lepisk, H., & Flamenco, E. A. (2016). Measuring leaf angle distribution in broadleaf canopies using UAVs. *Agricultural and Forest Meteorology, 218*, 204-208.

Mehner, H., Cutler, M., Fairbairn, D., & Thompson, G. (2004). Remote sensing of upland vegetation: the potential of high spatial resolution satellite sensors. *Global Ecology and Biogeography, 13*(4), 359-369.

Merzlyak, M. N., Gitelson, A. A., Chivkunova, O. B., & Rakitin, V. Y. (1999). Non-destructive optical detection of pigment changes during leaf senescence and fruit ripening. *Physiologia Plantarum, 106*(1), 135-141.

Met Office (2017). Sheffield climate. Retrieved 02 November 2017, from https://www.metoffice.gov.uk/public/weather/climate/gcqzwtdw7

Met Office (2019). England and Wales Fire Severity Index. Retrieved 05 October 2019, from https://www.metoffice.gov.uk/public/weather/fire-severity index/#?tab=map&fcTime=1570618800&zoom=5&lon=-4.00&lat=55.74.

Miller, G., & Cummins, R. (1987). Role of buried viable seeds in the recolonization of disturbed ground by heather (Calluna vulgaris [L.] Hull) in the Cairngorm mountains, Scotland, UK. *Arctic and Alpine Research, 19*(4), 396-401.

Milton, E. (1987). Review article: Principles of field spectroscopy. *Remote Sensing, 8*(12), 1807-1827.

Misra, P. N., Wheeler, S. G. and Oliver, R. E. (1977) Kauth-Thomas brigthness and greenness axes. Contract NASA 9-14350, RES 23-46.

Moritz, M. A., Morais, M. E., Summerell, L. A., Carlson, J., & Doyle, J. (2005). Wildfires, complexity, and highly optimized tolerance. *Proceedings of the National Academy of Sciences of the United States of America, 102*(50), 17912-17917.

Müller-Linow, M., Pinto-Espinosa, F., Scharr, H., & Rascher, U. (2015). The leaf angle distribution of natural plant populations: assessing the canopy with a novel software tool. *Plant Methods, 11*(1), 1-11.

Mumby, P., Green, E., Edwards, A., & Clark, C. (1997). Measurement of seagrass standing crop using satellite and digital airborne remote sensing. *Marine Ecology Progress Series, 159*, 51-60.

NCAVEO (2006). The Natural Radiation Environment. Retrieved 25th March 2018, from http://www.ncaveo.ac.uk/special_topics/field_spectroscopy/natural_environment/

Nisha Upadhyay (2016). Radiative Transfer Model. Retrieved 15th March 2017, from http://slideplayer.com/slide/7055822/

Olden, J. D., & Jackson, D. A. (2000). Torturing data for the sake of generality: how valid are our regression models? *Ecoscience, 7*(4), 501-510.

Ottmar, R. D., Sandberg, D. V., Riccardi, C. L., & Prichard, S. J. (2007). An overview of the Fuel Characteristic Classification System-Quantifying, classifying, and creating fuelbeds for resource planning. *Canadian Journal of Forest Research, 37*(12), 2383-2393.

Palmer, S., & Bacon, P. (2001). The utilization of heather moorland by territorial Red Grouse Lagopus lagopus scoticus. *Ibis, 143*(2), 222-232.

PDNPA (2001). The Peak District National Park Biodiversity and Action Plan: wildfire in the Peak District. Available at: http://www.peakdistrict.gov.uk/looking-after/biodiversity/biodiversity-action-plan. (accessed 15th April 2016).

PDNPA (2009). The Peak District National Park Landscape Strategy and Action Plan 2009-2019: introduction and overview. Final report. Available at: http://www.peakdistrict.gov.uk/data/assets/pdf_file/0003/90831/landscapestrategyandactionplan.pdf. (accessed 15th April 2016).

PDNPA (2014). The Peak District National Park Biodiversity and Action Plan: wildfire in the Peak District. Available at: https://www.peakdistrict.gov.uk/microsites/sopr/welcoming/tourism/volume. (accessed 8th November 2018).

PDNPA (2015). The Peak District National Park State of the Park. Available at: http://www.peakdistrict.gov.uk/microsites/sopr/landscape/climate. (accessed 7th June 2016).

PDNPVS (2015). Peak District National Park Visitor Survey 2014 & 2015 and Non-Visitor Surveys 2014 & 2015. Available at: https://www.peakdistrict.gov.uk/__data/assets/pdf_file/0011/775325/Visitor-and-Non-Visitor-2014-15.pdf. (accessed 5th November 2017).

PDNPVS (2014). Peak District National Park Visitor Survey 2014 and Non-Visitor Surveys 2014. Available at: https://www.peakdistrict.gov.uk/__data/assets/pdf_file/0005/538772/vistor-non-visitor-survey-2014.pdf. (accessed 5th November 2017).

Peak District National Park (2018). Map showing constituent authorities in the Peak District National Park. Retrieved 20th April 2018, from http://www.peakdistrict.gov.uk/visiting/maps/constituent-authorities.

Pearson, R. L., & Miller, L. D. (1972). *Remote mapping of standing crop biomass for estimation of the productivity of the shortgrass prairie.* Paper presented at the proceedings of the Eighth International Symposium on Remote Sensing of Environment, held October 2-6, 1972. p.1355. Michigan. USA.

Penuelas, J., Filella, I., Biel, C., Serrano, L., & Save, R. (1993). The reflectance at the 950–970 nm region as an indicator of plant water status. *International Journal of Remote Sensing, 14*(10), 1887-1905.

Perarnaud, V., Seguin, B., Malezieux, E., Deque, M., & Loustau, D. (2005). Agrometeorological research and applications needed to prepare agriculture and forestry to 21st century climate change. *Climatic Change, 70*(1-2), 319-340.

Perry, C. R., & Lautenschlager, L. F. (1984). Functional equivalence of spectral vegetation indices. *Remote Sensing of Environment, 14*(1), 169-182.

Pfitzner, K., Bartolo, R., Carr, G., Esparon, A., & Bollhöfer, A. (2011). Standards for reflectance spectral measurement of temporal vegetation plots: Supervising Scientist, Department of Sustainability, Environment, Water, Population and Communities. Australia.

Pinty, B., & Verstraete, M. (1992). GEMI: a non-linear index to monitor global vegetation from satellites. *Vegetatio, 101*(1), 15-20.

Piragnolo, M., Lusiani, G., & Pirotti, F. (2018). Comparison of vegetation indices from rpas and sentinel-2 imagery for detecting permanent pastures. *International*

Pivovaroff, A. L., Emery, N., Sharifi, M. R., Witter, M., Keeley, J. E., & Rundel, P. W. (2019). The effect of ecophysiological traits on live fuel moisture content. *Fire*, *2*(2), 28.

Pleniou, M., Xystrakis, F., Dimopoulos, P., & Koutsias, N. (2012). Maps of fire occurrence–spatially explicit reconstruction of recent fire history using satellite remote sensing. *Journal of Maps, 8*(4), 499-506.

Plummer, S., North, P., & Briggs, S. (1994). *The Angular Vegetation Index: An Atmospherically Resistant Index for the Second Along Track Sacnning Radiometer (ATSR-2).* In Proc. Sixth Int. Symp. Physical Measurements and Signatures in Remote Sensing, Val d'Isere, France.

Pollet, J., and Brown, A., 2007, *Fuel Moisture Sampling Guide.* Bureau of Land Management Utah State Office Salt Lake City, Utah.

Potter, B. E. (2012). Atmospheric interactions with wildland fire behaviour–I. Basic surface interactions, vertical profiles and synoptic structures. *International Journal of Wildland Fire*, *21*(7), 779-801.

Poulos, H. M., Camp, A. E., Gatewood, R. G., & Loomis, L. (2007). A hierarchical approach for scaling forest inventory and fuels data from local to landscape scales in the Davis Mountains, Texas, USA. *Forest Ecology and Management, 244*(1), 1-15.

Qi, J., Chehbouni, A., Huete, A., Kerr, Y., & Sorooshian, S. (1994). A modified soil adjusted vegetation index. *Remote Sensing of Environment, 48*(2), 119-126.

Quan, X., He, B., Yebra, M., Yin, C., Liao, Z., & Li, X. (2017). Retrieval of forest fuel moisture content using a coupled radiative transfer model. *Environmental Modelling & Software, 95*, 290-302.

Rein, G., Cleaver, N., Ashton, C., Pironi, P., & Torero, J. L. (2008). The severity of smouldering peat fires and damage to the forest soil. *Catena, 74*(3), 304-309.

Revel, C., Lonjou, V., Marcq, S., Desjardins, C., Fougnie, B., Coppolani-Delle Luche, C., . . . Miquel, C. (2019). Sentinel-2A and 2B absolute calibration monitoring. *European Journal of Remote Sensing, 52*(1), 122-137.

Riaño, D., Vaughan, P., Chuvieco, E., Zarco-Tejada, P. J., & Ustin, S. L. (2005). Estimation of fuel moisture content by inversion of radiative transfer models to simulate equivalent water thickness and dry matter content: Analysis at leaf and

canopy level. *IEEE Transactions on Geoscience and Remote Sensing, 43*(4), 819-826.

Riaño, D., Vaughan, P., Chuvieco, E., Zarco-Tejada, P. J., & Ustin, S. L. (2005). Estimation of fuel moisture content by inversion of radiative transfer models to simulate equivalent water thickness and dry matter content: analysis at leaf and canopy level. *Geoscience and Remote Sensing, IEEE Transactions on Geoscience and Remote Sensing, 43*(4), 819-826.

Richardson, A. J., & Wiegand, C. (1977). Distinguishing vegetation from soil background information. by gray mapping of Landsat MSS data.

Richter, R., Bachmann, M., Dorigo, W., & Müller, A. (2006). Influence of the adjacency effect on ground reflectance measurements. *IEEE Geoscience and Remote Sensing Letters, 3*(4), 565-569.

Richter, R., & Schläpfer, D. (2002). Geo-atmospheric processing of airborne imaging spectrometry data. Part 2: atmospheric/topographic correction. *International Journal of Remote Sensing, 23*(13), 2631-2649.

Rock, B., Vogelmann, J., Williams, D., Vogelmann, A., & Hoshizaki, T. (1986). Remote detection of forest damage. *BioScience, 36*(7), 439-445.

Rollins, M. G., Keane, R. E., & Parsons, R. A. (2004). Mapping fuels and fire regimes using remote sensing, ecosystem simulation, and gradient modeling. *Ecological Applications, 14*(1), 75-95.

Rollins, M. G., Morgan, P., & Swetnam, T. (2002). Landscape-scale controls over 20th century fire occurrence in two large Rocky Mountain (USA) wilderness areas. *Landscape Ecology, 17*(6), 539-557.

Rondeaux, G., Steven, M., & Baret, F. (1996). Optimization of soil-adjusted vegetation indices. *Remote Sensing of Environment, 55*(2), 95-107.

Rosema, A., Verhoef, W., Noorbergen, H., & Borgesius, J. (1992). A new forest light interaction model in support of forest monitoring. *Remote Sensing of Environment, 42*(1), 23-41.

Roujean, J.-L., & Breon, F.-M. (1995). Estimating PAR absorbed by vegetation from bidirectional reflectance measurements. *Remote Sensing of Environment, 51*(3), 375-384.

Rouse Jr, J. (1974). Monitoring the vernal advancement and retrogradation (green wave effect) of natural vegetation. Type II Report for period April 1973-September 1973. Texas A&M University Remote Sensing Centre College Station, Texas.

Rowland, C.S.; Morton, R.D.; Carrasco, L.; McShane, G.; O'Neil, A.W.; Wood, C.M. (2017) Land Cover Map 2015 (vector, GB). NERC Environmental Information Data Centre. Available at: https://doi.org/10.5285/6c6c9203-7333-4d96-88ab-78925e7a4e73. (accessed 15th January 2018).

Sakowska, K., Gianelle, D., Zaldei, A., MacArthur, A., Carotenuto, F., Miglietta, F., . . . Vescovo, L. (2015). WhiteRef: A new tower-based hyperspectral system for continuous reflectance measurements. *Sensors, 15*(1), 1088-1105.

San-Miguel-Ayanz, J., Carlson, J., Alexander, M., Tolhurst, K., Morgan, G., Sneeuwjagt, R., & Dudley, M. (2003). Current methods to assess fire danger potential. *Wildland Fire Danger Estimation and Mapping. The Role of Remote Sensing Data. World Scientific Publishing, Singapore*, pp. 21-61.

Sandberg, D. V., Ottmar, R. D., & Cushon, G. H. (2001). Characterizing fuels in the 21st century. *International Journal of Wildland Fire, 10*(4), 381-387.

Santana, V. M., & Marrs, R. H. (2014). Flammability properties of British heathland and moorland vegetation: models for predicting fire ignition. *Journal of Environmental Management, 139*, 88-96.

Schnitzer, M. (1982). Organic matter characterization. *Methods of soil analysis. Part 2. Chemical and Microbiological Properties*. Methods of soil. Part 2, 581-594. ASA-SSSA. USA.

Schowengerdt, R. A. (2006). *Remote sensing: models and methods for image processing*: Academic press. Elsevier. USA.

Serrano, L., Penuelas, J., & Ustin, S. L. (2002). Remote sensing of nitrogen and lignin in Mediterranean vegetation from AVIRIS data: Decomposing biochemical from structural signals. *Remote Sensing of Environment, 81*(2-3), 355-364.

Serrano, L., Ustin, S. L., Roberts, D. A., Gamon, J. A., & Penuelas, J. (2000). Deriving water content of chaparral vegetation from AVIRIS data. *Remote Sensing of Environment, 74*(3), 570-581.

Shang, B. Z., He, H. S., Crow, T. R., & Shifley, S. R. (2004). Fuel load reductions and fire risk in central hardwood forests of the United States: a spatial simulation study. *Ecological Modelling, 180*(1), 89-102.

Shen, L., Li, Z., & Guo, X. (2014). Remote sensing of leaf area index (LAI) and a spatiotemporally parameterized model for mixed grasslands. *International Journal of Applied Science and Technology, 4*(1).

Sims, D. A., & Gamon, J. A. (2002). Relationships between leaf pigment content and spectral reflectance across a wide range of species, leaf structures and developmental stages. *Remote Sensing of Environment, 81*(2), 337-354.

Sommers, W. T., Loehman, R. A., & Hardy, C. C. (2014). Wildland fire emissions, carbon, and climate: Science overview and knowledge needs. *Forest Ecology and Management, 317,* 1-8.

Sow, M., Mbow, C., Hély, C., Fensholt, R., & Sambou, B. (2013). Estimation of herbaceous fuel moisture content using vegetation indices and land surface temperature from MODIS data. *Remote Sensing, 5*(6), 2617-2638.

Spindelböck, J. P., Cook, Z., Daws, M. I., Heegaard, E., Måren, I. E., & Vandvik, V. (2013). Conditional cold avoidance drives between-population variation in germination behaviour in Calluna vulgaris. *Annals of Botany, 112*(5), 801-810.

Sprintsin, M., Karnieli, A., Berliner, P., Rotenberg, E., Yakir, D., & Cohen, S. (2007). The effect of spatial resolution on the accuracy of leaf area index estimation for a forest planted in the desert transition zone. *Remote Sensing of Environment, 109*(4), 416-428.

Sripada, R. P., Heiniger, R. W., White, J. G., & Weisz, R. (2005). Aerial color infrared photography for determining late-season nitrogen requirements in corn. *Agronomy Journal, 97*(5), 1443-1451.

Stimson, H. C., Breshears, D. D., Ustin, S. L., & Kefauver, S. C. (2005). Spectral sensing of foliar water conditions in two co-occurring conifer species: Pinus edulis and Juniperus monosperma. *Remote Sensing of Environment, 96*(1), 108-118.

Stonex, S., Stewart, C., Bastik, R., Michaud, K., Smith, J., Sahd, K., Halperin, J., Kearny, D., Roller, T., Rodgers, M., Dennett, C., Swanson, D., Gatewood, R., Maxwell, C., and Ellington, J., (2004). Southwest Area Fuel Moisture Monitoring

Program: Standard Methods and Procedures. USDA Forest Service, Southwest Region. Albuquerque, New Mexico.

Taiz, L. and Zeiger, E. (2002). *Plant Physiology*, 3rd and 5th Edition. The Benjamin Cummings Publishing Company, Redwood City. California.

Tharme, A., Green, R., Baines, D., Bainbridge, I., & O'brien, M. (2001). The effect of management for red grouse shooting on the population density of breeding birds on heather-dominated moorland. *Journal of Applied Ecology*, *38*(2), 439-457.

The Guardain. (2018). Firefighters from seven counties fight Greater Manchester moor fires. 1st July. available at: https://www.theguardian.com/uk-news/2018/jul/01/firefighters-from-seven-counties-fight-greater-manchester-moor-fires. (accessed 15th January 2019).

Thompson, D., MacDonald, A., Marsden, J., & Galbraith, C. (1995). Upland heather moorland in Great Britain: a review of international importance, vegetation change and some objectives for nature conservation. *Biological Conservation*, *71*(2), 163-178.

Tucker, C. J. (1980). Remote sensing of leaf water content in the near infrared. *Remote Sensing of Environment*, *10*(1), 23-32.

Turner, D. P., Cohen, W. B., Kennedy, R. E., Fassnacht, K. S., & Briggs, J. M. (1999). Relationships between leaf area index and Landsat TM spectral vegetation indices across three temperate zone sites. *Remote Sensing of Environment*, *70*(1), 52-68.

Urbanski, S. P., Hao, W. M., & Baker, S. (2008). Chemical composition of wildland fire emissions. *Developments in Environmental Science*, *8*, 79-107.

USGS (2017). Spectral Characteristics Viewer Retrieved 12th November 2017, from https://landsat.usgs.gov/spectral-characteristics-viewer.

Usher, M., & Thompson, D. (1993). Variation in the upland heathlands of Great Britain: conservation importance. *Biological Conservation*, *66*(1), 69-81.

Ustin, S. L., Riaño, D., Koltunov, A., Roberts, D. A., & Dennison, P. E. (2009). Mapping Fire Risk in Mediterranean Ecosystems of California: Vegetation type, Density, Invasive Species, and Fire Frequency *Earth Observation of Wildland Fires in Mediterranean Ecosystems* (pp. 41-53). Springer. Verlag Berlin Heidelberg.

Van Der Werff, H., & Van Der Meer, F. (2016). Sentinel-2A MSI and Landsat 8 OLI provide data continuity for geological remote sensing. *Remote Sensing, 8*(11), 883-898.

Van Wijk, M. T., & Williams, M. (2005). Optical instruments for measuring leaf area index in low vegetation: application in arctic ecosystems. *Ecological Applications, 15*(4), 1462-1470.

Verhoef, W. (1984). Light scattering by leaf layers with application to canopy reflectance modeling: the SAIL model. *Remote Sensing of Environment, 16*(2), 125-141.

Villaescusa-Nadal, J. L., Franch, B., Roger, J. C., Vermote, E. F., Skakun, S., & Justice, C. (2019). Spectral adjustment model's analysis and application to remote sensing data. *IEEE Journal of Selected Topics in Applied Earth Observations and Remote Sensing, 12*(3), 961-972.

Viney, N. R. (1991). A review of fine fuel moisture modelling. *International Journal of Wildland Fire, 1*(4), 215-234.

Walter-Shea, E. A., & Biehl, L. L. (1990). Measuring vegetation spectral properties. *Remote Sensing Reviews, 5*(1), 179-205.

Wang, J., Xu, R., & Yang, S. (2009). Estimation of plant water content by spectral absorption features centered at 1,450 nm and 1,940 nm regions. *Environmental Monitoring and Assessment, 157*(1-4), 459-469.

Wang, L., Hunt Jr, E. R., Qu, J. J., Hao, X., & Daughtry, C. S. (2013). Remote sensing of fuel moisture content from ratios of narrow-band vegetation water and dry-matter indices. *Remote Sensing of Environment, 129*, 103-110.

Wang, L., & Qu, J. J. (2007). NMDI: A normalized multi-band drought index for monitoring soil and vegetation moisture with satellite remote sensing. *Geophysical Research Letters, 34*(20), 1-5.

Wang, L., Qu, J. J., Hao, X., & Hunt Jr, E. R. (2011). Estimating dry matter content from spectral reflectance for green leaves of different species. *International Journal of Remote Sensing, 32*(22), 7097-7109.

Wang, L., Qu, J. J., Hao, X., & Zhu, Q. (2008). Sensitivity studies of the moisture effects on MODIS SWIR reflectance and vegetation water indices. *International Journal of Remote Sensing, 29*(24), 7065-7075.

Wang, X., Wotton, B. M., Cantin, A. S., Parisien, M.-A., Anderson, K., Moore, B., & Flannigan, M. D. (2017). CFFDRS: an R package for the Canadian forest fire danger rating system. *Ecological Processes, 6*(1), 5-16.

Whalley, W., Leeds-Harrison, P., & Bowman, G. (1991). Estimation of soil moisture status using near infrared reflectance. *Hydrological Processes, 5*(3), 321-327.

Williams, D. L. (1991). A comparison of spectral reflectance properties at the needle, branch, and canopy level for selected conifer species. *Remote Sensing of Environment, 35*(2), 79-93.

Wotton, B., Martell, D., & Logan, K. (2003). Climate change and people-caused forest fire occurrence in Ontario. *Climatic Change, 60*(3), 275-295.

Wu, C., Niu, Z., Tang, Q., & Huang, W. (2009). Predicting vegetation water content in wheat using normalized difference water indices derived from ground measurements. *Journal of Plant Research, 122*(3), 317-326.

Wulder, M. A., Hilker, T., White, J. C., Coops, N. C., Masek, J. G., Pflugmacher, D., & Crevier, Y. (2015). Virtual constellations for global terrestrial monitoring. *Remote Sensing of Environment, 170*, 62-76.

Xiao, X., Zhang, Q., Braswell, B., Urbanski, S., Boles, S., Wofsy, S., . . . Ojima, D. (2004). Modeling gross primary production of temperate deciduous broadleaf forest using satellite images and climate data. *Remote Sensing of Environment, 91*(2), 256-270.

Xie, Y., Sha, Z., & Yu, M. (2008). Remote sensing imagery in vegetation mapping: a review. *Journal of Plant Ecology, 1*(1), 9-23.

Xue, J., & Su, B. (2017). Significant remote sensing vegetation indices: A review of developments and applications. *Journal of Sensors, 2017*, 1-17.

Yakubu, I., Mireku-Gyimah, D., & Duker, A. (2015). Review of methods for modelling forest fire risk and hazard. *African Journal of Environmental Science and Technology, 9*(3), 155-165.

Yallop, A., Thacker, J., Thomas, G., Stephens, M., Clutterbuck, B., Brewer, T., & Sannier, C. (2006). The extent and intensity of management burning in the English uplands. *Journal of Applied Ecology, 43*(6), 1138-1148.

Yazdani, R., Ryerson, A., & Derenyi, E. (1981). *Vegetation change detection in an area—a simple approach for use with geo-data base.* Paper presented at the

Proceedings of the 7th Canadian Symposium on Remote Sensing. Winnipeg, Manitoba. Canada.

Yebra, M., Aguado, I., García, M., Nieto, H., Chuvieco, E., & Salas, J. (2007). *Fuel moisture estimation for fire ignition mapping.* Paper presented at the Actas de la IV Conferencia Internacional sobre Incendios Forestales, Sevilla (España).

Yebra, M., & Chuvieco, E. (2009). Linking ecological information and radiative transfer models to estimate fuel moisture content in the Mediterranean region of Spain: Solving the ill-posed inverse problem. *Remote Sensing of Environment, 113*(11), 2403-2411.

Yebra, M., Chuvieco, E., & Riano, D. (2008). Estimation of live fuel moisture content from MODIS images for fire risk assessment. *Agricultural and Forest Meteorology, 148*(4), 523-536.

Yebra, M., Dennison, P. E., Chuvieco, E., Riaño, D., Zylstra, P., Hunt, E. R., . . . Jurdao, S. (2013). A global review of remote sensing of live fuel moisture content for fire danger assessment: Moving towards operational products. *Remote Sensing of Environment, 136*, 455-468.

Yebra, M., Scortechini, G., Badi, A., Beget, M. E., Boer, M. M., Bradstock, R., . . . de Dios, V. R. (2019). Globe-LFMC, a global plant water status database for vegetation ecophysiology and wildfire applications. *Scientific Data, 6*(1), 1-8.

Yilmaz, M. T., Hunt Jr, E. R., Goins, L. D., Ustin, S. L., Vanderbilt, V. C., & Jackson, T. J. (2008). Vegetation water content during SMEX04 from ground data and Landsat 5 Thematic Mapper imagery. *Remote Sensing of Environment, 112*(2), 350-362.

Zarco-Tejada, P. J., Berjón, A., López-Lozano, R., Miller, J. R., Martín, P., Cachorro, V., . . . De Frutos, A. (2005). Assessing vineyard condition with hyperspectral indices: Leaf and canopy reflectance simulation in a row-structured discontinuous canopy. *Remote Sensing of Environment, 99*(3), 271-287.

Zarco-Tejada, P. J., González-Dugo, V., & Berni, J. A. (2012). Fluorescence, temperature and narrow-band indices acquired from a UAV platform for water stress detection using a micro-hyperspectral imager and a thermal camera. *Remote Sensing of Environment, 117*, 322-337.

Zarco-Tejada, P. J., Rueda, C., & Ustin, S. (2003). Water content estimation in vegetation with MODIS reflectance data and model inversion methods. *Remote Sensing of Environment, 85*(1), 109-124.

Zhang, H. K., Roy, D. P., Yan, L., Li, Z., Huang, H., Vermote, E., . . . Roger, J.-C. (2018). Characterization of Sentinel-2A and Landsat-8 top of atmosphere, surface, and nadir BRDF adjusted reflectance and NDVI differences. *Remote Sensing of Environm*ent. 215, 482-494.

Zhang, J., Xu, Y., Yao, F., Wang, P., Guo, W., Li, L., & Yang, L. (2010). Advances in estimation methods of vegetation water content based on optical remote sensing techniques. *Science China Technological Sciences, 53*(5), 1159-1167.

Zheng, X., Huang, Q., Wang, J., Wang, T., & Zhang, G. (2018). Geometric accuracy evaluation of high-resolution satellite images based on Xianning test field. *Sensors, 18*(7), 2121.

Zhang, Y., & Zhao, F. (2011). Study of environmental vegetation index based on environment satellite CCD data and LAI inversion. *Spectroscopy and Spectral Analysis, 31*(10), 2789-2793.

Zhu, X., & Liu, D. (2015). Improving forest aboveground biomass estimation using seasonal Landsat NDVI time-series. *ISPRS Journal of Photogrammetry and Remote Sensing, 102*, 222-231.

Appendices

Appendix I

Table of vegetation indices found in the literature from 1972 to 2014.

Index	Abbreviation	Author and Year
Adjusted Green Vegetation Index	AGVI	Jackson, Slater, and Pinter (1983)
Anth Reflectance Index	ARI	Gitelson, Merzlyak, and Chivkunova (2001)
Atmospherically Resistant Vegetation Index	ARVI	Kaufman and Tanre (1992)
Adjusted Soil Brightness Index	ASBI	Jackson et al. (1983)
Angular Vegetation Index	AVI	Plummer et al. (1994)
Blue Green Pigment Index	BGI	Zarco-Tejada et al. (2005)
Blue Red Pigment Index	BRI	Zarco-Tejada, González-Dugo, and Berni (2012)
Chlorophyll Absorption Reflectance Index	CARI	Kim, Daughtry, Chappelle, McMurtrey, and Walthall (1994)
Cellulose Absorption Index	CAS	Daughtry (2001)
Canopy Chlorophyll Content Index	CCCI	Li et al. (2014)
Continuum Removed Chlorophyll Well Depth	CRCWD	Broge and Leblanc (2001)
Crop Water Stress Index	CWSI	Idso, Jackson, Pinter Jr, Reginato, and Hatfield (1981)
Differenced Vegetation Index	DVI	Clevers (1989)
Enhanced Vegetation Index	EVI	Huete et al. (2002)
Green Atmospherically Resistant Vegetation Index	GARVI	Gitelson, Kaufman, and Merzlyak (1996)
Green Difference Vegetation Index	GDVI	Sripada, Heiniger, White, and Weisz (2005)
Global Environment Monitoring Index	GEMI	Pinty and Verstraete (1992)
Green normalized difference vegetation index	GNDVI	Gitelson et al. (1996)
Greenness Above Bare Soil	GRABS	Hay et al. (1979)
Green-Red Vegetation Index	GRVI	Falkowski, Gessler, Morgan, Hudak, and Smith (2005)
Green Vegetation Index	GVI	Kauth and Thomas (1976)
Global Vegetation Moisture Index	GVMI	Ceccato et al. (2002)
Greenness Vegetation and Soil Brightness	GVSB	Badhwar (1981)
Healthy Index	HI	Mahlein et al. (2013)
Huan Jing vegetation Index	HJVI	Zhang and Zhao (2011)
Leaf Water Stress Index	LWSI	Hunt et al. (1987)

Modified Chlorophyll Absorption in Reflectance Index	MCARI	Daughtry, Walthall, Kim, De Colstoun, and McMurtrey Iii (2000)
Maximum Difference Water Index	MDWI	Eitel, Gessler, Smith, and Robberecht (2006)
Misra Green Vegetation Index	MGVI	Misra et al. (1977)
Misra Non Such Index	MNSI	Misra et al. (1977)
Modified SAVI	MSAVI	Qi et al. (1994)
Misra Soil Brightness Index	MSBI	Misra et al. (1977)
Moisture Stress Index	MSI	Hunt and Rock (1989)
Modified Simple Ratio	MSR	Chen (1996)
Multi-Temporal Vegetation Index	MTVI	Yazdani et al. (1981)
Misra Yellow Vegetation Index	MYVI	Misra et al. (1977)
Normalized Difference Greenness Index	NDGI	Chamard et al. (1991)
Normalized Difference Index	NDI	McNairn and Protz (1993)
Normalized Difference Infrared Index	NDII	Hardisky et al. (1983)
Normalized Difference Lignin Index	NDLI	Serrano, Penuelas, and Ustin (2002)
Normalized Difference Nitrogen Index	NDNI	Serrano et al. (2002)
Normalized Difference Vegetation Index	NDVI	Rouse et al. (1974)
Normalized Difference Water Index	NDWI	Gao (1996)
Non-Linear Index	NLI	Chen (1996)
Normalized Multi-band Drought Index	NMDI	Wang and Qu (2007)
Non Such Index	NSI	Kauth and Thomas (1976)
Optimal Soil Adjusted Vegetation Index	OSAVI	Rondeaux, Steven, and Baret (1996)
Physiological Reflectance Index	PRI	Gamon, Penuelas, and Field (1992)
Pigment-Specific Normalized Difference	PSND	Blackburn (1998)
Plant Senescence Reflectance Index	PSRI	Merzlyak, Gitelson, Chivkunova, and Rakitin (1999)
Pigment-Specific Simple Ratio	PSSR	Blackburn (1998)
Perpendicular Vegetation Index	PVI	Jackson et al. (1980)
Ratio Analysis of Reflectance Spectra	RARS	Chappelle, Kim, and McMurtrey III (1992)
Renormalized Difference Vegetation Index	RDVI	Roujean and Breon (1995)
Redness Index	RI	Escadafal and Huete (1991)
Ratio Vegetation-Index	RVI	Pearson and Miller (1972)
Shortwave Angle Slope Index	SASI	Khanna et al. (2007)
Soil Adjusted Vegetation Indices	SAVI	Chen (1996)
Soil Brightness Index	SBI	Kauth and Thomas (1976)
Soil Background Line	SBL	Richardson and Wiegand (1977)
Shortwave Infrared Water Stress Index	SIWSI	Fensholt and Sandholt (2003)
Simple Ratio Water Index	SRWI	Zarco-Tejada et al.(2003)
Transformed Chlorophyll Absorption in Reflectance Index	TCARI	Haboudane, Miller, Tremblay, Zarco-Tejada, and Dextraze (2002)

Transformed Difference Vegetation Index	TDVI	Bannari, Asalhi, and Teillet (2002)
Transformed Soil Atmospherically Resistant Vegetation Index	TSARVI	Bannari et al. (1994)
Transformed Soil Adjusted Vegetation Index	TSAVI	Baret and Guyot (1991)
Transformed Vegetation Index	TVI	Perry and Lautenschlager (1984)
Vegetation Condition Index	VCI	Kogan (1995)
Visible Atmospherically Resistant Index	VDVI	Gitelson, Kaufman, Stark, and Rundquist (2002)
Vegetation Index Number	VIN	Pearson and Miller (1972)
Vegetation Water Stress Index	VWSI	Ghulam et al. (2008)
Wide Dynamic Range Vegetation Index	WDRVI	Gitelson (2004)
Water Index	WI	Penuelas et al.(1993)
Yellow Vegetation Index	YVI	Kauth and Thomas (1976)

Appendix II:

Results of FMC measurement sampling from study area (Burbage Moor).

Table 1: Samples from Peak District (Burbage) 20-04-2016								
No of plot	GPS of the centre	Place of sampling	Height of the plant/cm	Fresh weight	Dry weight	Water weight (g)	Water Content %	FMC%
1	383257 N 427429 E	Centre	50	15.244	7.811	7.433	48.760	95.161
		NW	55	17.492	9.201	8.291	47.399	90.110
		NE	55	15.858	8.592	7.266	45.819	84.567
		SW	40	18.902	10.431	8.471	44.815	81.210
		SE	55	17.062	9.042	8.02	47.005	88.697
2	383186 N 427545 E	Centre	60	20.099	10.801	9.298	46.261	86.085
		NW	55	21.774	11.331	10.443	47.961	92.163
		NE	45	23.583	12.79	10.793	45.766	84.386
		SW	55	18.723	10.221	8.502	45.409	83.182
		SE	55	19.555	10.721	8.834	45.175	82.399
3	383197 N 427377 E	Centre	40	22.255	13.582	8.673	38.971	63.857
		NW	55	23.986	10.671	13.315	55.512	124.777
		NE	60	23.503	14.551	8.952	38.089	61.522
		SW	50	22.258	13.02	9.238	41.504	70.952
		SE	45	23.776	14.461	9.315	39.178	64.415
4	382962 N 426815 E	Centre	45	25.782	14.601	11.181	43.367	76.577
		NW	45	20.118	11.4	8.718	43.334	76.474
		NE	45	23.967	13.551	10.416	43.460	76.865
		SW	55	21.691	12.201	9.49	43.751	77.781
		SE	50	20.107	11.371	8.736	43.448	76.827
5	382976 N 426857 E	Centre	45	20.714	11.922	8.792	42.445	73.746
		NW	40	26.631	14.89	11.741	44.088	78.852
		NE	45	21.431	12.071	9.36	43.675	77.541
		SW	40	24.092	13.36	10.732	44.546	80.329
		SE	50	24.478	13.091	11.387	46.519	86.983

Table 2: Samples from Peak District (Burbage) 24-05-2016								
No of plot	GPS of the centre	Place of sampling	Height of the plant/cm	Fresh weight	Dry weight	Water weight (g)	Water Content %	FMC%
1	383257 N 427429 E	Centre	52	30.438	13.668	16.77	55.096	122.695
		NW	50	24.512	11.229	13.283	54.190	118.292
		NE	53	34.874	15.042	19.832	56.868	131.844
		SW	42	26.695	12.516	14.179	53.115	113.287
		SE	62	28.573	12.999	15.574	54.506	119.809
2	383186 N 427545 E	Centre	62	28.203	9.909	18.294	64.865	184.620
		NW	58	26.955	11.202	15.753	58.442	140.627
		NE	67	25.246	10.489	14.757	58.453	140.690
		SW	60	27.857	10.441	17.416	62.519	166.804
		SE	65	25.376	10.457	14.919	58.792	142.670
3	383197 N 427377 E	Centre	40	35.059	16.694	18.365	52.383	110.010
		NW	50	25.261	11.473	13.788	54.582	120.178
		NE	43	28.679	14.773	13.906	48.488	94.131
		SW	42	33.357	15.812	17.545	52.598	110.960
		SE	42	27.947	12.73	15.217	54.449	119.537
4	382962 N 426815 E	Centre	54	21.001	10.726	10.275	48.926	95.795
		NW	45	28.997	11.195	17.802	61.393	159.017
		NE	53	27.974	12.059	15.915	56.892	131.976
		SW	52	26.285	11.382	14.903	56.698	130.935
		SE	54	24.494	11.588	12.906	52.690	111.374
5	382976 N 426857 E	Centre	52	37.983	16.871	21.112	55.583	125.138
		NW	49	34.908	16.4	18.508	53.019	112.854
		NE	42	38.387	17.916	20.471	53.328	114.261
		SW	50	32.671	13.696	18.975	58.079	138.544
		SE	43	36.119	14.131	21.988	60.877	155.601

Table 3: Samples from Peak District (Burbage) 21-06-2016								
No of plot	GPS of the centre	Place of sampling	Height of the plant/cm	Fresh weight	Dry weight	Water weight (g)	Water Content %	FMC%
1	383257 N 427429 E	Centre	45	20.001	8.696	11.305	56.522	130.002
		NW	40	21.075	8.054	13.021	61.784	161.671
		NE	50	19.881	7.457	12.424	62.492	166.609
		SW	40	19.001	8.924	10.077	53.034	112.920
		SE	55	27.581	11.232	16.349	59.276	145.557
2	383186 N 427545 E	Centre	60	22.951	8.711	14.24	62.045	163.472
		NW	55	29.587	11.092	18.495	62.511	166.742
		NE	55	24.011	9.375	14.636	60.955	156.117
		SW	60	25.282	9.369	15.913	62.942	169.847
		SE	65	26.739	9.657	17.082	63.884	176.887
3	383197 N 427377 E	Centre	45	25.697	12.791	12.906	50.224	100.899
		NW	40	23.002	9.9	13.102	56.960	132.343
		NE	25	26.251	11.781	14.47	55.122	122.825
		SW	40	23.651	10.685	12.966	54.822	121.348
		SE	40	31.032	14.008	17.024	54.860	121.531
4	382962 N 426815 E	Centre	45	27.942	13.486	14.456	51.736	107.193
		NW	55	26.382	10.944	15.438	58.517	141.064
		NE	50	21.872	8.755	13.117	59.972	149.823
		SW	50	21.961	9.534	12.427	56.587	130.344
		SE	65	30.795	12.041	18.754	60.900	155.751
5	382976 N 426857 E	Centre	55	37.082	15.553	21.529	58.058	138.424
		NW	55	39.412	15.827	23.585	59.842	149.018
		NE	40	28.141	12.986	15.155	53.854	116.703
		SW	55	33.592	14.645	18.947	56.403	129.375
		SE	45	23.741	10.004	13.737	57.862	137.315

Table 4: Samples from Peak District (Burbage) 19-07-2016								
No of plot	GPS of the centre	Place of sampling	Height of the plant/cm	Fresh weight	Dry weight	Water weight (g)	Water Content %	FMC%
1	383257 N 427429 E	Centre	54	17.094	6.359	10.735	62.800	168.816
		NW	48	23.618	8.602	15.016	63.579	174.564
		NE	54	21.287	7.462	13.825	64.946	185.272
		SW	46	22.854	8.685	14.169	61.998	163.143
		SE	50	19.258	6.328	12.93	67.141	204.330
2	383186 N 427545 E	Centre	58	16.34	6.618	9.722	59.498	146.902
		NW	72	26.837	8.89	17.947	66.874	201.879
		NE	64	22.897	8.735	14.162	61.851	162.129
		SW	44	24.67	10.362	14.308	57.998	138.082
		SE	52	27.235	10.598	16.637	61.087	156.982
3	383197 N 427377 E	Centre	39	23.38	9.826	13.554	57.973	137.940
		NW	48	26.433	9.938	16.495	62.403	165.979
		NE	45	22.82	9.183	13.637	59.759	148.503
		SW	40	22.419	9.157	13.262	59.155	144.829
		SE	40	23.479	9.232	14.247	60.680	154.322
4	382962 N 426815 E	Centre	44	28.509	10.61	17.899	62.784	168.699
		NW	48	26.302	9.651	16.651	63.306	172.531
		NE	64	27.751	9.573	18.178	65.504	189.888
		SW	46	24.355	9.224	15.131	62.127	164.040
		SE	51	25.77	9.712	16.058	62.313	165.342
5	382976 N 426857 E	Centre	50	30.112	12.627	17.485	58.067	138.473
		NW	43	28.237	9.251	18.986	67.238	205.232
		NE	53	25.591	10.139	15.452	60.381	152.402
		SW	54	28.75	9.732	19.018	66.150	195.417
		SE	47	26.038	9.341	16.697	64.126	178.750

Table 5: Samples from Peak District (Burbage) 15-08-2016								
No of plot	GPS of the centre	Place of sampling	Height of the plant/cm	Fresh weight	Dry weight	Water weight (g)	Water Content %	FMC%
1	383257 N 427429 E	Centre	52	24.107	10.419	13.688	56.780	131.375
		NW	56	27.465	13.431	14.034	51.098	104.490
		NE	51	30.404	11.171	19.233	63.258	172.169
		SW	45	28.967	12.322	16.645	57.462	135.084
		SE	50	34.174	14.518	19.656	57.517	135.391
2	383186 N 427545 E	Centre	70	20.631	8.829	11.802	57.205	133.673
		NW	60	26.299	11.065	15.234	57.926	137.677
		NE	65	25.785	10.708	15.077	58.472	140.801
		SW	40	25.792	11.026	14.766	57.250	133.920
		SE	68	41.16	16.665	24.495	59.512	146.985
3	383197 N 427377 E	Centre	40	26.01	10.484	15.526	59.692	148.092
		NW	45	32.9	15.473	17.427	52.970	112.628
		NE	38	38.985	19.326	19.659	50.427	101.723
		SW	42	28.165	12.661	15.504	55.047	122.455
		SE	40	29.068	14.39	14.678	50.495	102.001
4	382962 N 426815 E	Centre	49	36.248	16.926	19.322	53.305	114.156
		NW	40	28.491	11.99	16.501	57.917	137.623
		NE	60	34.027	14.567	19.46	57.190	133.590
		SW	58	34.309	13.761	20.548	59.891	149.321
		SE	55	33.743	13.847	19.896	58.963	143.685
5	382976 N 426857 E	Centre	60	36.518	16.482	20.036	54.866	121.563
		NW	48	30.824	14.886	15.938	51.706	107.067
		NE	40	33.033	13.942	19.091	57.794	136.932
		SW	58	34.269	15.013	19.256	56.191	128.262
		SE	45	31.879	14.087	17.792	55.811	126.301

Table 6: Samples from Peak District (Burbage) 27-09-2016								
No of plot	GPS of the centre	Place of sampling	Height of the plant/cm	Fresh weight	Dry weight	Water weight (g)	Water Content %	FMC%
1	383257 N 427429 E	Centre	47	35.97	16.567	19.403	53.942	117.118
		NW	50	36.992	16.462	20.53	55.498	124.711
		NE	53	36.23	15.494	20.736	57.234	133.832
		SW	45	29.73	13.886	15.844	53.293	114.101
		SE	40	37.788	17.07	20.718	54.827	121.371
2	383186 N 427545 E	Centre	69	35.661	15.546	20.115	56.406	129.390
		NW	57	36.936	16.583	20.353	55.103	122.734
		NE	60	41.099	18.549	22.55	54.868	121.570
		SW	58	35.742	15.37	20.372	56.997	132.544
		SE	63	32.818	15.23	17.588	53.593	115.483
3	383197 N 427377 E	Centre	43	33.49	16.942	16.548	49.412	97.674
		NW	50	35.599	18.514	17.085	47.993	92.282
		NE	45	39.1	19.514	19.586	50.092	100.369
		SW	39	33.649	17.215	16.434	48.839	95.463
		SE	45	32.6	15.171	17.429	53.463	114.884
4	382962 N 426815 E	Centre	55	29.809	14.976	14.833	49.760	99.045
		NW	42	28.142	13.432	14.71	52.271	109.515
		NE	62	28.572	12.909	15.663	54.819	121.334
		SW	55	23.81	10.957	12.853	53.982	117.304
		SE	57	34.206	15.494	18.712	54.704	120.769
5	382976 N 426857 E	Centre	60	27.291	13.127	14.164	53.942	117.118
		NW	49	30.339	11.511	18.828	55.498	124.711
		NE	40	32.123	15.945	16.178	57.234	133.832
		SW	52	32.987	15.172	17.815	53.293	114.101
		SE	45	35.66	17.025	18.635	54.827	121.371

Table 7: Samples from Peak District (Burbage) 27-10-2016								
No of plot	GPS of the centre	Place of sampling	Height of the plant/cm	Fresh weight	Dry weight	Water weight (g)	Water Content %	FMC%
1	383257 N 427429 E	Centre	45	36.532	17.543	18.989	51.979	108.243
		NW	46	29.697	13.607	16.09	54.181	118.248
		NE	54	36.109	16.971	19.138	53.001	112.769
		SW	46	26.691	13.489	13.202	49.462	97.872
		SE	45	29.774	13.244	16.53	55.518	124.811
2	383186 N 427545 E	Centre	70	34.102	14.169	19.933	58.451	140.680
		NW	48	36.28	17.344	18.936	52.194	109.179
		NE	62	32.127	13.041	19.086	59.408	146.354
		SW	54	35.574	15.821	19.753	55.527	124.853
		SE	62	29.827	14.598	15.229	51.058	104.323
3	383197 N 427377 E	Centre	47	26.726	13.478	13.248	49.570	98.294
		NW	56	24.209	12.557	11.652	48.131	92.793
		NE	40	28.151	15.624	12.527	44.499	80.178
		SW	35	26.33	12.148	14.182	53.863	116.744
		SE	43	29.722	13.373	16.349	55.006	122.254
4	382962 N 426815 E	Centre	58	21.942	14.631	7.311	33.320	49.969
		NW	50	26.705	15.446	11.259	42.161	72.893
		NE	43	28.492	15.018	13.474	47.290	89.719
		SW	52	26.718	13.25	13.468	50.408	101.645
		SE	45	28.893	11.97	16.923	58.571	141.378
5	382976 N 426857 E	Centre	48	33.122	10.719	22.403	67.638	209.003
		NW	40	30.43	13.261	17.169	56.421	129.470
		NE	58	32.341	14.47	17.871	55.258	123.504
		SW	55	27.776	13.583	14.193	51.098	104.491
		SE	52	33.697	14.617	19.08	56.622	130.533

Table 8: Samples from Peak District (Burbage) 16-11-2016								
No of plot	GPS of the centre	Place of sampling	Height of the plant/cm	Fresh weight	Dry weight	Water weight (g)	Water Content %	FMC%
1	383257 N 427429 E	Centre	45	31.331	12.609	18.722	59.756	148.481
		NW	52	29.243	12.113	17.13	58.578	141.418
		NE	54	28.512	12.362	16.15	56.643	130.642
		SW	46	26.132	10.924	15.208	58.197	139.216
		SE	47	33.217	14.386	18.831	56.691	130.898
2	383186 N 427545 E	Centre	68	37.35	15.526	21.824	58.431	140.564
		NW	49	34.41	14.294	20.116	58.460	140.730
		NE	58	26.459	11.248	15.211	57.489	135.233
		SW	62	29.22	12.001	17.219	58.929	143.480
		SE	64	29.809	13.308	16.501	55.356	123.993
3	383197 N 427377 E	Centre	42	23.965	10.711	13.254	55.306	123.742
		NW	54	23.753	10.872	12.881	54.229	118.479
		NE	40	21.041	10.062	10.979	52.179	109.114
		SW	40	29.055	13.826	15.229	52.414	110.148
		SE	43	30.582	11.51	19.072	62.363	165.699
4	382962 N 426815 E	Centre	45	32.916	12.27	20.646	62.723	168.264
		NW	42	32.259	12.407	19.852	61.539	160.006
		NE	56	34.684	12.586	22.098	63.712	175.576
		SW	52	33.828	12.729	21.099	62.371	165.755
		SE	50	34.21	12.901	21.309	62.289	165.173
5	382976 N 426857 E	Centre	55	23.483	9.54	13.943	59.375	146.153
		NW	47	25.887	10.475	15.412	59.536	147.131
		NE	40	33.685	12.842	20.843	61.876	162.303
		SW	52	26.4	9.716	16.684	63.197	171.717
		SE	46	29.357	11.109	18.248	62.159	164.263

Table 9: Samples from Peak District (Burbage) 16-12-2016								
No of plot	GPS of the centre	Place of sampling	Height of the plant/cm	Fresh weight	Dry weight	Water weight (g)	Water Content %	FMC%
1	383257 N 427429 E	Centre	45	61.421	21.377	40.044	65.196	187.323
		NW	43	32.852	12.464	20.388	62.060	163.575
		NE	54	31.93	12.188	19.742	61.829	161.979
		SW	45	30.721	11.485	19.236	62.615	167.488
		SE	50	25.037	12.271	12.766	50.989	104.034
2	383186 N 427545 E	Centre	57	37.941	14.497	23.444	61.791	161.716
		NW	54	35.757	13.939	21.818	61.017	156.525
		NE	55	40.939	15.74	25.199	61.553	160.095
		SW	62	34.666	13.385	21.281	61.389	158.991
		SE	65	38.712	15.219	23.493	60.687	154.366
3	383197 N 427377 E	Centre	47	29.999	11.418	18.581	61.939	162.734
		NW	52	26.978	6.794	20.184	74.817	297.086
		NE	44	25.425	9.463	15.962	62.781	168.678
		SW	42	24.123	9.851	14.272	59.163	144.879
		SE	40	39.342	15.321	24.021	61.057	156.785
4	382962 N 426815 E	Centre	45	39.148	11.632	27.516	70.287	236.554
		NW	43	36.369	13.917	22.452	61.734	161.328
		NE	54	44.668	15.513	29.155	65.270	187.939
		SW	50	40.936	10.404	30.532	74.585	293.464
		SE	48	41.9	15.107	26.793	63.945	177.355
5	382976 N 426857 E	Centre	58	30.516	10.548	19.968	65.435	189.306
		NW	52	27.626	9.197	18.429	66.709	200.381
		NE	36	28.271	7.238	21.033	74.398	290.591
		SW	52	26.012	9.032	16.98	65.278	187.998
		SE	50	27.86	9.448	18.412	66.088	194.877

Table 10: Samples from Peak District (Burbage) 25-01-2017								
No of plot	GPS of the centre	Place of sampling	Height of the plant/cm	Fresh weight	Dry weight	Water weight (g)	Water Content %	FMC%
1	383257 N 427429 E	Centre	43	23.194	10.731	12.463	53.734	116.140
		NW	50	17.748	7.566	10.182	57.370	134.576
		NE	55	19.744	8.025	11.719	59.355	146.031
		SW	42	14.633	6.239	8.394	57.363	134.541
		SE	48	21.932	10.075	11.857	54.063	117.687
2	383186 N 427545 E	Centre	66	27.34	11.402	15.938	58.296	139.783
		NW	56	27.891	11.651	16.24	58.227	139.387
		NE	58	26.735	12.433	14.302	53.495	115.033
		SW	57	25.813	11.028	14.785	57.277	134.068
		SE	60	28.8	12.17	16.63	57.743	136.648
3	383197 N 427377 E	Centre	42	19.391	8.187	11.204	57.779	136.851
		NW	46	17.118	7.799	9.319	54.440	119.490
		NE	37	17.498	7.031	10.467	59.818	148.869
		SW	40	19.241	8.386	10.855	56.416	129.442
		SE	43	16.38	6.91	9.47	57.814	137.048
4	382962 N 426815 E	Centre	48	32.535	13.941	18.594	57.151	133.376
		NW	42	33.788	13.715	20.073	59.409	146.358
		NE	64	32.054	13.855	18.199	56.776	131.353
		SW	50	29.169	12.976	16.193	55.514	124.792
		SE	62	32.234	13.409	18.825	58.401	140.391
5	382976 N 426857 E	Centre	56	19.509	8.958	10.551	54.083	117.783
		NW	58	18.948	7.953	10.995	58.027	138.250
		NE	40	20.297	8.75	11.547	56.890	131.966
		SW	50	21.53	9.678	11.852	55.049	122.463
		SE	42	20.381	9.02	11.361	55.743	125.953

Table 11: Samples from Peak District (Burbage) 24-02-2017								
No of plot	GPS of the centre	Place of sampling	Height of the plant/cm	Fresh weight	Dry weight	Water weight (g)	Water Content %	FMC%
1	383257 N 427429 E	Centre	42	28.689	13.596	15.093	52.609	111.011
		NW	45	29.265	14.247	15.018	51.317	105.412
		NE	48	30.298	14.993	15.305	50.515	102.081
		SW	43	20.318	9.733	10.585	52.097	108.754
		SE	37	25.532	12.721	12.811	50.176	100.708
2	383186 N 427545 E	Centre	63	24.387	11.466	12.921	52.983	112.690
		NW	58	21.655	10.759	10.896	50.316	101.273
		NE	60	23.496	11.451	12.045	51.264	105.187
		SW	52	25.796	12.338	13.458	52.171	109.078
		SE	61	25.363	12.527	12.836	50.609	102.467
3	383197 N 427377 E	Centre	50	17.002	8.681	8.321	48.941	95.853
		NW	52	12.001	6.159	5.842	48.679	94.853
		NE	44	16.38	8.61	7.77	47.436	90.244
		SW	39	13.612	6.923	6.689	49.140	96.620
		SE	38	11.929	6.485	5.444	45.637	83.948
4	382962 N 426815 E	Centre	41	17.42	8.513	8.907	51.131	104.628
		NW	37	16.796	8.193	8.603	51.221	105.004
		NE	54	16.339	6.309	10.03	61.387	158.979
		SW	50	13.933	5.844	8.089	58.056	138.416
		SE	51	14.843	5.921	8.922	60.109	150.684
5	382976 N 426857 E	Centre	48	26.827	13.065	13.762	51.299	105.335
		NW	51	28.925	13.66	15.265	52.774	111.750
		NE	38	29.832	15.335	14.497	48.595	94.535
		SW	52	26.241	12.855	13.386	51.012	104.131
		SE	48	26.595	14.081	12.514	47.054	88.872

Table 12: Samples from Peak District (Burbage) 26-03-2017								
No of plot	GPS of the centre	Place of sampling	Height of the plant/cm	Fresh weight	Dry weight	Water weight (g)	Water Content %	FMC%
1	383257 N 427429 E	Centre	47	30.486	15.074	15.412	50.554	102.242
		NW	54	29.663	14.754	14.909	50.261	101.051
		NE	52	26.713	13.365	13.348	49.968	99.873
		SW	50	32.900	16.998	15.902	48.334	93.552
		SE	48	34.44	17.133	17.307	50.253	101.016
2	383186 N 427545 E	Centre	67	19.274	10.281	8.993	46.659	87.472
		NW	60	23.295	11.978	11.317	48.581	94.482
		NE	55	25.848	13.676	12.172	47.091	89.003
		SW	53	22.23	11.397	10.833	48.731	95.051
		SE	65	20.378	11.024	9.354	45.902	84.851
3	383197 N 427377 E	Centre	52	20.949	11.764	9.185	43.845	78.077
		NW	50	15.527	8.309	7.218	46.487	86.870
		NE	42	13.698	7.655	6.043	44.116	78.942
		SW	33	19.135	10.387	8.748	45.717	84.221
		SE	41	19.316	10.678	8.638	44.719	80.895
4	382962 N 426815 E	Centre	47	28.138	14.725	13.413	47.669	91.090
		NW	42	25.111	13.71	11.401	45.402	83.158
		NE	56	21.563	10.692	10.871	50.415	101.674
		SW	53	15.011	7.652	7.359	49.024	96.171
		SE	56	19.338	9.428	9.91	51.246	105.112
5	382976 N 426857 E	Centre	53	31.06	16.001	15.059	48.484	94.113
		NW	52	32.263	16.349	15.914	49.326	97.339
		NE	40	28.134	14.368	13.766	48.930	95.810
		SW	55	27.675	13.63	14.045	50.750	103.045
		SE	48	31.02	15.897	15.123	48.752	95.131

Appendix III:

Meteorological Office weather station data 1981 - 2010, Sheffield, located at 53.38º N, 1.48º W at 131.0 m above mean sea level.

Mean monthly temperature				
Month	Max. temp Sheffield	Min. temp Sheffield	Max. temp UK	Min. temp UK
Jan	6.7	1	6.4	0.9
Feb	7	0.8	6.6	0.7
Mar	9.7	2.4	8.9	2.1
Apr	12.5	3.7	11.4	3.4
May	15.9	6.5	14.7	6
Jun	18.8	9.4	17.3	8.8
Jul	21.1	11.5	19.4	10.9
Aug	20.8	11.3	19.1	10.8
Sep	17.8	9.3	16.5	8.8
Oct	13.7	6.5	12.8	6.2
Nov	9.6	3.5	9.1	3.3
Dec	6.9	1.3	6.7	1.1

Mean monthly rainfall		
Month	Rainfall (mm) Sheffield	Rainfall (mm) UK
Jan	74	121.7
Feb	54	88.6
Mar	58.8	95.1
Apr	59.1	72.7
May	58.5	70
Jun	62.3	73.4
Jul	60.8	78.1
Aug	66.9	89.5
Sep	66.2	96.4
Oct	82	127.1
Nov	77.1	121.2
Dec	78.7	120.2

Mean monthly sunshine		
Month	Sunshine (hours) Sheffield	Sunshine (hours) UK
Jan	52.1	47.2
Feb	71.4	69.8
Mar	104.8	101.8
Apr	147	148.1
May	183.2	185.9
Jun	174.7	169.5
Jul	189.6	172.4
Aug	177.6	163
Sep	132.2	124.7
Oct	99.4	92.5
Nov	61.2	57.2
Dec	45	40.8

Appendix IV:

The Landsat images from http://earthexplorer.usgs.gov, and Sentinel-2a images from https://scihub.copernicus.eu.

04-05-2016 L8OLI

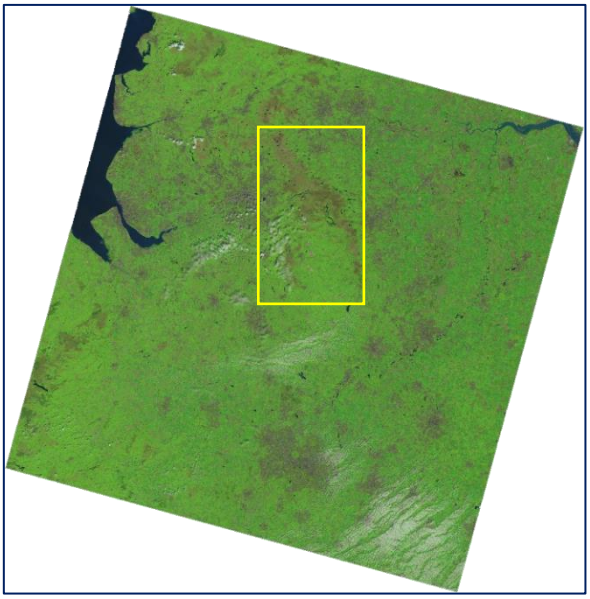

05-06-2016 L8OLI

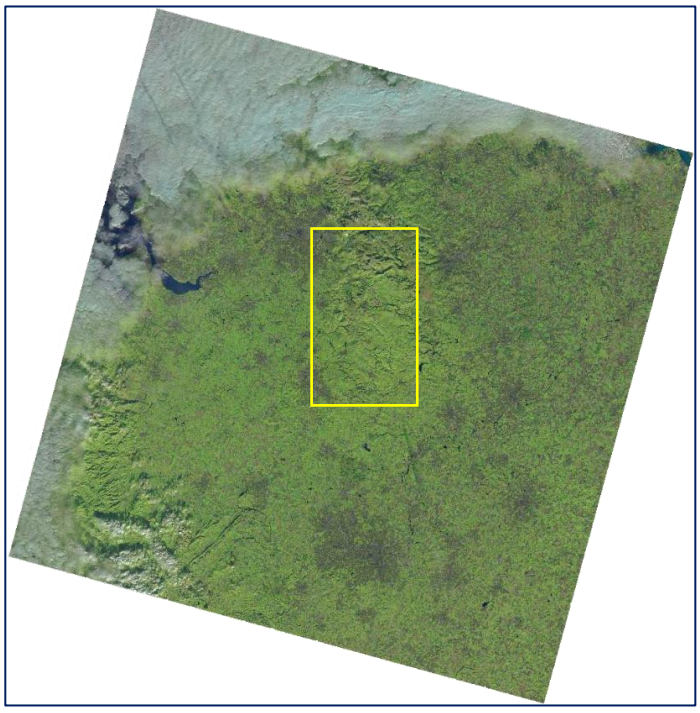

28-11-2016 L8OLI

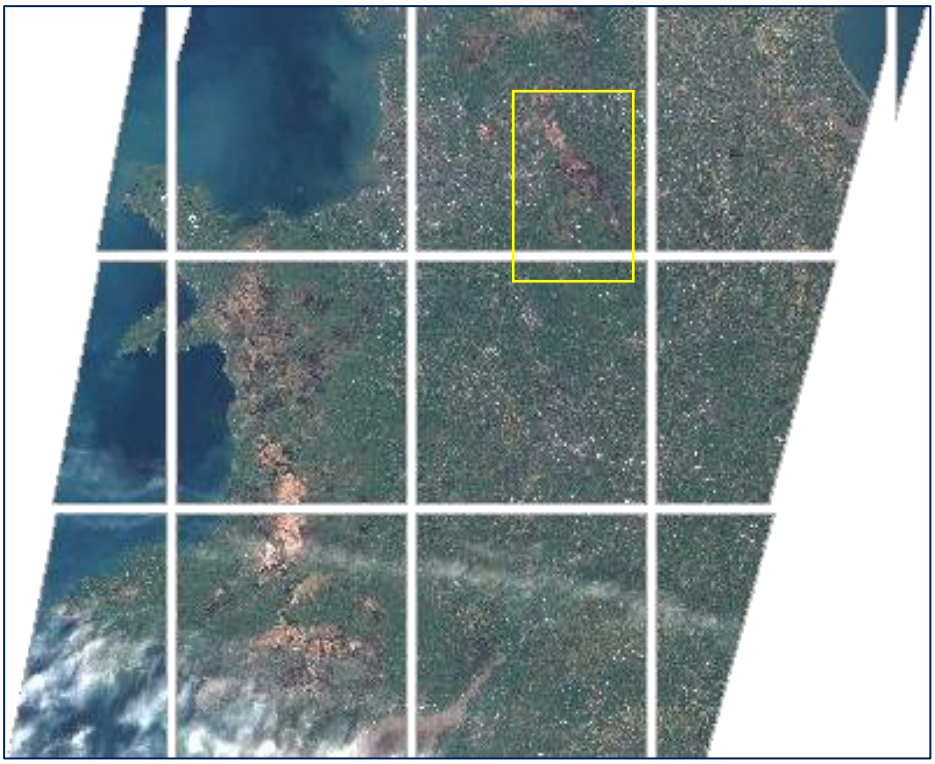

20-04-2016 S2A MSI

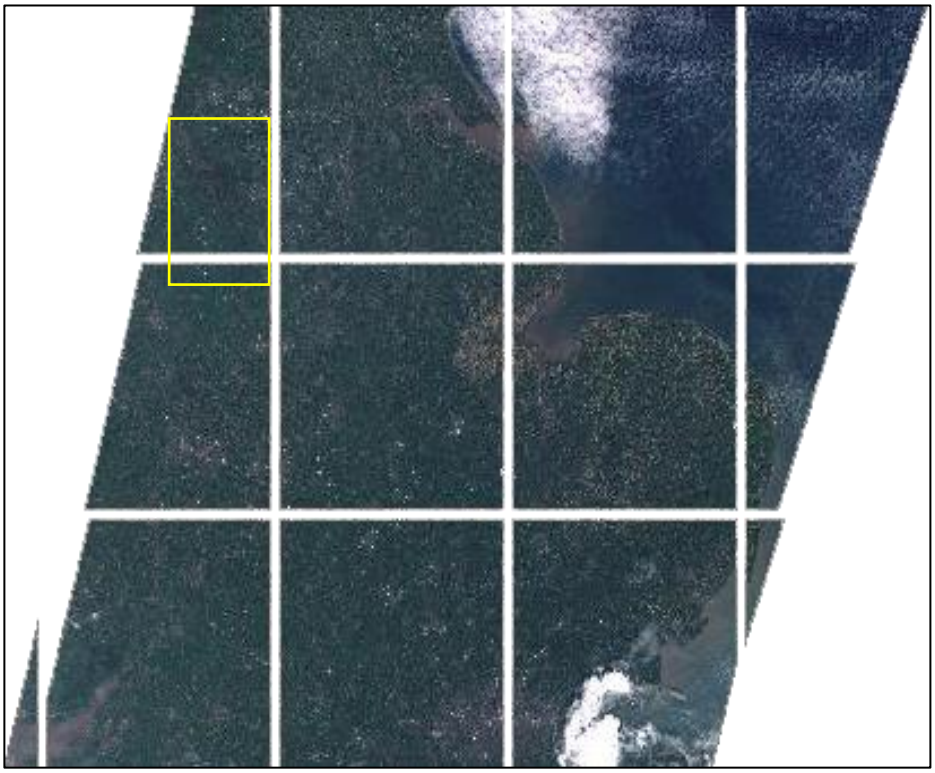

06-06-2016 S2A MSI

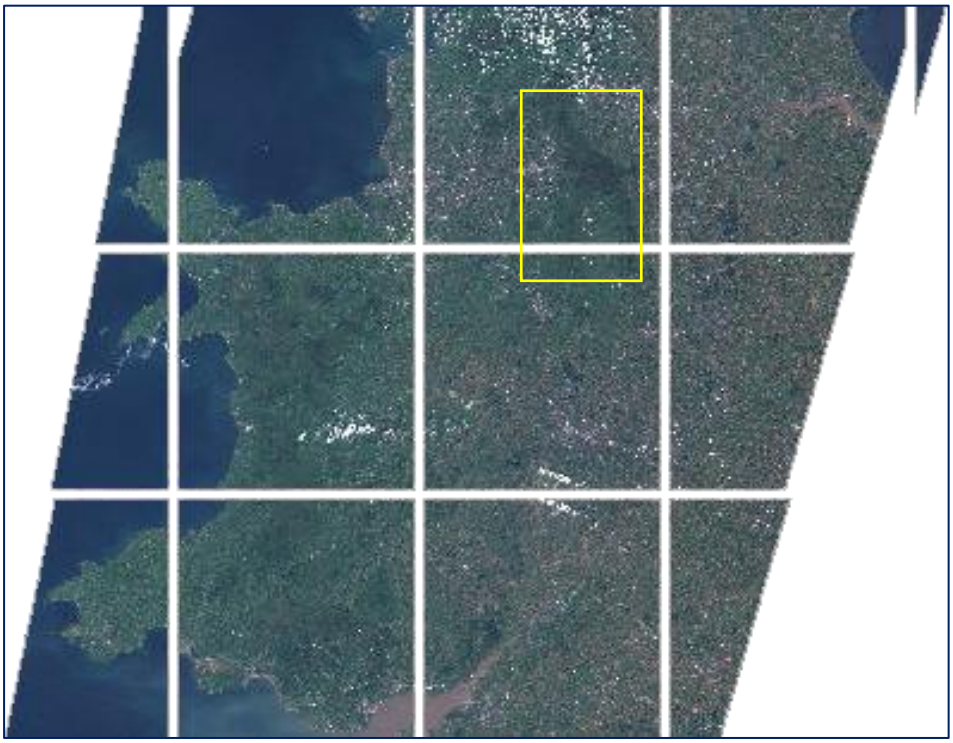

19-07-2016 S2A MSI

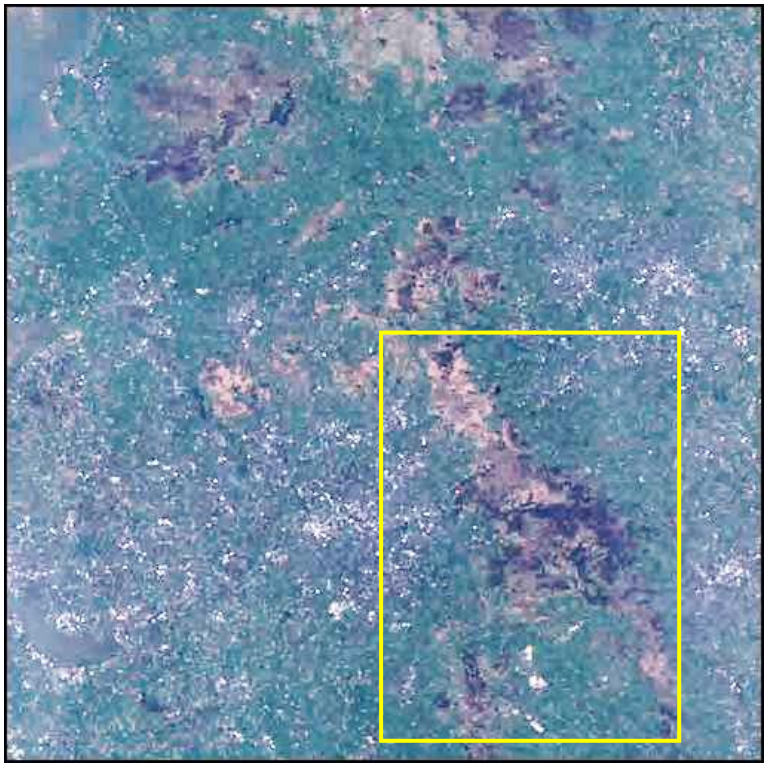

26-03-2017 S2A MSI

Appendix V:

Calluna FMC model computed in Erdas Imagine

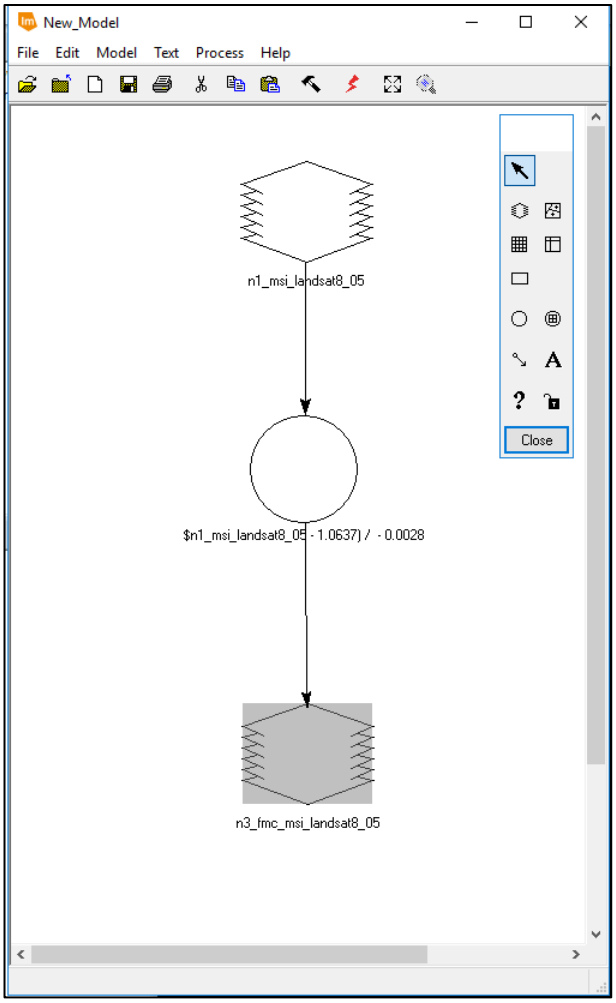

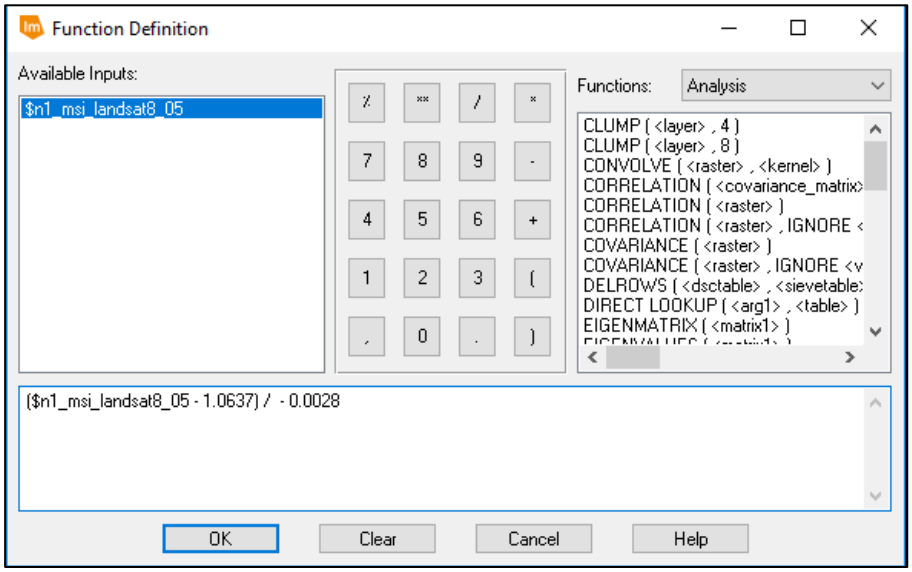

Appendix VI:

Shapefile for Heather for Peak District from UK Land Cover Map 2015.

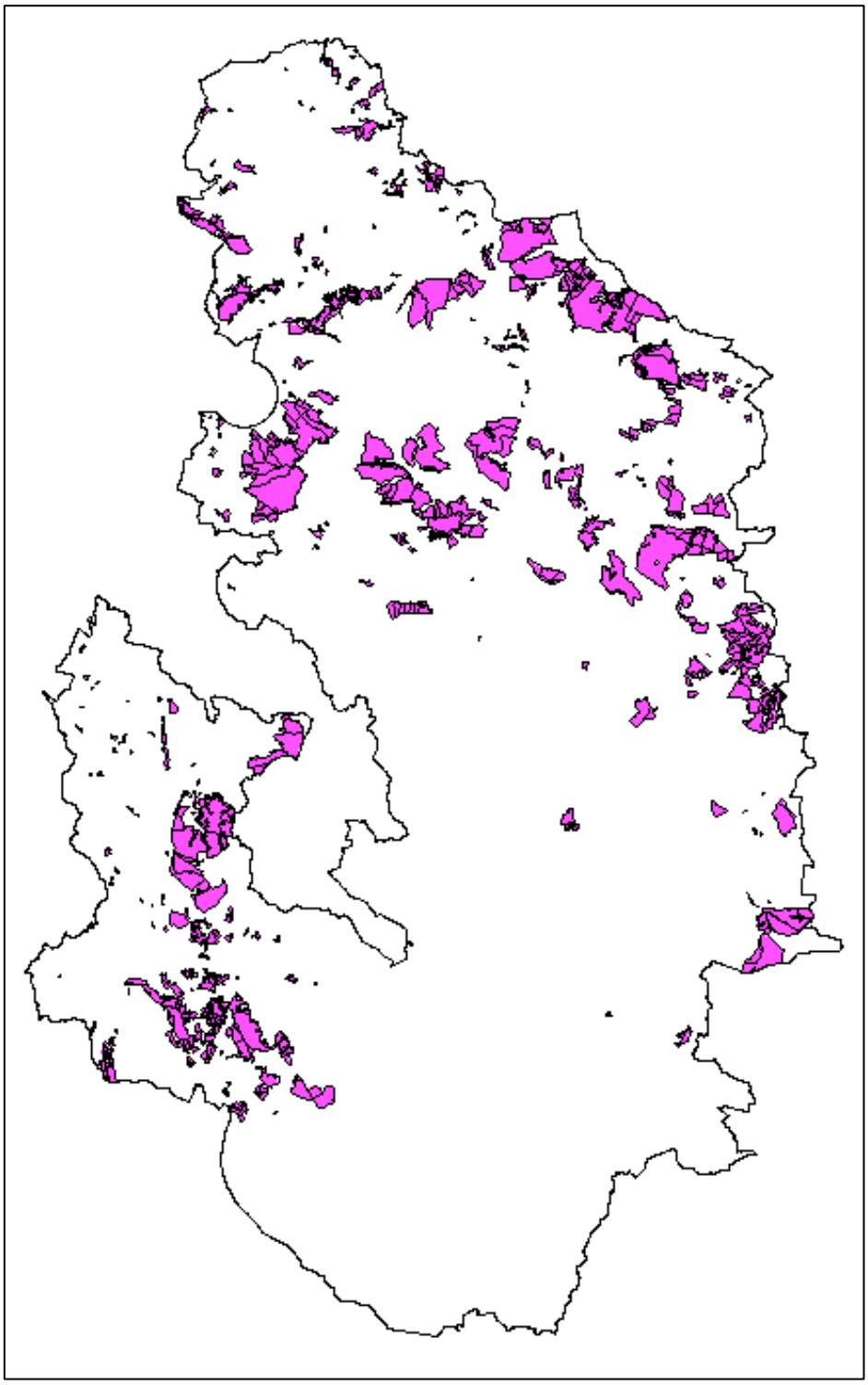

Appendix IX:

Sectors and key agencies which have contributed to of wildfire management in the UK adapted from (Gazzard et al, 2016).

Sector	Organization/Agency/Group	Scale
Contingency planning	Cabinet Office Civil Contingency Secretariat	National
	Department for Communities and Local Government Resilience and Emergency Planning Directorate	National
	Scientific Advisory Group of Experts	National
	Local Resilience Forums based within 39 Police Areas in England	Regional
Fire	Chief Fire Officers Association, Wildfire Group, National Operations Programme Group	National
	49 FRS in England and Wales, managed by regional Fire Authorities, and overseen by the DCLG	Regional
Environment	DEFRA Wildfire Group, within DEFRA Contingency Planning Team	National
	Forestry Commission	National to local
	Met Office	National
	Natural England	National to local
	Wildlife and landscape conservation groups: Royal Society for the Protection of Birds (RSPB), National Trust, Wildlife Trusts, etc.	National to local
	Land management community: practitioner associations such as the Moorland Association, the Heather Trust, Game and Wildlife Trust	National to local
Under represented sectors	Development control planning	Regional to local
	Department for Energy and Climate Change	National
	Insurance industry	National
Cross-sector	England and Wales Wildfire Forum, Scottish Wildfire Forum	National
	Local wildfire groups, also known as Fire Operations Groups	Regional to local
	Academic-led initiatives	National